UNFOLDED PROTEIN RESPONSE PATHWAY OF CANDIDA AURIS, ITS ROLE IN DISEASE PROGNOSIS AND TREATMENT

Thesis Submitted for the Award of the Degree of

DOCTOR OF PHILOSOPHY

in

Biotechnology

By

NAHID AKHTAR

Registration Number: 11816326

Supervised By

Dr. Mohammad Aminul Mannan

(20597)

Department of Molecular Biology and Genetic Engineering

School of Bioengineering and Biosciences,

Lovely Professional University, Punjab, India

LOVELY PROFESSIONAL UNIVERSITY, PUNJAB

2024

DECLARATION

I, hereby declare that the presented work in the thesis entitled "**Unfolded protein response pathway of *Candida auris*, its role in disease prognosis and treatment**" in fulfilment of degree of **Doctor of Philosophy (Ph. D.)** is outcome of research work carried out by me under the supervision of Dr. Mohammad Amin ul Mannan, working as Assistant Professor, in the School of Bioengineering and Biosciences, Lovely Professional University, Punjab, India. In keeping with general practice of reporting scientific observations, due acknowledgements have been made whenever work described here has been based on findings of other investigator. This work has not been submitted in part or full to any other University or Institute for the award of any degree.

(Signature of Scholar)

Name of the scholar: Nahid Akhtar

Registration No.: 11816326

Department/school: School of Bioengineering and Biosciences

Lovely Professional University,

Punjab, India

CERTIFICATE

This is to certify that the work reported in the Ph. D. thesis entitled "**Unfolded protein response pathway of *Candida auris*, its role in disease prognosis and treatment**" submitted in fulfillment of the requirement for the reward of degree of **Doctor of Philosophy (Ph.D.)** in the School of Bioengineering and Biosciences, Lovely Professional University, is a research work carried out by Nahid Akhtar, 11816326, is bonafide record of his/her original work carried out under my supervision and that no part of thesis has been submitted for any other degree, diploma or equivalent course.

(Signature of Supervisor)

Name of supervisor: Dr. Mohammad Amin ul Mannan

Designation: Assistant Professor

Department/school: School of Bioengineering and Biosciences

University: Lovely Professional University

ABSTRACT

Candida auris was reported for the first time in 2009 and since then the number of reported cases is rising steadily. *C. auris* that constitutes of five distinct geographical clades have been reported in 40 countries, in all the seven continents except Antarctica. Due to the multidrug resistance and rapid rate of transmission, it can be regarded as a key emergent public health issue. Various isolates of *C. auris* have been described which demonstrate unsusceptibilities to major antifungal classes: polyenes, echinocandins, flucytosine and azole. Furthermore, *C. auris* can evade innate immunity and has high mortality ranging between 30-60 percent. Due to these concerns, the research for novel antifungal drugs and drug targets to treat and prevent *C. auris* infections is imperative. Unfolded protein response (UPR) pathway could be one such drug target that could be manipulated for the identification and generation of different antifungal compounds. UPR pathway is a proteostatic pathway to maintain equilibrium due to the build-up of unfolded or misfolded proteins inside the cell. In previous studies, UPR element *HAC1* has been described as a key element in the virulence and pathogenesis of different human pathogenic fungi. Hence, this study aims to analyse the *HAC1* gene of *C. auris* and identify novel molecules that could target *C. auris* UPR pathway. Furthermore, this study aims to identify new antifungal molecules against *C. auris* and understand their antifungal mechanism. Lastly, to protect individuals from *C. auris* infections a novel prospective vaccine has been designed by immunoinformatics approach.

The bioinformatics analysis determined that the *C. auris HAC1* intron is 440 bp and has 5' hairpin loop surrounding 5' splice site. However, the 3' hairpin loop surrounding the 3' splice site is absent in *C. auris*. The cloning of *HAC1* gene in pESC-URA plasmid and genetic complementation in *Saccharomyces cerevisiae HAC1* delete strain showed that the *C. auris HAC1* could complement *HAC1* gene in *S. cerevisiae HAC1* delete strain and help it to sustain endoplasmic reticulum stress similar to wild type *S. cerevisiae* strain. For identifying molecules that could target the two hallmark proteins of the UPR pathway, Hac1p and Ire1p, various computational analyses were performed. The bioinformatics tools determined the molecular property, bioactivity, toxicity, drug-likeness of different molecules. The small molecules showing the best properties were analysed for their ability to interact with UPR proteins by molecular docking study and molecular dynamics simulation analysis. Flinderole-B, drummondin-E, betulinic acid, ursolic acid, oleanolic acid, stigmasterol showed good drug-likeness scores, were non-carcinogenic, non-toxic; and followed Lipinski's rule of five. Based on the molecular docking and molecular dynamics simulation analysis betulinic acid

and drummondin-E showed the potential to target Hac1 and Ire1p, respectively. Betulinic acid and drummondin E could be potential UPR pathway inhibitors in *C. auris*. Further laboratory and animal model experiments are necessitated to corroborate their antifungal potential.

Furthermore, betulinic acid (BA) has been evaluated for their antifungal property against *C. auris* in-vitro. To comprehend the antifungal mechanism of BA against *C. auris* scanning electron microscopy, ergosterol synthesis inhibition assay, H_2O_2 sensitivity assay and RNA sequencing were performed. The studies showed that the BA could inhibit *C. auris* growth, exerted oxidative stress and affected ergosterol synthesis. RNA sequencing of *C. auris* treated with BA showed down-regulation of genes appertaining to oxidative stress. BA also downregulated KRE9 domain-containing protein, which is a part of cell wall biogenesis and (1->6)-beta-D-glucan biosynthetic process. Finally, 3-(4,5-dimethylthiazol-2-yl)-2,5-diphenyltetrazolium bromide (MTT) assay exhibited that BA exerted low cytotoxicity on HEK293T cell line even at 2x MIC concentration of *C. auris*. Moreover, GC-MS analysis to assess the impact of BA administration on the metabolite secretion by *C. auris* was also performed. Metabolites belonging to different classes such as 2,5-diketopiperazines, delta lactam, fatty alcohol, piperazinone, pyrazine derivative, triterpene were detected in the metabolite extract of BA treated *C. auris*. These metabolites have wide array of properties such as antioxidant, auto-antibiotic, fungal metabolite, biofilm forming metabolite and hyphae inhibition. Tyrosol and phenylethyl alcohol which are biofilm forming metabolite and hyphae inhibiting metabolite respectively were also identified in the metabolites of BA treated cells.

As this study also intends to detect different molecules and drug targets for developing antifungals against *C. auris*, the antifungal property of ethnomedicinal plant *Sarcochlamys pulcherrima* and the ability of molecules present in *S. pulcherrima* to target carbonic anhydrase protein of *C. auris* were evaluated. The extracts of the plant's leaves (ethyl acetate and methanol) repressed the growth of *C. auris* and *C. albicans*. High-performance thin-layer chromatography analysis detected gallic acid in the plant's leaves extract. Further, *in vitro* antifungal assay revealed the suppression of the growth of six strains of *C. auris* by gallic acid. The computational experiments showed that the gallic acid could interact with *C. auris* carbonic anhydrase protein's active sites and affect its catalytic activity.

Finally, a distinct multi-epitope prospective vaccine has been designed through immunoinformatics for protection of individuals from *C. auris* infection. The Als3 protein of *C. auris* was targeted to identify strong binding epitopes to human major histocompatibility complex (MHC) alleles using online available servers. Various parameters such as the allergic potential, antigenicity, conservancy, interferon-gamma eliciting activity, and toxicity of the predicted epitopes were studied using various computational tools. Out of several epitopes, only those epitopes that were assessed as non-allergic, antigenic, conserved among different *C. auris* isolates, elicited interferon-gamma, and non-toxic were chosen to design vaccine candidate. The chosen epitopes were joined with adjuvants by GGS linker to design the prospective vaccine candidate. Different in-silico analyses indicated that the prospective candidate *C. auris* vaccine could be antigenic, non-allergic, and stable. Ramachandran plot analysis was performed to validate the tertiary model of the vaccine construct generated using I-TASSER software. Through the molecular docking and molecular dynamics analysis, it was determined that the vaccine could bind to the MHC and Toll-like receptor (TLR) with stability. The immunoinformatics research have produced promising findings for the *C. auris* vaccine construct but further experiments in candidiasis animal models must be carried out to determine the vaccine's efficacy and safety.

Acknowledgements

I want to express my sincere gratitude towards my supervisor Dr. Mohammad Aminul Mannan, Assistant Professor, Lovely Professional University for his guidance, support and co-operation. His ideas and comments always made this work and my research papers productive. His expertise and valuable guidance are acknowledged with gratitude.

I express my gratitude to my parents, sister and brother-in-law for their incessant and unconditional love, support and encouragement.

I am also thankful to my colleagues and friends, Mr. Atif Khurshid Wani, Mr. Tahir ul Gani Mir, Dr. Amit Joshi, Mr. Saikat Sena, Mr. Yogesh Chaudhary, Mr. Zahir Ahmad, Mr. Nirdesh Ranjan and Mr. Pranay Raut for their constant encouragement and support throughout my PhD journey.

Table of Contents

List of Tables

List of figures

List of abbreviations

ACE: Atomic contact energy

ADMET: Absorption, distribution, metabolism, excretion and toxicity

AP: 4,6-dimethyl alpha pyrone

BA: Betulinic acid

BLAST: Basic local alignment search tool

CAI: Codon adaptation index

CDC: Centre for Disease Control and Prevention, United States of America

CGD: Candida genome database

EDTA: Ethylenediaminetetraacetic acid

EI: Enzyme inhibitor

EUCAST: European committee on antimicrobial susceptibility testing

FESEM: Field emission scanning electron microscopy

DMEM: Dulbecco modified Eagle medium

DTT: Dithiothreitol

DPPH: 2,2-diphenyl-1-picrylhydrazyl

FBS: Fetal bovine serum

GA: Gallic acid

HCCDA: HiChrome *Candida* differential agar

HCI: HiCandida identification kit

HDAC: Histone deacetylase

HEK: Human embryonic kidney cells

HPTLC: High performance thin-layer chromatography

ICM: Ion-channel modulators

IEDB: Immune epitope database

KI: Kinase inhibitor

LogP: Partition coefficient

MD: Molecular docking

MDS: Molecular dynamics simulation

MFC: Minimum fungicidal concentration

MHCI: Major histocompatibility complex 1

MHCII: Major histocompatibility complex 2

MIC: Minimum inhibitory concentration

MTT: 3-(4,5-dimethylthiazol-2-yl)-2,5-diphenyltetrazolium bromide

NCCPF: National culture collection of pathogenic fungi

NCCS: National Centre for Cell Science

nOHN: Number of hydrogen bonds acceptors

nON: Number of hydrogen bonds donors

NRL: Nuclear receptor ligand

OD: Optical density

PBS: Phosphate-buffered saline

PCI: Phenol-chloroform-Isoamyl alcohol

PDB: Protein data bank

PI: Protease inhibitor

PMSF: Phenylmethylsulfonyl fluoride

RMSD: Root mean square deviation

RMSF: Root mean square fluctuation

SDA: Sabouraud dextrose agar

SDB: Sabouraud dextrose broth

SDF: Structure data file

SDS: Sodium dodecyl sulphate

SMILES: Simplified molecular input line entry system

SOT: Solid organ transplant

TPSA: Total polar surface area

YPDA: Yeast extract-peptone-dextrose agar

YPDB: Yeast extract-peptone-dextrose broth

Introduction

Introduction

Infectious diseases encompass a broad range of illnesses caused by various pathogens, including bacteria, viruses, parasites, and fungi. Diseases caused by viruses such as SARS-CoV-2, dengue, Zika virus, monkeypox virus and human immunodeficiency virus have affected millions of people across the world [1–3]. Bacterial diseases such as cholera, tuberculosis, influenza and pneumonia have also had a profound impact on human health throughout history [4,5], which has been further exacerbated by the emergence of antimicrobial resistance in recent years [6]. Human parasitic diseases have been acknowledged as significant threats to public health in different regions of the world for many decades [7–9]. While much attention is typically focused on bacterial and viral infections, fungal diseases often find themselves in the shadows and are frequently neglected by public health authorities [10]. Fungal diseases are often underestimated in terms of their impact on global health [11]. This underestimation stems from a lack of comprehensive surveillance systems, reporting and diagnostic tools for fungal infections especially in developing countries [12]. Consequently, a considerable number of instances remain untreated or are subject to misdiagnosis, thereby fostering the misconception that the prevalence of certain ailments is lower than their real occurrence [10]. Furthermore, compared to bacterial and viral infections, public awareness and understanding of fungal diseases are generally low [13]. Fungal diseases are prevalent in specific regions or climates, which limits their global visibility [10,14]. Some fungal infections are more common in tropical or subtropical areas, where resources for healthcare and research may already be limited [15–17]. Consequently, diseases that predominantly affect low-resource regions tend to receive less attention and funding from the global health community [18]. This lack of investment hampers the development of improved diagnostic tools, treatment options, and preventive measures [19]. The limited availability of data and research on fungal diseases further exacerbates the neglect.

The prevalence of fungal illnesses and their consequential effects on public health are seeing a significant and concerning escalation on a global scale [20]. Fungal infections can cause grave and occasionally life-threatening illnesses. Some of the most common fungal infections include candidiasis, histoplasmosis, aspergillosis, cryptococcosis and pneumocystosis [21]. These infections are often challenging to treat and can cause complications in individuals with weakened immune systems, such as those undergoing cancer treatment or receiving

organ transplants [22]. Infections caused by fungi are estimated to affect up to 1 billion people around the world. In India alone more than 57 million people have been estimated to be affected by fungal infections [23]. Almost 150 million of these 1 billion cases could result in patient death [12]. Fungal infections are not only a significant public health issue, but they are also a major economic issue. Centre for Disease Control and Prevention (CDC), a prominent public health organization based in the USA has estimated that almost 6.7-7.5 billion dollars are spent in the USA alone on treating fungi-related illnesses [24]. Currently, multiple antifungal medications are accessible for treating fungal infections. Azole antifungals, such as fluconazole, itraconazole, and voriconazole, are widely prescribed for various fungal infections, which function by suppressing the ergosterol synthesis, a crucial element present in fungal cell membranes [25]. Polyene antifungals, entailing amphotericin B and nystatin, function via binding to fungal cell membrane ergosterol, causing damage and leakage of cell membrane which ultimately leads to fungal cell death [26]. Echinocandins which include caspofungin, micafungin, and anidulafungin target the cell wall of fungi by inhibiting the synthesis of beta-glucan, a key component necessary for its integrity [27]. Allylamines are usually applied topically (butenafine and naftifine) or used both topically and orally (terbinafine) for more severe infections and inhibit an enzyme called squalene epoxidase, thereby disrupting the synthesis of ergosterol in the cell membranes of various fungi [28]. Flucytosine is a unique antifungal drug often availed in combinatorial therapy, commonly with amphotericin B, which interferes with fungal DNA and RNA synthesis, inhibiting fungal cell growth and replication [27]. Two newly developed antifungal drugs, Isavuconazole (broad spectrum azole) and Ibrexafungerp (glucan synthase inhibitor) have been ratified by the FDA for the treatment of mucormycosis and aspergillosis in adults, and vulvovaginal candidiasis respectively [29,30]. Other antifungals with novel mechanisms, such as albaconazole, aureobasidin A, enfumafungin, encochleated amphotericin B, fosmanogepix, nikkomycin Z, olorofim, opelconazole, oteseconazole, rezafungin, and tetrazole VT-1129 are currently under development [29,31,32]. Unsatisfactory outcomes, low bioavailability of the antifungal medicines, lack of drug-drug interaction information and adverse effects of the currently available antifungals are further concerns associated with fungal infections [11]. The problem is being further worsened by the development of resistance to different classes of antifungals in various infectious fungi.

There are about 300 fungal pathogenic species, mostly belonging to *Aspergillus, Blastomyces, Candida, Coccidioides, Histoplasma, Paracoccidioides* and *Pneumocystosis*

genus of Ascomycota division, which cause diseases in humans [33–35]. Among the Basidiomycetes, *Cryptococcus sp.* are of major concern along with *Trichosporon sp.* and *Malassezia furfur* which may cause opportunistic infections in immunosuppressed individuals [35]. Furthermore, there are Mucorales which can affect severely immunocompromised patients. During the COVID-19 pandemic, there were increasing reports of secondary infections due to mucors in COVID-19 patients [36]. Among all Ascomycetes, *Candida sp.* is of great interest in public health [37]. They are ubiquitous part of the human microbiome where it exists as commensal and transferred to the child from the mother vertically [38]. However, some of them like *C. albicans* and *C. auris* are opportunist pathogens that cause systemic and mucosal infections in those with weakened immune systems [39–41]. Despite treatment, disseminated candidiasis has a significant death rate of 35-60% [42,43]. Oropharyngeal candidiasis affects 20-40% of AIDS and cancer patients, while recurrent vulvovaginal candidiasis affects more than 8% of all women [44,45]. *Candida* infection has a huge direct cost to the US healthcare system ($1-2 billion a year) [46]. Recently, *Candida auris* has been emerging rapidly and causing global health concern [47]. Studies have revealed the emergence of antifungal drug unsusceptible *C. auris* infection in immunocompromised patients [47].

First discovered in 2009 in a Japanese patient's outer ear canal, *C. auris* has been related to invasive healthcare-linked outbreaks and has spread to a multitude of countries all over the world [48]. World Health Organization has placed *C. auris* in a critical priority group, along with *C. albicans*, *A. fumigatus* and *C. neoformans*, for public health action, research and development purposes [49,50]. *C. auris* belongs to the Metschnikowiaceae family of fungi, which are commonly found on human skin and in mucous membranes [51,52]. However, unlike other *Candida* species, *C. auris* could resiliently persevere on different surfaces in healthcare environments for weeks or months, increasing the risk of transmission to patients [52]. Furthermore, *C. auris* is resistant to multiple classes of antifungal drugs, making it difficult to treat and control [53,54]. CDC has enlisted *C. auris* as an urgent threat in "antibiotic resistance threat reports in the United States of America [55]. Additionally, the drugs recommended for *C. auris* treatment are not available in several countries [50]. Since its discovery, *C. auris* has spread rapidly around the world. The CDC has reported over 2,377 incidents of *C. auris* in the United States alone during a period between January 2022 to December 2022 [53]. India has also experienced a significant burden of *C. auris* infections [56–58]. In a research in north-western India, *C. auris* was determined as one of the highly

prevalent fungi leading to septicaemia in COVID-19 patients [59]. Multiple outbreaks of *C. auris* were also reported at a hospital in South India [60]. *C. auris* is concerning due to its high prevalence and incidence in vulnerable populations, such as hospitalized patients and those with weakened immune systems [61]. Individuals who have undergone organ transplantation, take medications to suppress their immune system, have diabetes, have recently used antibiotics, use catheters, and have spent extended periods in hospitals or nursing homes are at risk of being susceptible to *C. auris* infections. [62]. The exact prevalence of *C. auris* is difficult to determine, as it is often misidentified by routine laboratory methods and may be underdiagnosed in some regions [63]. The diagnosis of *C. auris* requires specialized laboratory techniques, as routine laboratory methods may misidentify the fungus as other *Candida* species [64]. Molecular identification methods, such as polymerase chain reaction (PCR) of internal transcribed spacer region and sequencing, are often used to accurately identify *C. auris* [65]. Raman spectroscopy, CHROMagar^{TM}, Candida Plus media, and MALDI-TOF may also be availed for the detection and confirmation of *C. auris* [66–68].

C. auris can result in a myriad of infections, including eye and ear infections, central nervous system, bone, wound, internal organs and bloodstream infections [50,53]. These infections can be severe and difficult to treat, particularly in patients with underlying health conditions or weakened immune systems [69]. In some cases, *C. auris* infections can lead to death; mortality rate ranging between 30-60% [56,70–72]. Furthermore, *C. auris* infected people have been observed to spend more time in intensive care units or hospitals than the sufferers of other fungal candidemia. *C. auris* is unsusceptible to most of the prominent classes of antifungal agents, making the infection management and cure further challenging [53,54]. The optimal treatment approach for *C. auris* infections is not well-established, as there have been few clinical trials conducted on this topic. Treatment typically involves the use of antifungal drugs, such as echinocandins (caspofungin, micafungin, anidulafungin), and may require a combination of drugs to achieve a successful outcome [53,73,74]. *C. auris* can infect and colonize humans, even in the hospital settings. These nosocomial infections have been mostly attributed to the biofilm formation on hospital equipments, surgical instruments, and beds. The transmission is from person to person contact and in some cases the source of infections can be traced back to the health care professionals and hospital environment [75,76]. Preventing the breakout of *C. auris* in healthcare settings requires a multifaceted approach, including strict infection control practices, such as hand hygiene, environmental

cleaning, and the use of personal protective equipment [77]. Additionally, early identification and isolation of infected patients can help prevent further transmission [53].

Rapidly developing *C. auris* is a global public health hazard that requires ongoing observation and investigation. Its capacity to remain on surfaces, induce serious infections, and acquire resistance to numerous antifungal classes highlights the need for effective prevention and treatment. Hence, there is a dire necessity for identifying new drug targets (genes, pathways) and potential antifungal molecules with low toxicity for effectively treating *C. auris* infection. Phytochemicals from various herbal medicinal plants could be an important source of potentially safe and novel antifungal drugs [78,79]. Furthermore, small molecules from marine algae and cyanobacteria could also be delved into for the advancement of antifungal drugs [80–82].

The unfolded protein response (UPR) pathway could be one such drug target that could be manipulated for the development of novel antifungal compounds. The UPR pathway is a proteostatic pathway to maintain equilibrium due to the accrual of unfolded or misfolded proteins inside the cell especially in the endoplasmic reticulum [83]. In previous studies, the role of UPR elements *HAC1* has been described to play a critical part in the pathogenesis of different fungi such as *Cryptococcus neoformans, Aspergillus fumigatus, Candida albicans and Candida parapsilosis* [84,85]. The UPR pathway and their role in the virulence and pathogenicity of different pathogenic fungi have been discussed in detail in the review of literature, sections 2.3-2.5. The deletion of the genes associated with the UPR pathway has inhibited the ability to uptake nutrients, hyphal growth, biofilm formation, melanin synthesis, and made the cells sensitive to antifungal agents, temperature and cell wall disrupting compounds [84]. The association of the UPR with fungal pathogenesis opens a new avenue to combat fungal diseases and the antifungal agent tolerance in pathogenic fungi. As, the UPR elements *HAC1* and *IRE1* play a key part in the fungal pathogenesis they could be prospective targets for developing novel drugs for the cure and management of fungal infections. Hence, the objectives 2 and 3 of this research try to decipher *C. auris* UPR pathway and find compounds that could target *C. auris* UPR pathway for developing antifungal drugs.

Despite several studies, only a few novel antifungal drugs are under clinical trials such as Ibrexafungerp which inhibits 1,3-β-D-glucan synthesis, MGCD290 which is a fungal HDAC inhibitor, VT-1129 which interferes with cytochrome P450 activity, Fosmanogepix

(APX001) which inhibits fungal GPI anchor protein [86–89]. Furthermore, the currently used antifungals such as polyenes, azoles, and echinocandins exert a high selective pressure on the pathogen survival leading to the development of drug unsusceptibility in the pathogenic fungi [90]. Because of the tremendous transmission rate and mortality linked to the fungus, it is imperative to look for novel and effective compounds that can treat *C. auris* infections. One of the major sources of novel antimicrobial molecules can be plants, which have been used as part of traditional and herbal medicine for ages. Therefore, as part of the objective 4, plant extracts and phytochemicals have been examined for their antifungal activity in *C. auris*. In this objective, betulinic acid (BA) has been evaluated for its antifungal property. BA is a triterpenoid found in various plants such as *Betula alba* (stem bark), *Diospyros leucomelas* (stem), *Eucalyptus camaldulensis* (leaves), *Millettia richardiana* (stem bark), *Morus alba* (stem and root), *Salvia officinalis* (leaves) [91,92]. Previous studies have reported the antioxidant, anti-diabetic, anti-tumour, anti-inflammatory, hepato-protective, antiviral, antiprotozoal, antimalarial, and neuroprotective properties of BA [93–99]. Additionally, in the objective 4, the antifungal property of an ethnomedicinal plant *Sarcochlamys pulcherrima* plant extract was evaluated by *in vitro* and *in silico* studies. *S. pulcherrima* is an evergreen tree that grows in the forests of northeastern states of India, Thailand, Bhutan, Myanmar and Indonesia [100]. Various tribes in India and Bangladesh use different parts of this plant to treat several ailments such as fever blisters, tongue ulcers, flatulence, boils, dysentery, diarrhoea, digestion problem, and itching of the eyes [100]. The antibacterial and antifungal properties of *S. pulcherrima* have been reported in previous studies [101,102]. Moreover, the currently employed antifungals, exert significant selective pressure on the survival of pathogens, leading to the occurrence of drug unsusceptibility in pathogenic fungi [90]. Given the high transmission rate and mortality linked to the fungus, it is crucial to seek new and effective compounds for treating *C. auris* infections. Plants, which have been utilized in traditional and herbal medicine for centuries, present a promising source of novel antimicrobial molecules. As part of objective 4, plant extracts and phytochemicals were evaluated for their antifungal activity against *C. auris*. Specifically, the antifungal property of a triterpenoid molecule BA was assessed. Furthermore, within objective 4, the antifungal activity of *S. pulcherrima*, an evergreen ethnomedicinal plant, was evaluated through *in vitro* and *in silico* studies.

Another strategy that can be used to protect fungal infections is the development of antifungal vaccine candidates. The research into developing safer and potent vaccines against fungi can

help in reducing the dependency on antifungal drugs, some of which can have adverse effects; and aid in overcoming antifungal drug resistance which has been increasingly reported in various human pathogens as a result of the haphazard use of the existing antifungal agents [103]. Furthermore, the fungal vaccines could be beneficial in preventing those fungal infections that afflict both the immunocompetent individuals and immunocompromised patients, such as coccidioidomycosis [104]. Vaccines can aid in preventing these infections by eliciting the immune system to produce protective antibodies that can identify and neutralize the pathogenic fungi [105]. By preventing these infections, vaccines can not only save lives but also reduce healthcare costs associated with treating fungal infections [106]. So far, various live-attenuated vaccines, inactivated vaccines, radioattenuated yeasts, recombinant vaccines, synthetic peptide vaccines, DNA vaccines and glycoconjugate peptide vaccines have been developed for immunization against different pathogenic fungi in animal models [107–110]. The NDV-3A vaccine comprising of the *C. albicans* Als3p N-terminal region has shown safety and efficacy against vulvovaginal candididasis in phase two clinical trials [111]. Although these vaccine candidates have shown encouraging results, only three candidates have reached the human clinical trial phage and no vaccine has been approved for human use by the FDA yet [112]. So, the goal of the objective 5 is to use in silico immunoinformatics to identify a unique prospective epitope-based candidate vaccine for protection from *C. auris* infection. The usage of computational methods for designing prospective candidate vaccines has rapidly increased in the past decade and this method has been applied to the design of vaccine candidates against a multitude of bacteria, viruses, fungi and cancer [113–116]. The epitope-based vaccines designed using immunoinformatics could be an alternative to live attenuated or avirulent fungal vaccine candidates. Additionally, these vaccines could also overcome challenges like antigenic shift, antigenic drift and genetic variations [117]. Moreover, immunoinformatics can also reduce the cost and time used for the development and selection of novel, safe and effective fungal vaccine candidates [117]. Immunoinformatics approach has been applied for the development of peptide/epitope-based prospective vaccine constructs against different candidiasis-causing pathogenic fungi for example *Candida tropicalis*, *C. albicans* and *Candida dubliniensis* [118–121]. Furthermore, the immunoinformatics approach has also been used for the design of prospective novel vaccines for protection against aspergillosis and mucormycosis [122,123]. The immunoinformatics studies generally target different virulent proteins such as secreted aspartyl proteinases, Ftr1, and agglutinin-like sequence-3 to determine various B-cell epitopes ranging in length between 9-20 amino acids, MHC-restricted $CD8^+$ and $CD4^+$ T-

cell-specific peptides [119,121]. Then, from the hundreds of epitopes those epitopes are selected which are determined to possess the capability for inducing the elicitation of different cytokines (interferon, interleukin) and are predicted as antigenic, non-allergic, non-toxic, conserved by different computational tools. The selected epitopes are linked with adjuvants using linker sequences such as GGS, GPGPG, AAY, and EAAAK to design a final vaccine construct [118,123]. Then, different computational tools are availed to determine the antigenicity, secondary structure and tertiary structure of the designed prospective candidate vaccines. Finally, the ability of the designed vaccine constructs to bind with different toll-like receptors and MHC molecules is analysed using molecular docking and molecular dynamics simulation studies [120,124]. Moreover, the immune response activated by the designed prospective fungal candidate vaccines can also be studied computationally [125].

Review of Literature

Review of Literature

2.1 Human fungal infections

Fungi are widely distributed throughout the environment and have emerged approximately 1.6 million years ago. Presently, the global fungal population is believed to have a range of 1.5-5 million species [81,82]. However, only a few hundred species are commonly associated with human diseases. Few of these fungi are recognized as genuine pathogens, leading to the development of infections like histoplasmosis and paracoccidioidomycosis in healthy hosts, whereas most of them are typically regarded as opportunistic pathogens (e.g., *Cryptococcus* and *Candida*), primarily infecting the immunocompromised patients.

Most fungi are harmless and only cause nail and skin infections, but some can cause life-threatening diseases. Ringworm, athletes' foot, and nail infections impact 1.7 billion people worldwide and these infections are straightforward to treat, but invasive fungal infections kill about 1.5 million people with an aggravated mortality of 50% [33].

The infections due to *Candida sp.* are of two types: mucocutaneous candidiasis and invasive candidiasis. The mucocutaneous candidiasis can be either vulvovaginal candidiasis infecting healthy women or oesophageal and oropharyngeal infection mostly affecting AIDS patients or individuals undergoing corticosteroid therapy. Invasive candidiasis can of two forms: intra-abdominal candidiasis infecting patients undergoing abdominal surgery and disseminated candidiasis infecting individuals with weak immunity like HIV/AIDS patients, premature neonates, patients under corticosteroids, and solid organ transplant (SOT) recipients [126]. The *Aspergillus sp.* infections may lead to pulmonary aspergillosis or disseminated aspergillosis in patients under immunosuppression or allergic bronchopulmonary aspergillosis in atopic individuals [127]. *Cryptococcus sp*. usually infects HIV/AIDS patients, haematopoietic stem cell transplant recipients or individuals using corticosteroids and ibrutinib where it may cause pneumonia, cryptococcosis of the central nervous system, or disseminated cryptococcosis [128]. Pneumocystosis caused by *Pneumocystis jirovecii* infection can cause pneumonia or disseminated pneumocystosis in HIV/AIDS patients or patients receiving corticosteroid therapy. Histoplasmosis, which is afflicted because of *Histoplasma capsulatum*, is prevalent in North and South America and primarily affects individuals with weakened immune systems, including those with diminished CD4 cells such as individuals with malignancies, HIV/AIDS patients, COVID-19 patients, and SOT recipients [129]. Furthermore, filamentous molds such as *Rhizomucor,*

Mucor, and *Rhizopus* may cause rhinocerebral, sinopulmonary or disseminated mucormycosis in COVID-19 patients, diabetic ketoacidosis patients, individuals with neutropenia, transplant recipients and patients using corticosteroids [36].

Exogenous fungi cause most fungal infections. However, the host's endogenous fungi, or mycobiome that makes up a minor percentage of the microbiota, has been linked to various diseases [130]. Pathogenic fungi can live in the fungal microbiome as commensals for an extended period, nonetheless when the hosts' immunity is compromised or on antibiotics, the fungi bloom and lead to disease conditions. *Candida* species frequently colonize mucosal surfaces, with 30-70% of healthy adults serving as carriers. During favourable situations, such as under immunosuppression or antibiotic therapy, these species can lead to conditions like invasive candidiasis or candidemia. Likewise, *Cryptococcus* and *Pneumocystis* species can occur as lung commensals but can inflict severe and life-threatening conditions in individuals with weakened immune systems [130]. The human gut fungal microbiota has also been implicated in the progression of inflammatory bowel diseases like Ulcerative colitis and Crohn's disease; pouchitis and colorectal cancer [131]. In patients with colorectal cancer, there is an abundance of *Aspergillus sp.*, mainly *Aspergillus flavus* which produces carcinogen aflatoxin, thus implicating the association of mycobiome in colorectal cancer [132]. Reports have also suggested an association between mycobiome and oral cancer. Oral lesions infected with *Candida* can transform into tumours because of the production of carcinogens like nitrosamines and acetaldehyde by *Candida sp.* [133]. The mycobiome can also cause mucocutaneous candidiasis in low-birth-weight infants and premature neonates. Candida colonization also helps to promote allergic airway inflammation by producing prostaglandin which causes macrophage polarization and food allergy by promoting mast cell degranulation [131]. Similarly, the enhancement of the gut commensal *Wallemia mellicola* population in mice exacerbated the allergic airway disease by altering the pulmonary immune response [134]. The role of *W. mellicola* in allergic airway diseases in humans remains unexplored. Fungal infections have been reported as the risk factor for multiple sclerosis, a neurological inflammatory disease. However, the source of the fungi whether exogenous or endogenous is yet to be explored [135].

2.2 Antifungal drug resistance in human pathogenic fungi

Fungal diseases, either superficial or systemic, have been emerging as a severe public health matter throughout the globe, with a mortality rate of up to 70% for some invasive fungal

diseases, including trichosporonosis, cryptococcosis, pneumocystosis and zygomycosis in immunocompromised individuals [136]. Antifungal drugs play a critical role in the control and cure of fungal infections. However, the increasing prevalence of antifungal agents unsusceptibility in human pathogenic fungi is a major challenge in the treatment of fungal infections [137].

Antifungal drug resistance can occur through several mechanisms, including genetic alterations in the target binding sites of the drug, increased efflux of the drug, biofilm formation and modifications in the metabolic pathways of the fungus [137,138]. Resistance can also arise through target overexpression, stress adaptation-signalling, acquisition of resistance genes from other fungi, cross-resistance from strains that have become resistant due to the use of agricultural fungicides, mutations in existing genes, or through the selection of pre-existing resistant subpopulations [139]. The mechanism of antifungal agents' unsusceptibility against different classes of antifungal drugs has been extensively reviewed in previous studies (Figure 2.1) [137–139].

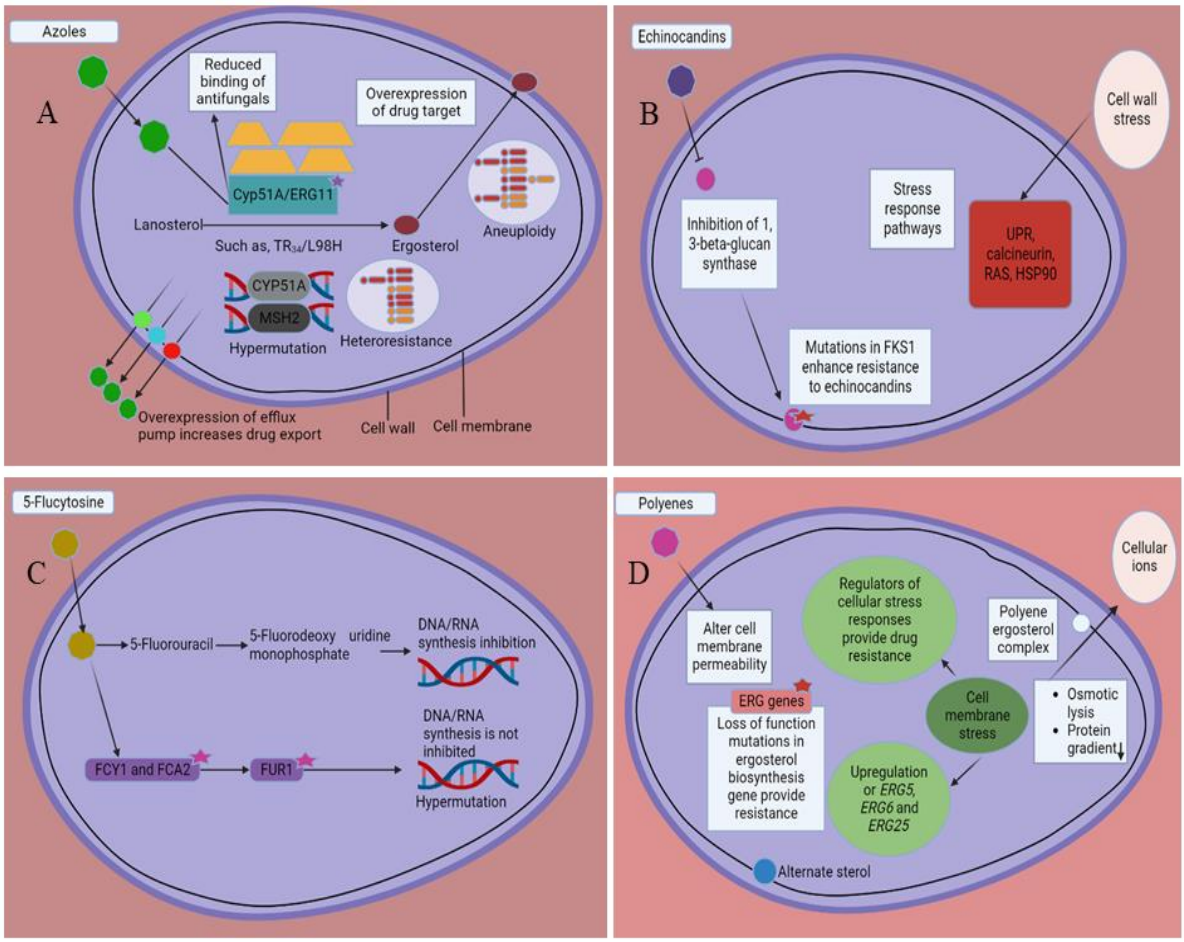

Figure 2.1: The methods by which antifungal resistance develops in different pathogenic fungi. A. Resistance to azole drugs mainly occurs due to their augmented removal from the cell and alterations in the sterol synthesis pathway due to genetic changes like promoter insertions in the *CYP51A* gene and point mutations. The elevated expression of the efflux and drug target pumps due to chromosomal aneuploidy and hypermutation also causes resistance to azoles. B. Echinocandins work by suppressing the activity of the enzyme 1,3-β-D-glucan synthase, and mutations in this particular gene may lead to drug resistance. Additionally, exposure to echinocandins can induce stress on the cell wall by repressing β-glucan synthase. This, in turn, indirectly activates the HSP90/mTOR pathway or Ca2+/calcineurin pathway, which plays a role in echinocandin tolerance. C. 5-flucytosine hinders the synthesis of DNA and resistance to it can occur through point mutations in *FCY1* gene (target of 5-flucytosine) and hypermutations. D. Polyene antifungals bind to ergosterol and affect cell membrane permeability, and resistance is caused by mutations that impair the function of genes associated with ergosterol synthesis and by upregulating the expression of *ERG5, ERG6,* and *ERG25* genes. Cell membrane stress can lead to the development of echinocandin tolerance by affecting the HSP90 regulators (Figure is adapted from [137].

The most commonly encountered antifungal drug-resistant fungi in clinical practice include *Candida* spp., *Pneumocystis* spp., *Aspergillus* spp., *C. neoformans,* and dermatophytes [140]. *C. albicans* is the most commonly detected fungal pathogen from clinical samples, and it accounts for up to 40-50% of all *Candida* infections [141–144]. Unsusceptibility to fluconazole, the most generally applied antifungal drug in the cure and management of candidiasis, has been characterized in up to 3-7% of isolates from some geographic regions [141,145]. Compared to *C. albicans,* the incidence of fluconazole unsusceptibility in non-albicans *Candida spp.,* for example *C. tropicalis, C. parapsilosis* and *C. glabrata* is higher [144,145]. Unsusceptibilty to other antifungal drugs such as echinocandins has also been reported in different *Candida sp.* [146,147]. Moreover, resistance to both echinocandins and fluconazole has been reported in *Candida* spp [148].

Members of the *Aspergillus* genus are some of the major causes of invasive fungal diseases in individuals with compromised immunity [149]. Unsusceptibility to antifungal molecules such as azoles, polyenes and echinocandins has been reported in some *Aspergillus* isolates [150–152]. *C. neoformans* is a common cause of meningitis in immunocompromised individuals, and unsusceptibility to antifungal molecules including fluconazole, flucytosine and

amphotericin B has been reported [153]. In dermatophytes, resistance to azoles and allylamines, which are the primary drugs used in the treatment of dermatophytosis, has been reported [154]. Antifungal resistance has also been reported in *P. jirovecii*, and *H. capsulatum* [155,156].

The management of antifungal agents' unsusceptibility in human fungal pathogens is challenging. There are few treatment choices available for fungal infections resistant to drugs, and the progress in developing new antifungal medications is extremely sluggish. Combining antifungal drugs with other therapeutic modalities, and using immunomodulatory agents, may be necessary to improve treatment outcomes of fungal infections [157,158]. In conclusion, antifungal drug unsusceptibility in human fungal pathogens is a significant public health problem that requires urgent attention. Increased awareness of the problem, the development of novel antifungal agents, and the employment of effective infection-limiting measures are necessary to reduce the burden of antifungal drug-resistant fungal infections.

2.3 Candida auris

C. auris is an ascomycete yeast and an emergent human pathogenic fungi belonging to the *Candida* genus. It forms small and round colonies exhibiting cream colour on agar media, and on CHROMagar media it forms colonies having creamy pink colour surrounded by blue halo [159]. It does not form pseudohyphae or hyphae but may form but may develop pseudohyphae-like forms under high salt stress conditions [160]. Its genome is 12-13kb and has between 5200-5600 protein coding genes [54]. The cell wall composition of *C. auris* is similar to *C. albicans* but the content of chitin is relatively higher in *C. auris* than *C. albicans* [161]. *C. auris* is an evolving pandrug-tolerant yeast species, which has gained significant attention in recent years because of its capability to afflict severe infections, particularly in healthcare settings [47]. A hypothesis suggests that global warming triggered the transformation of an environmental ancestor into a pathogen via thermal adaptation, which subsequently disseminated *C. auris* across the world through an intermediate host [162]. *C. auris* infections are perplexing to detect and treat, and they have been associated with high mortality rates [62]. Genomic analysis has revealed that *C. auris* is a genetically diverse species, with multiple clades (clades 1-5) [163]. These clades show geographic specificity (Clade 1: South Asia, Clade 2: East Asia, Clade 3: Africa, Clade 4: South America, Clade 5: Iran) and possess unique characteristics related to their pathogenesis, antifungal drug resistance, virulence, and biochemical and phenotypic properties [163–165]. Most of the

isolates belonging to the clade 1, 3 and 4 are resistant to fluconazole whereas those belonging to clade 2 usually show susceptibility to azoles and other antifungal drugs [163]. Similarly, the clade 1, 3 and 4 isolates are associated with invasive infections and clade 2 mainly infects ears [166]. A recent study has reported that in the silkworm model the isolates belonging to clade 4 had higher virulence and mortality rates in comparison to other clades [167]. The clade II isolates' genomes exhibit significant rearrangements, lack substantial subtelomeric regions which contain conserved cell wall proteins found in all other clades and have translocations nearby GC-deficient regions [166]. Isolates from clade 3 exhibit a greater tendency to form large aggregates and can assimilate L-rhamnose compared to isolates from other clades [165,168]. On the other hand, clade 1 isolates show a significant occurrence of pronounced pseudohyphae formation [165]. Data regarding the fifth clade is limited at the moment but so far clade 5 isolates have shown resistance to fluconazole, and utilize L-rhamnose like the clade 3 [163,166]. Furthermore, the genome of clade 5 shows a high degree of synteny in clades 1, 3 and 4, despite having a significantly different sequence compared to the other clades [166].

The proper and timely determination of *C. auris* infections is vital for efficacious management and infection regulation. Conventional laboratory methods, such as culture, assimilation tests, microscopy and enzyme colorimetric assays, are often inadequate for its identification [168]. Initially, existing yeast identification systems mistakenly identified *C. auris* as *Rhodotorula glutinis*, and *Candida haemulonii*, a closely related fungi to *C. auris* [169,170]. However, diagnostic methods for characterizing *C. auris* have significantly advanced in the previous decade. Molecular techniques, such as real-time polymerase chain reaction and multiplex PCR of internal transcribed spacer region, D1/D2 region and glycosylphosphatidylinositol-modified protein-encoding gene have been employed for *C. auris* detection [171–173]. FDA has approved MALDI-TOF mass spectrometry for the detection of *C. auris* [174]. Biochemistry-based detection platforms like using the VITEK 2 system can detect, some but not all, *C. auris* so it is recommended to send the isolates for further identification at reference labs [68]. Recently, CHROMagar™ Candida Plus media has been developed, which can be employed for the presumptive detection of *C. auris* [159].

C. auris has been reported in numerous countries across the globe, including the United States, Portugal, South Africa, Spain, Qatar, Italy, United Kingdom, India, and several others [175]. The exact prevalence is challenging to determine due to inconsistent surveillance systems and underreporting. However, *C. auris* has been responsible for outbreaks in

healthcare facilities, particularly in intensive care units and long-term care settings [47,52,56]. *C. auris* could transmit from person-to-person or contact with contaminated surfaces, equipments and medical devices; and inflict a myriad of infections, for example eye and ear infections, central nervous system infections, bone infections, wound infections, internal organs and bloodstream infections [50,53]. These infections can be severe and difficult to treat, particularly in patients with underlying health conditions or weakened immune systems [69]. In some cases, *C. auris* infections can lead to death; mortality rate ranging between 30-60% [56,70–72]. The risk factors of *C. auris* infection include tracheostomy, indwelling catheter/device, admission to intensive care units, recent surgery, immunosuppression, use of broad-spectrum antibiotics, presence of comorbidities like diabetes, and chronic kidney disease [70,160].

The exact mechanisms of *C. auris* pathogenesis are still under investigation. However, several factors contribute to its virulence which are mostly similar to *C. albicans* such as phospholipase, lipase and proteinase activities [176]. They can evade killing being killed by neutrophils and evade innate immune response [72,160]. Moreover, *C. auris* can evade interleukin-17 mediated skin clearance and persist for prolonged periods in deep skin tissues [177]. It can induce cytokine synthesis and can be phagocyted by human peripheral blood-derived macrophages, in a manner similar to *C. albicans* [161]. Furthermore, *C. auris* produces biofilms which have reduced biomass in comparison to *C. albicans* [176]. Biofilms allow the yeast to adhere to various surfaces, including medical devices and hospital surfaces, enhancing its ability to persist and cause infections [176]. *C. auris* has demonstrated higher tolerance to cell wall stress molecules, oxidative stress, and cationic stress than *C. albicans* [178]. The *HOG1* gene exhibits a significant association in virulence and tolerance to various stresses in *C. auris* [178]. The adhesin genes and *SSK1* gene also play a key role in *C. auris* virulence and stress condition adaptation [179]. *C. auris* also possesses resistance to multiple antifungal agents, including azoles, polyenes, and echinocandins (Figure 2.2) [180,181]. The formation of biofilms can help in developing tolerance to antifungals in *C. auris* [182,183]. This multidrug resistance can also be attributed to specific genetic mutations in genes like *FKS1* and *ERG11* [184,185]. The alterations in drug efflux pumps genes such as *CDR1*, and drug transporter gene like *TAC1B* can further contribute to its resistance [185]. Recently, Rpn4, a transcription factor has been implicated in developing unsusceptibility to fluconazole by inducing the expression of *CDR1* efflux pump [186].

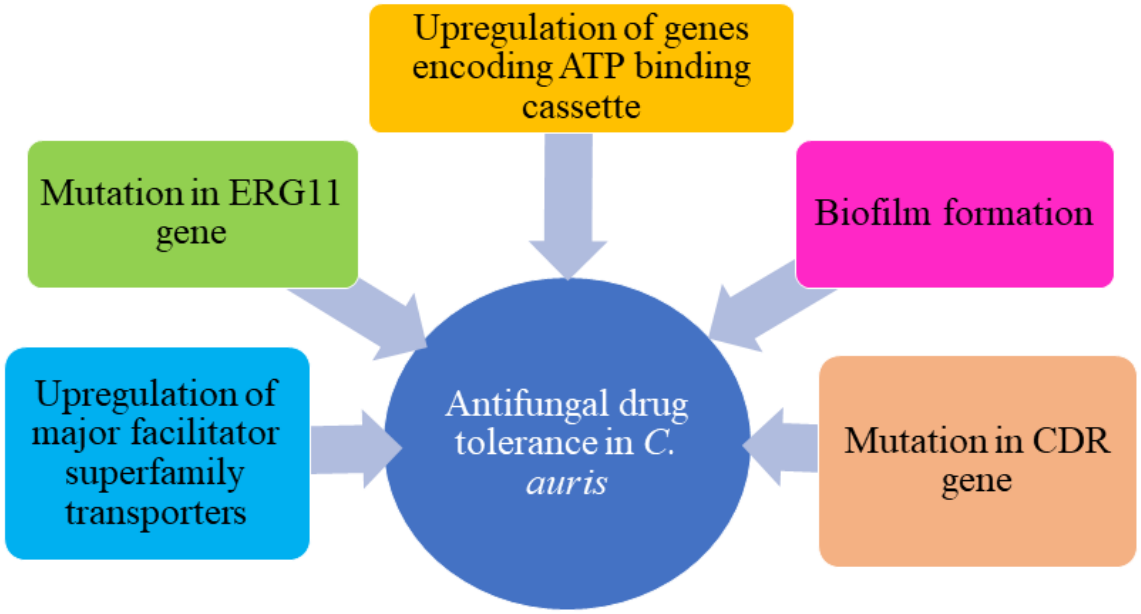

Figure 2.2: Mechanism of antifungal drug tolerance in *C. auris*

The management of *C. auris* infections is challenging due to its multidrug resistance. The selection of antifungal therapy hinges upon the susceptibility profile of the specific strain. In general, echinocandins (such as caspofungin, micafungin, or anidulafungin) are recommended by the CDC as the first-line treatment against invasive infections of *C. auris* [187]. Nevertheless, unsusceptibility to echinocandins has also been described, necessitating alternative treatment options. If the patient does not respond to echinocnadins or suffers from fungemia for more than five days the use of liposomal amphotericin B is recommended [187]. In addition to antifungal therapy, strict infection limitation strategies are crucial to impede the spread of *C. auris* within healthcare settings. These measures include hand hygiene, contact precautions, environmental cleaning, patient isolation, equipment disinfection and adherence to appropriate personal protective equipment (PPE) protocols [160].

2.4 UPR and mRNA degradation pathway

Although the primary UPR pathway was expounded in the 1990s, recent and interesting insights continue to emerge. Investigating the UPR elements in several fungi, including both non-pathogenic and pathogenic species, remains a crucial area of research [188]. Normally, under ER stress the *IRE1* gets activated and splices the mRNA *HAC1* [189]. Studies have shown that apart from splicing the 252 nucleotide intron from the mRNA that produces *HAC1* transcription factor, *IRE1* is also associated with the decay of other mRNA targeted to

the endoplasmic reticulum, ribosomal RNA and the mRNA coding for IRE1 (Figure 3) [189,190]. The *IRE1* uses different methods to cleave the *HAC1* mRNA and other mRNA undergoing decay. *IRE1* subunits engaged in *HAC1* mRNA splicing are present cooperatively in *IRE1* oligomer whereas the *IRE1* performing mRNA decay reside in the monomer or dimer of *IRE1* [191]. It has also been suggested that there is a difference in *IRE1* binding sites for *HAC1* mRNA and mRNA undergoing degradation pathway [191]. The *IRE*-mediated mRNA degradation occurs at cotranslational translocation and requires signal sequences to bring the mRNA close to the ribonuclease domain of *IRE1* for their eventual degradation [190]. The degradation of these mRNA cleaved by *IRE1* has been termed as the regulated *IRE1* dependent decay (RIDD) pathway which is important for maintaining homeostasis inside endoplasmic reticulum by reducing the protein folding load [192].

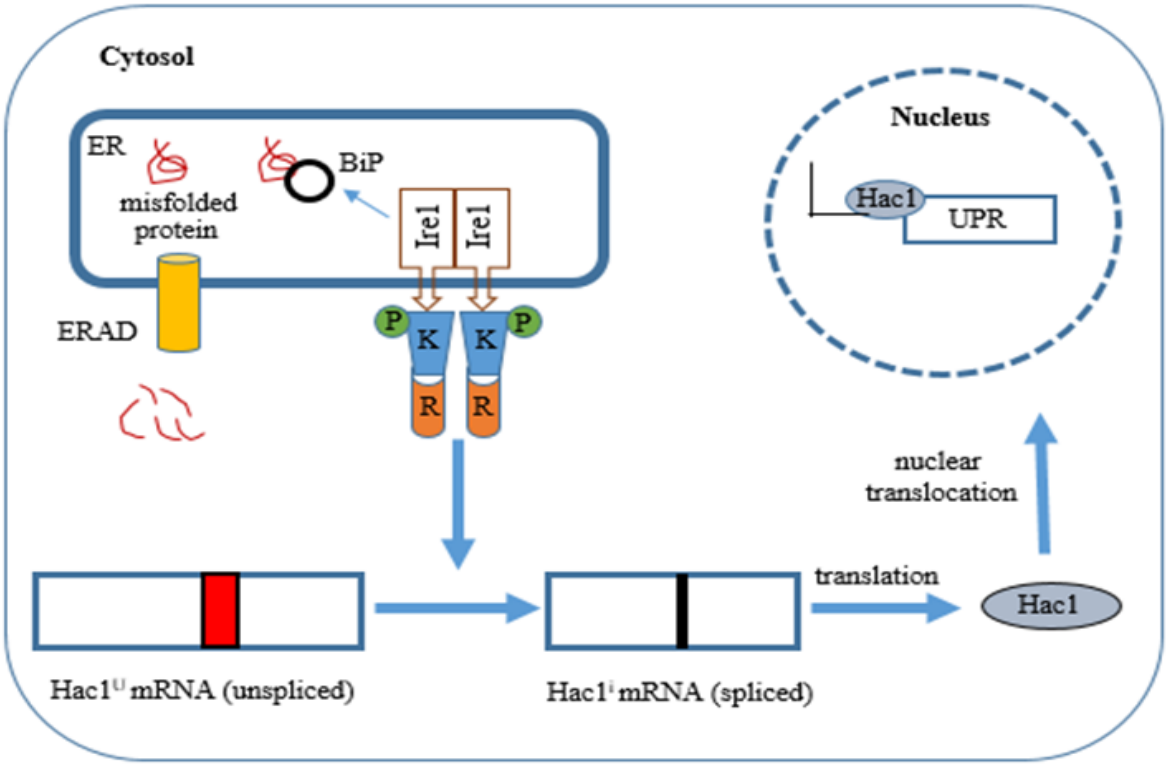

Figure 2.3: UPR pathway activation: The misfolded proteins accumulated due to endoplasmic reticulum stress are sensed by the BiP, a chaperone protein in endoplasmic reticulum, or by direct interaction of Ire1 protein with the misfolded proteins. This leads to the oligomerization of Ire1 protein, which causes its autophosphorylation through the cytoplasmic kinase domain. The autophosphorylation then activates the RNAse domain, which splices the *HAC1* mRNA in the cytoplasm to form a bZIP (basic leucine zipper) transcripton factor Hac1. Hac1 is translocated to the nucleus where it regulates transcription

of several genes such as members of the endoplasmic reticulum-associated degradation pathway, endoplasmic reticulum chaperone proteins, and enzymes involved in post-translational modifications, which will help the cell to tolerate the endoplasmic reticulum stress [193–196].

Only the splicing of *HAC1* mRNA occurs in *Saccharomyces cerevisiae* and there is no mRNA decay. But, in the fission yeast *Saccharomyces pombe* which lacks the *HAC1* ortholog, there is degradation of few other mRNAs which code for endoplasmic reticulum bound proteins. The degradation of these mRNA reduces the protein flux by 15% which helps to mitigate the ER stress in *S. pombe* [197] These mRNAs are cleaved by *IRE1* at UGC consensus sequence between G and C nucleotide to induce the mRNA decay [192]. However, in *S. pombe* despite the degradation of Bip1 mRNA by *IRE1*, the mRNA avoids the decay [197]. For the mRNA decay, *IRE1* also requires the activity of cellular exoribonucleases and exosomes with Ski complex (exosome/Ski) in the 5'-3' direction and 3'-5' direction respectively [192,197]. After the cleavage of mRNA sequence, the associated ribosomes are arrested at the end of the mRNA because the *IRE1* cleavage sites are within the coding sequence. Usually, the ribosomes associated with mRNA are separated when they reach a stop codon. But in the mRNA severed by the *IRE1*, the ribosomes do not reach to stop signal and hence have to be rescued by the "no go decay pathway" for the reuse of these stalled ribosomes in the translation of other mRNA [192]. To rescue the stalled ribosomes Dom34/Hbs1, Rli1 and an unidentified endonuclease referred as NGDase and exosome/Ski play an important role. NGDase cleaves the mRNA 1 or 2 nucleotides upstream of the stalled ribosome inside the channel from where mRNA exits the ribosome, Dom34/Hbs1 recycles the ribosome and exosome/Ski degrades the fragment of RNA [192].

2.5 Intricate link between fungal pathogenesis and UPR

UPR plays a vital role in attenuating then ER stress (Table 2.1). However, there is a plethora of evidences suggesting their role in the pathogenesis of different fungi [188]. The UPR pathway aids fungi in resistance to temperature, nutrient acquisition, biofilm formation, resistance to cell wall disruptors and antifungal agents, hyphal growth, melanin synthesis and capsule formation. These properties significantly contribute to the pathogenesis of different fungi. Other proteins involved in pathways other than canonical UPR pathway also activate the UPR and help in the virulence of *C. albicans* [198,199]. The role of other proteins in UPR activation and pathogenesis is yet to be explored in other pathogenic fungi. The recent

evidence showing the role of UPR in pathogenesis of *C. parapsilosis*, *C. neoformans*, *Cryptococcus deneoformans*, *Cryptococcus deuterogatti*, *C. albicans*, *C. glabrata* and *A. fumigatus* has been discussed in the following sections.

Table 2.1: Unfolded protein response pathway elements in different pathogenic fungi and their characteristics

Fungi	***IRE1* gene size**	***HAC1/HXL* gene size**	**Intron size**	**Functional significance or drug susceptibility**	**References**
S. cerevisiae	3348bp	969bp	252bp	Regulation of unfolded protein response, and transcription in meiosis	[84,193,200]
C. albicans	3672bp	1123bp	19bp	Pathogenesis and virulence, antifungal tolerance, regulation of proteins involved in cell wall synthesis, UPR activation	[84,200,201]
C. tropicalis	NA	912	19bp	NA	[200]
C. dubliniensis	3669bp	1098bp	22bp	NA	[200]
C. glabrata	3111bp	990bp	379	no role of *HAC1* and *IRE1* in antifungal susceptibility, no role of *IRE1* in maintaining cell wall integrity, IRE1 may be important for virulence, IRE1 is only related to governing endoplasmic stress	[83,84,200,202]
C. parapsilosis	3573bp	1158bp	626bp	Maintaining cell wall integrity, ketoconazole	[203]

				tolerance, endoplasmic stress tolerance	
Aspergillus fumigatus.	3498p	1359bp	20bp	endoplasmic stress tolerance, virulence, antifungal drug tolerance, nutrient acquisition	[84,200,204]
Cryptococcus species	3514bp	1137bp	56bp (HXL gene)	Helps in survival at body temperature, endoplasmic stress tolerance, resistance to azoles	[205–207]

2.5.1 Cryptococcus species

The unfolded protein response is important for the pathogenicity of *C. neoformans* and *Cryptococcus gatti*. In immunocompromised individuals, *C. neoformans* reaches to the brain via pulmonary route and causes lethal meningoencephalitis and also cause diseases of the lung and skin [205,208]. *C. gatti* causes diseases of the respiratory system and central nervous system in both healthy and immunocompromised animals and humans [205,209]. In both of these species, the activation of UPR is necessary for the resistance to ER stress and cell wall unstabilizing molecules [205]. They utilise *IRE1*-dependent activation of UPR to mediate ER stress. However, instead of *HAC1* transcription factor the *Cryptococcus sp.* use HXL1 protein, a phylogenetically distant protein of yeast *S. cerevisiae* to activate UPR [84]. *C deneoformans* and *C. neoformans* with disrupted *HXL1* and *IRE1* genes have shown severe growth defects at mammalian body temperature. Also in *C. deuterogatti* the role of UPR pathway in helping the fungi survive at 37°C has been seen [205]. However, in C. *deuterogatti* despite the disruption of *HXL1* gene the fungi showed increased level of thermotolerance at 37°C and 39°C suggesting that the *HXL1* has a minor role in thermotolerance [205]. These studies show the importance of the UPR pathway in providing thermotolerance in pathogenic *Cryptococcus* fungi. The UPR also plays vital role in the resistance to azole drugs in pathogenic *Cryptococcus* fungi. The disruption of *HXL1* and *IRE1* in *C. neoformans* makes it more susceptible to azole drugs [206]. *C. deuterogatti* with disrupted *IRE1* and *HXL1* genes also showed growth defects upon treatment with different

azole drugs [205]. The disruption of *IRE1* makes *C. deuterogatti* more susceptible to azoles whereas in *C. neoformans* the deletion of *HXL1* makes it more sensitive to azole drugs [205]. Melanin synthesis, phospholipase activity, capsule formation and extracellular vesicles are important for the virulence of the pathogenic *Cryptococcus* fungi [210,211]. In both *C. neoformans* and *C. deuterogatti* the disruption of *IRE1*, but not *HXL1* disruption, caused delayed synthesis of melanin. The UPR pathway does not play a major role in the capsule formation in *Cryptococcus* species [205]. Mice models of systemic cryptococcosis when infected with *C. deuterogatti* mutants with deleted *IRE1* and *HXL1* did not cause disease in the mice [205]. These studies show that the UPR elements in *Cryptococcus* species are linked with several factors such as melanin synthesis, antifungal drug unsusceptibility, thermotolerance and maintaining the infection in mice and insect models. Thus, implying the importance of the UPR components in the pathogenesis of *Cryptococcus* species.

2.5.2 Candida parapsilosis

C. parapsilosis is an important non-albicans *Candida sp*., and is the second most commonly isolated *Candida sp*. in South America, South Europe and Asia [212]. Research by Iracane et al has shown the possible activity of UPR in mediating the pathogenesis of *C. parapsilosis* [85]. The deletion of *HAC1* caused the fungi to be more sensitive to calcoflour white, congo red and antifungal drug ketoconazole [85]. Congo red and calcofluor white disrupt the synthesis of glucan, a crucial component of the fungal cell wall. Ketoconazole affects the synthesis of ergosterol which is an integral part of the fungal cell membrane [213]. The study suggests the significance of *HAC1* in conserving the integrity of cell membrane and cell wall in *C. parapsilosis*. The integrity of the cell wall is vital for growth, formation of hyphae, division and resistance to antifungal drugs. These factors are indispensable for the fungi to maintain the pathogenesis and sustained infection. Thus, the study corroborates the role of UPR element *HAC1* in sustaining the pathogenicity of *C. parapsilosis* and can be targeted for developing antifungal drugs against both the resistant and sensitive strains of pathogenic fungi *C. parapsilosis.*

2.5.3 Candida albicans

In *C. albicans* the canonical *IRE1*- HAC1 pathway mediates the ER stress [84]. As reviewed by Krishnan and Askew UPR pathway plays a key part in pathogenesis of *C. albicans* by helping in the transition of yeast form to pathogenic hyphal form and regulating expression of proteins pertaining to the biosynthesis of cell wall and adhesion [84]. The deletion of *IRE1*

gene in *C. albicans* has made the fungi susceptible to antifungal compound caspofungin suggesting the role of UPR in their pathogenesis [214]. Another study has shown the significance of IRE1 in maintaining cell wall integrity, adaptation to low iron stress, and biofilm development [201], Not only the proteins involved in the canonical pathway *IRE1-HAC1* pathway cause pathogenesis of *C. albicans* but proteins involved in other pathways that activate UPR also play significant role in *C. albicans* virulence. A study has shown that stress-associated endoplasmic reticulum protein 1 (SERP1) which is activated by endoplasmic reticulum stress and autophagy-related protein 8 (Atg8) are associated with unfolded protein response and virulence [198]. Li et al deleted both the SERP1 also known as Ysy6 and Atg8 genes and showed that their deletion caused a reduction in the *HAC1* mRNA splicing and UPR activation. They also showed that the double deletion caused the virulence loss and made *C. albicans* sensitive to tunicamycin. Both SERP1 and Atg8 are important for maintaining the mitochondrial function during endoplasmic reticulum stress [198]. This study shows that apart from *HAC1* transcription factor, *SERP1* and Atg8 synergistically could have a key part in the activation of UPR pathway. Msb2 a signaling protein involved in the regulation of environmental stress is also associated with the activation of UPR pathway [199]. Saraswat et al described that the Msb2 protein is associated with the expression of UPR pathway regulators like *IRE1* and *HAC1* and has a crucial role in the survival and hyphae formation of *C. albicans* at 42^0C [199]. *RTA2*, an effector of the calcineurin pathway is important for regulating the *HAC1* mediated UPR activation under ER stress [215]. These studies reveal that Serp1, Atg8 and Msb2 are important for activation of UPR pathway and also have a significant role in the virulence of *C. albicans*. These proteins involved in UPR pathway can be target for novel antifungal drugs. These studies also show that not only the canonical *IRE1-HAC1* pathway play role in the UPR activation but proteins involved in other pathways like calcineurin pathway and environmental stress are also involved in the UPR activation and *C. albicans* virulence.

2.5.4 Candida glabrata

C. glabrata is devoid of the canonical *IRE1-HAC1* dependent signalling for the activation of UPR. The *IRE1* of *C. glabrata* does not splice the *HAC1* mRNA during ER stress showing the UPR activation by *IRE1* is independent of *HAC1* but possesses the RIDD pathway mediated by *IRE1* which might alleviate the ER stress [83]. Similar to *C. albicans* the ER stress in *C. glabrata* is also co-ordinately mediated by crosstalk among *IRE1* and other signalling pathways like calcineurin pathway and Slt2 MAPK pathway [83]. But, there is no

role of *HAC1* and *IRE1* in antifungal susceptibility and also there is no part of *IRE1* in maintaining integrity of the cell wall in *C. glabrata*. However, the *IRE1* deletion reduced the *C. glabrata* virulence in the mice models of systemic *C. glabrata* infection [83,202]. *HAC1* is not necessary for the ER stress response and virulence in *C. glabrata* [83]. These studies show that there is no direct involvement of the canonical *HAC1-IRE1* pathway in mediating ER stress but the UPR element *IRE* might exert a crucial role in the *C. glabrata* virulence.

2.5.5 Aspergillus fumigatus

A. fumigatus uses the canonical *IRE1-HAC1* facilitated UPR pathway to attenuate the ER stress. However, it also uses the UPR pathway under normal conditions to regulate the expression of about 10% of its total genome [216]. In *A. fumigatus* there is absence of RIDD pathway but the ERAD pathway is present. The cell wall integrity pathway and UPR coexist and are affected reciprocally [217]. Other than alleviating the ER stress the UPR and ERAD pathways are also involved in maintaining the virulence of *A. fumigatus* [84]. The disruption of *HAC1* in *A. fumigatus* yielded the fungi sensitive to cell wall-disrupting antifungal agents and reduced the virulence in mice models of aspergillosis [204]. The *HAC1* deletion also made the fungi sensitive to heat by inhibiting the growth of young hyphae at 45^0C and reduced the secretion of proteolytic enzymes necessary for the nutrition uptake [204]. Thermotolerance, secretion of proteases, resistance to antifungal drugs and cell wall disruptors are important for the virulence of *A. fumigatus*. Along with UPR, ERAD another mechanism to alleviate ER stress also exhibits a major part in the virulence of *A. fumigatus*. The ERAD elements HrdA and DerA help to mitigate ER stress but not in the virulence of the fungi. But when the ERAD elements and UPR element HacA were deleted there was inhibition of protease secretion, hyphal growth, and made the fungi sensitive to antifungal drugs [84,218]. These studies show that UPR can have a key role in the pathogenesis of *A. fumigatus*.

2.6 Targeting UPR pathway-Reducing Fungal infections

Resistance to azole in *A. fumigatus,* echinocandins in *C. glabrata*, and unsusceptibility to fluconazole in non-*albicans Candida* species have been reported and pose a serious clinical threat that has to be mitigated. Currently, there are several antifungal compounds under study which can overcome the antifungal resistance in pathogenic fungi and help in controlling the fungal infections [219]. A novel strategy can be identifying compounds that can target the UPR pathway. As discussed in the earlier sections of the review of literature section, the UPR

elements like *IRE1*, *HAC1* and other proteins that activate the UPR have been implicated in the pathogenesis of *C. albicans*, *C. parapsilosis*, *C. glabrata*, *C. neoformans*, *C. deneoformans*, *C. deuterogatti*, and *A. fumigatus*. The deletion of the genes associated with UPR pathway has affected the virulence, pathogenesis and drug-resistant abilities of various human fungal pathogens (Figure 2.4) [84]. The association of the UPR in fungal pathogenesis opens a new avenue to combat fungal diseases and the antifungal agent unsusceptibility in pathogenic fungi. Furthermore, the conservation of the *IRE1-HAC1* reliant UPR-pathway in various fungal pathogens indicates that this pathway could be utilized for the generation of broad-spectrum antifungal medications. Various novel strategies should be developed to target the UPR elements and other elements that help in the activation of UPR under ER stress.

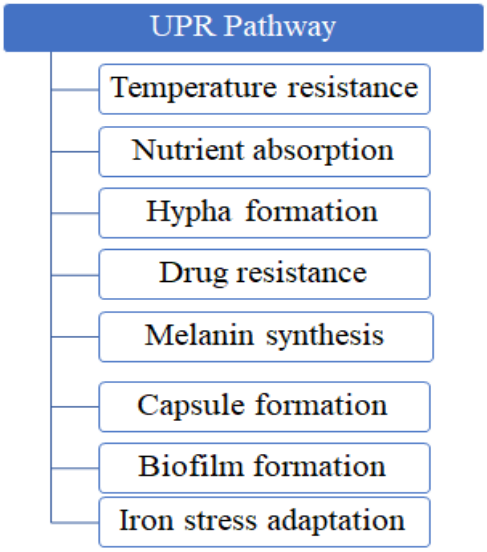

Figure 2.4: Role of UPR elements in fungal virulence and pathogenesis

2.7. Importance of phytochemicals in the treatment of fungal infections

Phytochemicals, also known as plant chemicals, are natural compounds found in plants that play a significant role in their defence against various pathogens, including fungi [78]. Phytochemicals have been extensively studied for their antifungal properties, and their potential use in the treatment of fungal infections is a growing area of interest in modern medicine [220].

Fungal diseases are one of the major health issues across the world, and conventional antifungal drugs are often associated with side effects and the evolution of drug unsusceptible

strains [221]. Therefore, there is an urgent need for alternative and complementary therapies for managing fungal infections. Phytochemicals have been described to possess antifungal activities against a multitude of fungal pathogens, including *C. albicans, A. fumigatus*, and *C. neoformans* (Figure 2.5, Table 2.2) [78,222]. As part of the thesis, a review paper has been published comprehensively discussing the role of different classes of phytochemicals along with compounds from different bacteria and fungi as potential antifungal drugs [78].

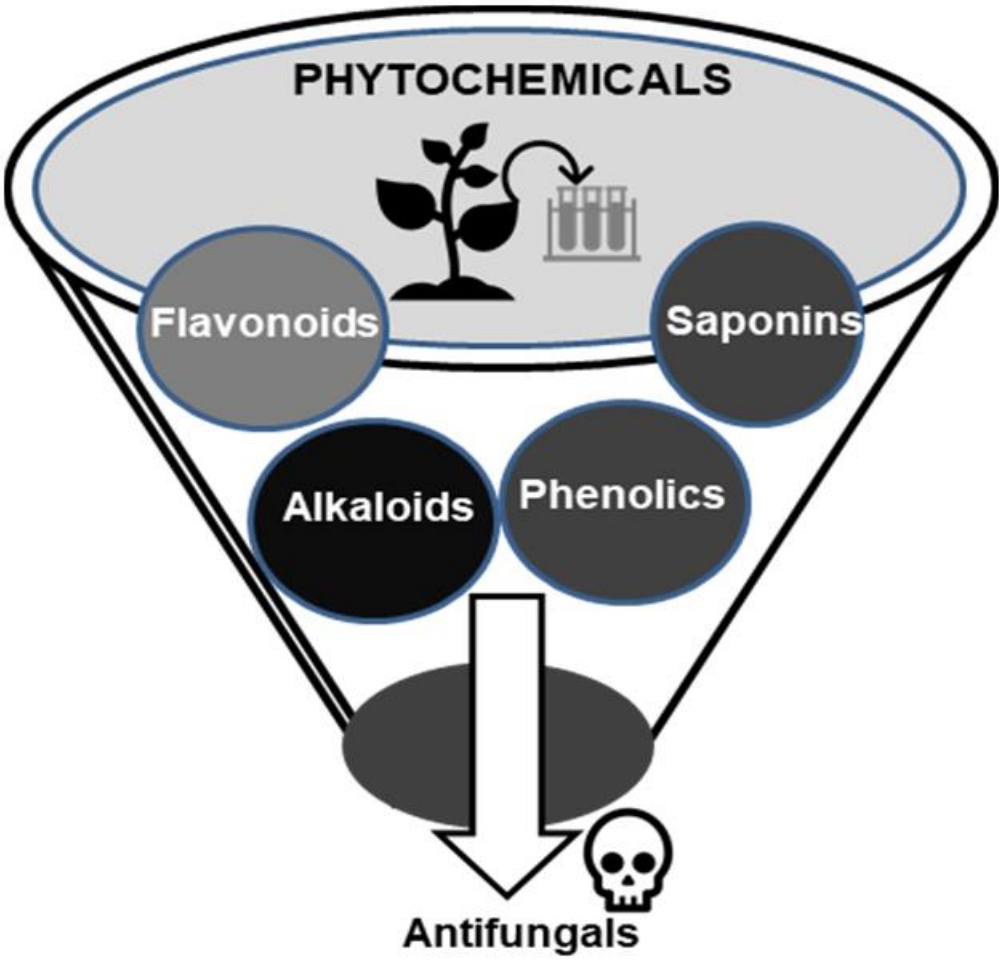

Figure 2.5: Phytochemicals as potential sources of antifungal drugs

One of the very comprehensively analyzed classes of phytochemicals with antifungal properties is polyphenols. Polyphenols are plant secondary metabolites found in a wide range of fruits, vegetables, and medicinal plants. They have been described to limit fungal growth by destabilizing fungal cell walls, interfering with fungal DNA replication, plasma membrane disruption and inhibiting fungal enzymes (cytochrome P450 monooxygenase, 1,3-β-glucan lysase and isocitrate lyase) [223,224].

Table 2.2: Antifungal property of various classes of phytochemicals

Class of phytochemicals	**Name of phytochemicals/secondary metabolites**	**Source plant**	**Targeted fungi**	**References**
Alkaloids	Tetrandrine	*Stephaniae tetrandrae*	*C. albicans*	[225]
	Tryptanthrin	*Polygonum tinctorium*	*C. neoformans, C. krusei, C. albicans*	[226]
	Pellitorine	*Zanthoxylum zanthoxyloides*	*A. fumigatus, Rhizopus sp.*	[227]
	Anagyrine, ammodendrine, and sparteine	*Retama monosperma*	*Aspergillus niger, C. albicans*	[228]
Flavonoids	8-prenylpinocembrin	*Dalea elegans*	*C. albicans*	[35]
	Myricetin	*Plinia cauliflora*	*Trichophyton rubrum, C. krusei*	[229]
	Nictoflorin, rutin	*Cirsium hypoleucum*	*C. krusei*	[230]
	Naringin	*Coffea arabica*	*A. fumigatus*	[231]
	Quercetin	*Senna siamea*	*C. albicans*	[232]

Lignan	Sesamin	*Sesamum indicum*	*C. glabrata, C. parapsilosis, C. albicans, C. krusei*	[233]
Phenolic acids	Gallic acid, catechin,	*Cistus ladanifer*	*C. glabrata, C. parapsilosis, C. albicans*	[234,235]
	Protocatechuic acid, caffeic acid, dihydroxyphenylacetic acid	*Ferocactus species*	*Aspergillus sp.*	[236]
Saponins	Kaikasaponin	*Desmodium salicifolium*	*C. glabrata*	[237]
	Anagallisin	*Anagallis arevnsis*	*C. albicans*	[238]
	Glinusopposide	*Glinus oppositifolius*	*Microsporum gypseum, T. rubrum*	[239]
	Hostaside	*Hosta plantaginea*	*C. albicans*	[240]

Flavonoids, a subclass of polyphenols, have been found to possess antifungal properties against a wide range of human pathogenic fungi. For example, the flavonoid quercetin has been described to repress the growth of *C. albicans, C. neoformans*, and *A. fumigatus* by disrupting the fungal cell wall, downregulation of fatty acid synthesis genes and interfering with fungal DNA replication [229,230,241]. Similarly, the flavonoid kaempferol has been reported to possess antifungal activities against *C. albicans* and *A. fumigatus* [242].

Terpenoids, another class of phytochemicals, have also been found to possess antifungal properties. Terpenoids are natural compounds found in plants, and they have been described to suppress fungal growth by destabilizing the fungal cell membranes, inducing Ca2+/Calcineurin pathway-associated apoptosis and interfering with fungal enzymes [243–245]. For example, the terpenoid carvacrol, found in essential oils of oregano and thyme, has been reported to possess antifungal properties against *C. albicans, A. fumigatus* and *C. neoformans* [245,246].

In addition to polyphenols and terpenoids, other classes of phytochemicals, such as alkaloids and saponins, have also been found to possess antifungal properties. Alkaloids are naturally occurring nitrogen-containing compounds found in plants, and they have been described to repress fungal growth through interference with fungal enzymes like DNA topoisomerase, and disruption of the iron-sulfur cluster biosynthesis [228,247,248]. Saponins are glycosides found in a wide range of plants, and they have been shown to possess antifungal activity by disrupting fungal cell membranes [249–251].

In conclusion, phytochemicals are a promising source of natural antifungal agents that can be used in the cure and control of human fungal diseases. Phytochemicals have been shown to possess antifungal properties against myriad of pathogenic fungi, and their use as complementary and alternative therapies for managing fungal diseases is an area of active research. Further studies are needed to examine the safety and effectiveness of phytochemicals in the treatment of fungal infections, but their potential as natural antifungal agents is certainly worth exploring.

2.8 Possibilities of natural products for C. auris treatment

Various reports of *C. auris* isolates have been described which are resistant to all the 3 major antifungal classes: polyenes, echinocandins, and azole [53,54]. Recently, *C. auris resistant* to flucytosine, another class of antifungal drug, has also been reported [252]. Moreover, the low bioavailability of the currently available antifungal drugs also hinders the course of *C. auris* infection treatment [221]. Due to the concerns of the evolution of pan-resistant *C. auris* isolates [253], side effects and low bioavailability of existing antifungals the search for novel, effective and safe antifungal drugs to treat *C. auris* infections is imperative. Phytochemicals could be one of the major sources of a novel class of antifungal drugs. Plants and plant-based products have been used for a long time in Chinese traditional medicine and Ayurveda.

Plethora of plant metabolites have shown antifungal properties against different yeast and filamentous fungi [78]. Other than phytochemicals, various peptides, essential oils and microbial metabolites could also be potential antifungal agents against *C. auris* (Table 2.3).

Previously various studies have been conducted to identify compounds such as carvacrol, palmatine, berberine, ceragenin, Cm-p5 peptide, silver nanoparticles, and bis-benzodioxolylindolinone, that could inhibit the growth of *C. auris* [254–257,257,258]. Various phytochemicals that have inhibited *C. auris* growth are listed in Table. Furthermore, drugs that could inhibit *C. auris* growth such as Fosmanogepix, MGCD290 and Ibrexafungerp have reached clinical trial stage [86–89].

Table 2.3: Antifungal property of various phytochemicals against *C. auris*

Phytochemical	**Mechanism**	**References**
6-shogaol (extracted from *Zingiber officinale)*	Downregulation of efflux pump-related *CDR1* gene, reduction of aspartyl proteinase level	[259]
Farnesol	Affects transcription of genes associated with fatty acid metabolism. intracellular metal ion contents, and growth	[260]
essential oil from *Lavandula angustifolia*	Affects expression of biofilm associated genes	[261]
Caffeic acid and ellagic acid	Modification of fungal cell wall	[262]
Myrtenol	Downregulation of *ERG1*1, *FKS1* and *ALS5* genes	[263]
Essential oil from leaves and bark of *Cinnamomum zeylanicum*	Disruption of cell membrane	[264]

fluconazole in combination with *C. zeylanicum* essential oil	Reduction of the ATPases activity	[265]
Oil from *Withania somnifera* seed	Targeting cell membrane and cell wall	[266]
Dehydrocurvularin (extracted from *Curvularia aeria*, a marine fungus)	Downregulation of genes associated with hyphal morphogenesis and adhesion to epitherlial cells	[267]
Penta- O-galloyl-β-d-Glucose	Iron chelation	[268]
Geraniol	Biofilm formation inhibition, ergosterol synthesis inhibition and imparing the activity of efflux pump	[269]
Chitosan	Not available (NA)	[270]
Gallic acid	NA	[79]
Rubiginosin C	NA	[271]
Medical grade honey	NA	[272]
diterpenediol 8(14),15-sandaracopimaradiene-7alpha,18-diol (extracted from *Tetradenia riparia*)	NA	[273]
Hakuhybotrol (extracted from *Hypomyces*	NA	[274]

pseudocorticiicola, a mycoparasictic fungi)		
Piper nigrum extract	NA	[275]
Crotamine (peptide from rattlesnake)	NA	[276]
Essential oils from cinnamon bark, lemongrass and clove bud	NA	[277]
Freshwater snail *Pomacea poeyana* peptides	NA	[278]
Leaf extract of *Syzygium samarangense*	NA	[279]

Research Gaps

I. Function of unfolded protein response elements, *HAC1* and *IRE1*, in *C. auris* pathogenesis is yet to be discovered.

II. As, *C. auris* exhibits resistance to most of the major classes of antifungal drugs, there is demand for novel antifungal drug. So, study about developing new drug based on phytochemicals as drug molecule against *C. auris* infection is to be studied.

III. Despite multiple attempts, no fungal vaccine has been approved. Immunoinformatics could be an interesting approach which could help in developing fungal vaccine. Hence, there is need of novek strategies to develop vaccine against pathogenic fungi such as *C. auris*.

OBJECTIVES

I. Collection of clinical isolates of *Candida* spp. and to study multi-drug resistance profile of those isolates.

II. Disruption and cloning of *HAC1* gene of *C. auris* and to study its role in the virulence and unfolded protein response pathway.

III. *In-silico* identification of small molecules targeting unfolded protein response proteins (*HAC1* and *IRE1*) of *C. auris*.

IV. To test the efficacy and safety of small molecules or its compounds in controlling *C. auris* infection and its mechanism thereof.

V. To develop a potent multivalent epitope based vaccine against *C. auris* using *in-silico* approach.

Materials and Methods

Table 4.1: Media composition

Media for fungal growth	**Composition**
HiChrome *Candida* differential agar media (HCCDA)	Chloramphenicol (0.05%), Yeast extract (0.4%), Chromogenic mix (0.72%), Agar (1.5%), Peptone (1.5%), Dipotassium hydrogen phosphate (0.1%)
Sabouraud dextrose broth (SD broth)	Peptone (1%), Dextrose (2%)
YPD media	Yeast extract (1%), Dextrose (2%), Peptone (2%)
Media for bacterial growth	
Luria broth	Sodium chloride (0.5%), Yeast extract (0.5%), Tryptone (1%),
SOC media	NaCl (0.05%), Glucose (0.36%), Yeast extract (0.5%), Tryptone (2%), Potassium chloride (2.5mM), Magnesium chloride (10mM)

Objective 1: Collection of clinical isolates of *Candida* spp. and to study multi-drug resistance profile of those isolates

4.1.1 Collection of Candida species and their identification

Blood samples were isolated from patients who have cancer and diabetes with their written consent by nurses from the Punjab Institute of Medical Sciences (PIMS), Jalandhar, Punjab, India (Ethical committee approval PIMS/DP/Gen.163/6085). Malignancies and diabetes are risk factors for *C. auris* infection and the patients suffering from cancer and diabetes are immunocompromised. Hence, samples from these patients are collected as per the protocol [280,281]. The identification of the fungal species was made by observing the colour of the colonies on HiChrome *Candida* differential agar media (HCCDA) (HiMedia, India, Catalogue number M1297A, Table 4.1). For the HCCDA analysis, 100 µl of blood samples were spread plated on HiChrome agar and then the plates were kept in the incubator for 48 hours at 35°C. Followed by the incubation, the colours of the colonies formed on the plates were observed and the *Candida* species were identified by following the manual provided by

the manufacturer of the HCCDA media. Furthermore, the identity of the *Candida* species isolated from the blood samples was also confirmed using HiCandida Identification (HCI, Catalogue number: KB006) kit manufactured by HiMedia Laboratories, India. The HCI kit identifies different *Candida* species on the basis of their ability to utilize 11 different carbohydrate substrates like trehalose, raffinose, dulcitol, xylose, inositol, cellobiose, galactose, sucrose, maltose, lactose and melibiose; and synthesize urease. The determination of the *Candida* species using the HCI kit was done by following the user guidelines provided by the manufacturer. In brief, the inoculation was prepared by growing single colonies of *Candida* species in yeast extract-peptone-dextrose broth (YPDB) for 6 hours. Then, the absorbance of the cells was adjusted to 0.5 OD at 600nm wavelength. After that, the 50µl of the inoculum was pipetted on each of the wells in the kit. Following, this the kits were incubated at 25^0C for 48 hours. The outcomes were inferred by following the identification index in the manual provided by the manufacturer. Furthermore, different *Candida* species clinical isolates were also obtained from NCCPF "(National Culture Collection of Pathogenic Fungi), Chandigarh, India". The confirmation of the NCCPF isolates was also done using the HCCDA and HCI kit as per the methods discussed above.

4.1.2. Drug resistance profile of Candida isolates

The drug resistance profile of the *Candida* species were done by following the guidelines issued by "European Committee on Antimicrobial Susceptibility Testing (EUCAST definitive document E.DEF 7.3.1)" for yeasts with modifications [282]. The susceptibilities of the isolates of the *Candida* species were assessed against fluconazole and amphotericin B in triplicates. Fluconazole (Catalogue number: 22239) and amphotericin B (Catalogue number: 54713) were purchased from Sisco Research Laboratories, India. The stock solution of fluconazole was diluted in the SDB media to obtain concentrations in the range between 0.25-128 µg/mL. Similarly, the stock solution of amphotericin B was diluted in SDB to obtain concentrations between 0.031-16 µg/mL. Then, 100 µL of the SDB were added to respective wells in 96 well microtiter plates. After, that 100 µL (2x concentration) of either fluconazole or amphotericin B was added to the first well and mixed with SDB to obtain the highest test concentration (Figure 4.1).

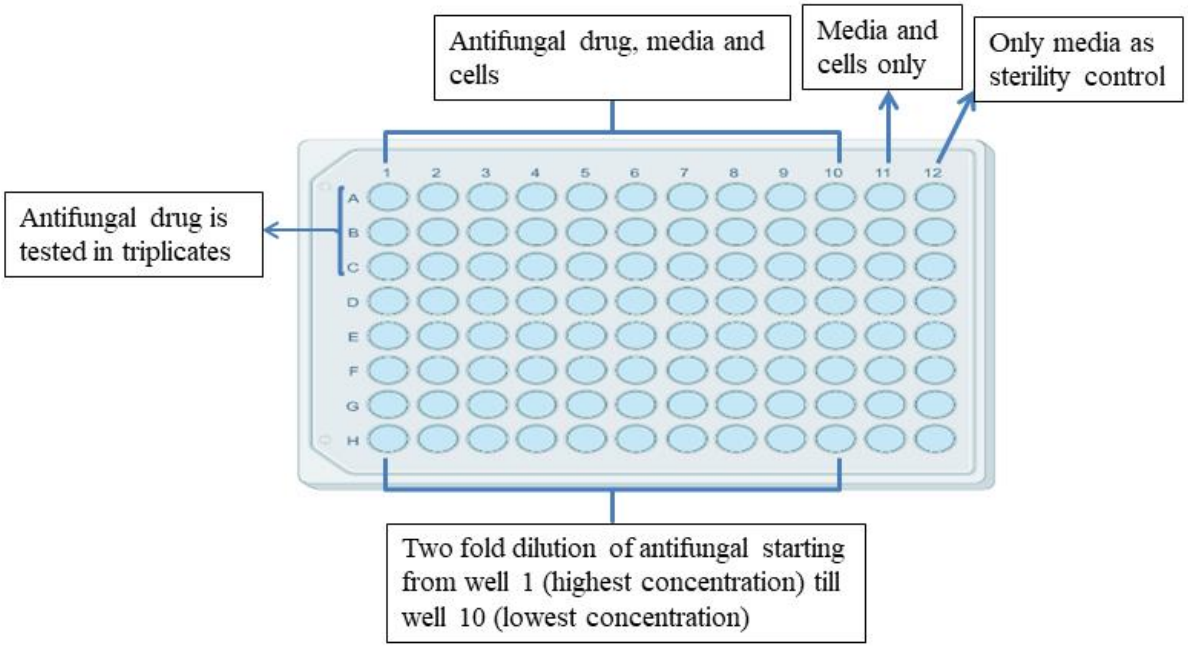

Figure 4.1: MIC assay scheme against *Candida* isolates

Then, 100 µL of SDB and drug mix were added to the second well to obtain two-fold dilution. The two-fold dilution was done till the 10^{th} well and 100 µL SDB and compound mix were discarded from the 10^{th} well to maintain equal volume (100 µL) in each well. 11^{th} well only contained media and *Candida* cells whereas the 12^{th} well was used as sterility control (only contained 100 µL of SDB). The inoculum size was $0.5x10^4$ CFU/mL. Then, the microtiter plate was kept in an incubator at 37°C for 24 hours without agitation. Afterwards the incubation, the MIC (50%) was determined by measuring the absorbance at 530nm. The MIC 50% was determined by the formula:

$$MIC\ (\%) = \{(Abs_c - Abs_s)/Abs_c\} x100$$

Where Abs_c= Absorbance of well-containing media and cells

Abs_s= Absorbance of well-containing media, drug and cells

Objective 2: Disruption and cloning of *HAC1* gene of *C. auris* and to study its role in the virulence and unfolded protein response pathway

4.2.1. Bioinformatics analysis of the determination of intron and cleavage sites of C. auris HAC1

The sequences of *HAC1* genes of different fungi were obtained from "Candida Genome Database (CGD), Saccharomyces Genome Database (SGD)" or GenBank. The accession numbers of the *HAC1* genes are provided in Table 4.2. The phylogenetic tree was made by the use of Clustal Omega software available at https://www.ebi.ac.uk/Tools/msa/clustalo/. While using Clustal Omega, the DNA sequences were input in FASTA format; and for rest of the parameters the default settings were used. For the identification of the intron size and splice sites, the DNA sequences of *C. parapsilosis* and *C. auris HAC1* genes were compared by pairwise sequence alignment. EMBOSS Needle which uses the Needleman-Wunsch's algorithm, was employed for the pairwise sequence alignment [283]. While using EMBOSS Needle, the DNA sequences were input in FASTA format; and for the rest of the parameters the default settings were used. The information regarding the splice sites was obtained from Iracane et al, 2018 [203]. The secondary structure of the *C. auris HAC1* was developed by employing RNAfold webserver with the default conditions (http://rna.tbi.univie.ac.at/cgi-bin/RNAWebSuite/RNAfold.cgi).

Table 4.2: List of *HAC1* genes from different yeast and the database from where the sequences were obtained

Yeast	**Accession number**	**Database**
C. albicans	C1_06130C_A/HAC1	CGD
C. auris	B9J08_001826	CGD
C. dubliniensis	Cd36_05800	CGD
C. glabrata	CAGL0K12540g/HAC1	CGD
C. parapsilosis	CPAR2_103720/HAC1	CGD
C. tropicalis	XM_002549933.1	GenBank
S. cerevisiae	S000001863	SGD

4.2.2 Cloning of C. auris HAC1 gene

The *HAC1* gene along with 1kb downstream sequence (that contains introns) were synthesized by GenScript, USA. The synthesized gene was then cloned in pESC-URA plasmid (Figure 4.2) by SmaI/XhoI restriction enzymes. The plasmid map is shown in Figure. Sanger sequencing was done to verify the inserted gene in the vector (GenScript, USA).

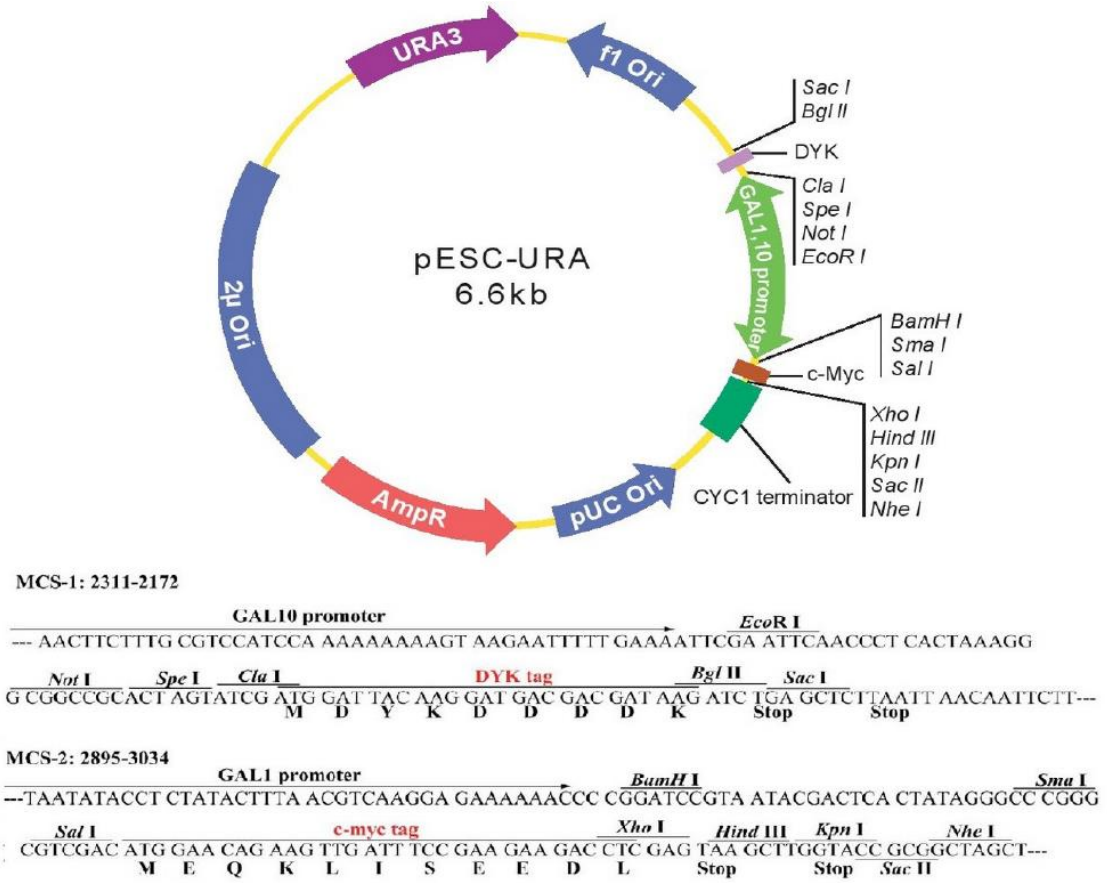

Figure 4.2: pESC-URA vector map

4.2.3. Genetic complementation analysis

4.2.3.1 Lithium acetate mediated transformation

The pESC-URA plasmid containing the *C. auris HAC1* gene was transformed into *Saccharomyces cerevisiae HAC1* delete strain obtained as a courtesy from Dr. Madhusudan's lab, University of Wisconsin, Milwaukee, USA using lithium acetate-based transformation method [284]. The strains studied in this experiment are mentioned in Table 4.3. The *S. cerevisiae HAC1* delete strain are auxotrophs of histidine, leucine, uracil and methionine [285]. For transformation, *S. cerevisiae HAC1* delete strain was cultured overnight in YPD broth followed by secondary inoculation of 0.1 OD cells in 20 ml YPD broth (Figure 4.3). The secondary inoculated cells were grown until 0.8 OD cells were obtained (about 4 hours).

After that, the cells were pelleted by centrifugation (6000rpm, 3 minutes) and the pellet was washed with 100mM lithium acetate in Tris-EDTA buffer (5ml). The solution was centrifuged and pelleted followed by resuspension of the pellet in 100mM lithium acetate in Tris-EDTA buffer (5ml). The resuspended cells were incubated at 28°C for half an hour with shaking. After incubation, the cells were centrifuged at 6000rpm for 3 minutes and the supernatant was discarded. In the pellet transformation mix (350µl of 50% polyethylene glycol, 135 µl of 100mM lithium acetate, 10 µl of 2mg/ml salmon sperm DNA and 5 µl of 100ng pESC-URA plasmid containing the *C. auris HAC1* gene) were added and kept in the incubator at 28°C for sixty minutes. Afterwards the incubation, the cells were subjected to heat shock at 42°C for 20 minutes. Then, the cells with the transformation mix were kept at room temperature for two minutes and centrifuged for pelleting down the cells. The supernatant was discarded and the pellet was centrifuged after the addition of sterile water. Following the washing step with sterile water, the supernatant was removed and the pellet was resuspended in 1ml YPD broth. Finally, 100µl of the resuspension was spread on SC minus uracil media with either glucose or galactose; and the plates were kept for incubation for 48 hours at 28°C.

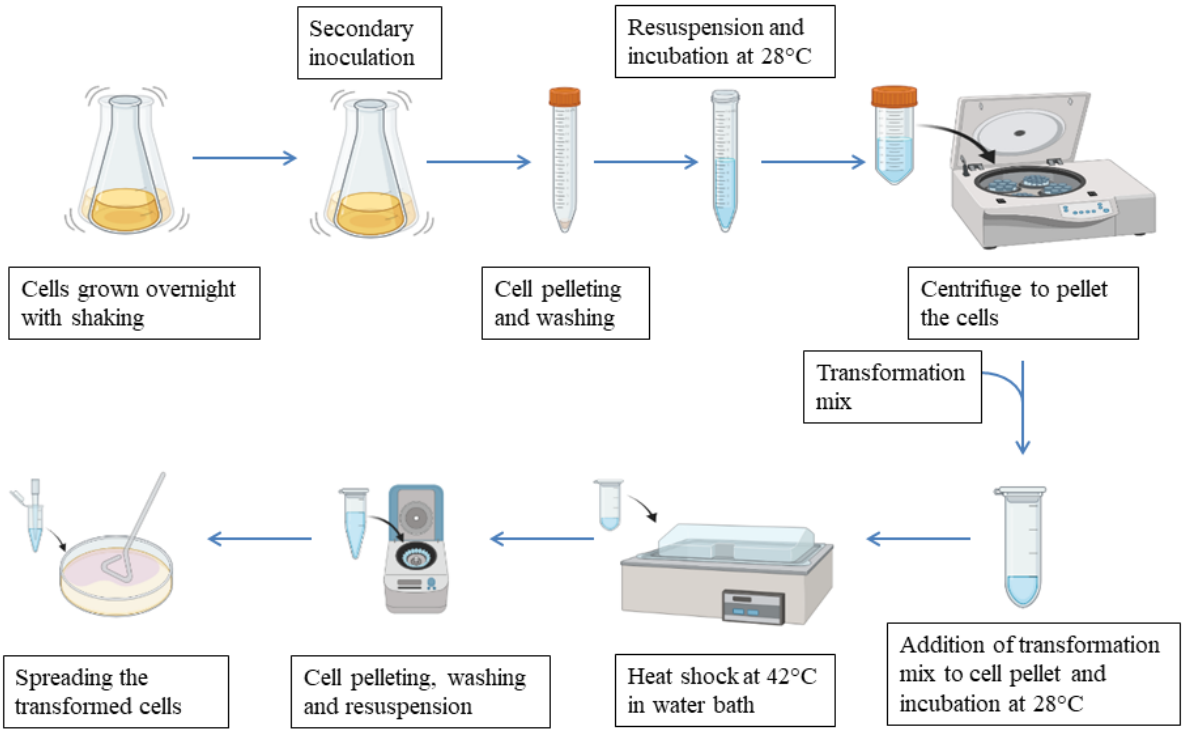

Figure 4.3: Lithium acetate *S. cerevisiae* transformation

Table 4.3: Strains of fungi used

Strains	**Provided by**
Saccharomyces cerevisiae BY4741	Dr. Madhusudan Dey, University of Wisconsin-Milwaukee, USA
S. cerevisiae Δhac1	Same as above strain
C. parapsilosis CL1B214	Dr. Geraldine Butler, University College Dublin, Ireland
C. parapsilosis Δhac1	Dr. Geraldine Butler, University College Dublin, Ireland

4.2.3.2 Patching and replica plating of the transformed cells

From the transformed cells, eight randomly selected cells were patched in circular form on SC minus uracil plates and incubated for 24 hours at 28°C. Then, the patches of cells were replica plated using velveteen cloth on SC minus uracil plates containing different concentrations of DTT (0mM, 5mM, 10mM and 20mM). Afterwards, the replica plates were incubated for 24 hours at 28°C.

4.2.3.3 Dilution spotting

Dilution spotting was performed for *S. cerevisiae* wild type strain (BY4741), *S. cerevisiae HAC1* delete strain and transformed *S. cerevisiae* to compare their growth under endoplasmic reticulum stress caused by DTT. The cells were grown overnight in YPD broth at 28^0C. Then, the cells were adjusted for equal OD (0.2 OD) based on spectrophotometric analysis. Afterwards, the cells were serially diluted in autoclaved water from 10^{-1} to 10^{-5} dilutions. Then 5µl of cells from each dilution was pipetted on grids marked on SC minus uracil plates with or without DTT.

Objective 3: In-silico identification of small molecules targeting unfolded protein response proteins (HAC1 and IRE1) of *C. auris*

4.3.1. Determination of the bioactivity, molecular properties and the drug-likeness of the small molecules

The SMILES formulas of the small molecules were retrieved from the PubChem website [286]. The small molecules chosen for analysis in this objective have been provided in Table 15. The SMILES formulas of the selected small molecules were provided as input in Molinspiration software to predict the molecular characteristics and bioactivity of the small molecules using default settings [287]. Molinspiration aids in predicting several molecular characteristics such as LogP, molecular weight, nON, nOHN and TPSA of different compounds. These characteristics of small compounds will help in determining whether the small molecules have the potential to be a human active drug compound depending upon Lipinski's rule of 5 [288]. Additionally, the Molinspiration software helps to predict various bioactivities of the compounds such as enzyme, protease or kinase inhibitors activities. Molinspiration also aids in determining if the small molecules are GPCR (G-protein coupled receptor), ICM (ion-channel modulators), and NRL (Nuclear-receptor ligand). Molsoft webserver was employed to assess the predict the molecular property and drug-likeness of the small molecules [289]. The SMILES formulas of the selected small molecules were used as input and default parameters of the Molsoft webserver were used.

4.3.2 ADMET property prediction of the small molecules

AdmetSAR2 online server was used for assessing the "ADMET (Absorption, distribution, metabolism, excretion and toxicity)" properties of the small molecules selected in this study [290]. The SMILES formula of the small molecules was given as input and the admetSAR2 server provided data regarding the carcinogenicity, Caco-2 permeability, capability to cross the blood-brain barrier, human intestinal absorption potential, AMES toxicity, hepatotoxicity, and several other properties of the small molecules which can be useful in assessing the ADMET property.

4.3.3 Determination of tertiary structure of the HAC1 and IRE1 proteins of Candida auris and validation of their predicted tertiary structure

The amino acid sequences of the Ire1p and Hac1p proteins were taken from the CGD [291]. *C. auris* strain B8441_V2, protein sequences B9J08_001826, and B9J08_001611 were used

to predict the tertiary structures of Hac1p and Ire1p respectively. The tertiary structure's models of the proteins were determined by the I-Tasser tool which uses iterative template-based fragments assembly simulations and multiple threading approaches to predict the 3D model of proteins [292]. The amino acid sequence of the Hac1p and Ire1p were provided as input to the I-Tasser online server in FASTA format for the prediction of their tertiary structures. Finally, the tertiary structures of the modelled Hac1p and Ire1p were validated by the Rampage web server [293]. This server generates Ramachandran plot which is used to assess the quality of the tertiary structures of proteins.

4.3.4. Molecular docking analysis of the small molecules with Hac1p and Ire1 of Candida auris

The PatchDock server was used to perform molecular docking (MD) of the selected small molecules with Hac1p and Ire1p of *C. auris* to analyse the interactions between them [294]. PatchDock server analyses the interactions among the ligands (small molecules) and the receptors (Hac1p and Ire1p of *C. auris*) on the basis of atomic contact energy and molecular shape complementarity [294]. Prior to the MD analysis, the small molecules' SDF (Structure data file) were obtained from the PubChem server and were transformed into PDB (Protein data bank) file using the MarvinView tool (http://www.chemaxon.com/). After that, the PDB files of the small molecules and PDB files of the predicted tertiary structure of Hac1p and Ire1p were uploaded as ligands and receptors to the PatchDock server for performing molecular docking analysis. In the PatchDock, server protein-small ligand docking was selected and RMSD (Root mean square deviation) value of 1.5 was used.

4.3.5 Molecular dynamics simulation analysis of the docked small molecule-protein complexes

To comprehend the molecular dynamics of all the best-scoring docked sets, molecular dynamics simulation (MDS) was done by the Amber 18 tool [295]. Molecular topographies were produced utilizing the vestibule [296]. With TIP3P water box and sodium particles, entire frameworks were solvated and maintained to a neutral regime. Delicate energy mimimizations in two stages were performed to relax all the systems followed by warming. Particle Mesh Ewald calculation for short- and long-range associations was likewise utilized. A sum of 50 ns recreation for every framework was performed [297]. CPPTRAJ and PTRAJ were utilized to assess the directions for stability (RMSD) and residual adaptability or flexibility (RMSF) [298].

Objective 4: To test the efficacy and safety of small molecules or its compounds in controlling *C. auris* infection and its mechanism thereof.

4.4.1. Minimum inhibitory concentration (MIC) determination of betulinic acid

The antifungal activity of betulinic acid (BA) against different *C. auris* isolates, *Candida albicans* and other non-*albicans Candida* isolates were assessed using the broth microdilution method using EUCAST guidelines (for MIC), with few changes [282]. Table 4.4 lists all the isolates of *C. auris, C. albicans* and other non-albicans species against which the MIC and MFC of BA were determined. These strains were obtained from NCCPF (National Culture Collection of Pathogenic Fungi), Chandigarh, India. All the *C. auris* isolates evaluated in this study were found to be sensitive to fluconazole and amphotericin B (AmpB) except NCCPF: 470149 which is resistant to fluconazole. Similarly, the rest of *Candida* species were also sensitive to both AmpB and fluconazole. BA (lot number: 855057-100MG) were purchased from Sigma-Aldrich, USA. The stock solution of BA was diluted in SDB to obtain the concentration of BA in the range between 0.5-256 µg/mL. Then, 100 µL of the SDB were added to respective wells in 96 well microtiter plates. After, that 100 µL (2x concentration) of BA was added to the first well and mixed with SDB to obtain the highest test concentration. Then, 100 µL of SDB and drug mix were added to the second well to obtain two-fold dilution. The two-fold dilution was done till the 10^{th} well and 100 µL SDB and compound mix were discarded from the 10^{th} well to maintain equal volume (100 µL) in each well. The 11^{th} well only contained media and Candida species cells whereas 12^{th} well was used as sterility control (only contained 100 µL of SDB). The inoculum size was $0.5x10^4$ CFU/mL. Then, the plates were kept in the incubator at 35ºC for 24 hours without agitation. After the incubation, the MIC (50%) was assessed by measuring the absorbance at 530nm. The MIC 50% was determined by the formula:

$$MIC\ (\%) = \{(Abs_c - Abs_s)/Abs_c\} x100$$

Where Abs_c= Absorbance of well-containing media and cells

Abs_s= Absorbance of well-containing media, drug and cells

Table 4.4: List of *Candida* species against which the MIC of BA was determined

NCCPF accession number	***Candida* species**
17783	*C. tropicalis*
NCCPF: 400063	*C. albicans*

NCCPF: 420226	*C. tropicalis*
NCCPF: 410002	*C. kefyr*
NCCPF: 440027	*C. krusei*
NCCPF: 450030	*C. parapsilosis*
NCCPF: 470049	*C. auris*
NCCPF: 470055	*C. auris*
NCCPF: 470097	*C. auris*
NCCPF: 470098	*C. auris*
NCCPF: 470110	*C. auris*
NCCPF: 470111	*C. auris*
NCCPF: 470112	*C. auris*
NCCPF: 470138	*C. auris*
NCCPF: 470149	*C. auris*

4.4.2. Minimum fungicidal concentration (MFC) determination of betulinic acid

The MFC of BA against the different isolates of *C. auris*, *C. albicans* and other non-albicans *Candida* isolates has been analyzed by following the procedure of Espinel-Ingroff *et al*, 2002 [299]. From the wells that showed complete inhibition (optically clear microtiter plate wells obtained after treating the *Candida* isolates for the determination of MIC), 20µl were spread plated on SDA plates and stored in the incubator at 35ºC for 48 hours. The MFC was determined as the lowermost concentration which yielded less than 3 colonies [299].

4.4.3. Field emission scanning electron microscopy to determine the effect of BA on the cell surface of the C. auris isolates

The effects of the *C. auris* treatment with BA were visualized through field emission scanning electron microscopy (FESEM). Two clinical isolates of *C. auris* namely NCCPF: 470149 (insusceptible to fluconazole) and NCCPF: 470097 (susceptible to fluconazole) were treated with 2x MIC concentration of BA separately and kept in the incubator overnight at 35ºC along with shaking (100rpm). Cells grown overnight at 35ºC without any treatment were used as the control for FESEM analysis. After the overnight incubation, the cells were pelleted down by using centrifuge machine at 5000rpm for 3 minutes, which was followed by discarding of the supernatant. Following this, the cells were spread on a glass coverslip with a toothpick. Then, the cells were fixed on the glass coverslips by using 200 µL 2.5 percent

glutaraldehyde made 0.1 molar phosphate buffer (pH=7.2). After this, the coverslips were kept in the fridge at 4ºC for 24 hours to complete the fixation process. Then dehydration of cells was done by treating the fixed cells with a series of ethanol (25%, 50%, 75%, 95% and 100%) for 15 minutes. Then, the fixed cells on glass cover slips were sent to Central Instrumentation Facility, Lovely Professional University, India for FESEM analysis. The fixed cells were gold coated and visualized by FESEM analyser (JEOL Ltd, Japan).

4.4.4 Determination of ergosterol synthesis inhibition by BA treatment on C. auris

The ergosterol synthesis inhibition analysis was done according to the methodology by Arthington-Skaggs *et al*, 1999 and Prasath *et al*, 2020 [300,301]. *C. auris* cells were treated in the presence (MIC and 2x MIC concentration) and the absence of BA for 24 hours at 35ºC in this assay. Then, the cells were pelleted by centrifugation for 10 minutes at 8000rpm. After that, the cells were washed thrice with 1x-phosphate buffered saline (2mL, pH=7.2, HiMedia, India, Lot number: TL1032-100ml). Following the washing step, the cells were pelleted. The pelleted cells were treated with 2mL of 20% alcoholic potassium hydroxide and kept in the incubator for sixty minutes at 85ºC. The alcoholic potassium hydroxide by mixing 20 grams of potassium hydroxide and 35 mL of sterile distilled water and bringing the final volume to 100 mL with the addition of 100% ethanol. After the incubation, sterile distilled water (1ml) and n-heptane (3mL) were pipetted to the cell suspension and robustly vortexed (3 minutes) for phase separation. Then, the n-heptane layer (upper layer) was separated and stored overnight at -20ºC. Finally, the n-heptane layer was diluted five times in 100 percent ethanol and absorbance was measured between 200-300nm using Lasany UV-Vis spectrophotometer (Model: LI-2800). Ergosterol displays a distinctive spectrophotometric absorbance profile in the 240-300 nm range. The occurrence of ergosterol and its intermediatary compound 24(28) dehyrdorerosterol in the samples generates a distinct graph in the 240-300nm range.

4.4.5. Hydrogen peroxide sensitivity assay

The hydrogen peroxide sensitivity test was performed by adhering to the protocol of Muthamil *et al*, 2020 and Prasath et al, 2019 [302,303]. *C. auris* cells were treated in the presence (MIC and 2x MIC concentration) and absence of BA overnight. The absorbance of the overnight culture was measured at 600nm. Then, the absorbance was adjusted to 0.3 and spread on SDA plates. 100µl of the 0.3 OD600 cells were spread on the plates. Then, sterile discs were kept in the centre of the plates. On the sterile 15µL of hydrogen peroxide (30%)

was added. The plates were kept in the incubator for 24 hours at 35^0C and afterwards the incubation, the zone of inhibition was measured.

4.4.6. RNA sequencing

C. auris cells were treated for 6 hours with 2x MIC concentration of BA. The concentration of the drug and period of treatment were determined based on the growth kinetics study. The dose of drugs and time for which the cells were to be treated before RNA isolation for RNA sequencing was determined by growing cells for up to 6 hours and taking absorbance at 600nm every 2 hours. The growth of the *C. auris* decreased in a concentration-dependent manner with time. Based on the data shown in Table 4.5, it was deduced that cells treated with 2x MIC of BA were suitable for RNA isolation for RNA sequencing. The RNA was isolated from the treated and untreated cells after 6 hours of treatment using Qiagen RNA isolation kit and sent to Nucleome Informatics Private Limited, Hyderabad, India for RNA sequencing and predicting differentially expressed genes of *C. auris* upon treatment with BA.

Table 4.5: Growth kinetics to deduce the drug concentration and treatment time for RNA sequencing

BA	**T_0 (OD_{600})**	**T_2 (OD_{600})**	**T_4 (OD_{600})**	**T_6 (OD_{600})**
No treatment	0.130	0.182	0.564	1.024
32µg/ml (MIC)	0.130	0.208	0.564	1.124
64µg/ml (2x MIC)	0.128	0.190	0.364	0.718
128µg/ml (4x MIC)	0.152	0.190	0.238	0.336

4.4.7 GC-MS analysis to study the effect of BA treatment on the metabolite secretion by C. auris

The GC-MS analysis was done according to Semreen *et al*, 2019 (see Table 4.6) [304]. *C. auris* cells were grown for 24 hours in YPD broth containing fluconazole (4ug/ml) or BA (2x MIC). After, 24 hours the cells were filtered using 0.2 µM Whatman filter paper and the supernatant was collected. Then, the metabolites in the supernatant were extracted by mixing the supernatant and ethyl acetate in a 1:1 ratio. Ethyl acetate has been previously used for the

extraction of secondary metabolites from fungi [305,306]. Organic solvents like ethyl acetate can help in the extraction of diverse types of metabolites and improve the stability of the extracted metabolites [307]. After the formation of two distinct layers, the ethyl acetate layer was collected. Then, ethyl acetate was evaporated by rotatory evaporation until 500 µl of the solvent containing the extract was left. Then, the extract was sent to AAL Research and Solutions, Panchkula, Haryana, India for GC-MS analysis.

Table 4.6: Parameters for GC-MS analysis

Carrier gas	Helium
Sample injection volume	1µl
Sample injection temperature	250^0C
Sample injection mode	Splitless
Mass spectrometer electron energy	70eV
Mass spectrometer ion source temperature	240^0C
Mass spectrometer interface temperature	250^0 C
Mass spectrometer scan mode	initiating from 35m/z and ending at 450 m/z having a scan rate of 1428
Library	NIST

4.4.8 Cytotoxicity analysis of BA

The MTT assay to determine the *in vitro* cytotoxicity of BA was done according to Leon *et al*, 2011 [308]. The cytotoxic effect of BA was determined against NRK (normal rat kidney epithelial cells) and human embryonic kidney (HEK293T) cell lines. The cell lines were bought from "National Centre for Cell Science" (NCCS, Pune, India). The cells were cultivated in DMEM media (GIBCO Laboratories) added with 25 mM glucose, streptomycin 100 g/mL, 10% fetal bovine serum, and penicillin 100 IU/mL at 37°C in 95% air and 5% carbon dioxide. HEK293T was subcultured in 96-well plates and cultured between 80-90% confluency. Next, HEK293T was treated with varying doses of BA (0, 16 µg/ml, 32 µg/ml, 64 µg/ml and 128 µg/ml) and kept in the CO_2 incubator for a day. Afterwards, the PBS was washed, followed by MTT administration (5mg in 10ml) and kept in the CO_2 incubator for 120 minutes. At last, the formazan crystals generated because of of MTT mitochondrial reduction were dissolved in DMSO (100 µL/well) and the optical densities were determined at the wavelength of 570 nm.

4.4.9 Determination of antifungal potential of Sarcochlamys pulcherrima extract and identification of potential small molecules from S. puclcherrima extract as antifungals against C. auris

4.4.9.1 Sample collection and preparation of extract

The leaves and bark from one *S. pulcherrima* tree were collected from the New Halflong region of North Cachar Hills (Assam, India) in July 2019. The samples were washed thoroughly with water to remove any dust and other impurities from the plant sample. After that, the samples were air-dried in a hot air oven at 45-50°C until the samples dried completely. Then, the dried samples were powdered with the help of a grinder, packed in airtight packets, and stored at 4°C for future use. The extract was obtained by the Soxhlet-mediated extraction method. The extracts were obtained using two solvents: 90% methanol and ethyl acetate. For obtaining the plant extract 30 grams of leaves powder was added to 100 ml of each solvent [309]. The Soxhlet apparatus was run at ~65°C (methanol extraction) and ~77°C (ethyl acetate extraction) for 25 cycles [309]. The crude solvent extract was then concentrated to 5 ml to remove the excess solvent by using a rotatory evaporator at 40 rpm and 50°C temperature. The concentrate (5ml) was further stored at 50°C to remove the remaining solvent until the concentrate had a dry paste-like consistency. The amount of the extract in the paste form was measured and kept in the fridge at 4°C up till further usage.

4.4.9.2 Determination of the antifungal activity of S. pulcherrima plant extract against C. auris

The *C. auris* strain YG19 which is sensitive to fluconazole and amphotericin B was obtained from NCCPF, Chandigarh, India. The antifungal activities of *S. pulcherrima* plant extract against *C. auris* were evaluated by the disc diffusion procedure. The yeast strains were grown in YPD broth overnight at 150 rpm shaking at 28°C. Then, the overnight grown culture was serially diluted to obtain 0.05 OD. From the diluted culture, 100µl was taken and spread over solidified SDA. After spreading the cells, filter discs containing different concentrations of the methanol and ethyl acetate plant extract were placed on the SDA plates. The Petri dishes were kept in the incubator for 48 hours at 28°C. Afterwards, the incubation time was over, the Petri dishes were observed and the diameters of the zones of inhibition were measured. Fluconazole disc (Himedia, India,10 µg), was used as control.

4.4.9.3 Determination of the antioxidant activity of S. pulcherrima plant extract

The antioxidant capabilities of the extract of *S. pulcherrima* leaves were determined *in vitro* through DPPH free radical scavenging experiment. For the assay, 0.135 mM DPPH (2,2-diphenyl-1-picrylhydrazyl) was prepared in methanol and the *S. pulcherrima* leaves extract was prepared in DMSO with concentrations ranging from 0-200 µg/ml. One ml of 0.135 mM DPPH and 1 ml of plant extract of varying concentrations were added into test tubes and kept for 45 minutes in the absence of light at room temperature. All the experiments were performed in triplicates and ascorbic acid was applied as standard. Following the incubation, absorbance was determined at 517nm. The DPPH scavenging activity was calculated as:

% DPPH scavenging activity = $\{(Abs_c - Abs_s)/ Abs_c\} X 100$

Abs_c = Average absorbance of methanol + DPPH

Abs_s = Average absorbance of sample (different concentrations of plant extract/ Ascorbic acid) +DPPH

4.4.9.4 Determination of total phenolic content of S. pulcherrima plant extract

The phenolic contents in the extract were estimated by the use of the Folin-Ciocalteu reagent. The leaves extract, 200 µL of different concentrations (160 µg/ml and 320 µg/ml prepared in distilled water), was mixed with 2% sodium carbonate (2 mL) and 10% Folin-Coicalteu reagent (2.5 mL). Then, the reaction mix was warmed at 45°C in a water bath for 20 minutes. After the incubation, the absorbance was measured at 765 nm. All the experiments were performed in triplicate and gallic acid (Sisco Research Laboratories, India) was used as standard.

4.4.9.5 HPTLC detection of phenols in the plant extract

After detecting phenols in the plant extract by the Folin-Ciocalteu method, the extract was analyzed by HPTLC to detect the specific phenolic compounds such as gallic acid and quercetin in the *S. pulcherrima* extract. The presence of phenols in the plant extract was determined by using HPTLC at Herbal Health Research Consortium Private Limited, Amritsar, Punjab, India. The silica gel TLC plate coated with fluorescent indicator F_{254} with dimensions 5.0 x 10.0 cm (Merck, Germany) was used. The sample i.e., ethyl acetate extract of *S. pulcherrima* (2 µL) was loaded in the forms of bands (6mm) using the CAMAG Linomat 5 semi-automatic sample application system. After the development of the TLC plates in hexane-chloroform-acetic acid (4:5:1 ratio), they were air-dried and scanned using a CAMAG TLC scanner at 270 nm wavelength with a Deuterium lamp in absorption mode. A

gallic acid standard (Sisco Research Laboratories, India) of 1mg/ml was used for the analysis.

4.4.9.6 Determination of in vitro antifungal activity of gallic acid against C. auris

The antifungal property of gallic acid was determined in triplicates against 6 different clinical isolates of *C. auris*. These strains were obtained from NCCPF, Chandigarh, India. The NCCPF identification numbers of these strains are 470049, 470055, 470097, 470098, 470111, and 470149. All the samples of *C. auris* tested in this experiment were found to be sensitive to fluconazole and amphotericin B except NCCPF 470149 which is resistant to fluconazole. Gallic acid was purchased from Sisco Research Laboratories, India.

The antifungal activity of gallic acid against *C. auris* strains was assessed through the broth microdilution procedure using EUCAST guidelines, with modification [282]. The stock solution of gallic acid was diluted in Sabouraud dextrose broth (SDB) to achieve the concentration of gallic acid in the range of 0.06 mg/ml to 32 mg/ml. Then, 100 µL of the SDB with diluted gallic acid was put into the respective wells in 96 well microtiter plates, in triplicate. The inoculum size was $0.5x10^4$ CFU/mL. Then, the plates were kept in the incubator at 35ºC for 24 h without agitation. After the incubation, the MIC (50%) was measured by reading the absorbance at 530nm. The MIC 50% was determined by the formula:

$$MIC\ (\%) = \{(Abs_c - Abs_s)/Abs_c\} x100$$

Where Abs_c= Absorbance of well-containing media and culture

The minimum fungicidal concentration (MFC) of gallic acid against *C. auris* was examined by adhering to the procedure of Espinel-Ingroff et al, 2002 [299]. From the wells that showed complete inhibition (optically clear microtiter plate wells obtained after treating *C. auris* for the determination of MIC), 20µl were spread on SDA-containing Petri plates and kept in the incubator at 35ºC for 48 hours. The MFC was determined as the lowermost of the concentrations that yielded less than 3 colonies [299].

4.4.9.7 Structure prediction: modelling, validation and superimposition of C. auris carbonic anhydrase protein

The tertiary structure of the *C. auris* CA protein is not resolved yet. The amino acid sequence of *Candida auris* CA protein (269 amino acids) was retrieved from CGD (http://www.candidagenome.org/cgi-bin/locus.pl?locus=B9J08_000363) and the tertiary structure model of the *C. auris* CA protein was modelled through I-TASSER web interface [310]. To model a structure, I-TASSER uses a combination of different methodologies

including *ab-initio* loop modelling, fragment assembly, threading and structural refinements [310]. To identify the template protein structure, we performed a BLAST search against the PDB database [311,312]. The top hit obtained was of *C. albicans* CA protein with 79% sequence identity and 77% query coverage. Hence, the crystal structure of *C. albicans* CA (PDB ID: 6GWU) was used as a primary template for modelling the *C. auris* CA protein structure. The best structure model was selected based on a confidence score (C-score).

To estimate the quality of the modelled structure SAVES server (http://nihserver.mbi.ucla.edu/SAVES) was used. The backbone conformations and final geometric compatibility of interacting residues in the I-TASSER generated *C. auris* CA protein structure were determined via several structural assessment methods. The Ramachandran plot examination was applied to estimate the modelled CA protein backbone's phi/psi distribution. Additionally, the ERRAT program was employed to calculate non-bonded atomic interactions for the modelled proteins. To demonstrate the compatibility of the 3D atomic model of amino acid with its amino acid sequence (1D) was created through the verify-3D program. To check the structural consistency, we superimposed the modelled structure with the template structure (6GWU) and calculated root mean square deviation (RMSD) using the iPBA server (https://www.dsimb.inserm.fr/dsimb_tools/ipba/example.php). All the figures of the molecules and interactions have been made through UCSF Chimera software [313].

4.4.9.8 Molecular docking of gallic acid with C. auris carbonic anhydrase protein

Prior to docking, the crystal structures and the modelled proteins underwent energy reduction and refinement. This process involved 100 steps of steepest descent followed by 500 steps of conjugate gradient, conducted using the Swiss PDB viewer software platform [314]. The SDF of gallic acid was taken from the PubChem (https://pubchem.ncbi.nlm.nih.gov) database that contained PubChem ID: CID 370. After downloading the SDF structure, it was transformed into PDB file through an online tool available at: https://cactus.nci.nih.gov/translate/. Firstly, we docked the zinc metal-ion in the modeled structure of *C. auris* CA protein using Metal Ion-Binding site prediction and docking server (MIB) (http://140.128.63.8/MIB/). On the Zn coordinated *C. auris* CA gallic acid was docked using Patchdock web-server with the criteria to get a maximum of 10 docked poses [315]. The active site amino acids of *C. auris* CA modelled structure were marked based on *C. albicans* CA structure (PDD ID: 6GWU). The docked protein-ligand complexes were evaluated based on their ACE. The visualization of interacting residues of *C. auris* CA with the ligand was done using UCSF Chimera. All images of interaction were generated through UCSF Chimera [313].

Objective 5: To develop a potent multivalent epitope based vaccine against *C. auris* using *in-silico* approach.

4.5.1. Protein sequence retrieval and analysis

The sequence of the Als3p of *Candida auris* strain B8441(protein ID B9J08_004112) was retrieved from the CGD [316]. The cellular localization of the Als3p was reported by using the CELLO2GO web server [317]. The server uses BLAST homology searching and CELLO localization approaches to predict the subcellular localization of proteins [317]. Since a good vaccine candidate should be antigenic and elicit a strong immune response, the antigenicity of the Als3p was determined by Vaxijen 2.0 web server [318]. Vaxijen 2.0 webserver uses an auto cross-covariance method to predict bacterial, fungal, viral, and tumour antigenic proteins.

4.5.2. Prediction of T cell and B cell epitopes

For the determination of T helper cell epitopes that interact with MHC class II molecules, NETMHC 2.3 webserver was used [319]. It uses an artificial neural network to predict the binding of epitopes with various MHC class II alleles. The prediction of epitopes that may bind with MHC class I molecules and initiate cytotoxic T cell-mediated immune response was performed by NETMHC 4.0 webserver. This web server also uses an artificial neural network to predict peptides that can bind with different human and animal MHCI molecules [320]. The prediction of linear B cell epitopes was done by the IEDB B cell epitope prediction tool using the Bepipred linear epitope prediction method [321]. This server uses Hidden Markov Model to predict the linear B cell epitopes [321].

4.5.3. Prediction of toxicity, allergenicity, antigenicity and interferon-γ activating potential of the epitopes

Peptides that are non-toxic, antigenic, non-allergen, and induce the production of interferon-γ are considered an ideal candidate for vaccine engineering [322,323]. The ToxinPred web server was used to predict the toxicity of epitopes [324]. To predict the antigenicity of the peptides Vaxijen 2.0 webserver was used. This server uses an auto cross-covariance method to predict bacterial, fungal, viral, and tumour antigenic proteins [318]. The AllergenFP v.1.0 server was used to assess the allergenicity of the epitopes. It uses a Tanimoto coefficient to predict if a peptide is an allergen. Several studies have shown the role of interferon- γ in the

prevention of invasive Candidiasis and Aspergillosis [325,326]. Hence, in this study, the ability of the epitopes to induce interferon-γ production has been studied by the IFNepitope web server [327]. This server helps to predict and design epitopes that can elicit interferon-γ production [327].

4.5.4. Analysis of the conservancy of the epitopes

An ideal vaccine against *C. auris* must be able to elicit an immune response against its different strains. Hence, the conservation of the epitopes among different *C. auris* strains were analyzed by the IEDB Epitope Conservancy Tool [328]. The epitope conservancy was analyzed among the Als3p of *C. auris* strains B11221, B11220, and B11213. The accession numbers of the Als3p of *C. auris* strains B11221, B11220, and B11213 were XP_028889036.1, QEO24215.1, and PSK76860.1 respectively. The Als3p were confirmed in other strains of *C. auris* by performing protein-protein BLAST analysis with Als3p of *C. auris* strain B8441 [329]. Only epitopes with 100% identity among all the selected strains of *C. auris* were considered for further analysis.

4.5.5. Vaccine engineering and its physiochemical property determination

The epitopes that were predicted to be conserved among different *C. auris* strains, non-toxic, antigenic, non-allergenic, and induce the production of interferon-γ were chosen for the design of the final vaccine. Adjuvants derived from RS09 and the C and N terminals of the flagellin (UNIPROT ID: Q06971) protein of *Salmonella dublin* were utilized. These adjuvants have been previously used in the multivalent epitope-based vaccine design of Herpes Simplex Virus and Human Papilloma Virus [323,330,331]. PADRE sequence was incorporated into the vaccine to improve the vaccine stability [331]; and all the epitopes, adjuvants, and PADRE sequences were adjoined with each other by the GGS linker sequence. The physiochemical characteristics of the prospective vaccine have been determined by the ExPASyProtParam web server [332]. Using this tool stability, the number of amino acids, molecular weight, isoelectric point, total of negatively and positively charged amino acids, aliphatic index and various other properties of the vaccine construct can be determined [332]. The solubility of the prospective vaccine was evaluated by the Solpro web server [333]. This web server predicts the solubility of proteins with 74% accuracy after expression in *Escherichia coli* [333]. Then, the antigenicity and allergenic potential of the prospective vaccine were determined. Antigenicity was evaluated by Vaxijen 2.0 webserver [318] and allergenicity was predicted by the AllergenFP version 1.0 web server.

4.5.6. Determination of secondary and tertiary structure of the vaccine construct and validation of the predicted tertiary structure

To determine the secondary structure of the vaccine PSIPRED webserver was used [334]. This web server helps in the prediction of beta-sheets, alpha helices, and coils in proteins by applying the feed-forward neural networks program [310]. The models of the tertiary structure of the prospective vaccine were determined by using the I-Tasser server which uses iterative template-based fragments assembly simulations and multiple threading approaches to predict the 3D model of proteins [310]. Finally, the tertiary structure of the modelled prospective vaccine was validated by the Rampage web server [335]. This server generates a Ramachandran plot which is used to assess the quality of the tertiary structures of proteins.

4.5.7. Molecular docking of the vaccine construct with toll-like receptor molecule

The vaccine was docked with Toll-like receptor 5 molecule (PDB ID: 3J0A) and MHCII HLA DRB_0101 (PDB ID: 4AH2) by using the ClusPro 2.0 server [336]. ClusPro is a protein-protein docking server which results in 10 models of the docking complex by defining the centres of highly populated clusters of low-energy docked structures [336].

4.5.8. Molecular dynamics simulation

The interaction of the prospective vaccine with MHCI and TLR05 was analyzed under the G43A1 force field with spc216H2O model and a time step of 1 fs for overall 100 ns by deploying Gromacs 5.1.1 package [337,338]. During MD simulation phosphorylated threonine charges were defined at -2e [339], and for deamidated glutamine charges were set to 0. The antigenic domain had a total charge of -17e. To achieve an ionic strength of 140 mM, 74 Na+ ions and 57 Cl- ions were introduced to the system, substituting the H_2O molecules at indiscriminate positions. This ionic strength closely resembled that of cells [340]. Finally, RMSD and RMSF values of simulation trajectory were analyzed to study the interaction of vaccine construct with both receptors.

4.5.9. Codon adaptation and in-silico cloning

To assess the efficient cloning and expression of the prospective vaccine in expression vectors, the JCat webserver was used for codon optimization of vaccine candidate gene for expression in *E. coli* K12 strain [341]. During the codon optimization, the settings applied by Hasan *et al* were used [331]. SnapGene restriction cloning module developed by Insightful

Science was used for *in silico* cloning. During cloning the codon-optimized DNA sequence of the prospective vaccine was inserted between XhoI (158) and EcoRI (192) restriction sites of the pET28a(+) vector.

RESULTS AND DISCUSSION

Objective 1: Collection of clinical isolates of *Candida* spp. and to study multi-drug resistance profile of those isolates

5.1.1 Collection of Candida species and their identification

Collection and identification of human pathogenic fungi such as *Candida sp*. is very important. Accurate identification of the specific *Candida sp.* causing an infection is crucial for appropriate diagnosis and effective treatment. Different yeast species may exhibit varying levels of virulence and respond differently to antifungal drugs [342]. Furthermore, these studies help in the implementation of targeted surveillance programs and preventive measures. Collecting and characterizing these yeasts helps in monitoring the rise and spread of drug-resistant microbes [343]. This information guides the development of effective antifungal strategies and also helps in creating awareness about emerging pathogens such as *C. auris*.

From the 50 blood samples of cancer and diabetes patients, four *Candida* isolates were obtained (Figure 5.1), which is 8% of the total samples. The HCCDA test identified the isolates as *C. glabrata* (PIMS 6), *Candida tropicalis* (PIMS 7), *Candida krusei* (PIMS 13) and *Candida dubliniensis* (PIMS 20) (Figure 5.1).

Table 5.1: Colour of *Candida* sp. on chromogenic agar media

Yeasts	**Colour on ChromAgar media**
C. albicans	Light green [344]
C. dubliniensis	Dark bluish green [345]
C. glabrata	White and lavender [344]
C. krusei	Pink [344]
C. tropicalis	Blue, dark blue, metallic blue [344]
C. parapsilosis	Light brown [345]

The isolates obtained from NCCPF were also grown on HCCDA media (Table 4.1, Figure 5.2). The ability of the different NCCPF Candida isolates to produce urease and solubilize different carbohydrates present in the HCI kit is shown in Figure 5.3. The list of different substrates present in the wells of the HCI kit is provided in Table 5.2.

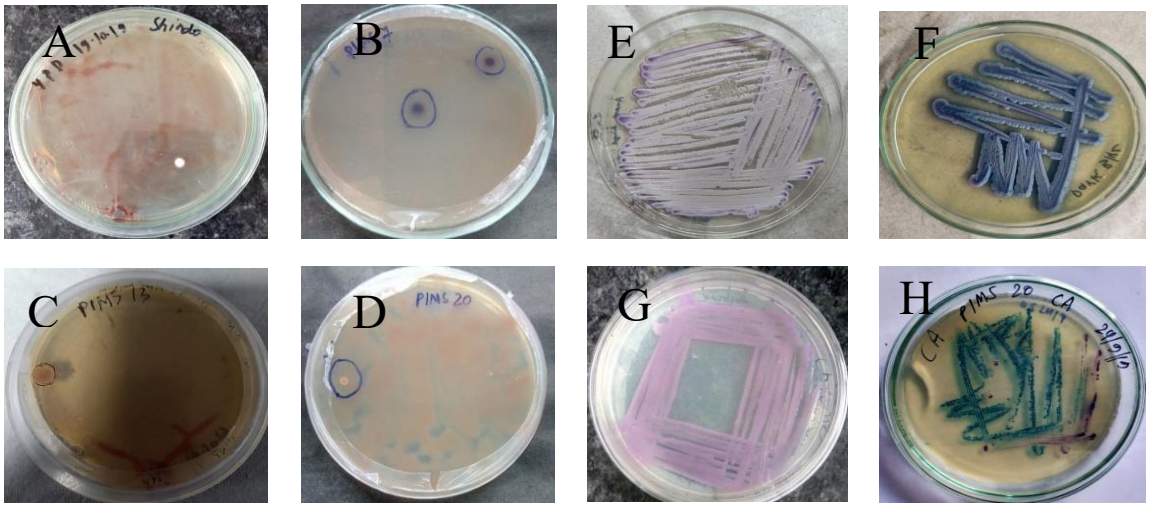

Figure 5.1: Fungi isolated from blood samples grown on SDA and HCCDA media A. Fungal isolate (PIMS6) on SDA plate B. Fungal isolate (PIMS7) on SDA plate C. Fungal isolate (PIMS13) on SDA plate D. Fungal isolate (PIMS20) on SDA plate. E. Fungal isolate (PIMS6) on HCCDA plate F. Fungal isolate (PIMS7) on HCCDA plate G. Fungal isolate (PIMS13) on HCCDA plate H. Fungal isolate (PIMS20) on HCCDA plate (Refer to the Table 5.1 for identification based on color on HCCDA media)

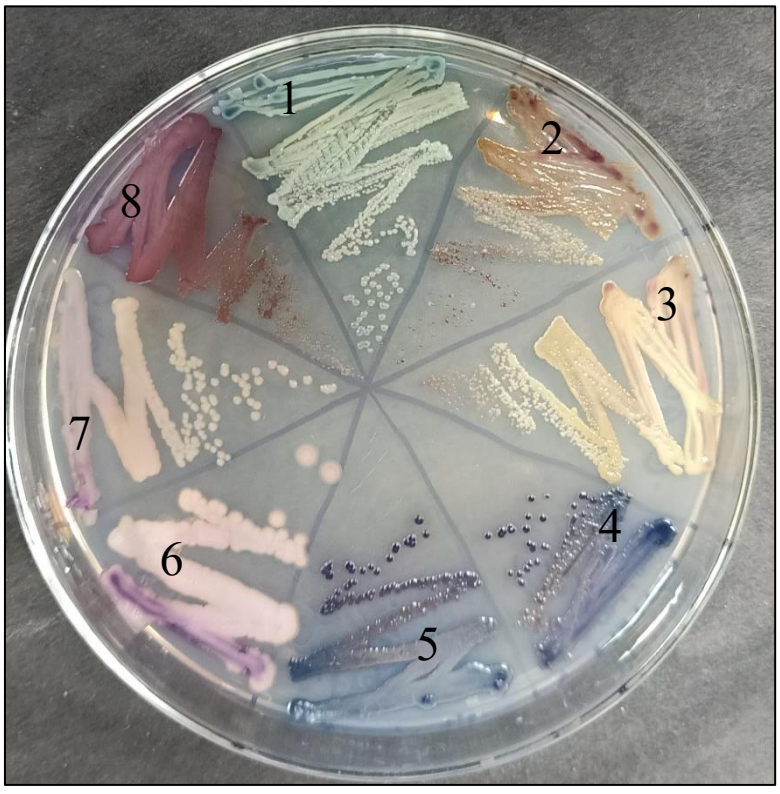

Where,

1= *C. albicans*

2= *C. auris (S)*

3= *C. auris (R)*

4= *C. tropicalis (S)*

5= *C. tropicalis (R)*

6= *C. krusei*

7= *C. kefyr*

8= *C. parapsilosis*

Figure 5.2: NCCPF *Candida* isolates grown on HCCDA media (Refer to Table for preliminary identification of the yeasts based on colour on HCCDA media)

Where,

1= *C. albicans*

2= *C. auris (S)*

3= *C. auris (R)*

4= *C. tropicalis (S)*

5= *C. tropicalis (R)*

6= *C. krusei*

7= *C. kefyr*

8= *C. parapsilosis*

Figure 5.3: Solubilisation of different carbohydrates by NCCPF *Candida* isolates where yellow/orange colour represents positive reaction (solubilisation of sugars) and pink/red colour represents negative reaction (did not solubilize the sugars). The name of substrates present in each well is provided in Table 5.2.

Table 5.2: Substrates present in the HCI kit

Well 1	**Well2**	**Well3**	**Well4**	**Well5**	**Well6**	**Well7**	**Well8**	**Well9**	**Well10**	**Well11**	**Well12**
Urease	Melibiose	Lactose	Maltose	Sucrose	Galactose	Cellobiose	Inositol	Xylose	Dulcitol	Raffinose	Trehalose

The main objective of this study was to investigate the susceptibility of fungal strains to antifungal agents. To achieve this, both plate-based and biochemical assays were employed. The plate-based assay involved culturing the fungal strains on agar plates and observing their growth in the presence of different antifungal agents. The biochemical assay, on the other hand, utilized specific biochemical markers to ascertain the susceptibility of the isolates. The

rationale behind using both plate-based and biochemical assays was to ensure a comprehensive evaluation of the fungal strains' susceptibility to antifungal agents. The plate-based assay provided a visual representation of the strains' growth inhibition, while the biochemical assay offered a more quantitative analysis based on specific markers.

Regarding the collection of other strains, the focus of this study was primarily on identifying susceptible and resistant fungal strains. As a result, the research did not pursue the collection of additional strains beyond those obtained from PIMS, Jalandhar. The main goal was to expand the repertoire of clinical isolates and gain a better understanding of their susceptibility to antifungal agents described in the next section 5.1.2.

5.1.2. Drug resistance profile of Candida isolates

The emergence of *C. auris* resistant clinical isolates is a significant concern in healthcare settings worldwide. *C. auris* is acknowledged for its ability to develop unsusceptibility to multiple antifungal agents, including echinocandins, azoles, and polyenes [252]. Intrinsic resistance, antifungal selected pressure and nosocomial transmission are distinct elements that add to the emergence and spread of resistant isolates. The drug susceptibility profiles of *C. auris* clinical isolates are indeed crucial for several reasons. Having accurate drug susceptibility information allows clinicians to make informed decisions regarding the selection of antifungal drugs for the control and cure of *C. auris* infections. By knowing what antifungal agents are effective against a particular isolate, clinicians can tailor treatment regimens to maximize efficacy and improve patient outcomes [346]. Monitoring the drug susceptibility profiles of *C. auris* isolates is imperative for tracking the emergence and spread of antifungal unsusceptibility [347]. By regularly analyzing susceptibility patterns, healthcare systems can detect trends in resistance and implement appropriate measures to check and control the dissemination of drug-resistant strains. Furthermore, understanding the drug susceptibility profiles of *C. auris* isolates is central to developing active infection control strategies. Drug susceptibility profiles play a vital role in promoting antifungal stewardship practices. By tailoring therapy based on the susceptibility profile of *C. auris* isolates, clinicians can avoid the unnecessary use of broad-spectrum antifungal drugs, which helps to minimize the development and spread of drug-tolerant isolates. This approach preserves the effectiveness of available antifungal agents and ensures their appropriate use [348].

The decision not to pursue further strain collection was driven by the specific objectives of the study and the lack of the availability of resources. The principal aim of the research was

to increase the repertoire of clinical isolates and since we have obtained enough isolates from PGI Chandigarh, further strain collection was not pursued. However, it is important to consider that strain diversity and the inclusion of isolates from different geographical locations can provide valuable insights into the epidemiology and drug susceptibility patterns of *C. auris*, and future studies may benefit from a broader strain collection strategy.

According to the EUCAST guidelines, the MIC for amphotericin B is the lowermost of the drug doses which inhibits at least 90% growth of cells in relation to drug-free control. Similarly, for fluconazole the MIC is the lowermost of the drug concentrations which inhibits at least 50% growth of cells in relation to drug-free control [282]. The tentative MIC breakpoints of different antifungal drugs are provided in Table 5.3 [349].

Table 5.3: Tentative MIC breakpoints

Antifungal	**MIC breakpoint (µg/mL)**
Fluconazole	≥32
Amphotericin B	≥2
Anidulafungin, Micafungin	≥4

The *Candida* species isolated from the blood samples were sensitive to both fluconazole and amphotericin B excluding the PIMS20 sample, which was unsusceptible to amphotericin B (Table 5.4). The antifungal susceptibility of 15 clinical isolates obtained NCCPF (9 *C. auris* isolates, 2 *C. tropicalis* isolates, and 1 clinical isolate each of *C. albicans. C. parapsilosis, C. krusei* and *C. kefyr*) against fluconazole and amphotericin B have been performed. All the isolates obtained from NCCPF were sensitive to amphotericin B (except NCCPF: 470097, *C. auris*) and fluconazole (except NCCPF: 470049 and 470149, both are *C. auris*) (Table 5.5).

Table 5.4: MIC of the antifungal drugs against the *Candida* isolates obtained from blood samples from PIMS, Jalandhar

Clinical Isolate	***Candida* species**	**Fluconazole (MIC) (µg/mL)**	**Amphotericin B (MIC) (µg/mL)**
PIMS 6	*C. glabrata*	0.25	0.25
PIMS 7	*C. tropicalis*	0.25	0.75
PIMS 13	*C. krusei*	ND	ND

PIMS 20	*C. dubliniensis*	0.5	Resistant

Table 5.5: MIC of the antifungal drugs against the *Candida* isolates from NCCPF

Clinical Isolate	***Candida* species**	**Fluconazole (MIC) (µg/mL)**	**Amphotericin B (MIC) (µg/mL)**
17783	*C. tropicalis*	2	1
NCCPF: 400063	*C. albicans*	0.125	0.5
NCCPF: 420226	*C. tropicalis*	2	0.5
NCCPF: 410002	*C. kefyr*	0.5	0.125
NCCPF: 440027	*C. krusei*	16	0.25
NCCPF: 450030	*C. parapsilosis*	8	0.031
NCCPF: 470049	*C. auris*	Resistant	0.125
NCCPF: 470055	*C. auris*	16	0.25
NCCPF: 470097	*C. auris*	8	0.25
NCCPF: 470098	*C. auris*	1	2 (Resistant)
NCCPF: 470110	*C. auris*	1	0.125
NCCPF: 470111	*C. auris*	16	0.25
NCCPF: 470112	*C. auris*	16	0.125
NCCPF: 470138	*C. auris*	8	0.25
NCCPF: 470149	*C. auris*	Resistant	0.025

CDC has reported that about 7% of *Candida sp.* isolated from blood samples are not susceptible to fluconazole and species like *C. glabrata, C. auris* and *C. parapsilosis* are more resistant than other species [350]. Similar, to previous studies in this study also the *C. auris* resistant (2 out of 9 samples) common antifungal drug fluconazole has been reported. One out of nine *C. auris* isolates was unsusceptible to amphotericin B. This study highlights the occurrence of antifungal drug unsusceptibilty in *C. auris* isolates obtained from patients in India. Hence, there is an urgent need for monitoring the transmission of different *Candida sp.* including *C. auris*. Furthermore, antifungal drug resistance testing should be done to guide the therapy that can be used for treating fungal infections. The *Candida* species collected in this objective were further used for the identification of novel antifungal molecules and their mechanism in objective 4.

Objective 2: Disruption and cloning of *HAC1* gene of *C. auris* and to study its role in the virulence and unfolded protein response pathway

5.2.1. Bioinformatics analysis of the determination of intron and cleavage sites of C. auris HAC1

The endoplasmic reticulum (ER) protein homeostasis is maintained via the unfolded protein response (UPR) stress response [84]. It is initiated when unfolded or misfolded proteins accumulate in the ER, which can happen during many physiological and pathological situations, including fungal infections (see section 2.5 and 2.6 in the review of literature). Candida species, *C. neoformans*, and *A. fumigatus* alter and exploit the UPR pathway to survive, proliferate, and cause disease [84,195,207]. Depending on the infection stage, the UPR pathway can help or hurt fungal infections. Fungal pathogens face host-induced stressors including nutrient constraints, oxidative stress, and immunological responses. Invading fungus can experience ER stress and UPR activation from these stress conditions. UPR activation enables fungal cells to adapt and survive in the host [84].

Understanding the interplay between the UPR pathway and fungal pathogenesis is crucial for developing new strategies to combat fungal infections. Targeting elements of the UPR pathway could offer potential avenues for the development of novel antifungal therapies. In this objective, we aimed to analyze the UPR pathway of *C. auris*, specifically focusing on the *IRE1* and *HAC1* components. At the time this study was initiated, there was limited or no information available regarding the UPR pathway in *C. auris*. This knowledge gap highlighted the importance of studying the UPR pathway in this emerging fungal pathogen.

To achieve this, we employed various experimental approaches to characterize the UPR pathway in *C. auris*. We first conducted extensive literature reviews to gather information about the UPR pathway in other fungal species and identify conserved components such as *IRE1* and *HAC1* (discussed in sections 2.5 and 2.6). While our study focused on the characterization of the UPR pathway in *C. auris*, it is imperative to note that our findings provide initial insights into its existence and functionality.

Based on the phylogenetic tree, comparison of *HAC1* intron size in other *Candida* species, multiple sequence alignment and manual pairwise sequence alignment the *HAC1* intron in *C. auris* was identified. The phylogenetic tree (Figure 5.4) shows that the *HAC1* genes of *C. albicans, C. tropicalis* and *C. dubliniensis* are more related and have much recent common ancestors in comparison to other *Candida* species. In fact, the size of introns in *C. albicans*

(19bp), *C. tropicalis* (19bp) and *C. dubliniensis* (22bp) are similar. Moreover, the phylogenetic tree shows that the *HAC1* genes of *C. parapsilosis* and *C. auris* are more related. Hence, we hypothesize that the *HAC1* intron of *C. auris* is similar to the *HAC1* intron of *C. parapsilosis*. To corroborate the hypothesis a pairwise sequence alignment was performed manually and EMBOSS Needle tool. The analysis showed that the *HAC1* intron in *C. auris* is 440 bp long (Figure 5.5). Similar to the *HAC1* intron of *C. parapsilosis*, the *C. auris HAC1* intron has a 5' hairpin loop surrounding the 5' splice site (Figure 5.5). The secondary structure of HAC1 RNA predicted by RNAfold also shows the presence of hairpin loop structure around the 5' splice site (Figure 5.6). However, the 3' hairpin loop surrounding the 3' splice site is absent in *C. auris*. In a previous research, it has been reported in different yeasts like *Candida guilliermondii*, *Candida lusitaniae*, *Pichia stipitis*, *Candida famata* and *Lodderomyces elongisporus* that the 3' hairpin loop has been lost [351]. Similarly, the bioinformatics analysis in our study also shows the absence of hairpin loop surrounding the 3' splice site.

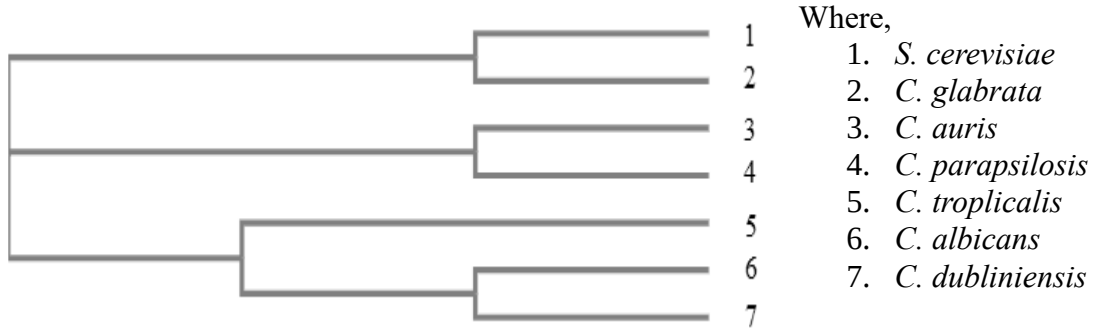

Figure 5.4: *HAC1* gene phylogenetic tree

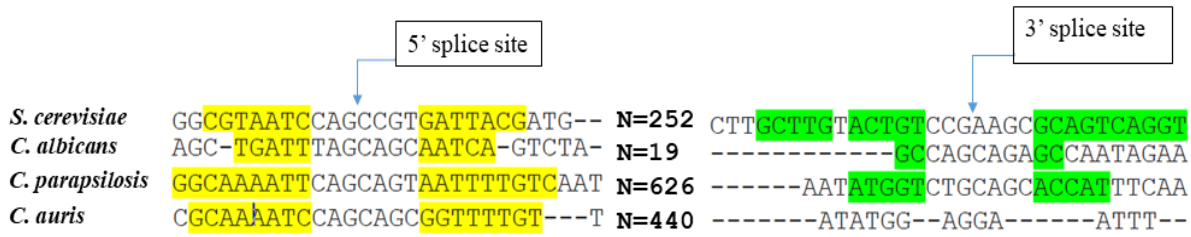

Figure 5.5: Splice sites of *C. auris HAC1*. Yellow highlighted region hairpin loop surrounding 5′ splice site and green highlighted region is hairpin loop surrounding 3′ splice site.

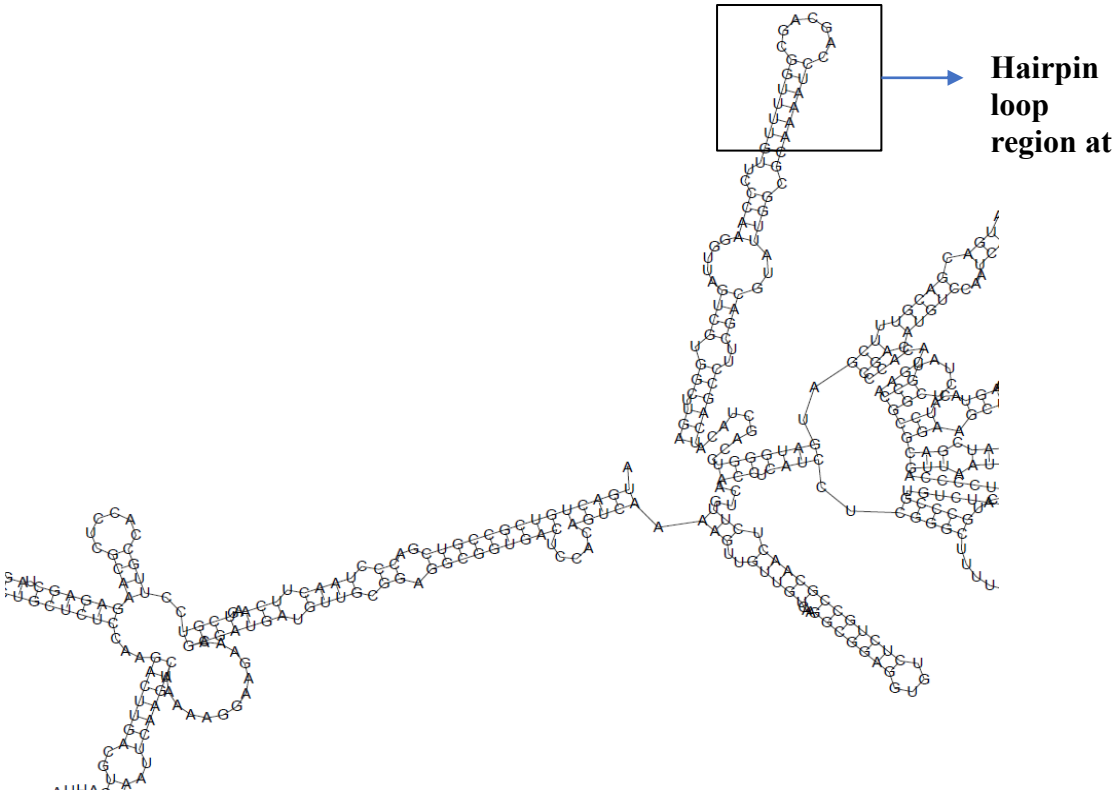

Figure 5.6: *C. auris HAC1* RNA secondary structure showing hairpin loop around 5' splice site

5.2.2 Cloning of C. auris HAC1 gene

The bioinformatics analysis showed the presence of UPR element *HAC1* in *C. auris*. Hence, to further understand if the *HAC1* gene is involved in mediating the ER stress, the cloning of

C. auris HAC1 gene was performed in the pESC-URA plasmid in the first step by using the service provided by GenScript, USA.

The *C. auris HAC1* gene was successfully synthesized and cloned into pESC-URA plasmid by SmaI/XhoI restriction. Sanger sequencing confirmed the *C. auris HAC1* sequence. Restriction digestion of the plasmid containing the *HAC1* gene by SmaI and XhoI enzymes showed the expected band on agarose gel (Figure 5.7).

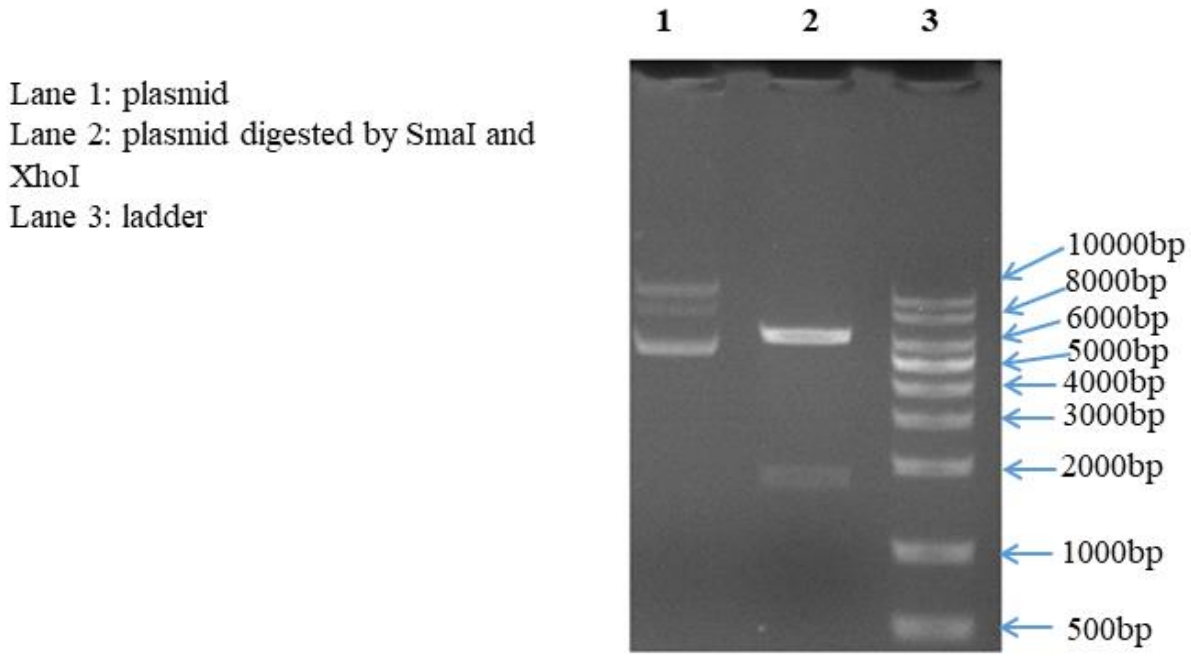

Figure 5.7: Restriction digestion of the pESC-URA plasmid containing *C. auris HAC1*

5.2.3. Genetic complementation analysis

5.2.3.1 Lithium acetate mediated transformation

The pESC-URA plasmid with the cloned *C. auris HAC1* gene was transformed in *S. cerevisiae HAC1* delete strain by using lithium acetate mediated transformation method as described in section 4.2.3.1. The *HAC1* containing plasmid was transformed into *S. cerevisiae HAC1* delete strain because of failure in generating *C. auris HAC1* delete strain even after multiple attempts.

The *S. cerevisiae HAC1* delete strain is histidine, leucine, methionine and uracil auxotroph. The formation of colonies in SC media without uracil suggests that the *S. cerevisiae HAC1* delete strain was transformed with *pESC-URA* plasmid containing the *C. auris HAC1* gene (Figure 5.8).

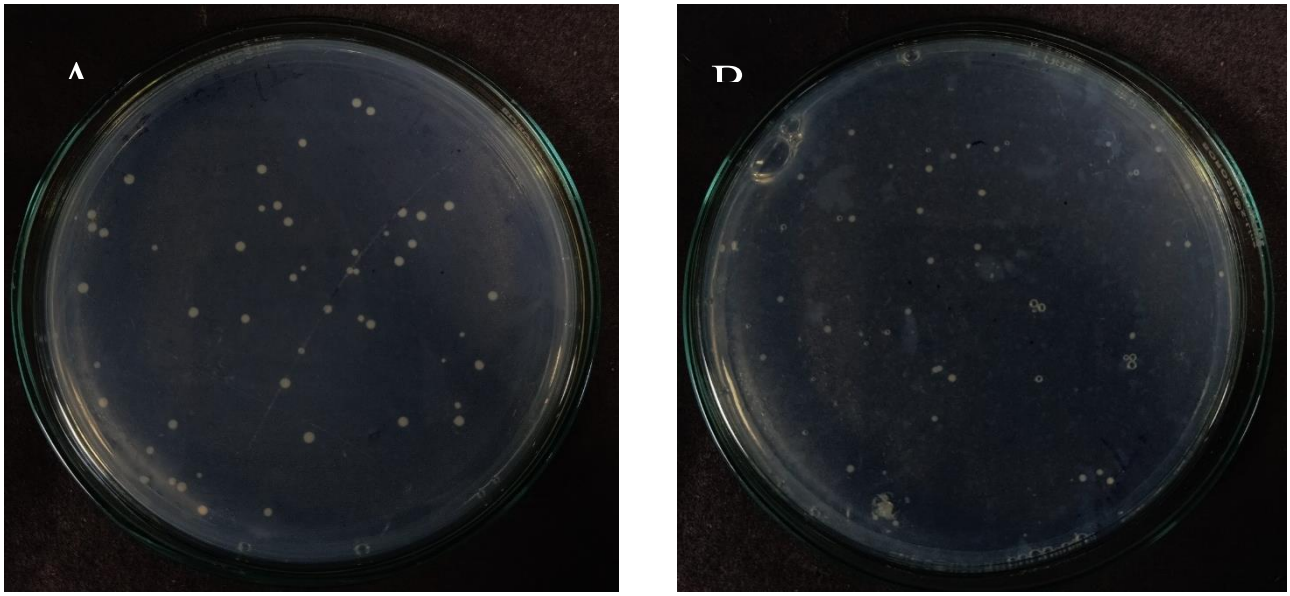

Figure 5.8: Transformation of *S. cerevisiae HAC1* delete strain with pESC-URA plasmid containing *C. auris HAC1*. A. Transformed *S. cerevisiae* (*HAC1* delete) after 48 hours on SC-URA plate with dextrose B. Transformed *S. cerevisiae* (*HAC1* delete) after 48 hours on SC-URA plate with galactose

5.2.3.2 Patching and replica plating of the transformed cells

The randomly selected colonies which were then patched on SC-URA plates also grew (Figure 5.9). The patched colonies were replica plated on SC-URA media containing different concentrations of DTT for inducing endoplasmic reticulum stress. The cells grew on media without DTT, 5mMM DTT and 10mMM DTT. However, at higher DTT concentrations the growth was significantly inhibited in comparison to the cells without DTT stress (Figure 5.10).

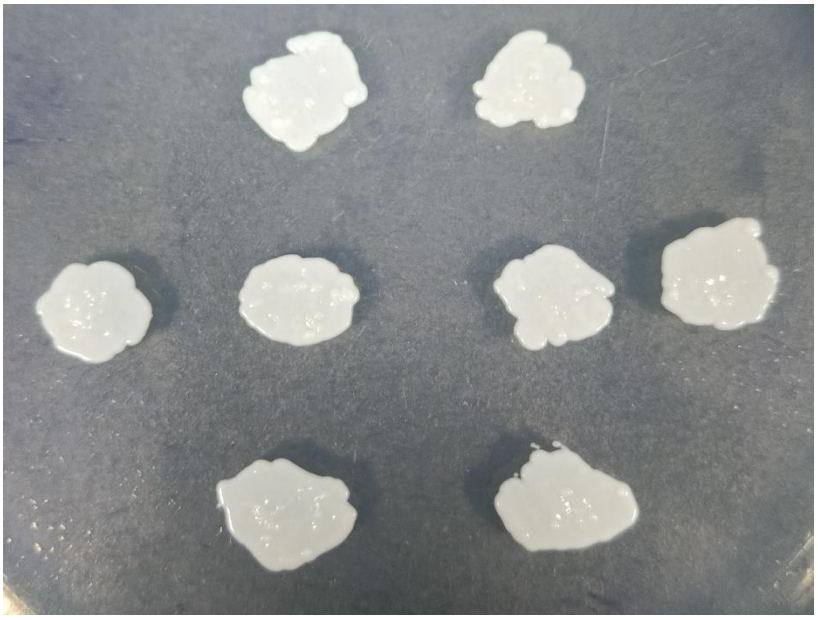

Figure 5.9: Patched transformants on SC-URA media

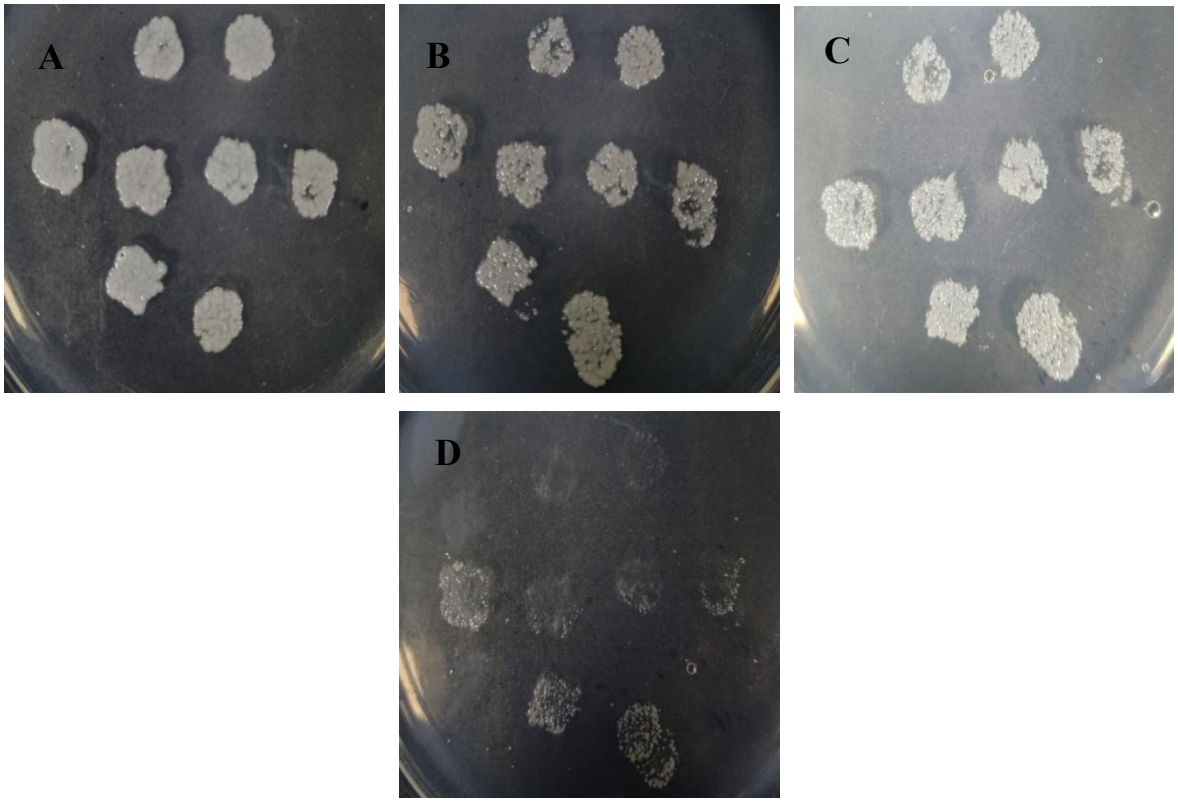

Figure 5.10: Growth of the transformants under DTT stress A. no DDT stress. B. 5mM DTT stress C. 10mM DTT stress D. 20mM DTT stress

5.2.3.3 Dilution spotting

The dilution spotting of *S. cerevisiae* WT strain (BY4741), *S. cerevisiae HAC1* delete strain and *S. cerevisiae HAC1* delete strain complemented with *C. auris HAC1* (SC-Cau-HAC1) gene on different concentrations of DTT shows that the SC-Cau-HAC1 strain can tolerate higher concentrations of DTT in comparison to wild type and *S. cerevisiae HAC1* delete strain (Figure 5.11). This analysis shows that the *C. auris HAC1* can complement the *S. cerevisiae HAC1* delete strain and help to bear endoplasmic reticulum stress.

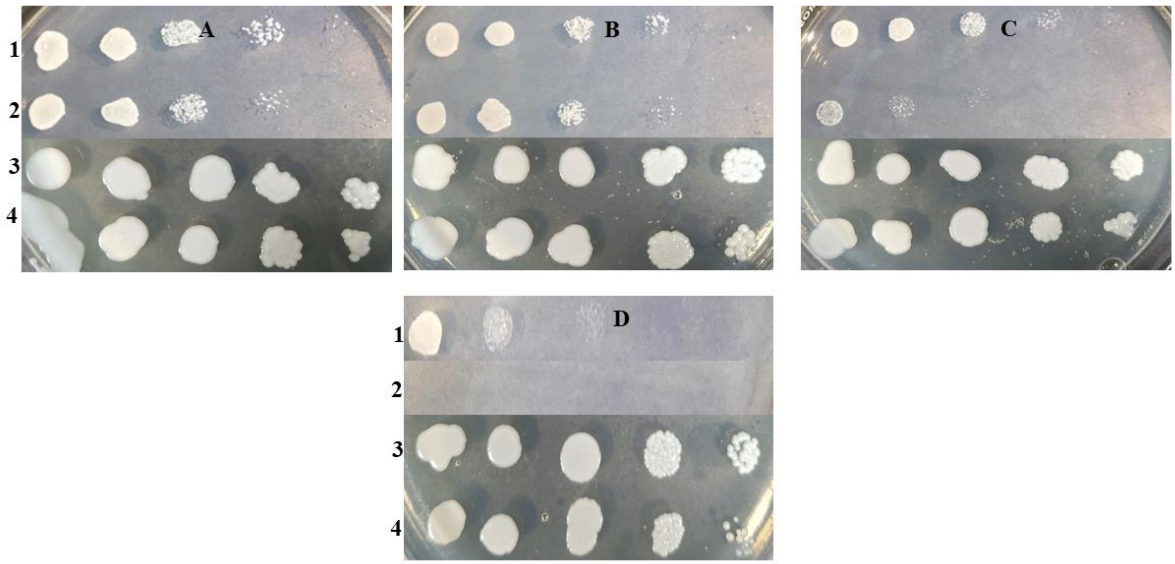

Figure 5.11: Growth of different strains under DTT stress. *S. cerevisiae* WT strain (1), *S. cerevisiae HAC1* delete strain (2) and SC-Cau-HAC1 strains (3 and 4) under DTT stress. A. No DTT B. 5mM DTT C. 10mM DTT D. 20mM DTT (Rows 1-2 and rows 3-4 are from separate plates)

The cloning of the *HAC1* gene in pESC-URA plasmid and genetic complementation in *S. cerevisiae HAC1* delete strain showed that the *C. auris HAC1* could complement *HAC1* gene in the *S. cerevisiae HAC1* delete strain. The *S. cerevisiae HAC1* delete strain's growth is gradually inhibited as the concentration of DTT increases whereas the *S. cerevisiase* complemented with *HAC1* gene from *C. auris* thrives even at higher DTT stress. This suggests that the *C. auris HAC1* is likely to be involved in mediating ER stress. However, future studies focusing on the splicing of the *C. auris HAC1* gene and further confirmation by RT-PCR analysis are required.

Objective 3: In-silico identification of small molecules targeting unfolded protein response proteins (HAC1 and IRE1) of *C. auris*

The UPR pathway is a cellular signalling pathway found in eukaryotes that helps maintain proteostasis within the cell. Various research indicate that even fungal pathogens employ this pathway as a means to evade the host's defences, maintain virulence and assimilate to ER stress [197,204,207]. Two key players in the UPR, Ire1p and Hac1p, serve as mediators and significantly contribute to the pathogenesis and virulence along with maintaining proteostasis under ER stress (discussed in sections 2.5 and 2.6 of the review of literature). The work done in objective 2 suggests that the *C. auris HAC1* gene could play an important role in maintaining homeostasis during DTT-mediated ER stress. Furthermore, the involvement of the UPR elements, Ire1p and Hac1p, in the virulence and pathogenesis of different *Candida sp.* suggests that these elements could also be responsible for virulence and pathogenesis in *C. auris* as well. Hence, the possibility of these elements as potential targets by using phytochemicals for drug discovery against *C. auris* has been evaluated using several computational approaches. The computational analysis could help in predicting the properties of different phytochemicals and identifying potential drug candidates. It can complement the experimental studies and enable virtual screening, and rational drug design, which can significantly accelerate the drug development process. Furthermore, the computational analysis can help in the prediction of potential binding sites or interactions between UPR proteins and phytochemicals that could act as potential antifungal drugs against *C. auris*. So in the subsequent sections, an attempt has been made to identify potential phytochemicals that can be used as drug molecules based on their molecular properties, biological activities and ADME properties. Furthermore, the binding and interactions of the phytochemicals with UPR elements, Ire1p and Hacp, have also been explored using MD and MDS studies.

5.3.1. Determination of the bioactivity, molecular properties, and the drug-likeness of the small molecules

The compounds selected in this study have shown different therapeutic effects in previous studies. Chloroquine phosphate is an approved anti-malarial drug [13]. Various in vitro and animal model studies have shown the antiviral, anti-diabetic, antimicrobial, and anti-sclerotic effects of mangiferin [14]. Flinderole-B has shown antimalarial property [15]. Drummondin-E has shown antibacterial activity [16]. Butanoic acid has shown a role in the treatment of inflammatory intestinal diseases [17]. As these compounds (Table 5.6) have already shown a

plethora of therapeutic effects, in this study we explored their potential as antifungal drugs. Furthermore, these phytochemicals were identified to be present in the extract of various plants in our lab and our collaborators' lab. So, these phytochemicals belonging to natural origin were of primary interest as they are more likely to be safer than chemically synthesized molecules.

Table 5.6: Classification of various phytochemicals used in this study

Serial Number	**Compound**	**PubChem ID**	**Smile Structure**	**Classification**
1	Linoleic acid	5280450	CCCCCC=CCC=CCCCCCCCC(=O)O	Fatty acid
2	Oleic acid	445639	CCCCCCCCC=CCCCCCCCC(=O)O (3D structure downloaded from drug database, ID DB04224	Fatty acid
3	Butanoic acid	264	CCCC(=O)O	Fatty acid
4	Benz(a)Anthracene,1,12-dimethyl	9407	CC1=C2C(=CC=C1)C=CC3=CC4=CC=CC=C4C(=C32)C	Phenanthrenes
5	Palmitic acid	985	CCCCCCCCCCCCCCCC(=O)O	Fatty acid
6	Mangiferin	5281647	C1=C2C(=CC(=C1O)O)OC3=C(C2=O)C(=C(C(=C3)O)C4C(C(C(C(O4)CO)O)O)O)O	Xanthonoid
7	Plumbagin	10205	CC1=CC(=O)C2=C(C1=O)C=CC=C2O	Naphthoquinone
8	Betulinic acid	64971	CC(=C)C1CCC2(C1C3CCC4C5(CCC(C(C5CCC4(C3(CC2)C)C)(C)C)O)C)C(=O)O 3D downloaded from drug database DB12480	Triterpenoid
9	1,7-Dihyroxy-3-methoxyxanthone	129716110	CC(=C)C=CC1=C(C=C2C(=C1O)C(=O)C3=C(O2)C=CC(=C3)O)OC	Xanthone
10	Ursolic acid	64945	CC1CCC2(CCC3(C(=CCC4C3(CCC5C4(CCC(C5(C)C)O)C)C)C2C1C)C)C(=O)O DB15588 3D downloaded from drug database	Triterpenoid
11	Oleanolic acid	10494	CC1(CCC2(CCC3(C(=CCC4C3(CCC5C4(CCC(C5(C)C)O)C)C)C2C1)C)C(=O)O)C	Triterpenoid
12	Chloroquine phosphate	64927	CCN(CC)CCCC(C)NC1=C2C=CC(=CC2=NC=C1)Cl.OP(=O)(O)O.OP(=O)(O)O	Quinoline
13	Alpha pyrone	11183167	CCCCCCC1=CC(=CC(=O)O1)C	Lactone
14	Flinderole B	25195148	CC(=CC1CC(N2C1=C(C3=CC=CC=C32)CCN(C)C)(C)C=CC4=C(C5=CC=CC=C5N4)CCN(C)C)C	Alkaloid

15	Gallic acid	370	C1=C(C=C(C(=C1O)O)O)C(=O)O	Phenolic acid
16	Drummondin E	132133	CC(=CCC1(C(=C(C(=C(C1=O)C(=O)C)O)CC2=C(C=C(C(=C2O)C(=O)C)O)OCC=C(C)C)O)C)C	Resorcinols
17	Stigmasterol	5280794	CCC(C=CC(C)C1CCC2C1(CCC3C2CC=C4C3(CCC(C4)O)C)C)C(C)C	Phytosterol
18	L-Homoserine lactone hydrochloride	2733667	C1COC(=O)C1N.Cl	Lactone
19	Coumarin	323	C1=CC=C2C(=C1)C=CC(=O)O2	Lactone

1,7-Dihyroxy-3-methoxyxanthone, Plumbain, Butanoic acid, Alpha pyrone, Drummondin E, and Gallic acid did not violate any rule in Lipinski's rule of five whereas other compound violated 1 or 2 rules. If a compound follows Lipinski's rule of five, it is more likely to be an active drug like molecule [288]. The results of the molecular property analysis by the Molinspiration tool are shown in Table 5.7. Molecular properties such as MW, nON, nOHN, and logP value of the compounds were predicted by the Molinspiration tool. The bioactivity of the compounds was also determined by the Molinspiration tool (Table 5.8). Molecules with a bioactivity score more than 0 are most likely to have significant bioactivity, while -0.50 to 0 will be moderately bioactive and below -0.50 is expected to be inactive. 1,7-Dihyroxy-3-methoxyxanthone was determined to be nuclear receptor ligand (NRL). Benz(a)anthracene is likely to be an enzyme inhibitor (EI) and kinase inhibitor (KI). Chloroquine phosphate is predicted as a GPCR ligand, ion channel modulator (ICM), and kinase inhibitor (KI). Betulinic acid exhibited the most bioactivity. It was predicted to be GPCR ligand, EI, KI, protease inhibitor (PI), NRL and ICM. Drummondin E and Mangiferin are predicted to be NRL and EI. Flinderole B is likely to be GPCR ligand and EI. Friedelin is expected to be NRL and EI. The bioactivities of all the compounds are listed in Table 5.8. Finally, chloroquine phosphate, Betulinic acid, Drummondin E, Ursolic acid, Flinderole B, Oleanolic acid, Mangiferin and Stigmasterol were predicted to be potential drug-like molecules on the basis of their drug-likeness score determined by Molsoft tool. The drug-likeness scores of all the compounds are listed in Table 5.9. Compounds with drug likeness score between 0-2.5 are more likely to be drugs.

Table 5.7: Molecular properties of the compounds

S.	Compound	Log	TPSA	Nato	MW	nO	nOH	nVi	nRo	Volum

N		P		m		N	N	o	t	e
1	Linoleic acid	6.86	37.3	20	280.45	2	1	1	14	312.65
2	Butanoic acid	1	37.3	6	88.11	2	1	0	2	89.80
3	Benz(a)Anthracene, 1,12-dimethyl	6.24	0	20	256.35	0	0	1	0	249.14
4	Oleic acid	7.58	37.3	20	282.47	2	1	1	15	318.84
5	Palmitic acid	7.06	37.3	18	256.43	2	1	1	14	291.42
6	Mangiferin	-0.16	201.27	30	422.34	11	8	2	2	335.80
7	Plumbagin	1.78	54.37	14	188.18	3	1	0	0	163.16
8	Betulinic acid	7.04	57.53	33	456.71	3	2	1	2	472.04
9	1,7-Dihyroxy-3-methoxyxanthone	4.47	79.9	24	324.33	5	2	0	3	285.87
10	Ursolic acid	6.79	57.53	33	456.71	3	2	1	1	471.49
11	Oleanolic acid	6.72	57.53	33	456.71	3	2	1	1	471.14
12	Chloroquine phosphate	5	28.16	22	319.88	3	1	1	8	313.12
13	Alpha pyrone	3.95	30.21	14	194.27	2	0	0	5	201.73
14	Flinderole B	7.58	27.2	38	508.75	4	1	2	9	516.62
15	Gallic acid	0.59	97.98	12	170.12	5	4	0	1	135.1
16	Drummondin E	4.68	141.36	33	498.57	8	4	0	9	463.71
1	Stigmasterol	7.87	20.23	30	412.7	1	1	1	5	450.33

7										
18	L-Homoserine lactone hydrochloride	-1.98	52.33	7	101.11	3	2	0	0	91.48
19	Coumarin	2.01	30.21	11	146.15	2	0	0	0	128.59

Table 5.8: Small molecules' bioactivities predicted by Molinspiration

Optimal parameters: a molecule with bioactivity score more than 0 is most likely to have considerable bioactivity, while -0.50 to 0 will be moderately bioactive and below -0.50 is expected to be inactive

S. N	Compound	GPCR	ICM	KI	NRL	PI	EI
1	Linoleic acid	0.29	0.17	-0.16	0.31	0.12	0.38
2	Butanoic acid	-3.34	-3.52	-3.77	-3.13	-3.32	-3.18
3	Benz(a)Anthracene, 1,12-dimethyl	-0.03	-0.17	0.05	-0.01	-0.23	0.06
4	Oleic acid	0.17	0.07	-0.22	0.23	0.07	0.27
5	Palmitic acid	0.02	0.06	-0.33	0.08	-0.04	0.18
6	Mangiferin	0.06	-0.04	0.06	0.14	-0.03	0.48
7	Plumbagin	-0.84	-0.31	-0.57	-0.69	-1.00	0.02
8	Betulinic acid	0.31	0.03	0.50	0.93	0.14	0.55
9	1,7-Dihyroxy-3-methoxyxanthone	-0.15	-0.26	-0.15	0.40	-0.20	0.27
10	Ursolic acid	0.28	-0.03	-0.5	0.89	0.23	0.69
11	Oleanolic acid	0.28	-0.06	-0.4	0.77	0.15	0.65
12	Chloroquine phosphate	0.32	0.32	0.38	-0.19	0.05	0.11
13	Alpha pyrone	-0.91	-0.79	-1.27	-0.84	-0.67	-0.26
14	Flinderole B	0.27	-0.12	0.09	-0.06	-0.08	0.17
15	Gallic acid	-0.77	-0.26	-0.88	-0.52	-0.94	-0.17
16	Drummondin E	0.32	0.32	0.38	-0.19	0.05	0.11
17	Stigmasterol	0.12	-0.08	-0.48	0.74	-0.02	0.53

18	L-Homoserine lactone hydrochloride	-3.22	-3.35	-3.60	-3.66	-2.97	-3.08
19	Coumarin	-1.44	-0.86	-1.57	-1.14	-1.43	-0.58

Table 5.9: Small molecules' drug-likeness predicted by Molsoft

Serial number	**Compound**	**Drug likeness score**
1	Linoleic acid	-0.30
2	Butanoic acid	-1.28
3	Benz(a)Anthracene, 1,12-dimethyl	-1.33
4	Oleic acid	-0.30
5	Palmitic acid	-0.54
6	Mangiferin	2.25
7	Plumbagin	-0.23
8	Betulinic acid	0.25
9	1,7-Dihyroxy-3-methoxyxanthone	0.01
10	Ursolic acid	0.66
11	Oleanolic acid	0.37
12	Chloroquine phosphate	1
13	Alpha pyrone	-0.85
14	Flinderole B	0.37
15	Gallic acid	-0.22
16	Drummondin E	0.38
17	Stigmasterol	0.62
18	L-Homoserine lactone hydrochloride	-1.10
19	Coumarin	-1.05

5.3.2 ADMET property prediction of the small molecules

For a compound to be successful under clinical trials it must have good absorption, distribution, metabolism and excretion (ADME) properties. Moreover, it must not be toxic. So, for the prediction of the ADMET properties admetSAR2 web server was used [290]. After the overall analysis of ADMET properties of the compounds Flinderole B, Linoleic acid, Butanoic acid, Oleic acid, Palmitic acid, Betulinic acid, Ursolic acid, Oleanolic acid, Alpha pyrone and Stigmasterol were found to have the ability to cross the blood-brain barrier, and could permeate and get absorbed in the human intestine. These two compounds were also found to be non-carcinogenic. The detailed ADMET properties of the other compounds are in Table 5.10.

Table 5.10: ADMET properties of the small molecules predicted by admetSAR

Compounds	**Blood-brain barrier**	**Human intestinal absorption**	**Caco-2 permeability**	**CYP inhibitory promiscuity**	**AMES toxicity**	**Hepatoxicity**	**Carcinogenicity**	**Rat cute toxicity LD_{50} mol/kg**
Linoleic acid	+	+	+	Low	Non-toxic	Non-toxic	Non-carcinogen	1.3991
Butanoic acid	+	+	+	Low	Non-toxic	Non-toxic	Non-carcinogen	1.6755
Benz(a)Anthracene, 1,12-dimethyl	+	+	+	Low	Toxic	Toxic	Non-carcinogen	2.1323
Oleic acid	+	+	+	Low	Non-toxic	Non-toxic	Non-carcinogen	1.3991
Palmitic acid	+	+	+	Low	Non-toxic	Non-toxic	Non-carcino	1.3275

							gen	
Mangiferin	-	+	-	Low	Toxic	Toxic	Non-carcinogen	2.3664
Plumbagin	+	+	+	High	Toxic	Toxic	Non-carcinogen	3.2704
Betulinic acid	+	+	+	Low	Non-toxic	Non-toxic	Non-carcinogen	3.8916
1,7-Dihyroxy-3-methoxyxanthone	-	+	+	High	Toxic	Toxic	Non-carcinogen	3.2405
Ursolic acid	+	+	+	Low	Non-toxic	Non-toxic	Non-carcinogen	2.3902
Oleanolic acid	+	+	+	Low	Non-toxic	Non-toxic	Non-carcinogen	2.3902
Chloroquine phosphate	+	+	+	Low	Toxic	Toxic	Non-carcinogen	2.6972
Alpha pyrone	+	+	+	Low	Non-toxic	Non-toxic	Non-carcinogen	2.0070
Flinderole B	+	+	-	Low	Toxic	Toxic	Non-carcinogen	2.9504
Gallic	-	+	-	Low	Non-	Non-	Non-	1.8670

acid					toxic	toxic	carcinogen	
Drummondin E	+	+	-	High	Non-toxic	Toxic	Non-carcinogen	2.4138
Stigmasterol	+	+	+	Low	Non-toxic	Non-toxic	Non-carcinogen	2.6561
L-Homoserine lactone hydrochloride	+	+	-	Low	Non-toxic	Toxic	Non-carcinogen	2.3093
Coumarin	-	+	+	Low	Non-toxic	Toxic	Non-carcinogen	2.4622

5.3.3 Determination of tertiary structure of the HAC1 and IRE1 proteins of Candida auris and validation of their predicted tertiary structure

The tertiary structures of the Hac1p of *S. cerevisiae, C. albicans* and *C. auris* are unavailable in the UNIPROT or PDB database. Furthermore, the tertiary structure of only Ire1p of *S. cerevisiae* is available in the PDB database. The molecular docking analysis for determining the binding of the phytochemicals with UPR elements requires the tertiary structures of the protein. Hence, the prediction of the *C. auris* Ire1p and Hac1p tertiary structure was performed computationally.

The models of the tertiary structures were predicted by the I-Tasser program and the structure was corroborated by creating Ramachandran plot using the Rampage program. The C-score of the top of the 3D models of *HAC1* is -2.35. The C-score of the best 3D model of *IRE1* is -0.84. Typically the C-score value ranges from -5 to 2 and higher C-score values imply a model of higher significance [292]. The C-score value of the models of *HAC1* and *IRE1* suggests the 3D model is of better quality. The tertiary structures of *HAC1* and *IRE1* proteins

are shown in Figure 5.12. The Ramachandran plots of the proteins are shown in Figure 5.13. Altogether 87.2% of the residues in *HAC1* protein of *C. auris* were present in favoured or allowed regions of the Ramachandran plot. Similarly, for the *IRE1* protein of *C. auris* 86.1% of the residues were present in favored or allowed region. The Ramachandran plot and C-score imply that the 3D models of the Ire1p and Hac1p are valid and of good quality.

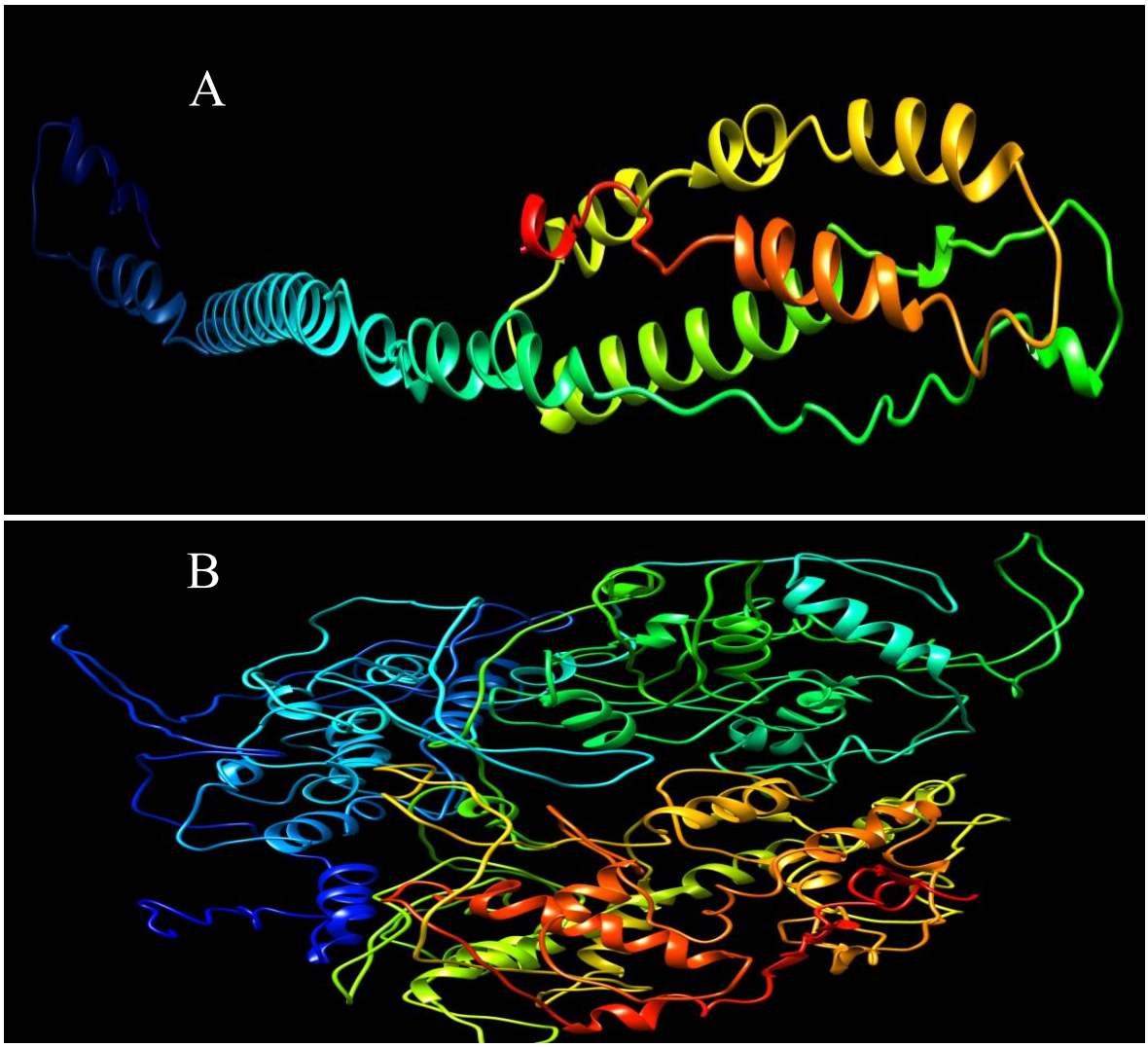

Figure 5.12: Tertiary structures of *C. auris* UPR elements. A. 3D Model of Hac1p of *C. auris* B. 3D Model of Ire1p of *C. auris*

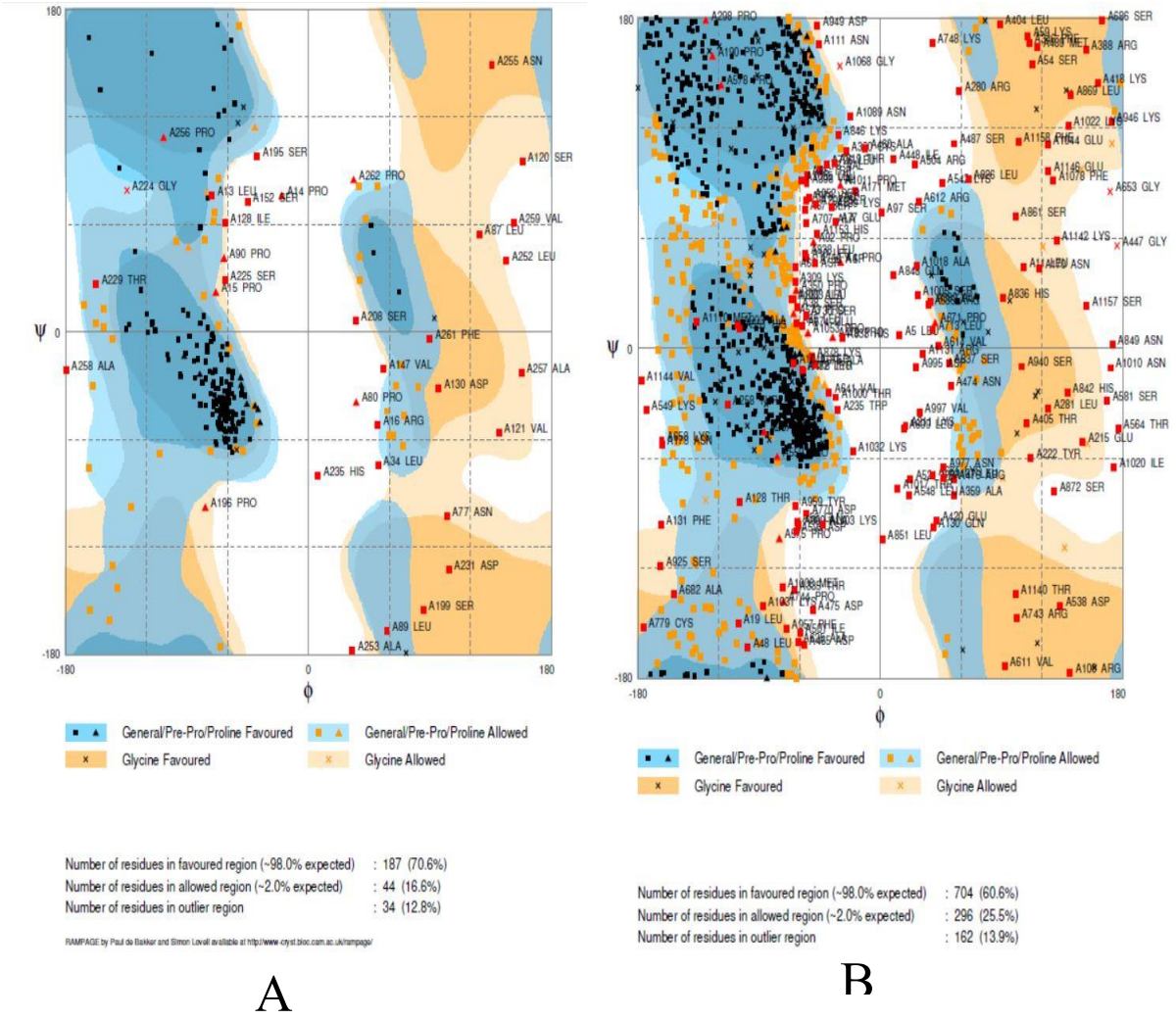

Figure 5.13: Validation of 3D Models of the HAC1 (A) and IRE1 (B) protein using Ramachandran plot

5.3.4. Molecular docking analysis of the small molecules with Hac1p and Ire1 of Candida auris

After the analysis of the molecular properties, drug-likeness, bioactivity and ADMET properties of the compounds, Flinderole B, Drummondin E, Betulinic acid, Ursolic acid, Oleanolic acid, Stigmasterol were selected for further analysis (see Tables 5.7-5.10). These compounds have good drug-likeness scores and ADME properties. They were found to be non-carcinogenic, nontoxic and non-hepatotoxic; and also followed Lipinski's rule of five. These findings suggest that these compounds are more likely to be drug compounds. Hence, the ability of these compounds to interact with the *HAC1* and *IRE1* proteins was determined by performing molecular docking analysis. The Patchdock server was used to perform molecular docking. This server predicts the Atomic contact energy, Geometric shape complementarity score and interface area between the interaction of ligand and receptor

molecules. The compounds with the maximum geometric shape complementarity value and minimum atomic contact energy when docked with the *HAC1* and *IRE1* proteins were chosen because the complexes with the maximum geometric shape complementarity value have minimum steric hindrances and have wide interface area [294] and lesser atomic contact energy indicates the complex is relatively stable and favourable because of the reduced desolvation energy [352]. The interaction between betulinic acid and *HAC1* has the lowest atomic contact energy suggesting the interaction between *HAC1* and betulinic acid is more stable. Similarly, for the docking between *IRE1* and Flinderole B has the lowest atomic contact energy. The molecular docking analysis outcomes of the small molecules with *HAC1* and *IRE1* are provided in Table 5.11 and Table 5.12 respectively. Furthermore, the types of bonds involved in the interaction of the compounds and the proteins and the length of these bonds were determined by Ligplot analysis (Figure 5.14) [353]. With *HAC1*, betulinic acid formed two H-bonds with SER 210 ($2A^0$) and ARG 114 ($2.4A^0$). Also, hydrophobic interactions were there. In the interaction of *HAC1* with stigmasterol and Drummondin E only hydrophobic interactions were involved. In the interaction of *HAC1* with Oleanolic acid (Ser112, $2.13A^0$), Flinderole B (Asn110, $2.31A^0$) and Ursolic acid (Ser210, $2.33A^0$) one hydrogen bond and hydrophobic interactions were involved. Drummondin E formed two H-bonds with *IRE1* at Lys28 ($2.48A^0$) and Gly727 ($3.07A^0$). Also, hydrophobic interactions were there. Flinderole B formed one H-bond with *IRE1* at Ser17 ($2.97A^0$). Also, hydrophobic interactions were there. However, in the interaction of *IRE1* with Betulinic acid, Oleanolic acid, Stigmasterol and Ursolic no H-bonds were formed, only hydrophobic interactions were involved.

Table 5.11: Docking of Hac1p with small molecules

Serial Number	**Receptor**	**Ligand**	**Score**	**Area**	**Atomic Contact Energy**
1	HAC1	Betulinic Acid	5194	698.00	-373.10
2	HAC1	Drummondin E	5726	744.20	-285.80
3	HAC1	Flinderole B	6726	869.10	-359.11
4	HAC1	Oleanolic	5410	695.50	-267.24

		acid			
5	HAC1	Stigmasterol	5724	796.40	-328.51
6	HAC1	Ursolic Acid	5418	734.80	-356.10

Table 5.12: Docking of Ire1p with small molecules

Serial Number	**Receptor**	**Ligand**	**Score**	**Area**	**Atomic Contact Energy**
1	IRE1	Betulinic Acid	5874	728.70	-260.67
2	IRE1	Drummondin E	6654	80.7.60	-189.74
3	IRE1	Flinderole B	7020	987.30	-271.78
4	IRE1	Oleanolic acid	6080	738.40	-192.52
5	IRE1	Stigmasterol	6356	804.40	-217.25
6	IRE1	Ursolic Acid	5798	732.00	-249.00

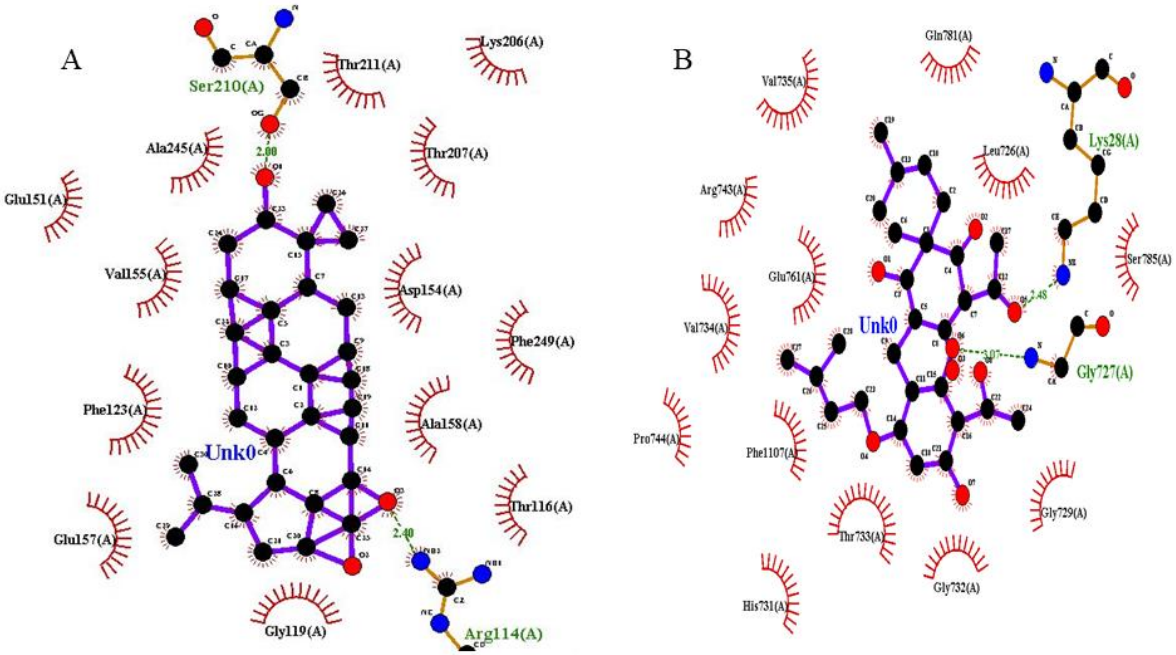

Figure 5.14: Ligplot analysis. (A) Hac1p with Betulinic acid (B) Ire1p with Drummondin-E. The hydrogen bonds are shown in the green dotted lines and others are hydrophobic interaction.

5.3.5. *Molecular dynamics simulation analysis of the docked small molecule-protein complexes*

Among the compounds that could interact with *HAC1*, Betulinic acid formed the most H-bonds and had better atomic contact energy and geometric shape complementarity score (Figure 22). Similarly, among the compounds that could interact with *IRE1*, Drummondin E formed the most H-bonds and had better atomic contact energy and geometric shape complementarity score. More the H-bonds, more stronger the interactions between the drug and receptor will be [354]. Hence, the docked complexes of *HAC1*-Betulinic acid and *IRE1*-Drummondin E were selected for molecular dynamics simulation by using the Amber 18 package (see section 4.3.5 for more detail about the methodology of MD simulations). Molecular dynamics simulation predicts the stability and residual adaptability of the interaction between the compounds and *HAC1 and IRE1* proteins. The graphs showing the stability (RMSD plot) and the residual adaptability (RMSF) plot of the molecular interactions are shown in Figure 5.15 and Figure 5.16 respectively. RMSD was found to be in the suitable range of 1 to 5 Å for both the docked complexes, indicating stable configuration for 50 ns run. RMSF was found to be less than 3.0 Å for both the docked complexes, indicating less fluctuation in configuration for 50 ns run. The molecular dynamics simulation studies show that the interactions between the compounds and *HAC1* and *IRE1* proteins are stable and have low fluctuation.

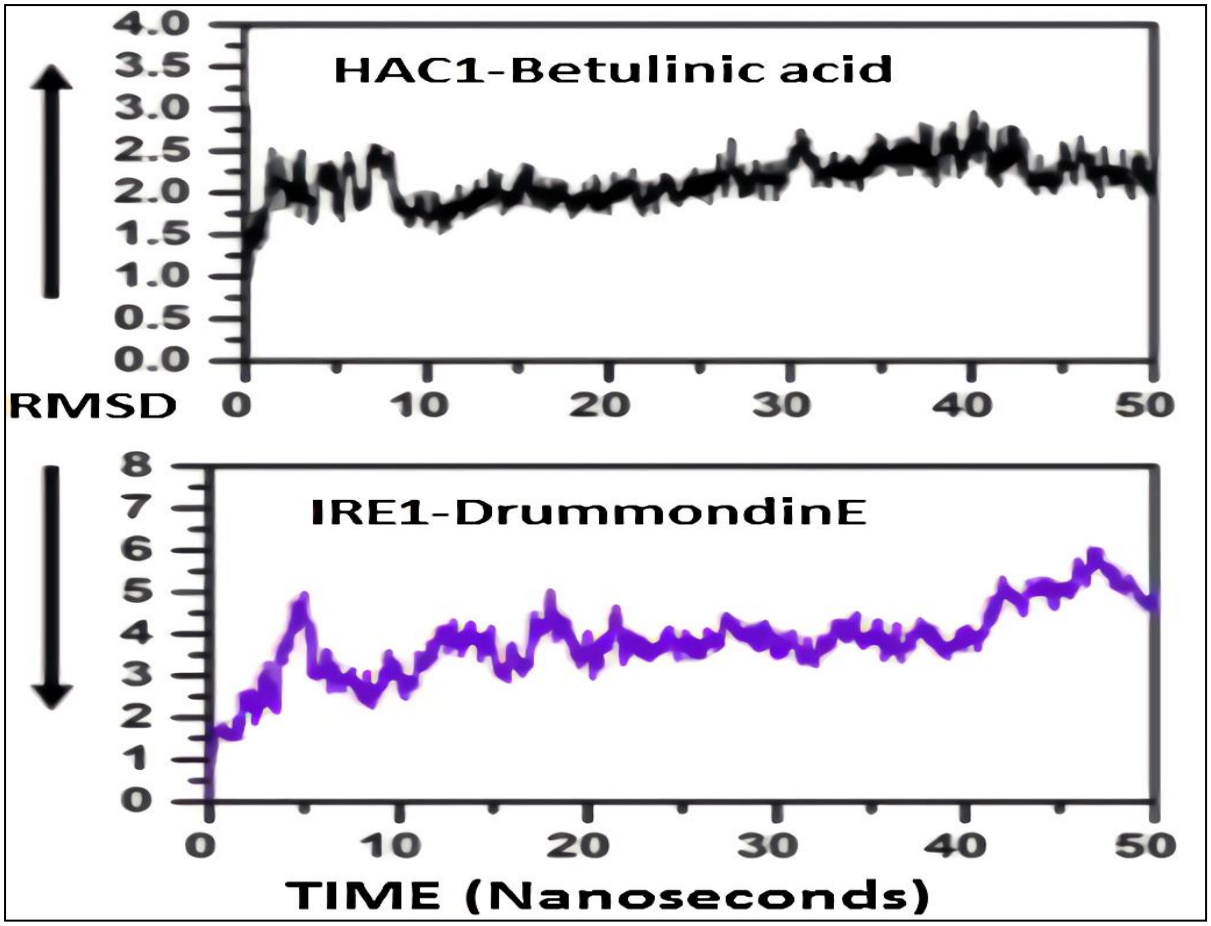

Figure 5.15: RMSD plot of *HAC1*-Betulinic acid and *IRE1*-Drummondin E complexes (In Å)

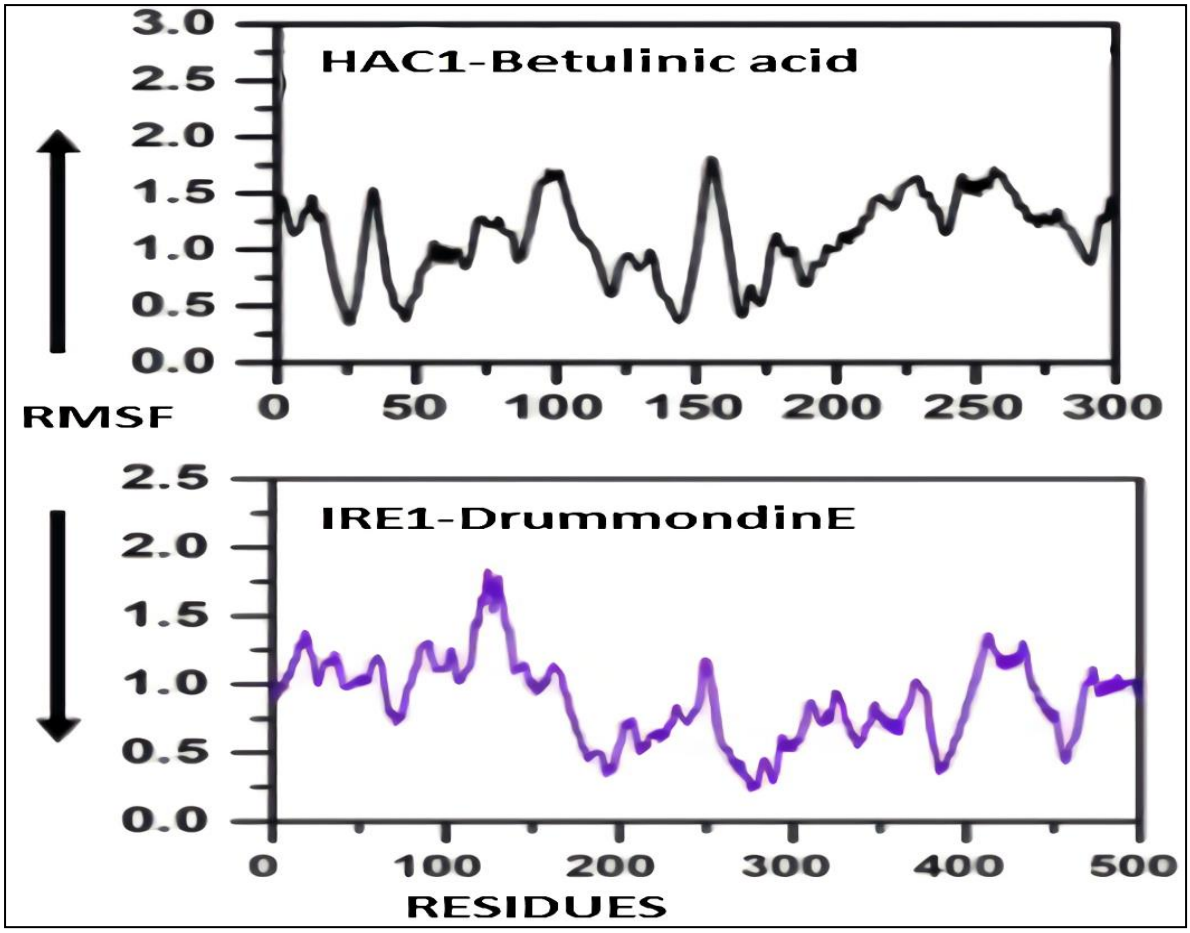

Figure 5.16: RMSF plot of *HAC1*-Betulinic acid and *IRE1*-DrummondinE complexes (In Å)

Discussion

Afterwards, the analysis of the molecular properties, drug likeness, bioactivity and ADMET properties of the compounds, flinderole B, drummondin E, betulinic acid, ursolic acid, oleanolic acid, and stigmasterol were selected for further analysis. These compounds have good drug-likeness score and ADME properties. They were found to be non-carcinogenic, non-toxic and non-hepatotoxic; and also followed Lipinski's rule of five. These findings suggest that these compounds are more likely to be drug compounds. Then, the ability of these compounds to interact with the *HAC1* and *IRE1* proteins was determined by performing the molecular docking analysis. Based on the atomic contact energy and number of hydrogen bonds created during the docking of phytochemicals with the *HAC1* and *IRE1* proteins, Betulinic acid was chosen as a potential small molecule to target the *HAC1* protein and drummondin E was chosen as a potential small molecule to target the *IRE1* protein of *C. auris*. More the number of H-bonds, more stronger the interactions between the drug and receptor will be [354]. Less atomic contact energy suggests the complex will be more stable

and favourable due to the low desolvation energy [352]. Further, the molecular dynamics simulations showed the interactions between the *HAC*1-Betulinic acid complex and *IRE1*-Drummondin E complex were found to have less fluctuations and good stability. Similar, studies have been performed to identify the phytochemicals to target different virulent proteins of *C. albicans* [354]. Jha *et al* reported different phytochemicals that can target cell wall proteins, transcriptional regulators, and proteins necessary for biofilm formation and hypha growth of *C. albicans* using *in silico* approach [354]. However, they did not perform molecular dynamics simulations analysis to determine the stability of the interactions in their study. Another study has also ascertained some ligands to inhibit the CPH1-MAP kinase pathway of *C. albicans* [355]. On the same line in this study also we report phytochemicals that can target unfolded protein response pathway. These phytochemicals could be a beneficial addition to the arsenal in treating *C. auris* infections and can be also tested for their antifungal properties against other pathogenic fungi. The capability of these compounds to suppress the growth of *C. auris* in vitro and in vivo can be determined in future studies. This study helped us to select compounds, from a list of various phytochemicals, which we could use for the next objective of the thesis which is to find novel antifungal compounds against *C. auris*. The possible antifungal molecules identified in this objective have been further evaluated for their ability to inhibit the growth of different *Candida sp.* in the next objective of the thesis.

Objective 4: To test the efficacy and safety of small molecules or its compounds in controlling *C. auris* infection and its mechanism thereof.

The efficacy and safety of small molecules or their compounds in controlling *C. auris* infection are important considerations in the development of potential antifungal agents. The efficacy can be assessed through various *in vitro* and *in vivo* studies. In vitro studies involve testing the compounds against *C. auris* isolates in laboratory settings and evaluating their antifungal activity, and MICs. *In vivo* studies involve testing the compounds in animal models to assess their therapeutic effects, such as reduction in fungal burden and improvement in survival rates. Understanding the mechanism of action of small molecules or their compounds is crucial to determine how they exert their antifungal effects. This can be elucidated through various approaches, including RNA sequencing, RT-PCR, molecular docking studies, molecular dynamics simulations, and biochemical assays. These methods help to identify the target proteins or pathways that the compounds interact with, leading to inhibition of fungal growth or virulence.

To evaluate small molecules as antifungal agents, safety is crucial. This includes testing their cytotoxicity to mammalian cells, drug-to-drug interactions, pharmacokinetics, and pharmacodynamics. Animal research and toxicity and safety analysis in cell lines or moths can help determine the safety and tolerance of the small molecules [356,357]. It has been well documented that *C. auris* may become antifungal unsusceptible after long-term exposure. Studying resistance mechanisms including target protein, efflux pump, and biofilm changes can assist design strategies to reduce resistance and enhance treatment outcomes [62,175,176]. Overall, the effectiveness and safety of small molecules or their compounds for controlling *C. auris* infection and understanding their underlying mechanisms require a comprehensive approach. Based on these parameters we sought to study the small molecules against clinical isolates of *C. auris*.

BA is a triterpenoid found in various plants such as *Betula alba* (stem bark), *Diospyros leucomelas* (stem), *Eucalyptus camaldulensis* (leaves), *Millettia richardiana* (stem bark), *Morus alba* (stem and root), *Salvia officinalis* (leaves) [91,92]. Previous studies have reported antioxidant, anti-diabetic, anti-tumour, anti-inflammatory, hepato-protective, antiviral, antiprotozoal, antimalarial, and neuroprotective properties [93–99]. Furthermore, the analysis in objective 3 also suggested that BA could be a potential antifungal drug by targeting the

UPR pathway. Hence, the antifungal ability of BA against *C. auris* and its possible mode of action was analysed in this objective.

5.4.1. Minimum Inhibitory concentration (MIC) and minimum fungicidal concentration (MFC) determination of betulinic acid

To analyse the antifungal activity of BA against *C. auris* along with other *Candida sp.*, MIC and MFC analysis were performed by following the method discussed in sections 4.4.1 and 4.4.2. The MIC of BA ranged between 16-32 µg/ml (Table 5.13). Similarly, the MFC of BA ranged between 128-512 µg/ml (Table 5.13). Two commonly used antifungals belonging to different classes namely fluconazole (azole) and amphotericin B (polyene) were used as control. The MIC of BA was comparatively higher in comparison to the fluconazole and amphotericin B.

Table 5.13: MIC and MFC of BA in µg/mL

Strains	**Fluconazole (µg/mL)**	**Amphotericin B (µg/mL)**	**MIC BA (µg/mL)**	**MFC BA (µg/mL)**
C. auris (S)	1	0.125	32	128
C. auris (R)	Resistant	0.25	32	128
C. auris 470049	16	0.25	16	512
C. auris 470055	8	0.25	32	256
C. auris 470098	16	0.25	32	128
C. auris 470110	16	0.125	32	256
C. auris 470111	Resistant	0.125	32	128
C. auris 470112	1	0.125	32	128
C. auris 470138	8	0.25	16	512
C. albicans	0.25	0.5	32	128
C. tropicalis 17783	2	1	32	128
C. tropicalis 420226	2	0.5	16	128
C. parapsilosis	4	0.31	32	128
C. krusei	16	0.0625	32	128
C. kefyr	0.25	0.0625	32	256

5.4.2. Field emission scanning electron microscopy to determine the effect of BA on the cell surface of the C. auris isolates

To assess the impact of the treatment of BA on the cell surface appearance and morphology the FESEM analysis of *C. auris* cells either treated with BA or without any treatment was performed as per the methodology discussed in section 4.4.3. After the observation of the cells by FESEM, *C. auris* cells without any treatment displayed smooth cell surfaces in comparison to cells treated with BA which exhibited wrinkled/distorted cell surfaces (Figure 5.17). This analysis shows that there is a likely possibility that BA is affecting the cell morphology either by hindering the cell wall synthesis or cell membrane stability. To understand the possible effects of BA treatment on cell surface further experiments like ergosterol synthesis inhibition assay and RNA sequencing are performed in sections 5.4.3 and 5.4.5.

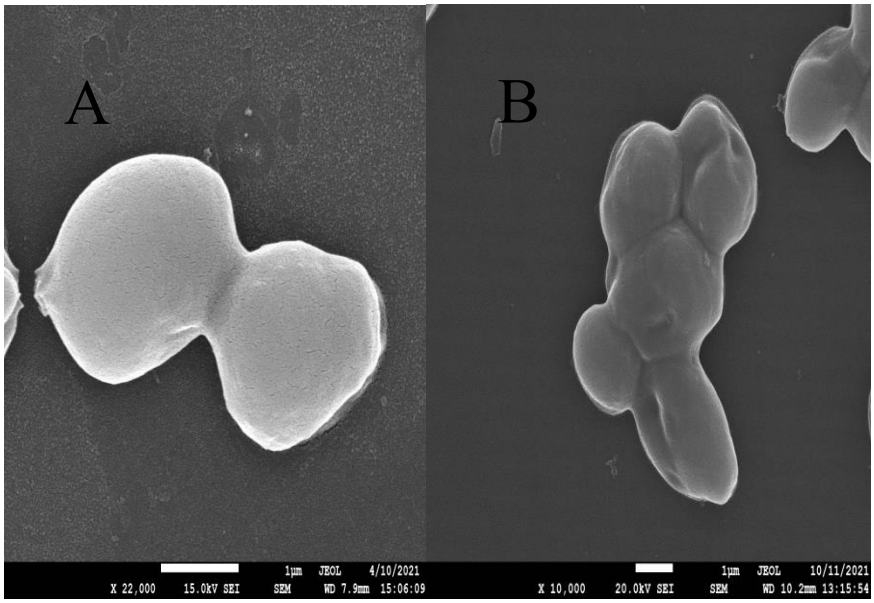

Figure 5.17: FESEM analysis for the comparison of *C. auris* cell surfaces after treatment of BA with *C. auris* cells without any treatment A. Cells without treatment B. Cells treated with BA

5.4.3 Determination of ergosterol synthesis inhibition by BA treatment on C. auris

Ergosterol shows a characteristic spectrophotometric absorbance profile in the range of 240-300 nm. The occurrence of ergosterol and its intermediary compound 24(28) dehyrdorerosterol in the samples generates a distinct graph between 240-300nm. There is a concentration-dependent decline in the concentration of ergosterol in *C. auris* treated with AP

and BA (MIC and 2x MIC) in comparison to the control (*C. auris* cells without any treatment) as implied by the decrease in the height of peaks in the graphs in Figure 5.18.

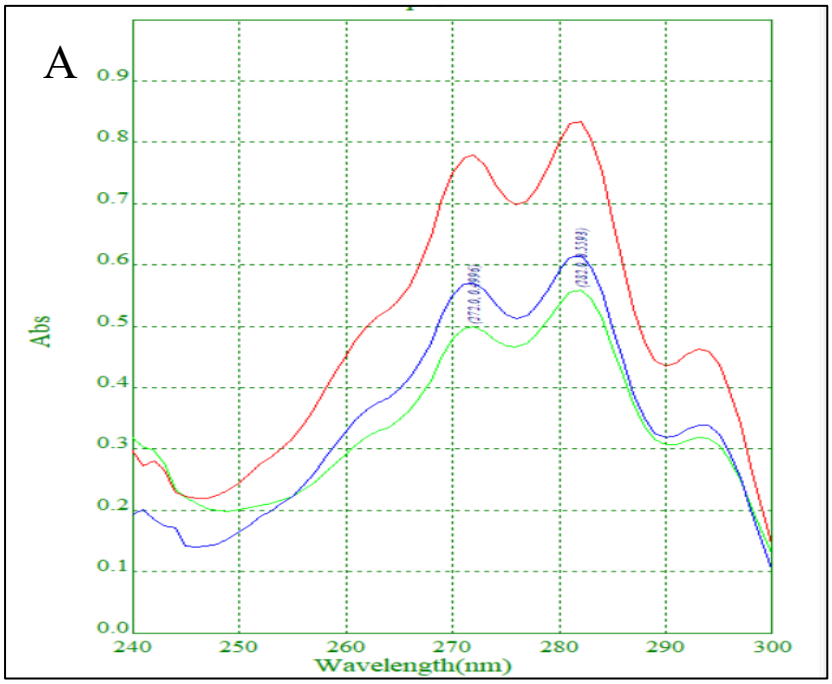

Figure 5.18: Ergosterol synthesis inhibition by BA

5.4.4 Hydrogen peroxide sensitivity assay

The outcomes of the H_2O_2 sensitivity assay are represented in Figure 5.19. The zone of inhibitions of control and cells treated with BA are listed in Table 5.14. As the concentration of BA increases, the *C. auris* cells become more susceptible to H_2O_2 as implied by the increase in the zone of inhibition in comparison to the control. This study suggests that the BA is likely to affect oxidative stress in *C. auris*.

Table 5.14: H_2O_2 sensitivity of *C. auris* treated with BA

SN	Drug Concentration (BA)	Zone of inhibition (BA)
1	0µg/ml	17mm
2	32µg/ml (MIC)	20mm
3	64 µg/ml (2MIC)	23mm

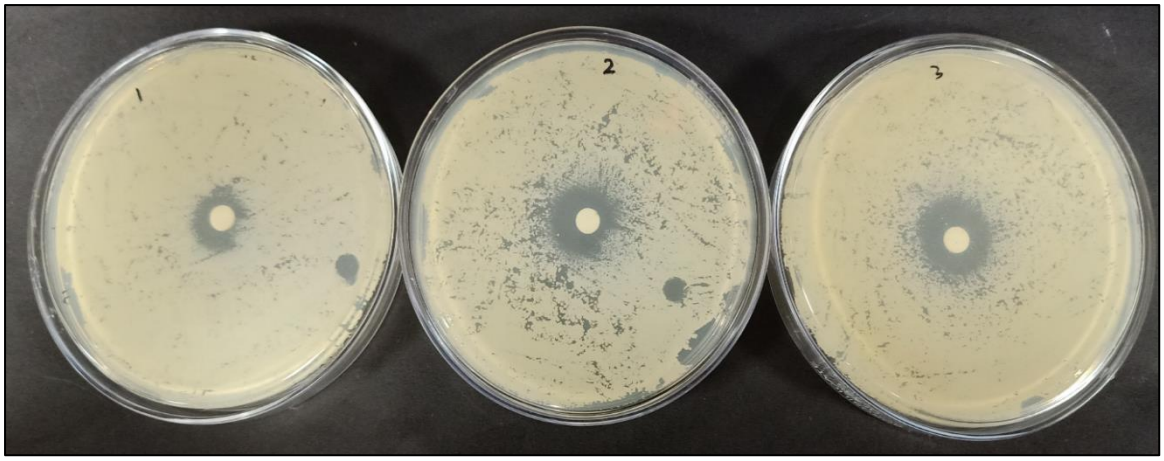

Figure 5.19: Effect of BA on sensitivity of *Candida auris* to H_2O_2. 1: Cells without BA treatment. 2. Cells treated with BA (MIC concentration). 3: Cells treated with BA (2x MIC concentration). With increase in drug concentration the cells show more sensitivity to H_2O_2.

5.4.5 RNA sequencing

The differentially expressed genes (DEGs) are shown in Figure 5.20 and Table 5.15. In *C. auris* cells treated with BA, 10 genes were downregulated logFC value -7 to -2. Of these 10 genes, 4 genes code for uncharacterized proteins. The downregulated genes are part of the superoxide metabolic process (Superoxide dismutase, Sod-Cu domain-containing protein), nucleotide biosynthetic pathway (Nucleoside diphosphate kinase, ATP synthase subunit 5), (1->6)-beta-D-glucan biosynthetic process, cell wall biogenesis. The downregulated genes have functions such as metal ion binding (n=2), ATP binding (n=2), proton-transporting ATP synthase activity, ornithine N5-monooxygenase activity and superoxide dismutase activity. Recently, it has been reported that Sod-Cu domain-containing protein is essential for the virulence of *C. auris* and could be a potential therapeutic antifungal target of *C. auris* [358].

In *C. auris* cells treated with BA, 87 genes were upregulated logFC values 2 to 7. Of these 87 genes, 30 genes code for uncharacterized proteins, 23 for tRNA, 2 for rRNA and 2 for 5s ribosomal RNA. The upregulated genes are part of a wide variety of pathways such as translation, protein folding, DNA replication, DNA-templated transcription, phospholipid biosynthetic process, and oxidative stress response, For 40 proteins the information regarding the process involved is unavailable. The upregulated genes have functions such as ATP binding (n=7), DNA binding (n=3), aminoacyl-tRNA editing activity (n=2), protein serine phosphatase activity (n=2), oxidoreductase activity (n=2), glutathione peroxidase activity.

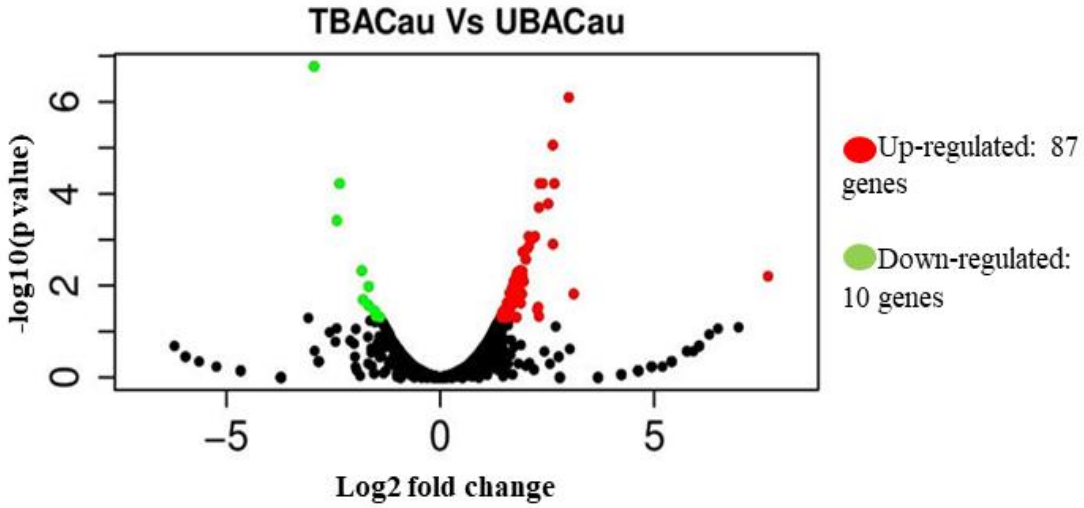

Figure 5.20: The volcano plot of the DEGs. The statistically significant DEGs are symbolized in red dots (up-regulated) or green dots (down-regulated). The x-axis represents the fold change, and the y-axis represents statistical significance.

Table 5.15: The DEGs after BA treatment

Protein	**log2FC**	**p-value**
Sod_Cu domain-containing protein	-2.95	0.00000000003
Superoxide dismutase [Cu-Zn]	-2.35	0.000000047
Nucleoside diphosphate kinase	-2.41	0.00000068
Uncharacterized	7.66	0.000033
Serine/threonine-protein phosphatase	3.12	0.00013
Transcription initiation factor	3.0	0.00000000028
PRELI/MSF1	2.66	0.000000065

domain-containing protein		
DASH complex subunit DAD4	2.63	0.0000033
PKS_ER domain-containing protein	2.63	0.0000000046

The studies in sections 5.4.2 and 5.4.3 show that the treatment of *C. auris* with BA affects the cell surface and the ergosterol synthesis. Ergosterol is a major fungal sterol and has a crucial part in the structure, function and biogenesis of fungal plasma membrane. Furthermore, ergosterol helps fungi in stress adaptation and the ergosterol synthesis pathway is the target of many antifungal drugs [359,360]. However, the RNA-sequencing of BA-treated cells did not show any effect on genes involved in ergosterol synthesis. Nevertheless, the gene KRE9 domain-containing protein which is involved in cell wall biogenesis and (1->6)-beta-D-glucan biosynthesis process of *C. albicans* was down-regulated in *C. auris* treated with BA. The H_2O_2 sensitivity assay performed in section 5.4.4 showed that the *C. auris* cells became more sensitive to oxidative in comparison to control after treatment of BA. The down-regulation of genes pertaining to oxidative stress tolerance in *C. auris* after BA treatment (Superoxide dismutase, Sod-Cu domain-containing protein) treatment shows BA exert oxidative stress in *C. auris*. The possible role of BA in oxidative stress and cell wall synthesis needs to be validated with RT-PCR analysis in future studies.

5.4.6 *GC-MS analysis to study the effect of BA treatment on the metabolite secretion by C. auris*

Microbes, such as *Candida sp.,* release certain substances called metabolites that exert a key part in regulating their pathogenesis and morphology [304]. Hence, GC-MS analysis to determine the impact of BA treatment on the metabolite secretion by *C. auris* was also performed as per the method discussed in section 4.4.7. The *C. auris* cells fluconazole sensitive (NCCPF: 470097) and fluconazole resistant (NCCPF: 470149) strains were treated

with fluconazole BA. Then the cells were subjected to GC-MS analysis for analysing their metabolic profile. The metabolic profile of cells treated with fluconazole was compared with the cells treated with BA. Different treatments given to the *C. auris* cells and the number of metabolites identified by GC-MS analysis are presented in Table 5.16. In Figure 5.21 the chromatogram of the different metabolites present in the ethyl acetate extract of *C. auris* cells treated with fluconazole have been shown.

Various metabolites belonging to different classes such as 2,5-diketopiperazines, delta lactam, fatty alcohol, piperazinone, pyrazine derivative, and triterpene were detected in the ethyl acetate metabolite extract of *C. auris* treated with fluconazole and BA (Table 5.17-5.20). They have a wide array of properties such as antioxidant, auto-antibiotic, fungal metabolite, biofilm-forming metabolite and hyphae inhibition. Earlier, the metabolite profiling of *C. auris* by Semreen et al, 2019 identified tyrosol and phenylethyl alcohol which are biofilm-forming metabolite and hyphae inhibiting metabolite respectively [304]. In our study also tyrosol and phenylethylalcohol were identified in the metabolites of cells treated with fluconazole, and BA. Other fungal metabolites such as benzeneacetic acid, pyrrolo[1,2-a]pyrazine-1,4-dione, 2-methyl-butaoic acid, butylated hydroxytoluene, squalene which have been reported as metabolites in *S. cerevisiae*, *C. albicans* and *Aspergillus spp*. were also identified. This GC-MS analysis of the metabolites secreted by *C. auris* can help to understand how *C. auris* behaves under stress caused by antifungal molecules like fluconazole and BA, which might help to understand its pathogenesis, virulence, growth and drug-resistance.

Table 5.16: Treatment of *C. auris* for metabolite profiling using GC-MS

Sample name	**Sample detail**	**Number of volatile organic compounds detected**
Yeast extract 1	*C. auris* (S) treated with 4ug/ml fluconazole	48
Yeast extract 2	*C. auris* (R) treated with 4ug/ml fluconazole	40
Yeast extract 3	*C. auris* (S) treated with 2MIC BA	38
Yeast extract 4	*C. auris* (R) treated with 2MIC	13

	BA	

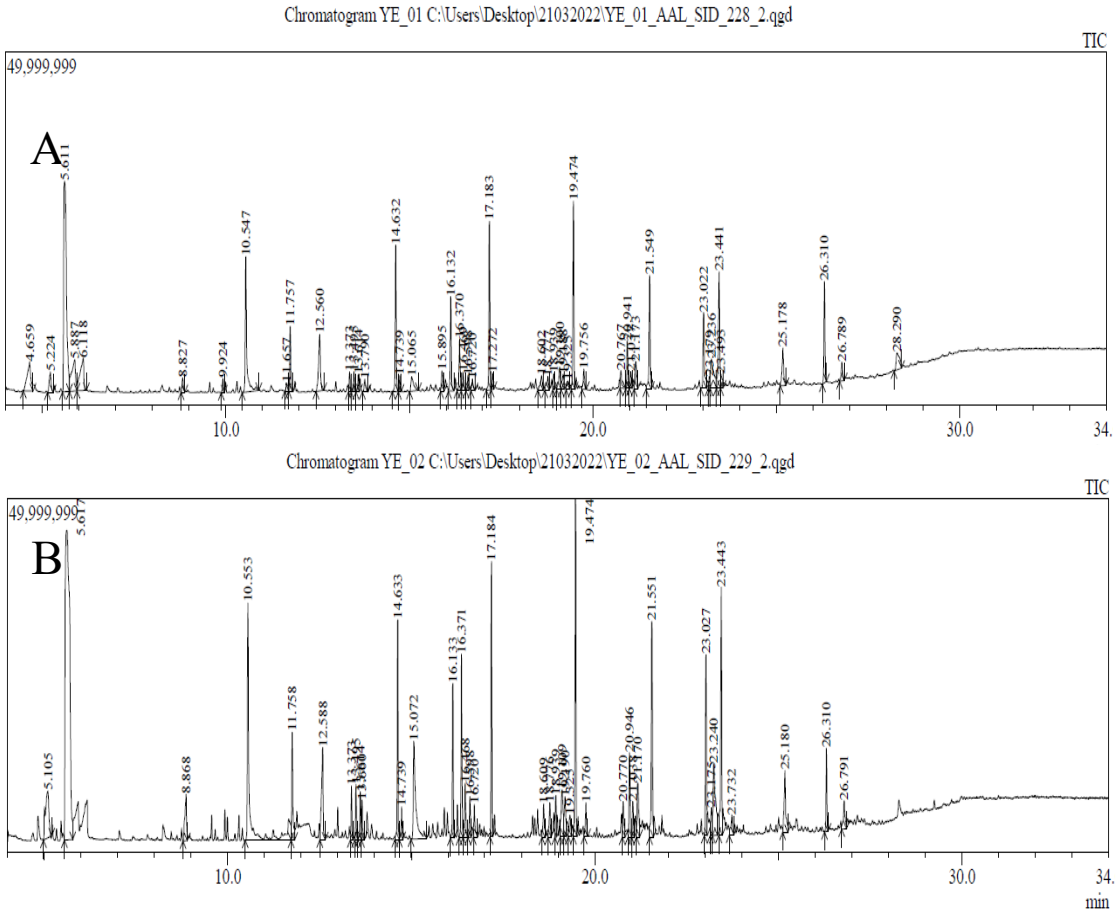
Chromatogram YE_01 C:\Users\Desktop\21032022\YE_01_AAL_SID_228_2.qgd
TIC
49,999,999
A
5.611
10.547
14.632
17.183
19.474
21.549
23.441
26.310
4.659
5.224
5.887
6.118
8.827
9.924
11.657
11.757
12.560
15.895
16.132
16.370
17.272
19.756
23.022
25.178
26.789
28.290
10.0
20.0
30.0
34.
Chromatogram YE_02 C:\Users\Desktop\21032022\YE_02_AAL_SID_229_2.qgd
TIC
49,999,999
B
5.105
5.617
8.868
10.553
11.758
12.588
14.633
15.072
16.133
16.371
17.184
19.474
19.760
21.551
23.027
23.443
25.180
26.310
26.791
10.0
20.0
30.0
34.
min

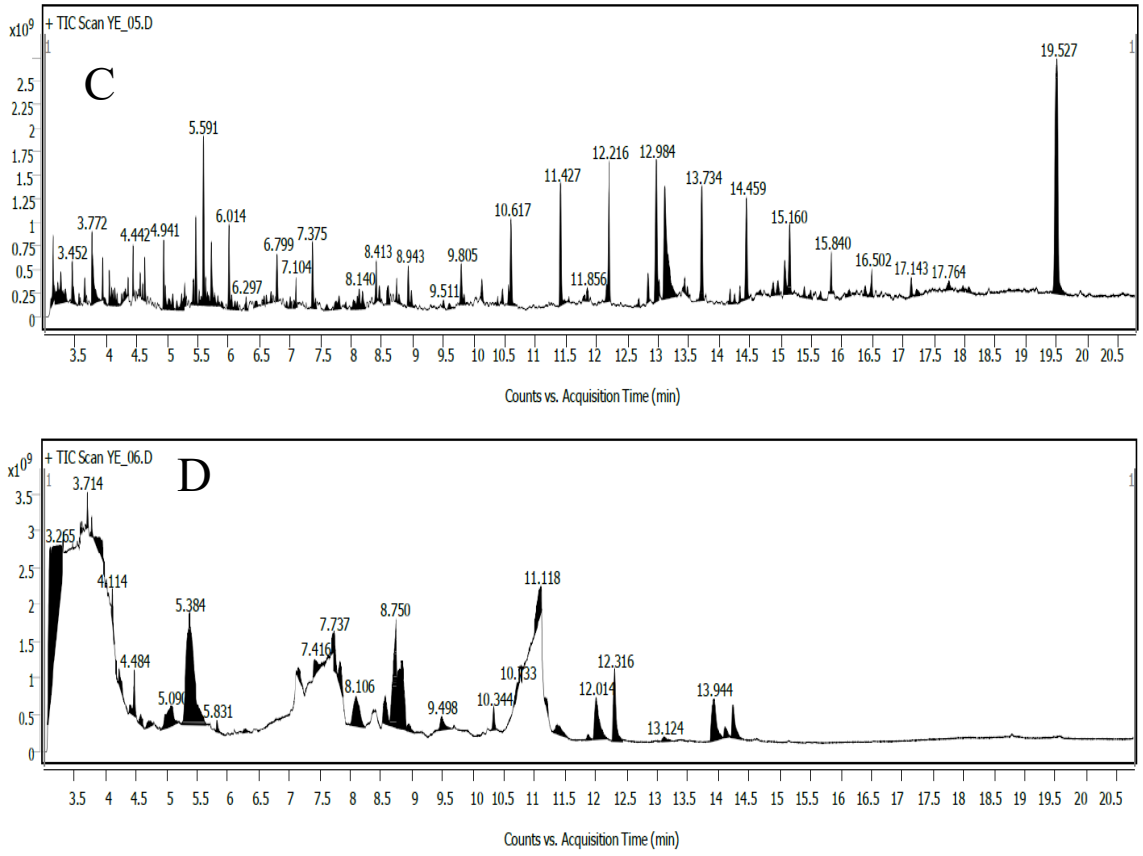

Figure 5.21: Chromatograms representing the metabolites in the ethyl acetate extract of C. auris treated with fluconazole and BA A. *C. auris* fluconazole sensitive strain (NCCPF: 470097) treated with 4ug/ml fluconazole B. *C. auris* fluconazole resistant strain (NCCPF: 470149) treated with 4ug/ml fluconazole C. *C. auris* fluconazole sensitive strain (NCCPF: 470097) treated with 2MIC BA D. *C. auris* fluconazole resistant strain NCCPF: 470149 treated with 2MIC BA

Table 5.17: Metabolites present in yeast extract 1

Metabolite	Properties	Class of metabolite
1,4-diazabicyclo[4.3.0]nonan-2,5-dione, 3-methyl	Antimicrobial	NA
11-Methyldodecanol (Isotridecanol)	A natural product found in *Vitis vinifera*	Fatty alcohol
1-Decanol, 2-hexyl-	Natural product found in *Nelumbo nucifera*	Branched alcohol

1-Heptacosanol	Antioxidant molecule isolated from *Aspergillus arcoverdensis*	Fatty alcohol
2,5-Piperazinedione, 3,6-bis(2-methylpropyl)-	A natural product found in *Kandelia candel*	2,5-diketopiperazines
2-Piperidinone	Role as L-glutamate gamma-semialdehyde dehydrogenase inhibitor. A natural product found in *Dichilus reflexus, Dichilus pilosus*.	Delta lactam
Benzeneacetic acid	*S. cerevisiae* metabolite, pyruvate carboxylase inhibitor, Aspergillus metabolite	Phenylacetic acid
Cyclo(L-prolyl-L-valine)	A natural product found in *Streptomyces albospinus, Penicillium herquei*	Piperazinone
Phenylethyl alcohol	Auto-antibiotic secreted by *Candida albicans*	Alcohol
Pyrrolo[1,2-a]pyrazine-1,4-dione, hexahydro-	Antioxidants, Fungal metabolite	Pyrazine derivative

Table 5.18: Metabolites present in yeast extract 2

Metabolite	**Properties**	**Class of metabolite**
Propanoic acid, 2-methyl-	A natural product found in *Myrtus communis, Coffea Arabica.* A volatile oil component and a plant metabolite.	Fatty acid
Succinic anhydride	A natural product found in *Pycnandra acuminata* and *Clerodendrum*	Acid anhydride

	japonicum	
Phenylethyl alcohol	Auto-antibiotic secreted by *Candida albicans*	Alcohol
Dodecane, 4,6-dimethyl-	Lignin-derived aromatic compound found in *Streptomyces.* Fungal metabolite (present in *Amanita rubescens* mushroom)	Alkane
1-Pentadecene	Involved in the defence of insects like *Palembus ocularis* and *Parastizopus armaticeps.* Natural product found in *Panax ginseng, Herrania cuatrecasana.*	Alkene
Benzeneethanol, 4-hydroxy-	Also known as tyrosol. It has a role as an anti-arrhythmia drug, an antioxidant, a cardiovascular drug, a protective and fungal metabolite	Tyrosol
Pyrrolo[1,2-a]pyrazine-1,4-dione, hexahydro-	Antioxidants, Fungal metabolite	Pyrazine derivative
Eicosane	A natural product found in *Ageratum conyzoides, Vaccinium virgatum* and *Agave attenuate*	Alkane
1-Nonadecene	Natural product found in *Nelumbo lutea, Tanacetum vulgare.* It acts as plant and	Alkene

	bacterial metabolites.	

Table 5.19: Metabolites present in yeast extract 3

Metabolite	Properties	Class of metabolite
2-Nonen-1-ol	Natural product found in *Bistorta manshuriensis, Houttuynia cordata,* and *Anomala albopilosa*	Aliphatic alcohol
1-Octadecyne	A product naturally occuring in *Lonicera japonica*	NA
1-Octanol, 2-butyl-	A product naturally occuring in *Vitis vinifera*	Fatty alcohol
Phenylethyl alcohol	Auto-antibiotic secreted by *Candida albicans*	Alcohol
Nonane	A volatile oil component and plant metabolite found in *Hypericum foliosum, Hypericum gentianoides*	Alkane
1-Undecene, 4-methyl-	Secreted by *Pseudomonas species* and shows antifungal activity against *Rhizoctonia solani*	Alkene
Hexadecane	A product naturally ocuring in *Vitis rotundifolia, Curcuma amada.* It is a constituent of essential oils obtained from	Alkane

	Piper longum. It acts as a plant metabolite and one of the constituents of volatile oils.	
2,4-Di-tert-butylphenol	Antifungal, antioxidant. A natural product found in *Bacillus subtilis, Streptomyces parvulus* (bacterial metabolite)	Phenol
Butylated hydroxytoluene	Antioxidant. Secreted by *C. albicans, Aspergillus conicus* and *Penicillium conicus.* Natural product found in *Thymus longicaulis, Teucrium leucocladum*	Phenol derivative
4-(1,5-Dihydroxy-2,6,6-trimethylcyclohex-2-enyl)but-3-en-2-one	Present in *Annona reticulata* leaves extract	NA
2-Piperidinone, N-[4-bromo-n-butyl]-	Present in *Streptomyces thermocarboxydus* and *pomegranate* extract	Delta lactam
tert-Hexadecanethiol	Present in *Dovyalis cafra* fruit extract	NA
7,9-Di-tert-butyl-1-oxaspiro(4,5)deca-6,9- diene-2,8-dione	Naturally occuring in *Euphorbia pulcherrima* whole plant extract and Morchella mushroom	Lactone
5-Octadecene, (E)-	Present in volatile oil of	Alkene

	Polianthes tuberosa	
5-Eicosene, (E)-	Present in volatile essential oils of *Rosa canina roots* and *Manglietia glauca* leaves extract	Unsaturated aliphatic hydrocarbons
Heptacosane	It acts as a volatile oil constituent and a plant metabolite found in *Quercus salicina, Quercus glauca*	Alkane
Glycidyl (Z)-9-Heptadecenoate	Present in hemp seed oil	Fatty acid ester
Hexadecanoic acid, 2-hydroxy-1-(hydroxymethyl)ethyl ester	Plant metabolites (*Coriandrum sativum, Pistia stratiotes and eichornia crassipes*)	NA
Sulfurous acid, hexyl pentadecyl ester	Volatile components of white *Hypsizygus marmoreus* fungi	NA
9-Octadecenamide, (Z)-	Also called oleamide. A natural product found in *Desmos cochinchinensis*, *Pseudo-nitzschia multistriata*	NA
Squalene	Plant metabolite and *S. cerevisiae* metabolite. Antioxidant, Anticancer.	Triterpine

Table 5.20: Metabolites present in yeast extract 4

Metabolite	Properties	Class of metabolite
Benzeneethanol, 4-hydroxy-	Also known as tyrosol. It has a role as an anti-arrhythmia drug, an antioxidant, a cardiovascular drug, a protective and fungal metabolite	Tyrosol
Benzeneacetic acid	*S. cerevisiae* metabolite, pyruvate carboxylase inhibitor, Aspergillus metabolite	Phenylacetic acid
Pyrrolo[1,2-a]pyrazine-1,4-dione, hexahydro-	Antioxidants, Fungal metabolite	Pyrazine derivative
Cyclo(L-prolyl-L-valine)	A natural product found in *Streptomyces albospinus, Penicillium herquei*	Piperazinone
Pyrrolo[1,2-a]pyrazine- 1,4-dione, hexahydro-3- (2-methylpropyl)-	Detected in the extracts of fungi *Mortierella alpina* and a fungal endophyte. Antibiofilm activity against *E.coli* and *P. mirabilis.* Antifungal activity against *Fusarium oxysporum, Aspergillus niger, Microsporum gypseum, Trichophyton mentagrophytes,* and *Trichoderma harzianum*	Pyrazine derivative

Octadecanoic acid	Also called stearic acid. Shows antiviral and anti-inflammatory activities.	Saturated fatty acid
2,5-Piperazinedione, 3,6-bis(2-methylpropyl)-	A natural product found in *Kandelia candel*	2,5-diketopiperazines
Pyrrolo[1,2-a]pyrazine- 1,4-dione, hexahydro-3-(phenylmethyl)-	A natural product found in *Streptomyces antioxidans* and *Streptomyces xiamenensis* (Bacterial metabolite)	Pyrazine derivative

5.4.7. Cytotoxicity analysis of BA

This study aimed to see if different concentrations of BA are toxic to human cell lines, which will provide preliminary analysis about the potential of using BA as an antifungal drug in humans. To analyse the preliminary safety of BA, if they can be used for human use in future, the cytotoxicity analysis of BA was done against human cell lines by MTT assay as discussed in section 4.4.9. The cytotoxicity of BA was determined by MTT assay of the HEK293T cell line. After the dissolution of formazan crystals, the purple-coloured solution was formed suggesting that the cells were viable at different concentrations of BA. At the highest concentration of BA (8x MIC of BA: 128 µg/ml) 55% of HEK-293T cells were inhibited (Table 5.21). The MIC cytotoxicity of BA was determined as 105µg/ml (Figure 5.22). This study showed that even at 2x, 4x and 8x MIC concentrations of BA were not much toxic to human cell lines. This is a preliminary toxicity and safety analysis of BA which needs to be further validated in animal models in future studies.

Table 5.21: Cytotoxicity of BA on HEK-293T cell

Concentration of BA	**Percentage inhibition of HEK-293T cell line**
16 µg/ml	6.22%
32 µg/ml	27.18%

64 µg/ml	38.12%
128 µg/ml	55.52%

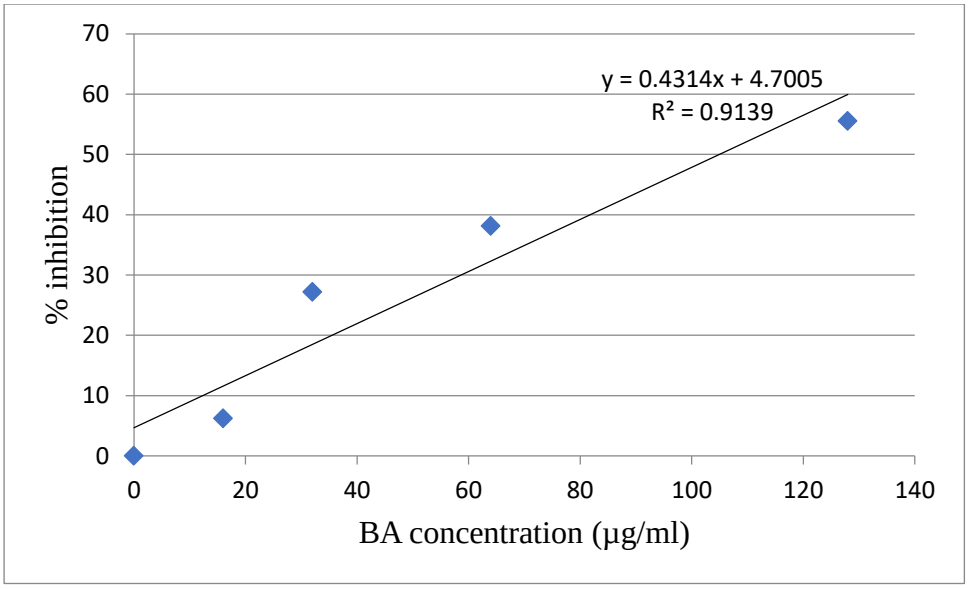

Figure 5.22: Scatter plot to calculate the 50% inhibition of the HEK-293T cell line by BA

5.4.8 Determination of antifungal potential of Sarcochlamys pulcherrima extract and identification of potential small molecules from S. pulcherrima extract as antifungals against C. auris

C. auris has exhibited resistance to multiple antifungal drugs, necessitating the exploration of alternative sources for antifungal compounds. A promising avenue lies in traditional and herbal medicine, where plants have shown potential as a rich reservoir of new antifungal molecules. Numerous studies have demonstrated the antimicrobial activity present in various herbs and medicinal plants [78,361,362]. In light of this, the present investigation sought to investigate the antifungal effects of leaves' extracts from the ethnomedicinal plant *Sarcochlamys pulcherrima* against *C. auris*. Native to the forests of northeastern states in India, Myanmar, Bhutan, Indonesia, and Thailand, *S. pulcherrima* is an evergreen tree with a history of use by different tribes in India and Bangladesh to treat diverse ailments such as flatulence, tongue ulcers, fever blisters, boils, dysentery, diarrhoea, indigestion, and eye itching [100]. Previous studies have already reported on the antibacterial and antifungal properties of *S. pulcherrima* [101,102].

5.4.8.1 Sample collection and extract preparation

In July 2018, leaves and barks were collected from a single *S. pulcherrima* tree located in the New Halflong region of North Cachar Hills in Assam, India. To ensure cleanliness, the plant samples were thoroughly washed with water to eliminate any dust or impurities. Subsequently, the samples were subjected to air-drying in a hot air oven set at temperatures between 45-50°C until complete dehydration was achieved. The dried samples were then finely ground into a powder using a grinder, carefully packed in airtight packets, and stored at a temperature of 4°C for future utilization.

The extraction process involved the use of two solvents, namely 90% methanol and ethyl acetate, through a Soxhlet apparatus. To obtain the plant extract, 30 grams of leaf powder were combined with 100 millilitres of each solvent. The methanol extraction was carried out at a temperature of 65°C, while the ethyl acetate extraction was performed at 77°C. This process was reiterated for a total of 25 cycles. Following extraction, the crude solvent extract was concentrated to a volume of 5 millilitres using a rotary evaporator operating at 40 revolutions per minute and a temperature of 50°C to eliminate excess solvent. The resulting concentrate was then subjected to further drying at 50°C until it reached a dry, paste-like consistency. The quantity of the extract in paste form was measured and stored at 4°C until it was ready for subsequent usage.

5.4.8.2 Determination of the antifungal activity of S. pulcherrima plant extract against C. auris

The antifungal property of *S. pulcherrima* methanol extract and ethyl acetate extract was determined against *C. auris* (NCCPF: 4700149) by disc diffusion method. The disc diffusion assay showed that the plant extract was able to inhibit the growth of *C. auris.* The zones of inhibition of methanol extract of *S. pulcherrima* against both *C. albicans* and *C. auris* strains were 11 mm, whereas the zones of inhibition of ethyl acetate extract of *S. pulcherrima* against *C. albicans* and *C. auris* strains were 10 and 15 mm, respectively. The comparison of a zone of inhibitions shows that the ethyl acetate plant extract showed better antifungal activity against *C. auris* than *C. albicans*. The zones of inhibition of fluconazole against *C. albicans* and *C. auris* were 26 mm and 24 mm respectively.

5.4.8.3 Antioxidant property of S. pulcherrima extract

The *S. pulcherrima* leaves extract showed antioxidant property by scavenging the DPPH free radicals. The IC_{50} values for determining the antioxidant property of the *S. pulcherrima* leaves extract was determined from the graph presented in Figure 5.23. The IC_{50} value of the

S. pulcherrima leaves extract was 57.16µg/ml, whereas the IC_{50} value of ascorbic acid was 18.61 µg/ml.

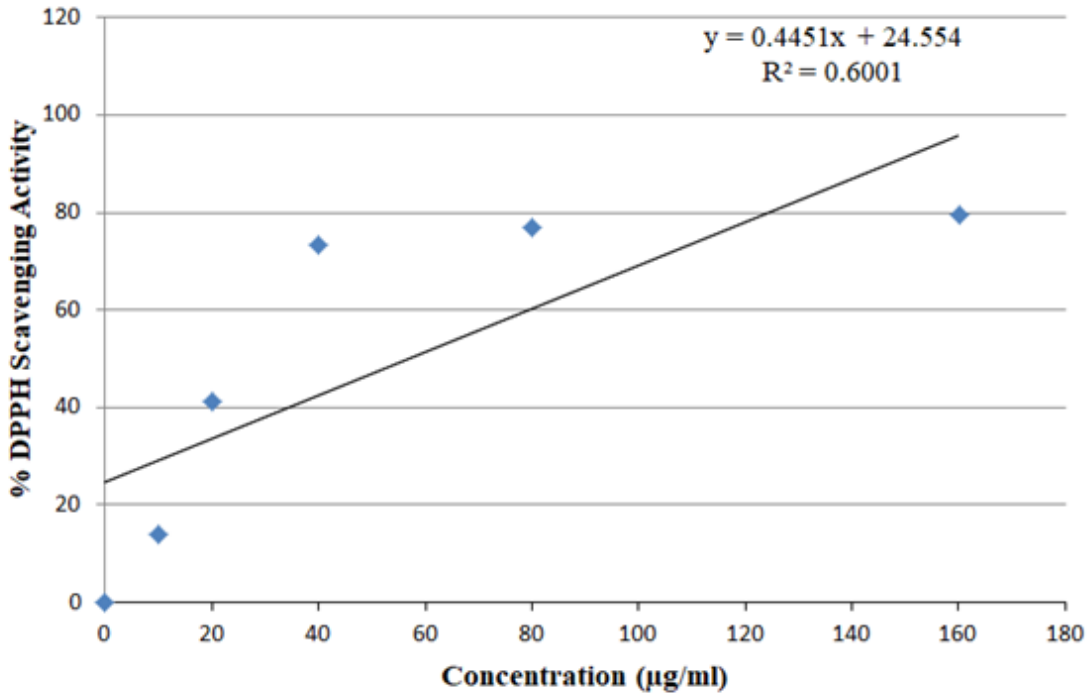

Figure 5.23: DPPH scavenging activity of *S. pulcherrima*

4.8.4 Determination of total phenol content of S. pulcherrima plant extract

The total phenol constituent in the methanol extract of *S. pulcherrima* leaves was appraised from the standard curve (Figure 5.24) obtained by plotting the concentration of gallic acid in the x-axis and the absorbance of gallic acid and Folin-Ciocalteu reagent mixture at 765nm in the y-axis. The absorbance values of *S. pulcherrima* extract for the determination of the TPC are provided in Table 5.22. It was estimated that the phenol content in the 160 µg/ml *S. pulcherrima* extract was equivalent to 40.31 µg/ml gallic acid. Similarly, the phenol content in the 320 µg/ml *S. pulcherrima* extract was equivalent to 79.46 µg/ml gallic acid.

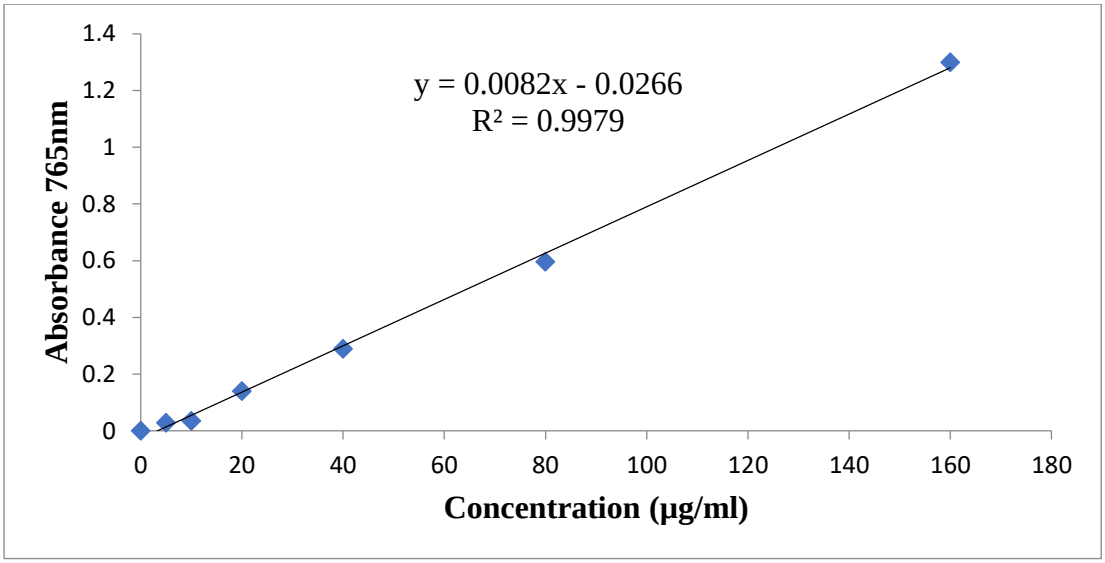

Figure 5.24: Standard graph of gallic acid for the determination of total phenol content in *S. pulcherrima* leaves extract

Table 5.22: The absorbance of *S. pulcherrima* extract for determination of total phenol content

Concentration (µg/ml)	Absorbance 765	Absorbance 765	Absorbance 765	Mean Absorbance
160	0.305	0.303	0.303	0.304
320	0.600	0.624	0.651	0.625

5.4.8.5 Detection of phenols in the S. pulcherrima plant extract

HPTLC analysis was used to detect gallic acid and quercetin in the *S. pulchherima* plant extract. The maximum R_f of the gallic acid standard was 0.43 and the peak area was 16416.6 While in the *S. pulcherrima* plant extract a peak was observed which had the maximum R_f of 0.45 and peak area of 1431.3. This peak of the plant extract coincided with the peak of gallic acid standard suggesting the occurrence of gallic acid in the *S. pulcherrima* plant extract. The HPTLC analysis did not show the presence of quercetin in the *S. pulcherrima* plant extract.

5.4.8.6 Determination of in vitro antifungal activity of gallic acid against C. auris

The *in vitro* antifungal assay exhibited that gallic acid repressed the growth of all the six isolates of *C. auris* used in this experiment. The MIC_{50} value of gallic acid (the lowermost

concentration of gallic acid that suppressed the 50% growth of *C. auris* in comparison to *C. auris* that were not treated with gallic acid) was determined in the range of 1.6-3.2 mg/mL. The MIC_{50} value of gallic acid (MIC_{50} GA) and minimum fungicidal concentration (MFC= lowest drug concentration that yields 3 or fewer colonies) value of gallic acid (MFC GA) against different *C. auris* strains are given in Table 5.23.

Table 5.23: MIC_{50} of gallic acid against different *C. auris* strains

***C. auris* isolate**	**NCCPF: 470149**	**NCCPF: 470111**	**NCCPF: 470098**	**NCCPF: 470055**	**NCCPF: 470097**	**NCCPF: 470049**
MIC_{50} GA (mg/ml)	3.2	1.6	3.2	1.6	1.6	1.6
MFC GA (mg/ml)	12.8	6.4	12.8	12.8	12.8	6.4

5.4.8.7 Structure modeling and assessment of C. auris carbonic anhydrase

The metallo-enzyme carbonic anhydrase (CA), EC number 4.2.1.1, presents a potential target for antifungal compounds, which effectively facilitates the conversion of carbon dioxide (CO_2) to bicarbonate [363]. Its role is significant in the virulence of *Cryptococcus spp*. and *C. albicans*, as well as in adaptation to fluctuating CO_2 levels inside the host, sporulation, elevation of cAMP concentration, and phenotypic switching [364–367]. Given its involvement in crucial biological processes such as CO_2 transport, fungal growth, pH regulation, virulence and respiration, CA becomes a pivotal target for the creation of novel antifungal agents. Earlier research has also highlighted the possibility of CA as a target for antifungal drugs [368]. Therefore, this study employed a computational approach to investigate whether gallic acid could potentially exert its function by binding to the CA enzyme of *C. auris*.

The 3D structure of the *C. auris* CA protein was predicted by the I-Tasser webserver where the amino acid sequence of *C. auris* CA protein was provided as input in FASTA format. The C-score (confidence score which is used to estimate the quality of predicted 3D models of proteins) of the modelled structure of *C. auris* carbonic anhydrase (CA) protein was found -1.66 (Table 5.24). Generally, the C-score value of protein models generated by I-Tasser ranges between −5 to 2 and a larger C-score implies that the generated model is of higher quality [310]. The C-score of the modelled *C. auris* CA protein was on the higher side suggesting the predicted model was of good quality. The quality of the predicted model of *C.*

auris CA protein was further assessed by generating a Ramachandran plot. Analysis of psi/phi angles showed that overall, 96% of residues in the modelled structure were localized in the allowed regions of the Ramachandran map. The mean ERRAT score of 93.10 of the modelled structure also confirmed the significant accuracy of the protein models predicted. Furthermore, the quality of the 3D model of *C. auris* CA protein was also assessed by Verfify3D software that decides the compatibiliness of the 3D model of proteins with its primary sequence (1D) by allocating a structural class on the basis of its environment (non-polar, polar, loop, helix, alpha, and beta etc) and location. Based on these factors the Verify3D software provides 3D-1D score for the protein model as output. Upon assessing the 3D model of *C. auris* CA protein by Verify3D software the 3D-1D score of 63.94% was obtained implying that 63.94% of amino acid residues of *C. auris* CA protein are compatible with its 3D model (Table 33). Thus, all three assessment methods namely, PROCHECK, ERRAT and Verify3D confirmed the quality of predicted 3D structures as being reliable. Superimposition of modelled CA protein structure of *C. auris* and experimentally determined CA structure of *C. albicans* showed RMSD value (provides the mean deviations among the corresponding atoms of two proteins and the lower RMSD value suggests higher structural similarity between proteins) of 0.43Å (Figure 5.25), which further confirms the high accuracy of modelled structure.

Table 5.24: Molecular modelling studies of *C. auris* CA protein

A: Target-Template details for selected modeled structure			
Protein Name	**No. of amino acid residues**	**Templates (PDB ID)**	**C-score of models**
C. auris CA	269	6GWU	-1.66

B: Model validation for selected modeled structure			
Protein Name	**Ramachandran Plot Statistics**	**ERRAT Statistics**	**Verify-3D**

							Statistics
	Residue in a most favorable region	Residue in the additional allowed region	Residue in the generously allowed region	Residue in the disallowed region	Number of non- proline and non-glycine residues	Score	Score
C. auris CA	68.4%	20.7%	7.2%	3.8%	269	93.10	63.94%

Figure 5.25: Superimposition of the modeled structure of *C. auris* (green) and crystal

structure of *C. albicans* (red) carbonic anhydrase protein

5.4.8.8 Molecular docking and evaluation of interacting residues

MIB web-server predicted the binding residues i.e., 94C, 149H and 152C where the Zn2+ metal ion can bind in the *C. auris* CA protein. When the modelled structure of CA of *C. auris* was docked with Zn2+ metal ion, we found that all active site residues i.e., 94C, 149H and 152C are interacting with it. The interacting residues are listed in (Table 5.25). The docking score and atomic contact energy which were obtained after docking the *C. auris CA* protein with gallic acid were 219 and -12.24 kcal/mol respectively (Table 5.26). We also evaluated the docked complexes of both the CA proteins of *C. auris* and *C. albicans* with gallic acid using Chimera software (all within 5 Å from the ligand) and found significant changes in the binding residues and the neighbouring residues (Table 5.27).

In the comparison of docking of *C. albicans* CA protein with gallic acid, the binding of gallic acid with *C. auris* CA protein was not energetically favoured as it was in *C. albicans* CA protein. In docking gallic acid with the CA protein of *C. albicans* the atomic contact energy was determined as -71.85 kcal/mol whereas the atomic contact energy while docking gallic acid with CA protein of C. auris was -12.24 kcal/mol. As the atomic contact energy for docking gallic acid with *C. auris* CA protein was higher than the docking of gallic acid with *C. albicans* CA protein, the binding of gallic acid with *C. albicans* CA protein was more favourable energetically. Lower atomic contact energy implies higher energetically favourbale binding. All three desired active site residues of *C. auris* CA protein did not interact with the gallic acid. Instead, interactions with only two active site residues (149H, 152C) were present in the docked complex, while in *C. albicans* CA docked complex with gallic acid, we found interactions with all the 3 desired active site residues. This indicated the presence of structural and mutational changes in the CA of *C. auris*. To verify this hypothesis, we analyzed the secondary structure distributions of all the interacting residues of both docked complexes with gallic acid (all within 5Å from the ligand), and we found a significant change in secondary structure in both docked structures (Figure 5.26). It has been reported in the crystal structure of carbonic anhydrase (PDB ID: 6GWU) of *C. albicans* that the active site residues (Ile 99, Gly 135, Phe 116 and Leu 121), most of which are hydrophobic create a narrow tunnel that acts as the point of entry to the positively charged active site. The analysis of the modelled structure of *C. auris* CA protein showed that the Ile 117, Gly 153, Phe 134 and Leu 139 residues of *C. auris* CA protein also created a narrow tunnel. In *C. albicans* CA protein there is a presence of a distinct salt bridge made up of

residues present between arginine amino acid at position 80 and aspartic acid amino acid at position 133 (Arg80 - Asp133) which adds to the development of the active site cavity in *C. albicans* CA protein [369]. The salt bridge regulates the tunnel's shape and openness and helps in the creation of the active site cavity in the *C. albicans* CA protein [369]. A similar salt bridge was also present in *C. auris* CA protein (Arg 98- Asp 151) but at four positions mutations were found (Figure 5.27). We infer these mutations hinder the accessibility of gallic acid to the active site of *C. auris* CA protein thereby decreasing the strength of binding.

Table 5.25: Interacting residues and secondary structure pattern of *C. auris* and *C. albicans* CA protein within 5Å from the Zn2+ metal ion

C. albicans		***C. auris* (+18 of *C. albicans* residues)**	
Within 5Å zinc ion & Secondary Structure (Sec Str) Analysis			
Amino Acid and Position	**Sec. Str**	**Amino Acid and Position**	**Sec. Str**
76 CYS	Strand	94 CYS	Coil
131 HIS	Strand	149 HIS	Coil
134 CYS	Coil	152 CYS	Coil
78 ASP	Coil	96 ASP	Coil
135 GLY	Helix	153 GLY	Coil
100 ALA	Helix	118 ALA	Coil
101 ASN	Helix	-	-
136 GLY	Helix	-	-
-	-	155 VAL	**Helix**
-	-	95 SER	**Coil**

Table 5.26: Docking studies of CA of *C. auris* and *C. albicans* yeast protein with gallic acid

Protein	**Ligand**	**Atomic Contact Energy (kcal/mol)**	**Docking Score**
CA of *C. albicans*	Gallic acid	-71.85	1850
CA of *C. auris**		-12.24	219

Table 5.27: Interacting residues and secondary structure pattern of CA of *C. auris* and *C. albicans* yeast protein within 5Å from the gallic acid

C. albicans		***C. auris* (+18 of *C. albican* residues)**	
Within 5Å Gallic Acid & Secondary Structure (Sec Str) Analysis			
Amino Acid and Position	**Sec. Str**	**Amino Acid and Position**	**Sec. Str**
76 CYS	Strand	-	-
131 HIS	Strand	149 HIS	Coil
134 CYS	Coil	152 CYS	Coil
133 ASP	Coil	151 ASP	Coil
80 ARG	Coil	98 ARG	Coil
79 SER	Coil	97 SER	Coil
78 ASP	Coil	96 ASP	Coil
77 SER	Coil	-	-
137 ILE	Helix	-	-
136 GLY	Helix	-	-
100 ALA	Helix	-	-
99 ILE	Helix	-	-
135 GLY	Helix	153 GLY	Coil
-	-	150 THR	Coil
-	-	236 VAL	Coil
-	-	36 LYS	Coil
-	-	38 GLN	Helix

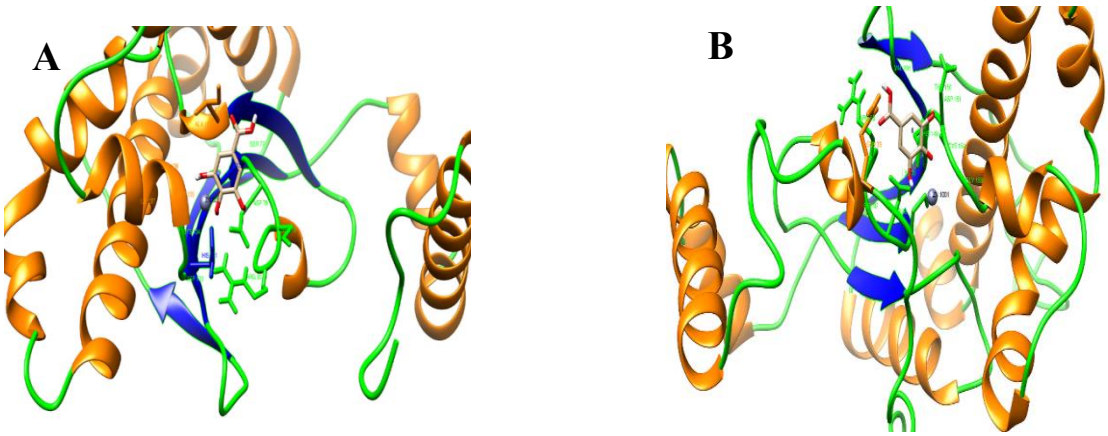

Figure 5.26: (A) Interacting residues and secondary structure (Helix: Orange, Coil: Green & Strand: Blue) pattern of *C. albicans* CA protein within 5Å from the ligand (gallic acid) (B) Interacting residues and secondary structure (Helix: Orange, Coil: Green & Strand: Blue) pattern of *C. auris* CA protein within 5Å from the ligand (Gallic Acid).

```
CLUSTAL O(1.2.4) multiple sequence alignment


C.albican       RAGDQCLATLPGEIFVHRNIANIVNANDISSQGVIQFAIDVLKVKKIIVCGHTD   54
C.auris         RAGEQCLATLPGEIFTHRNIANIVNANDISSQGVIQFAVDVLKVRKIIVCGHTD   54
                ***:**********.**********************:*****:*********
```

Figure 5.27: Sequence alignment of the 54 amino acids of *C. albicans* and *C. auris* carbonic anhydrase protein that forms the tunnel shape

Discussion

An amide derivative of betulinic acid has been described to repress the growth of *Cryptococcus neoformans* (MIC=0.25µg/ml) and *C. albicans* (MIC=32µg/ml) [370]. Similarly, in another study 16-hydroxy betulinic acid inhibited the growth of various filamentous plant pathogenic fungi such as *Rhizoctonia solani* (MIC=500µg/ml), *Pythium graminicola* (250µg/ml), and *Fusarium oxysporum* (1000µg/ml) [371]. In our study, the MICs of BA against *C. auris* and other *Candida* species were ranging between 16-32µg/ml and MFC value ranged between 128-256µg/ml. Furthermore, in our study the MFC value is 4-8 times higher than that of MIC value against *C. auris*, *C. parapsilosis*, *C. krusei*, *C. albicans* and *C. tropicalis*. In a previous study also, a derivative of BA had MFC values 4-8

times higher than that of MIC value against *C. albicans*, *C. krusei*, and *C. parapsilosis* [372]. However, the MIC and MFC of BA were lower than that of amphotericin B and fluconazole. Studies conducted by us show that the treatment of *C. auris* with BA affects the cell surface and affects the ergosterol synthesis as well. Ergosterol is a major fungal sterol and plays a critical role in the structure, function and biogenesis of fungal plasma membrane. Furthermore, ergosterol helps fungi in stress adaptation and ergosterol synthesis pathway is the target of many antifungal drugs [359,360]. However, the RNA-sequencing of BA-treated cells did not show any effect on genes involved in ergosterol synthesis. Nevertheless, the gene KRE9 domain-containing protein which is involved in cell wall biogenesis and (1->6)-beta-D-glucan biosynthesis process of *C. albicans* was down-regulated in *C. auris* treated with BA. The H_2O_2 sensitivity assay showed that the *C. auris* cells became more sensitive to oxidative in comparison to control after treatment of BA. The down-regulation of genes pertaining to oxidative stress tolerance in *C. auris* after BA (Superoxide dismutase, Sod-Cu domain-containing protein) treatment also shows that BA exerts oxidative stress in *C. auris*. Finally, the MTT assay to determine the cytotoxicity of BA on HEK293T cell lines showed that BA exhibited low cytotoxicity to the cell line even at 2xMIC concentration of *C. auris* suggesting possible safety of BA as a novel antifungal against *C. auris*. Previous study also showed low cytotoxicity of derivatives of BA in HEK293 cell line [370].

Furthermore, the antifungal property of *S. pulcherrima* leaves extract has been evaluated against *C. auris*. Then, the active compound responsible for the antifungal property was identified and the potential mode of action of the active compound was determined by *in silico* approach. The antioxidant and antifungal properties of *S. pulcherrima* methanolic extract against *C. albicans* (MIC 12.5 mg/ml) have been reported in previous studies [101,373,374]. However, its mode of action and efficacy against multidrug *Candida* spp. was not explored. In our study, both the methanol and ethyl acetate extract exhibited antioxidant and antifungal properties against *C. auris* and *C. albicans*. After determining the antifungal and antioxidant properties of the plant extract, we experimented to identify the potential active metabolite in the extract.

Previously, two triterpenoids namely tormentic acid and 23-hydroxycorosolic acid were identified and isolated from aerial parts of *S. pulcherrima* [102]. Furthermore, these two triterpenoids inhibited the biofilm formation by *Pseudomonas aeruginosa* [102]. As the *S. pulcherrima* plant extract showed the presence of phenolic compounds and antioxidant properties, we performed an HPTLC experiment to identify potential antioxidant compounds

such as quercetin and gallic acid in the plant extract. The HPTLC analysis found the existence of gallic acid in the extract. Gallic acid is a phenolic compound that naturally occurs in various herbal plants and fruits like *Camellia sinensis, Oenothera biennis*, *Vitis vinifera*, *Terminalia bellerica* and *Terminalia chebula* [375,376]. Different therapeutic potentials of gallic acid such as antimicrobial, antioxidant, anti-inflammatory, anticancer has been decribed in various *in vitro* and animal model studies [377–379]. Gallic acid has been reported to possess anti-inflammatory activity, cardioprotective property, chondroprotective activity, antidiabetic property, hepatoprotective activity, neuroprotective activity, and anticancer properties [380–386]. A homoeopathic drug manufactured by BioActive Nutritional, Florida, USA, where the active ingredient is gallic acid has been marketed for temporary relief from itching, back pain, joint pain, nasal congestion, fatigue, allergic rhinitis, and dyspepsia [387]. However, the safety and efficacy of this homoeopathic drug have not been evaluated by the FDA [387]. Previous *in vitro* research has reported the antifungal activity of gallic acid against different human fungal pathogens such *C. albicans, Candida krusei, Candida glabrata*, *Candida tropicalis*, *Microsporum canis*, and *Trichophyton species* [388,389]. In a study by Li et al. (2017) the MIC of gallic acid against *C. glabrata*, *C. albicans* and *C. troplicalis* between 12-100 µg/ml has been reported [388]. Similarly, in another study the MIC of the gallic acid against *C. krusei, C. albicans, C. glabrata,* and *C. tropicalis*; along with dermatophytes such as *M. canis* and *Trichophyton* species ranging between 0.25-1 mg/mL [389]. In our study, the MIC of gallic acid against *C. auris* ranged between 1.6-3.2 mg/mL. For four *C. auris* strains, the MIC was 1.6 mg/mL and for the remaining two *C. auris* strains the MIC value was measured as 3.2 mg/mL. The occurrence of antifungal drug unsusceptibility in *C. auris* could be the reason for the high MIC values of gallic acid. It was previously reported that administration of gallic acid to immunocompromised mice models with systemic *C. albicans* infection reduced mortality rate, inflammation, and fungal load in liver tissues of mice in comparison to mice in the control group that did not get any drugs [388]. Similarly, to these studies, the gallic acid also showed antifungal activity against *C. auris* in our study corroborating the hypothesis that the gallic acid is one of the potential active compounds in the *S. pulcherrima* for its antifungal properties.

Next, we determined the potential mode of action of gallic acid by performing *in silico* experiments. Previous studies reported the repression of ergosterol biosynthesis and reduction in *CYP51* enzyme activity as the mechanism by which gallic acid exerted its antifungal

activity [388,389]. In this objective, we assessed the CA protein of *C. auris* as a potential target of gallic acid. This protein is responsible for virulence and various other important biological functions in different fungi [363,365,368]. Targeting virulence proteins could minimize the adverse effects on host cells and limit the appearance of drug unsusceptibility in microbes by reducing the selective pressure [390,391]. Hence, CA can be a good target for discovering novel antifungal agents. In a previous study, it was reported that the repurposing of United States FDA-approved CA inhibitors such as ethoxzolamide, acetazolamide and methazolamide showed antibacterial properties against Vancomycin-resistant *Enterococcus faecalis* and *Enterococcus faecium* [392]. The molecular docking and molecular dynamics study showed that the CA of *E. faecium* might be the intracellular target of ethoxzolamide, acetazolamide, and methazolamide [392]. The results of our research imply that gallic acid could bind with the active site residues of *C. auris* and *C. albicans* CA proteins (Figure 34). The active site residues, majority of which are hydrophobic (Ile 99, Gly 135, Phe 116, Leu 121), form a narrow tunnel that could act as the point of entry to the +ly charged active site, according to a *C. albicans* crystal structure (6GWU). When we looked at the simulated structure of *C. auris*, we discovered that these residues (Ile 117, Gly 153, Phe 134, and Leu 139) were present in the protein as well, forming a small tunnel. The distinct salt bridges of 54 residues (Arg80-ASP133) which help in the creation of the active site cavity in *C. albicans* and regulate the shape and openness of the tunnel that also contributes to the formation of the active site cavity were also present in *C. auris* (ARG 98-ASP 151). The residues Asp 83, Val 95, Ile 118, and Lys 124 of *C. albicans* CA protein were mutated to Glu 101, Thr 113, Val 136 and Arg 142 respectively in *C. auris* CA protein. We believe that these changes make gallic acid less accessible to the active site, lowering the binding strength. Future studies can focus on making derivatives of gallic acid that can target CA of *C. auris* more efficiently. These derivatives could be novel antifungal drugs with new modes of action.

Objective 5: To develop a potent multivalent epitope based vaccine against *C. auris* using *in-silico* approach.

5.5.1. Protein sequence retrieval and analysis

According to the CELLO2GO web server, Als3p was predicted to be an extracellular protein or localized on the plasma membrane. The Als3p was also indicated to be highly antigenic. The Vaxijen score for the protein was 1.3035 which suggested a strong antigenic nature of Als3p. The results also showed that Als3p fulfils the preliminary criteria of being an antigenic and extracellular protein and having adhesion properties.

5.5.2. Prediction of T cell and B cell epitopes

For the prediction of T helper cell peptides HLA alleles: DRB1_1602, DRB1_1501, DRB1_1301, DRB1_1101, DRB1_1201, DRB1_0901, DRB1_1001, DRB1_0801, DRB1_0701, DRB1_0401, DRB1_0101, and DRB1_0301 were selected. The T helper cell (MHCII) epitopes that were classified as strong binder were selected for further analysis. For the prediction of T cytotoxic cell (MHCI) epitopes HLA alleles: HLA-B5801, HLA-B4001, HLA-A0101, HLA-B3901, HLA-A2601, HLA-A2402, HLA-A0201, HLA-B2705, HLA-B0801, HLA-B0702, and HLA-A0301 were selected.

5.5.3. Prediction of toxicity, allergenicity, antigenicity, interferon-γ activating potential and conservancy of the epitopes

All the epitopes that were predicted in the previous section were analyzed for their antigenicity, toxicity, conservancy, allergenicity, and interferon-γ activating potential. Altogether 12 epitopes were found to be non-allergen, non-toxic, antigenic, and could activate interferon-γ. Epitopes with a Vaxijen score ≥of 1.1 were selected as they are considered to be highly antigenic [393]. On further analysis using the Epitope Conservancy tool it was observed that only 8 epitopes were found to be conserved among the various strains of *C. auris*. These 8 conserved epitopes along with their toxicity, allergenicity, antigenicity, and interferon-γ activating potential are listed in Table 5.28.

Table 5.28: Epitopes that are conserved, antigenic (Vaxijen above 1.1), non-allergen, non-toxin, and induce interferon gamma synthesis. All the epitopes listed in the table are interferon-γ eliciting, non-toxic, non-allergic and antigenic

Epitope Type	Peptide	Vaxijen Score
T helper	FTSSSNTLQ	1.6882
T helper	SYQATVSFS	1.8102
T cytotoxic	GTDTLVIEV	3.2373
T cytotoxic	RPYININAA	1.5102
T cytotoxic	SSYQATVSF	1.5941
B cell	NAGSTSDEVNL	1.1967
B cell	RTWTGSVTTTETLTAPSGGTE	2.1727
B cell	PTPVTTITKTWTGSVTTTETIPAPSGGTET	1.3744

5.5.4. Vaccine engineering and its physiochemical property determination

The 8 conserved epitopes were further used for vaccine engineering. Two adjuvants RS09 (APPHALS), and the flagellin protein of *Salmonella dublin* were used as adjuvants. All these epitopes and adjuvants were linked by the GGS linker and the PADRE sequence was also added. The schematic diagram of the complete vaccine construct is plotted using Illustrator for Biological Sequences webserver [394] and is shown in Figure 5.28. Analysis of physiochemical properties (Table 5.29) of the vaccine construct by ExPASy ProtParam web server showed its instability index score was below 40, which indicated that the protein is stable and the negative GRAVY score implied the protein was hydrophilic [332]. The vaccine was also predicted as soluble after expression in *E. coli* using Solpro webserver [333]. The different physicochemical attributes of the prospective vaccine are listed in Table 38. The amino acid sequence of the prospective vaccine is: "MAQVINTNSLSLLTQNNLNKSQSALGTAIERLSSGLRINSAKDDAAGQAIANRFTANIKGLTQASRNANDGISIAQTTEGALNEINNNLQRVRELAVQSANSTNSQSDLDSIQAEITQRLNEIDRVSGQTQFNGVKVLAQDNTGGSAPPHALSGGSFTSSSNTLQGGSAKFVAAWTLKAAAGGSSYQATVSFSGGSGTDTLVIEVGGSRPYININAAGGSAKFVAAWTLKAAAGGSSSYQATVSFGGSNAGSTSDEVNLGGSAKFVAAWTLKAAAGGSRTWTGSVTTTETLTAPSGGTEGGSPTPVTTITKTWTGSVTTTETIPAPSGGTETLGNTVNNLTSARSRIEDSDYATEVSNMSRAQILQQAGTSVLAQANQVPQNVLSLLR".

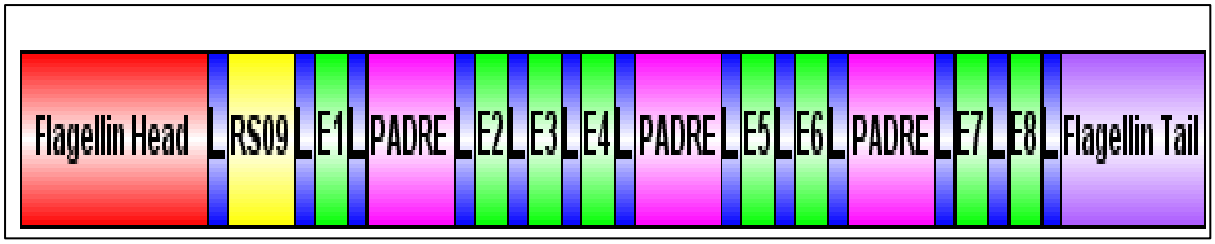

Figure 5.28: Design of the engineered *C. auris* vaccine candidate: The total length of the peptide vaccine is 388 amino acids. The N-terminal terminal and C-terminal is the flagellin protein sequence, followed by GSS (L) linker sequences, E1 to E8 depicts the selected epitopes and in between pan HLA DR-binding epitope (PADRE) sequence

Table 5.29: Physiochemical properties of the *C. auris* prospective vaccine

Number of amino acids	388
Molecular weight	39446.19
Instability index	39.98 (Stable)
Aliphatic index	76.57
Theoretical pI	6.63
Extinction coeffiecent	33460
Sum of -ve charged residues (Glu+Asp)	25
Sum of +ve charged residues (Lys+Arg)	25
Estimated half-life	30 hours in mammalian reticulocytes, >20 hours in yeast and > 10 hours in *E. coli*
Total number of atoms	5494
GRAVY	-0.244
Solubility (Solpro program)	Soluble (0.745210)
Allergenicity	Non-allergen
Antigenicity using Vaxijen sever	Antigen (Vaxijen score:1.2211)

5.5.5. Determination of secondary and tertiary structure of the vaccine construct and validation of the predicted tertiary structure

The analysis of the secondary structures of the vaccine construct by the PSIPRED server showed the presence of all three types of secondary structures namely coils, helix, and strands (Figure 5.29). The modelled tertiary structure by the I-Tasser server had the best C-score as -

1.08. The Rampage server webserver showed 93% of the residues of modelled protein were present in favoured or allowed regions of the Ramachandran plot (Figure 5.30).

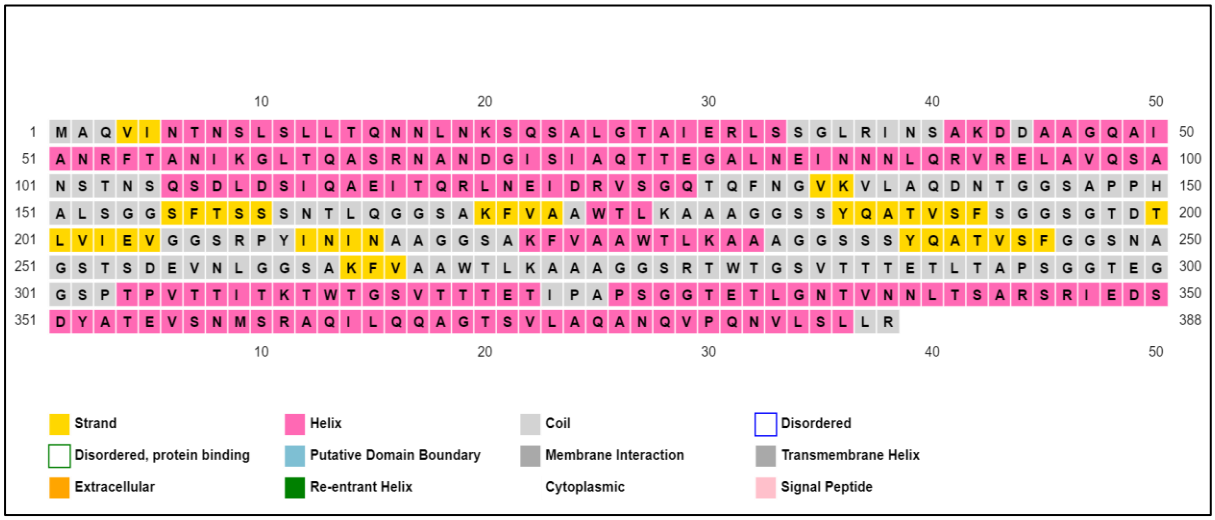

Figure 5.29: PSIPRED program predicted secondary structure of the potential vaccine candidate: The various regions shown are strand (yellow), helix (pink), membrane interaction, and transmembrane helix (Gray).

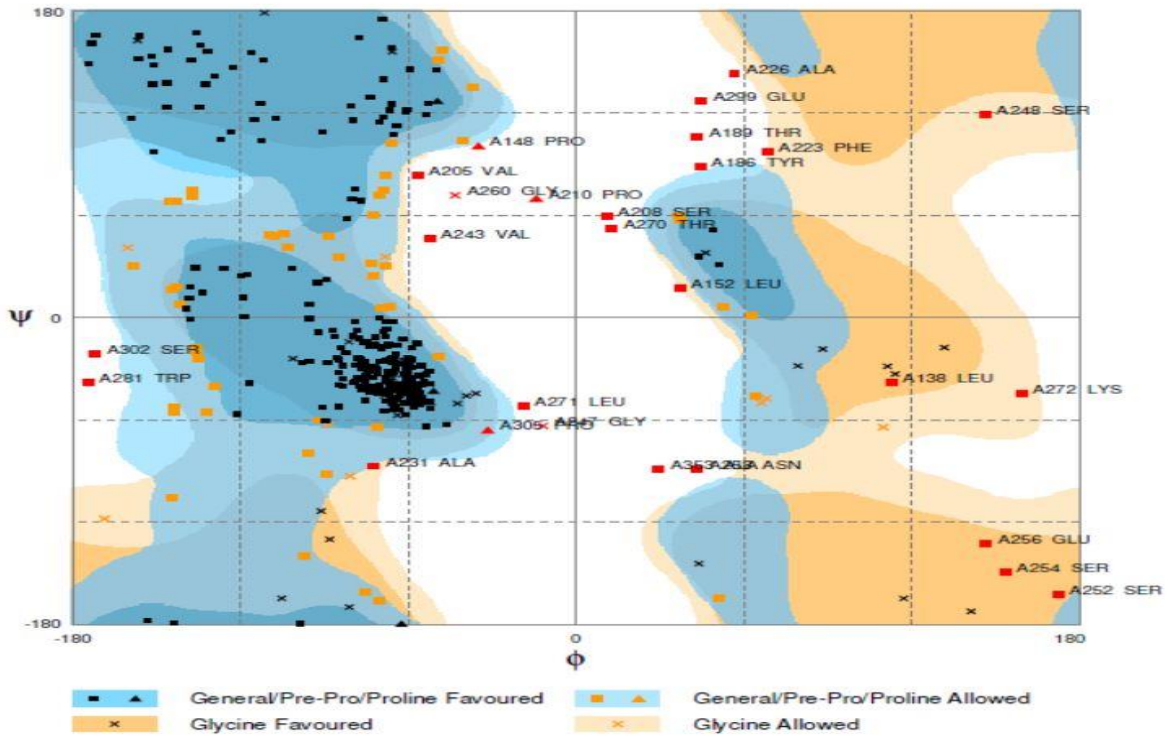

Figure 5.30: Ramachandran plot of the tertiary structure of *C. auris* vaccine construct

5.5.6. Molecular docking of the vaccine construct with toll-like receptor molecule and molecular dynamics simulation of vaccine and receptor complex

The molecular docking of the vaccine was performed with TLR5 and MHC class-II allele HLA DRB_0101 using the ClusPro 2.0 web server. After docking 29 models were obtained for both docking with TLR5 and MHC class-II HLA DRB_0101. Analysis of the docked complex with the lowest energy -1333.4 and -1025.6 respectively for TLR5 and MHCII HLA DRB_0101) showed that the vaccine construct occupied the receptor properly (Figure 5.31).

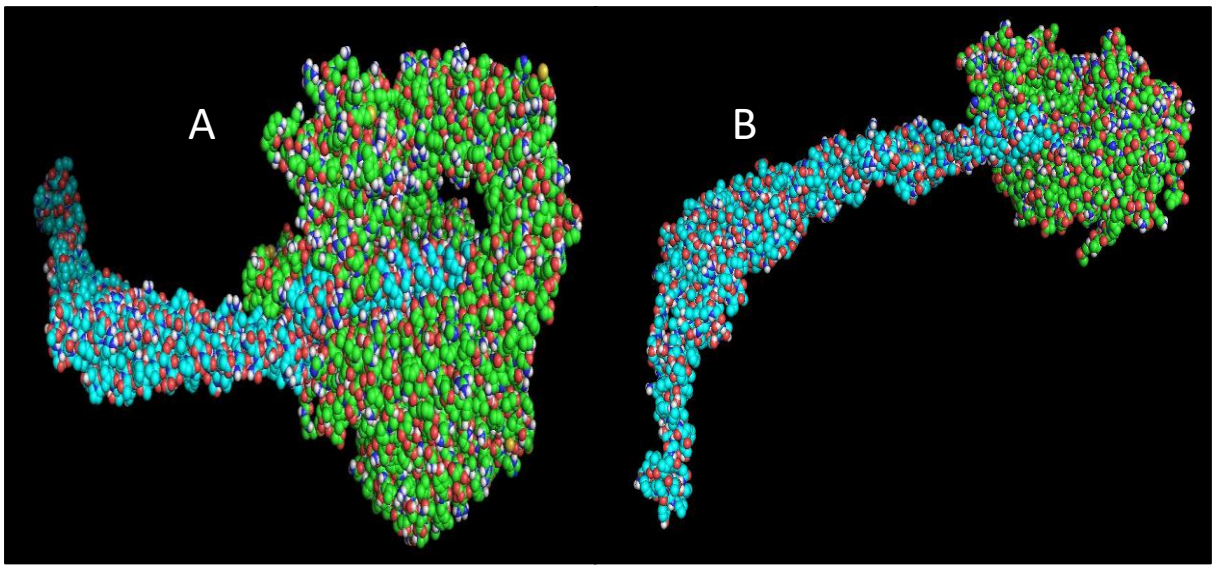

Figure 5.31: Molecular docking (A) Docking of vaccine construct (blue color) and TLR5 receptor (green). (B) Docking of vaccine construct (blue) and HLA allele (green in color).

5.5.7. Molecular dynamics simulation

Various molecular dynamics parameters such as RMSD, potential energy, temperature, the radius of gyration of free vaccine construct and vaccine construct with the receptors MHCI and TLR-5 in the last 10 ns are listed in Table 5.30. The RMSD and RMSF plots of the vaccine construct- MHCI complex and vaccine construct-TLR5 complex are shown in Figure 5.32. The RMSD for the vaccine construct-MHCI complex gradually increased up to 70 ns and afterwards, it became stable until 100 ns with an RMSD value of 0.46 nm. Similarly, for the vaccine, construct-TLR5 complex RMSD increased gradually up to 70 ns and afterwards it decreased and remained stable until 100 ns with an RMSD value of 0.37 nm. For the vaccine construct-MHCI complex, the RMSF was approximately 0.3 nm up to 16500 residues, then there was an abrupt rise up to 1.1 nm for the vaccine construct-TLR5 complex the RMSF was approximately 0.4 nm up to 13000 residues, then there was an abrupt rise of RMSF up to 0.7 nm between residues 13000–15000 residues followed by a decrease in the RMSF.

Table 5.30: Last 10 ns critical observations for free vaccine construct and docked vaccine construct

MD Parameter	**Free vaccine construct**	**Vaccine construct with MHCI**	**Vaccine construct with TLR-5**
RMSD (nm)	0.82 ± 0.03	0.46 ± 0.04	0.37 ± 0.02
Temperature (K)	300.3 ± 1.03	300.2 ± 1.9	300.1 ± 1.08
Potential Energy (KJ/mol)	-563049	- 1789736	- 1577342
Distance between center of mass of vaccine construct and MHCI antigenic determinant (nm)	-	3.05 ± 0.03	-
Distance between center of mass of vaccine construct and TLR-5 antigenic determinant (nm)	-	-	3.01 ± 0.02
H-bonds (protein-protein interaction)		278.7 ± 9.2	294.6 ± 8.3
Radius of gyration (nm)	-	2.92 ± 0.02	2.83 ± 0.05

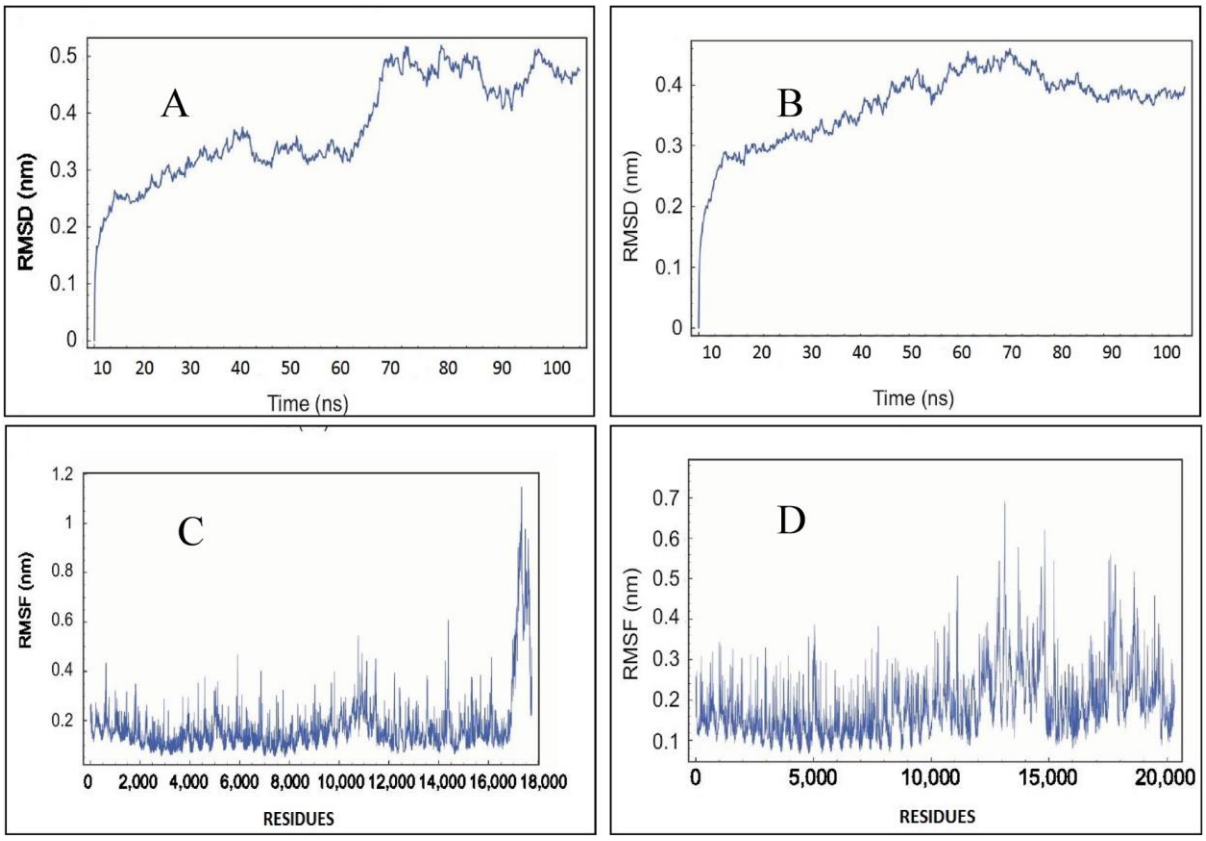

Figure 5.32: Molecular dynamics analysis (A) Vaccine construct +MHC1: RMSD Plot (B) Vaccine construct+ TLR05: RMSD Plot (C) Vaccine construct +MHC1: RMSF Plot (D) Vaccine construct+ TLR05: RMSF Plot.

5.5.8. Codon adaptation and in-silico cloning

To produce vaccines in large quantities, it needs to be cloned and expressed in a suitable vector. Codon adaptation analysis is one of the important criteria to delineate codon biases in the host. The Codon Adaptation Index of the candidate vaccine was 0.9731 which confirms the extraordinary degree of the sequence expression, and the GC content of the improved sequence was 53.17%. The vaccine construct was inserted between XhoI (158) and EcoRI (192) restriction sites of the pET28a (+) vector by using the restriction cloning module of SnapGene software. The size of the cloned product was 6503bp. The final cloned vaccine construct is shown in Figure 5.33, where the vaccine construct is shown in orange colour.

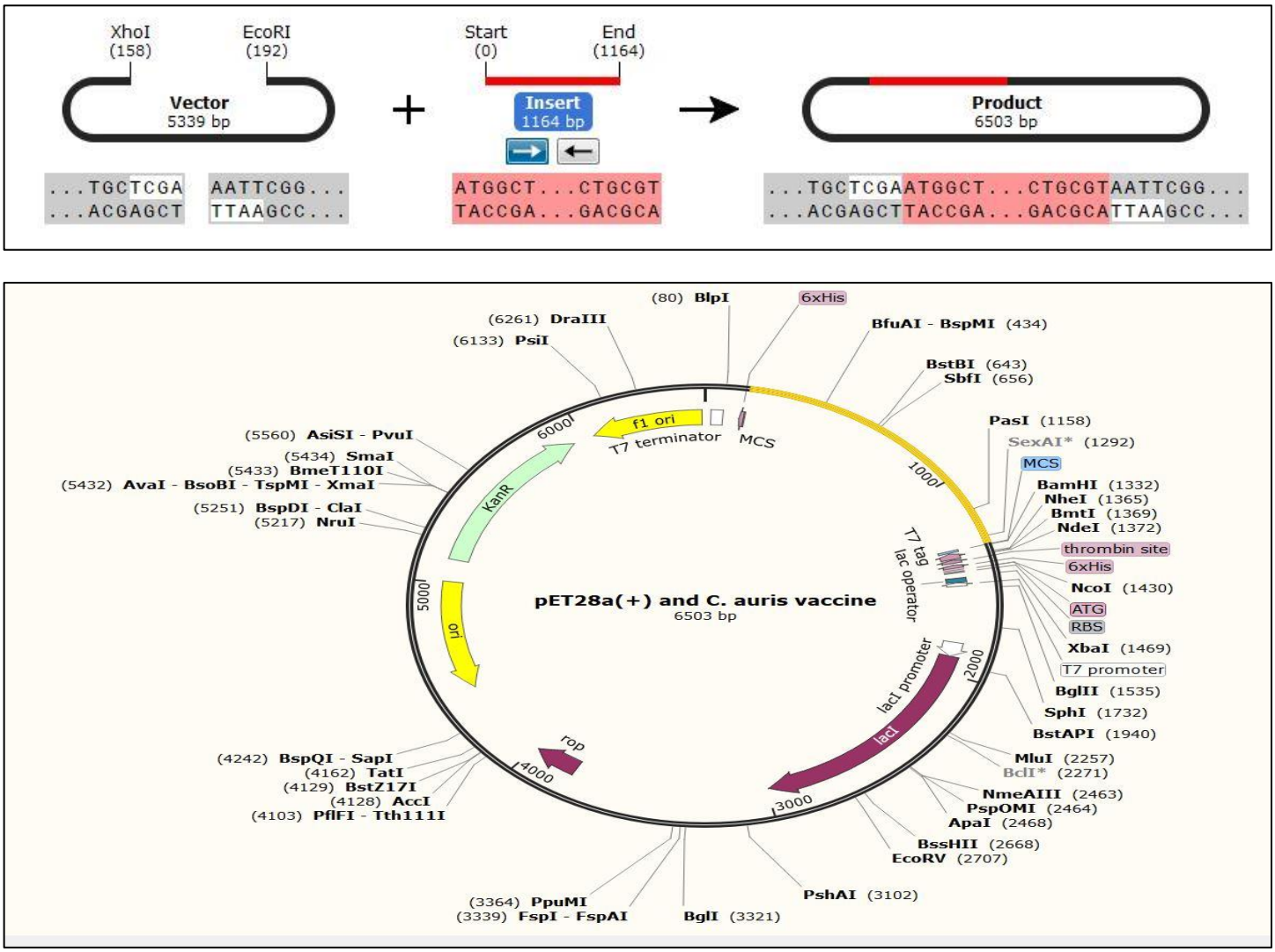

Figure 5.33: In silico cloning of the *C. auris* vaccine construct in pET28a (+) vector.

Discussion

The development of pan-drug unsusceptibility in fungi has highlighted the need to explore new treatment options for *C. auris*. A potential solution could be the creation of an effective and powerful vaccine to combat the pathogen. This objective aimed to use the in silico immunoinformatics technique to develop a unique multi-epitope prospective vaccine for protection from *C. auris* infection. To date, there have been no reports of immunoinformatics-based vaccine design for *C. auris*, although a multivalent vaccine for *Candida albicans* has been developed using in silico techniques [395]. Compared to other methods, designing a multiepitope-based vaccine using in silico immunoinformatics offers several advantages. It can save time and money in the vaccine design process [396,397]. Additionally, this approach can lead to the development of a vaccine that can generate a

strong immune response and overcome significant obstacles in vaccine design, such as antigenic drift, antigenic shift, and genetic variations [398].

The selection criteria outlined in Maria et al's review were taken into account when choosing a protein for this study and the Als3p protein was ultimately selected. Als3p is part of the agglutinin-like sequence protein family and is involved in the adherence of fungal cells to host cells, playing an important role in pathogenesis [322,399]. The sequence of Als3p protein was obtained from the Candida genome database and assessed for its subcellular localization and antigenicity. The protein was identified as highly antigenic and located in the cell membrane or extracellular environment. These are crucial factors that a protein must meet in order to be considered for vaccine design.[400]. Next, Als3p was used to predict several B-cells and T-cells epitopes, which were then evaluated for their antigenicity, allergenicity, conservancy among different *C. auris* strains, interferon-γ activating potential, and toxicity. Only the epitopes that were predicted to be antigenic, conserved among different *C. auris* strains, non-toxic, non-allergic, and capable of inducing interferon-γ production were selected for the final vaccine construct development. To ensure the safety of the final vaccine construct, the selected epitopes should not be toxic or allergic. Epitopes with high antigenicity, which have a Vaxijen score of at least 1.1, can be crucial for eliciting a strong immune response [401]. Conserved epitopes among different strains can overcome limitations like antigenic shifts and antigenic drifts. Interferon-γ has been found to possess a key part in preventing invasive aspergillosis and candidiasis, so epitopes that can activate interferon-γ synthesis could be useful in preventing *C. auris* infection further [402,403]. In the end, the chosen epitopes were linked together with adjuvants such as flagellin protein and RS09 using a linker sequence (GGS). RS09 and flagellin protein act as toll-like receptor (TLR) agonists, with RS09 being an agonist of TLR-4 4, and flagellin protein being an agonist of TLR-5 [404–406]. These TLR agonists help stimulate both adaptive immunity and innate immunity [404–406]. Previously, these adjuvants were utilized in the creation of a multivalent epitope-based vaccine against monkeypox virus, human cytomegalovirus, *C. dubliniensis*, *C. tropicalis* and Human papillomavirus [118,330,407–409]. To ensure the prospective vaccine's stability, the PADRE sequence was incorporated into the prospective vaccine construct design [410]. In the end, a prospective vaccine consisting of 388 amino acids was designed, which was anticipated to be strongly antigenic, soluble, stable, and lacking in allergenic properties. The 3D model of the prospective vaccine was designed by applying the I-Tasser program and confirmed by generating a Ramachandran plot and

measuring the C-score. The Ramachandran plot indicated that the majority (93%) of residues were located in the favourable or acceptable regions, indicating that the protein model was of high quality. Additionally, the C-score, another metric used to evaluate the accuracy of a protein's 3D model, was high, further confirming the model's quality. Once the 3D model of the vaccine was generated, MD analysis was conducted to examine how the vaccine binds to TLR molecules and MHC allele. The vaccine was found to effectively interact with these molecules, as indicated by the negative binding energy where low binding energy suggests higher binding affinity. The stability of the interactions among the vaccine candidate and TLR molecules and MHC alleles were then verified using molecular dynamics simulation analysis. Finally, computational cloning was performed, which suggested that the prospective *C. auris* vaccine could be efficiently expressed in *E. coli* for its commercial production. These results suggest that the vaccine candidate could be an effective and safe prevention strategy for *C. auris* infections. However, further validation through in vivo studies is necessary to support these claims.

Summary and Conclusion

Conclusion and Future perspectives

C. auris, a multidrug-resistant fungus has become a major public health threat because of its high mortality rate and rapid rate of transmission. The research for novel antifungal compounds and drug targets to treat and prevent *C. auris* infections is crucial. The unfolded protein response (UPR) pathway, which maintains equilibrium inside the cell by removing misfolded proteins, could be a potential drug target.

- The bioinformatics analysis determined that the *HAC1* intron in *C. auris* is 440 bp long and the *C. auris HAC1* intron has 5' hairpin loop surrounding 5' splice site. However, the 3' hairpin loop surrounding the 3' splice site is absent in *C. auris*.
- The cloning of the *HAC1* gene in pESC-URA plasmid and genetic complementation in the *S. cerevisiae HAC1* delete strain showed that the *C. auris HAC1* could complement the *HAC1* gene in *S. cerevisiae HAC1* delete strain and help it to sustain under endoplasmic reticulum stress similar to wild type *S. cerevisiae* strain.
- Using computational tools, the molecular properties of different molecules were analyzed, and BA and drummondin-E were predicted to be possible inhibitors of the C. *auris* UPR pathway.
- In vitro analysis showed that betulinic acid has the potential to thwart the growth of *C. auris* and affect genes involved in oxidative stress and cell wall biogenesis. Betulinic acid was found to have low cytotoxicity on human cell line even at 2x MIC concentration of *C. auris*.
- Furthermore, the antifungal activity of *S. pulcherrima* could be due to the presence of gallic acid, which may be a potential molecule for developing antifungals against *C. auris*.
- Computational studies also showed that gallic acid could interact with the active sites of *C. auris* carbonic anhydrase protein and affect its catalytic activity.
- Finally, a novel prospective vaccine has been designed by an immunoinformatics approach to protect individuals from *C. auris* infections. Additional in vivo experiments are necessary for establishing the effectiveness and safety of either the vaccine candidate or the selected epitopes.

Further studies should focus on showing the splicing of the *HAC1* gene by RT-PCR analysis. Future studies should also focus on in vitro and in vivo studies to corroborate the antifungal

potential of betulinic acid and drummondin-E by inhibiting the UPR elements. Additionally, studies should analyse the antifungal potential, safety and toxicity of the *S. pulcherrima* phytochemicals in mice models. The potential of targeting carbonic anhydrase as an antifungal drug target can also be explored to develop a novel class of antifungal drugs. In the future, research akin to Kaushik *et al* (2022) could be conducted, where the predicted antigenic peptides are synthesized and tested for their capability to produce protective antibodies in animals [411]. Additionally, the proposed vaccine design could be used as a recombinant vaccine which could then be administered to immunize animal models infected with *C. auris* and evaluated for its capability to generate an immune response and protect the mice from *C. auris*, adhering to the procedure akin to that of Shukla *et al* (2022) [412].

Bibliography

1. Philpott, D. Epidemiologic and Clinical Characteristics of Monkeypox Cases — United States, May 17–July 22, 2022. *MMWR Morb Mortal Wkly Rep* **2022**, *71*, doi:10.15585/mmwr.mm7132e3.
2. Sánchez, F.J.M.; Martínez-Sellés, M.; García, J.M.M.; Guillén, S.M.; Rodríguez-Artalejo, F.; Ruiz-Galiana, J.; Cantón, R.; Ramos, P.D.L.; García-Botella, A.; García-Lledó, A.; et al. Insights for COVID-19 in 2023. *Rev Esp Quimioter* **2023**, *36*, 114–124, doi:10.37201/req/122.2022.
3. Baluku, J.B.; Torpey, K. INTEREST 2022: New Perspectives in HIV Treatment, Pathogenesis and Prevention in Africa. *Ther Adv Infect Dis* **2023**, *10*, 20499361231177856, doi:10.1177/20499361231177856.
4. Piret, J.; Boivin, G. Pandemics Throughout History. *Frontiers in Microbiology* **2021**, *11*, 631736.
5. Sampath, S.; Khedr, A.; Qamar, S.; Tekin, A.; Singh, R.; Green, R.; Kashyap, R. Pandemics Throughout the History. *Cureus* **2021**, *13*, e18136, doi:10.7759/cureus.18136.
6. de Kraker, M.E.A.; Lipsitch, M. Burden of Antimicrobial Resistance: Compared to What? *Epidemiologic Reviews* **2021**, *43*, 53–64, doi:10.1093/epirev/mxab001.
7. Jagannathan, P.; Kakuru, A. Malaria in 2022: Increasing Challenges, Cautious Optimism. *Nat Commun* **2022**, *13*, 2678, doi:10.1038/s41467-022-30133-w.
8. Barry, A.E. Grand Challenges in Parasite Epidemiology and Ecology. *Frontiers in Parasitology* **2022**, *1*, 1034819.
9. Wang, J.-L.; Li, T.-T.; Huang, S.-Y.; Cong, W.; Zhu, X.-Q. Major Parasitic Diseases of Poverty in Mainland China: Perspectives for Better Control. *Infect Dis Poverty* **2016**, *5*, 67, doi:10.1186/s40249-016-0159-0.
10. Rodrigues, M.L.; Nosanchuk, J.D. Fungal Diseases as Neglected Pathogens: A Wake-up Call to Public Health Officials. *PLoS Negl Trop Dis* **2020**, *14*, e0007964, doi:10.1371/journal.pntd.0007964.
11. Almeida, F.; Rodrigues, M.L.; Coelho, C. The Still Underestimated Problem of Fungal Diseases Worldwide. *Front Microbiol* **2019**, *10*, 214, doi:10.3389/fmicb.2019.00214.
12. Bongomin, F.; Gago, S.; Oladele, R.O.; Denning, D.W. Global and Multi-National Prevalence of Fungal Diseases—Estimate Precision. *Journal of Fungi* **2017**, *3*, 57, doi:10.3390/jof3040057.
13. Benedict, K.; Molinari, N.A.M.; Jackson, B.R. Public Awareness of Invasive Fungal Diseases — United States, 2019. *MMWR Morb Mortal Wkly Rep* **2020**, *69*, 1343–1346, doi:10.15585/mmwr.mm6938a2.
14. Narayanasamy, S.; Dat, V.Q.; Thanh, N.T.; Ly, V.T.; Chan, J.F.-W.; Yuen, K.-Y.; Ning, C.; Liang, H.; Li, L.; Chowdhary, A.; et al. A Global Call for Talaromycosis to Be Recognised as a Neglected Tropical Disease. *The Lancet Global Health* **2021**, *9*, e1618–e1622, doi:10.1016/S2214-109X(21)00350-8.
15. Rodrigues, M.L.; Nosanchuk, J.D. Fungal Diseases as Neglected Pathogens: A Wake-Up Call to Public Health Officials. In *Advances in Clinical Immunology, Medical Microbiology, COVID-19, and Big Data*; Jenny Stanford Publishing, 2021 ISBN 978-1-00-318043-2.
16. He, Y.; Zheng, H.; Mei, H.; Lv, G.; Liu, W.; Li, X. Phaeohyphomycosis in China. *Frontiers in Cellular and Infection Microbiology* **2022**, *12*.
17. Hsu, L.Y.; Wijaya, L.; Shu-Ting Ng, E.; Gotuzzo, E. Tropical Fungal Infections. *Infect Dis Clin North Am* **2012**, *26*, 497–512, doi:10.1016/j.idc.2012.02.004.
18. Greener, M. Why Have We Neglected Fungal Infections? *Prescriber* **2022**, *33*, 20–23, doi:10.1002/psb.2008.

19. Rodrigues, M.L.; Albuquerque, P.C. Searching for a Change: The Need for Increased Support for Public Health and Research on Fungal Diseases. *PLoS Negl Trop Dis* **2018**, *12*, e0006479, doi:10.1371/journal.pntd.0006479.
20. Kmeid, J.; Jabbour, J.F.; Kanj, S.S. Epidemiology and Burden of Invasive Fungal Infections in the Countries of the Arab League. *Journal of Infection and Public Health* **2020**, *13*, 2082–2086, doi:10.1016/j.jiph.2019.05.007.
21. Brown, G.D.; Denning, D.W.; Gow, N.A.R.; Levitz, S.M.; Netea, M.G.; White, T.C. Hidden Killers: Human Fungal Infections. *Sci Transl Med* **2012**, *4*, 165rv13, doi:10.1126/scitranslmed.3004404.
22. Bongomin, F.; Gago, S.; Oladele, R.O.; Denning, D.W. Global and Multi-National Prevalence of Fungal Diseases—Estimate Precision. *J Fungi (Basel)* **2017**, *3*, 57, doi:10.3390/jof3040057.
23. Ray, A.; Aayilliath K, A.; Banerjee, S.; Chakrabarti, A.; Denning, D.W. Burden of Serious Fungal Infections in India. *Open Forum Infect Dis* **2022**, *9*, ofac603, doi:10.1093/ofid/ofac603.
24. CDC Impact of Fungal Diseases in the United States Available online: https://www.cdc.gov/fungal/cdc-and-fungal/burden.html (accessed on 12 March 2023).
25. Ghannoum, M.A.; Rice, L.B. Antifungal Agents: Mode of Action, Mechanisms of Resistance, and Correlation of These Mechanisms with Bacterial Resistance. *Clin Microbiol Rev* **1999**, *12*, 501–517.
26. Lakhani, P.; Patil, A.; Majumdar, S. Challenges in the Polyene- and Azole-Based Pharmacotherapy of Ocular Fungal Infections. *Journal of Ocular Pharmacology and Therapeutics* **2019**, *35*, 6, doi:10.1089/jop.2018.0089.
27. Robbins, N.; Wright, G.D.; Cowen, L.E. Antifungal Drugs: The Current Armamentarium and Development of New Agents. *Microbiology Spectrum* **2016**, *4*, 10.1128/microbiolspec.funk-0002–2016, doi:10.1128/microbiolspec.funk-0002-2016.
28. Hammoudi Halat, D.; Younes, S.; Mourad, N.; Rahal, M. Allylamines, Benzylamines, and Fungal Cell Permeability: A Review of Mechanistic Effects and Usefulness against Fungal Pathogens. *Membranes (Basel)* **2022**, *12*, 1171, doi:10.3390/membranes12121171.
29. Logan, A.; Wolfe, A.; Williamson, J.C. Antifungal Resistance and the Role of New Therapeutic Agents. *Curr Infect Dis Rep* **2022**, *24*, 105–116, doi:10.1007/s11908-022-00782-5.
30. Phillips, N.A.; Rocktashel, M.; Merjanian, L. Ibrexafungerp for the Treatment of Vulvovaginal Candidiasis: Design, Development and Place in Therapy. *Drug Des Devel Ther* **2023**, *17*, 363–367, doi:10.2147/DDDT.S339349.
31. Wall, G.; Lopez-Ribot, J.L. Current Antimycotics, New Prospects, and Future Approaches to Antifungal Therapy. *Antibiotics (Basel)* **2020**, *9*, 445, doi:10.3390/antibiotics9080445.
32. McCarty, T.P.; Pappas, P.G. Antifungal Pipeline. *Frontiers in Cellular and Infection Microbiology* **2021**, *11*.
33. Brown, G.D.; Denning, D.W.; Gow, N.A.R.; Levitz, S.M.; Netea, M.G.; White, T.C. Hidden Killers: Human Fungal Infections. *Science Translational Medicine* **2012**, *4*, 165rv13-165rv13, doi:10.1126/scitranslmed.3004404.
34. Kim, J.-Y. Human Fungal Pathogens: Why Should We Learn? *Journal of Microbiology* **2016**, *54*, 145–148, doi:10.1007/s12275-016-0647-8.
35. Köhler, J.R.; Casadevall, A.; Perfect, J. The Spectrum of Fungi That Infects Humans. *Cold Spring Harb Perspect Med* **2015**, *5*, a019273, doi:10.1101/cshperspect.a019273.
36. Akhtar, N.; Khurshid Wani, A.; Kant Tripathi, S.; Prakash, A.; Amin-ul Mannan, M. The Role of SARS-CoV-2 Immunosuppression and the Therapy Used to Manage

COVID-19 Disease in the Emergence of Opportunistic Fungal Infections: A Review. *Current Research in Biotechnology* **2022**, *4*, 337–349, doi:10.1016/j.crbiot.2022.08.001.
37. Turner, S.A.; Butler, G. The Candida Pathogenic Species Complex. *Cold Spring Harbor Perspectives in Medicine* **2014**, *4*, a019778–a019778, doi:10.1101/cshperspect.a019778.
38. d'Enfert, C.; Kaune, A.-K.; Alaban, L.-R.; Chakraborty, S.; Cole, N.; Delavy, M.; Kosmala, D.; Marsaux, B.; Fróis-Martins, R.; Morelli, M.; et al. The Impact of the Fungus-Host-Microbiota Interplay upon Candida Albicans Infections: Current Knowledge and New Perspectives. *FEMS Microbiology Reviews* **2021**, *45*, fuaa060, doi:10.1093/femsre/fuaa060.
39. Altinkaya Çavuş, M.; Sav, H. Opportunistic Candida Infections in Critical COVID-19 Patients. *Pol J Microbiol* **2022**, *71*, 411–419, doi:10.33073/pjm-2022-036.
40. Goravey, W.; Ali, G.A.; Ali, M.; Ibrahim, E.B.; Al Maslamani, M.; Abdel Hadi, H. Ominous Combination: COVID-19 Disease and Candida Auris Fungemia—Case Report and Review of the Literature. *Clinical Case Reports* **2021**, *9*, e04827, doi:10.1002/ccr3.4827.
41. Erfaninejad, M.; Zarei Mahmoudabadi, A.; Maraghi, E.; Hashemzadeh, M.; Fatahinia, M. Epidemiology, Prevalence, and Associated Factors of Oral Candidiasis in HIV Patients from Southwest Iran in Post-Highly Active Antiretroviral Therapy Era. *Frontiers in Microbiology* **2022**, *13*, 983348.
42. Hirano, R.; Sakamoto, Y.; Kudo, K.; Ohnishi, M. Retrospective Analysis of Mortality and Candida Isolates of 75 Patients with Candidemia: A Single Hospital Experience. *Infect Drug Resist* **2015**, *8*, 199–205, doi:10.2147/IDR.S80677.
43. Xiao, Z.; Wang, Q.; Zhu, F.; An, Y. Epidemiology, Species Distribution, Antifungal Susceptibility and Mortality Risk Factors of Candidemia among Critically Ill Patients: A Retrospective Study from 2011 to 2017 in a Teaching Hospital in China. *Antimicrobial Resistance & Infection Control* **2019**, *8*, 89, doi:10.1186/s13756-019-0534-2.
44. Patil, S.; Rao, R.S.; Majumdar, B.; Anil, S. Clinical Appearance of Oral Candida Infection and Therapeutic Strategies. *Frontiers in Microbiology* **2015**, *6*.
45. Yano, J.; Sobel, J.D.; Nyirjesy, P.; Sobel, R.; Williams, V.L.; Yu, Q.; Noverr, M.C.; Fidel, P.L. Current Patient Perspectives of Vulvovaginal Candidiasis: Incidence, Symptoms, Management and Post-Treatment Outcomes. *BMC Women's Health* **2019**, *19*, 48, doi:10.1186/s12905-019-0748-8.
46. Benedict, K.; Whitham, H.K.; Jackson, B.R. Economic Burden of Fungal Diseases in the United States. *Open Forum Infect Dis* **2022**, *9*, ofac097, doi:10.1093/ofid/ofac097.
47. Chowdhary, A.; Sharma, C.; Meis, J.F. Candida Auris : A Rapidly Emerging Cause of Hospital-Acquired Multidrug-Resistant Fungal Infections Globally. **2017**, doi:10.1371/journal.ppat.1006290.
48. Hegde, A. Candida Auris Is Coming. *Indian J Crit Care Med* **2022**, *26*, 543–544, doi:10.5005/jp-journals-10071-24223.
49. Fisher, M.C.; Denning, D.W. The WHO Fungal Priority Pathogens List as a Game-Changer. *Nat Rev Microbiol* **2023**, 1–2, doi:10.1038/s41579-023-00861-x.
50. WHO *WHO Fungal Priority Pathogens List to Guide Research, Development and Public Health Action*; Geneva, 2022;
51. Kühbacher, A.; Burger-Kentischer, A.; Rupp, S. Interaction of Candida Species with the Skin. *Microorganisms* **2017**, *5*, 32, doi:10.3390/microorganisms5020032.

52. Thatchanamoorthy, N.; Rukumani Devi, V.; Chandramathi, S.; Tay, S.T. Candida Auris: A Mini Review on Epidemiology in Healthcare Facilities in Asia. *J Fungi (Basel)* **2022**, *8*, 1126, doi:10.3390/jof8111126.
53. CDC Candida Auris Available online: https://www.cdc.gov/fungal/candida-auris/index.html (accessed on 14 October 2022).
54. Chybowska, A.D.; Childers, D.S.; Farrer, R.A. Nine Things Genomics Can Tell Us About Candida Auris. *Frontiers in Genetics* **2020**, *11*, 351, doi:10.3389/fgene.2020.00351.
55. CDC The Biggest Antibiotic-Resistant Threats in the U.S. Available online: https://www.cdc.gov/drugresistance/biggest-threats.html (accessed on 9 March 2023).
56. Sathyapalan, D.T.; Antony, R.; Nampoothiri, V.; Kumar, A.; Shashindran, N.; James, J.; Thomas, J.; Prasanna, P.; Sudhir, A.S.; Philip, J.M.; et al. Evaluating the Measures Taken to Contain a Candida Auris Outbreak in a Tertiary Care Hospital in South India: An Outbreak Investigational Study. *BMC Infectious Diseases* **2021**, *21*, 425, doi:10.1186/s12879-021-06131-6.
57. Chowdhary, A.; Tarai, B.; Singh, A.; Sharma, A. Multidrug-Resistant Candida Auris Infections in Critically Ill Coronavirus Disease Patients, India, April-July 2020. *Emerg Infect Dis* **2020**, *26*, 2694–2696, doi:10.3201/eid2611.203504.
58. Rudramurthy, S.M.; Chakrabarti, A.; Paul, R.A.; Sood, P.; Kaur, H.; Capoor, M.R.; Kindo, A.J.; Marak, R.S.K.; Arora, A.; Sardana, R.; et al. Candida Auris Candidaemia in Indian ICUs: Analysis of Risk Factors. *Journal of Antimicrobial Chemotherapy* **2017**, *72*, 1794–1801, doi:10.1093/jac/dkx034.
59. Rajni, E.; Singh, A.; Tarai, B.; Jain, K.; Shankar, R.; Pawar, K.; Mamoria, V.; Chowdhary, A. A High Frequency of Candida Auris Blood Stream Infections in Coronavirus Disease 2019 Patients Admitted to Intensive Care Units, Northwestern India: A Case Control Study. *Open Forum Infectious Diseases* **2021**, *8*, ofab452, doi:10.1093/ofid/ofab452.
60. Sathyapalan, D.T.; Antony, R.; Nampoothiri, V.; Kumar, A.; Shashindran, N.; James, J.; Thomas, J.; Prasanna, P.; Sudhir, A.S.; Philip, J.M.; et al. Evaluating the Measures Taken to Contain a Candida Auris Outbreak in a Tertiary Care Hospital in South India: An Outbreak Investigational Study. *BMC Infectious Diseases* **2021**, *21*, 425, doi:10.1186/s12879-021-06131-6.
61. Chen, J.; Tian, S.; Han, X.; Chu, Y.; Wang, Q.; Zhou, B.; Shang, H. Is the Superbug Fungus Really so Scary? A Systematic Review and Meta-Analysis of Global Epidemiology and Mortality of Candida Auris. *BMC Infectious Diseases* **2020**, *20*, 827, doi:10.1186/s12879-020-05543-0.
62. Sanyaolu, A.; Okorie, C.; Marinkovic, A.; Abbasi, A.F.; Prakash, S.; Mangat, J.; Hosein, Z.; Haider, N.; Chan, J. Candida Auris: An Overview of the Emerging Drug-Resistant Fungal Infection. *Infect Chemother* **2022**, *54*, 236–246, doi:10.3947/ic.2022.0008.
63. Cortegiani, A.; Misseri, G.; Chowdhary, A. What's New on Emerging Resistant Candida Species. *Intensive Care Medicine* **2019**, *45*, 512–515, doi:10.1007/s00134-018-5363-x.
64. Lockhart, S.R.; Etienne, K.A.; Vallabhaneni, S.; Farooqi, J.; Chowdhary, A.; Govender, N.P.; Colombo, A.L.; Calvo, B.; Cuomo, C.A.; Desjardins, C.A.; et al. Simultaneous Emergence of Multidrug-Resistant Candida Auris on 3 Continents Confirmed by Whole-Genome Sequencing and Epidemiological Analyses. *Clinical infectious diseases : an official publication of the Infectious Diseases Society of America* **2017**, *64*, 134–140, doi:10.1093/cid/ciw691.

65. de Jong, A.W.; Gerrits van den Ende, B.; Hagen, F. Molecular Tools for Candida Auris Identification and Typing. *Methods Mol Biol* **2022**, *2517*, 33–41, doi:10.1007/978-1-0716-2417-3_3.
66. Pezzotti, G.; Kobara, M.; Nakaya, T.; Imamura, H.; Fujii, T.; Miyamoto, N.; Adachi, T.; Yamamoto, T.; Kanamura, N.; Ohgitani, E.; et al. Raman Metabolomics of Candida Auris Clades: Profiling and Barcode Identification. *Int J Mol Sci* **2022**, *23*, 11736, doi:10.3390/ijms231911736.
67. Sasoni, N.; Maidana, M.; Latorre-Rapela, M.G.; Morales-Lopez, S.; Berrio, I.; Gamarra, S.; Garcia-Effron, G. Candida Auris and Some Candida Parapsilosis Strains Exhibit Similar Characteristics on CHROMagarTMCandida Plus. *Med Mycol* **2022**, myac062, doi:10.1093/mmy/myac062.
68. Lockhart, S.R.; Lyman, M.M.; Sexton, D.J. Tools for Detecting a "Superbug": Updates on Candida Auris Testing. *J Clin Microbiol* **2022**, *60*, e0080821, doi:10.1128/jcm.00808-21.
69. Forsberg, K.; Woodworth, K.; Walters, M.; Berkow, E.L.; Jackson, B.; Chiller, T.; Vallabhaneni, S. Candida Auris: The Recent Emergence of a Multidrug-Resistant Fungal Pathogen. *Medical Mycology* **2018**, *57*, 1–12, doi:10.1093/mmy/myy054.
70. Al-Rashdi, A.; Al-Maani, A.; Al-Wahaibi, A.; Alqayoudhi, A.; Al-Jardani, A.; Al-Abri, S. Characteristics, Risk Factors, and Survival Analysis of Candida Auris Cases: Results of One-Year National Surveillance Data from Oman. *Journal of Fungi* **2021**, *7*, 31, doi:10.3390/jof7010031.
71. Prayag, P.S.; Patwardhan, S.; Panchakshari, S.; Rajhans, P.A.; Prayag, A. The Dominance of Candida Auris: A Single-Center Experience of 79 Episodes of Candidemia from Western India. *Indian Journal of Critical Care Medicine : Peer-reviewed, Official Publication of Indian Society of Critical Care Medicine* **2022**, *26*, 560, doi:10.5005/jp-journals-10071-24152.
72. Johnson, C.J.; Davis, J.M.; Huttenlocher, A.; Kernien, J.F.; Nett, J.E. Emerging Fungal Pathogen Candida Auris Evades Neutrophil Attack. *mBio* **2018**, *9*, e01403-18, doi:10.1128/MBIO.01403-18.
73. Lamoth, F.; Kontoyiannis, D.P. The Candida Auris Alert: Facts and Perspectives. *The Journal of Infectious Diseases* **2018**, *217*, 516–520, doi:10.1093/infdis/jix597.
74. Eldesouky, H.E.; Li, X.; Abutaleb, N.S.; Mohammad, H.; Seleem, M.N. Synergistic Interactions of Sulfamethoxazole and Azole Antifungal Drugs against Emerging Multidrug-Resistant Candida Auris. *Int J Antimicrob Agents* **2018**, *52*, 754–761, doi:10.1016/j.ijantimicag.2018.08.016.
75. Du, H.; Bing, J.; Hu, T.; Ennis, C.L.; Nobile, C.J.; Huang, G. Candida Auris: Epidemiology, Biology, Antifungal Resistance, and Virulence. *PLoS Pathogens* **2020**, *16*, doi:10.1371/journal.ppat.1008921.
76. Forsberg, K.; Woodworth, K.; Walters, M.; Berkow, E.L.; Jackson, B.; Chiller, T.; Vallabhaneni, S. Candida Auris: The Recent Emergence of a Multidrug-Resistant Fungal Pathogen. *Medical Mycology* **2019**, *57*, 1–12, doi:10.1093/mmy/myy054.
77. Kean, R.; Sherry, L.; Townsend, E.; McKloud, E.; Short, B.; Akinbobola, A.; Mackay, W.G.; Williams, C.; Jones, B.L.; Ramage, G. Surface Disinfection Challenges for Candida Auris: An in-Vitro Study. *Journal of Hospital Infection* **2018**, *98*, 433–436, doi:10.1016/j.jhin.2017.11.015.
78. Akhtar, N.; Ayoubi, R.; Kour, V.; Goutam, U.; Mannan, M.A. Natural Products, for Fungal Diseases Management and Prevention. *The Natural Products Journal* **2021**, *11*, e110521193310, doi:10.2174/2210315511666210512035847.

79. Akhtar, N.; Mannan, M.A.; Pandey, D.; Sarkar, A.; Sharma, H.; Kumar, M.; Ghosh, A. Potent Antifungal Properties of Gallic Acid in Sarcochlamys Pulcherrima against Candida Auris. *BioTechnologia* **2023**, *104*, 105–119, doi:10.5114/bta.2023.127202.
80. Gautam, S.; Mannan, M.A. The Role of Algae in Nutraceutical and Pharmaceutical Production. In *Bioactive Natural products in Drug Discovery*; Singh, J., Meshram, V., Gupta, M., Eds.; Springer: Singapore, 2020; pp. 665–685 ISBN 9789811513947.
81. Wani, A.K.; Akhtar, N.; Datta, B.; Pandey, J.; Amin-ul Mannan, M. Cyanobacteria-Derived Small Molecules: A New Class of Drugs. In *Volatiles and Metabolites of Microbes*; Kumar, A., Singh, J., Samuel, J., Eds.; Academic Press, 2021; pp. 283–303 ISBN 978-0-12-824523-1.
82. Sarkar, A.; Akhtar, N.; Mannan, M.A. Antimicrobial Property of Cell Wall Lysed Chlorella, an Edible Alga. *Research Journal of Pharmacy and Technology* **2021**, *14*, 3695–3699, doi:10.52711/0974-360X.2021.00639.
83. Miyazaki, T.; Kohno, S. ER Stress Response Mechanisms in the Pathogenic Yeast Candida Glabrata and Their Roles in Virulence. **2014**, 365–370.
84. Krishnan, K.; Askew, D.S. Endoplasmic Reticulum Stress and Fungal Pathogenesis. *Fungal biology reviews* **2014**, *28*, 29–35, doi:10.1016/j.fbr.2014.07.001.
85. Iracane, E.; Donovan, P.D.; Ola, M. Identification of an Exceptionally Long Intron in the HAC1. **2018**, *3*, 1–10.
86. Oliver, J.D.; Sibley, G.E.M.; Beckmann, N.; Dobb, K.S.; Slater, M.J.; McEntee, L.; du Pré, S.; Livermore, J.; Bromley, M.J.; Wiederhold, N.P.; et al. F901318 Represents a Novel Class of Antifungal Drug That Inhibits Dihydroorotate Dehydrogenase. *Proc Natl Acad Sci U S A* **2016**, *113*, 12809–12814, doi:10.1073/pnas.1608304113.
87. Ghannoum, M.; Arendrup, M.C.; Chaturvedi, V.P.; Lockhart, S.R.; McCormick, T.S.; Chaturvedi, S.; Berkow, E.L.; Juneja, D.; Tarai, B.; Azie, N.; et al. Ibrexafungerp: A Novel Oral Triterpenoid Antifungal in Development for the Treatment of Candida Auris Infections. *Antibiotics* **2020**, *9*, E539, doi:10.3390/antibiotics9090539.
88. Gintjee, T.J.; Donnelley, M.A.; Thompson, G.R. Aspiring Antifungals: Review of Current Antifungal Pipeline Developments. *J Fungi (Basel)* **2020**, *6*, E28, doi:10.3390/jof6010028.
89. Yu, Y.; Albrecht, K.; Groll, J.; Beilhack, A. Innovative Therapies for Invasive Fungal Infections in Preclinical and Clinical Development. *Expert Opin Investig Drugs* **2020**, *29*, 961–971, doi:10.1080/13543784.2020.1791819.
90. Srinivasan, A.; Lopez-Ribot, J.L.; Ramasubramanian, A.K. Overcoming Antifungal Resistance. *Drug Discov Today Technol* **2014**, *11*, 65–71, doi:10.1016/j.ddtec.2014.02.005.
91. Pai, S.R.; Joshi, R.K. Distribution of Betulinic Acid in Plant Kingdom. *Plant Science Today* **2014**, *1*, 103–107, doi:10.14719/pst.2014.1.3.58.
92. Rajemiarimiraho, M.; Banzouzi, J.-T.; Nicolau-Travers, M.-L.; Ramos, S.; Cheikh-Ali, Z.; Bories, C.; Rakotonandrasana, O.L.; Rakotonandrasana, S.; Andrianary, P.A.; Benoit-Vical, F. Antiprotozoal Activities of Millettia Richardiana (Fabaceae) from Madagascar. *Molecules* **2014**, *19*, 4200–4211, doi:10.3390/molecules19044200.
93. Cunha, A.B.; Batista, R.; Castro, M.Á.; David, J.M. Chemical Strategies towards the Synthesis of Betulinic Acid and Its More Potent Antiprotozoal Analogues. *Molecules* **2021**, *26*, 1081, doi:10.3390/molecules26041081.
94. Jiang, W.; Li, X.; Dong, S.; Zhou, W. Betulinic Acid in the Treatment of Tumour Diseases: Application and Research Progress. *Biomed Pharmacother* **2021**, *142*, 111990, doi:10.1016/j.biopha.2021.111990.
95. Loe, M.W.C.; Hao, E.; Chen, M.; Li, C.; Lee, R.C.H.; Zhu, I.X.Y.; Teo, Z.Y.; Chin, W.-X.; Hou, X.; Deng, J.; et al. Betulinic Acid Exhibits Antiviral Effects against

Dengue Virus Infection. *Antiviral Res* **2020**, *184*, 104954, doi:10.1016/j.antiviral.2020.104954.
96. Lou, H.; Li, H.; Zhang, S.; Lu, H.; Chen, Q. A Review on Preparation of Betulinic Acid and Its Biological Activities. *Molecules* **2021**, *26*, 5583, doi:10.3390/molecules26185583.
97. Mu, Q.; Wang, H.; Tong, L.; Fang, Q.; Xiang, M.; Han, L.; Jin, L.; Yang, J.; Qian, Z.; Ning, G.; et al. Betulinic Acid Improves Nonalcoholic Fatty Liver Disease through YY1/FAS Signaling Pathway. *FASEB J* **2020**, *34*, 13033–13048, doi:10.1096/fj.202000546R.
98. Prados, M.E.; García-Martín, A.; Unciti-Broceta, J.D.; Palomares, B.; Collado, J.A.; Minassi, A.; Calzado, M.A.; Appendino, G.; Muñoz, E. Betulinic Acid Hydroxamate Prevents Colonic Inflammation and Fibrosis in Murine Models of Inflammatory Bowel Disease. *Acta Pharmacol Sin* **2021**, *42*, 1124–1138, doi:10.1038/s41401-020-0497-0.
99. Wu, C.; Chen, H.; Zhuang, R.; Zhang, H.; Wang, Y.; Hu, X.; Xu, Y.; Li, J.; Li, Y.; Wang, X.; et al. Betulinic Acid Inhibits Pyroptosis in Spinal Cord Injury by Augmenting Autophagy via the AMPK-mTOR-TFEB Signaling Pathway. *Int J Biol Sci* **2021**, *17*, 1138–1152, doi:10.7150/ijbs.57825.
100. Mazumder, A.H.; Das, J.; Gogoi, H.K.; Paul, S.B. Pharmaceutical Scope of a Phytochemically Unexplored Medicinal Plant, Sarcochlamys Pulcherrima (Roxb.) Gaud.: A Review. *Pharmacogn Rev* **2015**, *9*, 81–83, doi:10.4103/0973-7847.156358.
101. Mazumder, A.H.; Das, J.; Gogoi, H.K.; Chattopadhyay, P.; Paul, S.B. Antimicrobial Activity of Methanol Extract and Fractions from Sarcochlamys Pulcherrima. *Bangladesh Journal of Pharmacology* **2014**, *9*, 4–9, doi:10.3329/bjp.v9i1.16760.
102. Ghosh, C.; Bhowmik, J.; Ghosh, R.; Das, M.C.; Sandhu, P.; Kumari, M.; Acharjee, S.; Daware, A.V.; Akhter, Y.; Banerjee, B.; et al. The Anti-Biofilm Potential of Triterpenoids Isolated from Sarcochlamys Pulcherrima (Roxb.) Gaud. *Microbial Pathogenesis* **2020**, *139*, 103901, doi:10.1016/j.micpath.2019.103901.
103. Pattison, H.; Millar, B.; Moore, J. Fungal Vaccines. *British Journal of Biomedical Science* **2021**, *78*, 167–176, doi:10.1080/09674845.2021.1907953.
104. Martinez, M.; Clemons, K.V.; Stevens, D.A. Heat-Killed Yeast as a Pan-Fungal Vaccine. In *Vaccines for Invasive Fungal Infections: Methods and Protocols*; Kalkum, M., Semis, M., Eds.; Methods in Molecular Biology; Springer: New York, NY, 2017; pp. 23–30 ISBN 978-1-4939-7104-6.
105. Santos, E.; Levitz, S.M. Fungal Vaccines and Immunotherapeutics. *Cold Spring Harb Perspect Med* **2014**, *4*, a019711, doi:10.1101/cshperspect.a019711.
106. Velayuthan, R.D.; Samudi, C.; Lakhbeer Singh, H.K.; Ng, K.P.; Shankar, E.M.; Denning, D.W. Estimation of the Burden of Serious Human Fungal Infections in Malaysia. *Journal of Fungi* **2018**, *4*, 38, doi:10.3390/jof4010038.
107. do Nascimento Martins, E.M.; Reis, B.S.; Fernandes, V.C.; Costa, M.M.S.; Goes, A.M.; de Andrade, A.S.R. Immunization with Radioattenuated Yeast Cells of Paracoccidioides Brasiliensis Induces a Long Lasting Protection in BALB/c Mice. *Vaccine* **2007**, *25*, 7893–7899, doi:10.1016/j.vaccine.2007.09.011.
108. Milan, R.; Alois, R.; Josef, C.; Jana, B.; Evzen, W. Recombinant Protein and DNA Vaccines Derived from Hsp60 Trichophyton Mentagrophytes Control the Clinical Course of Trichophytosis in Bovine Species and Guinea-Pigs. *Mycoses* **2004**, *47*, 407–417, doi:10.1111/j.1439-0507.2004.01028.x.
109. Nanjappa, S.G.; Mudalagiriyappa, S.; Fites, J.S.; Suresh, M.; Klein, B.S. CBLB Constrains Inactivated Vaccine-Induced CD8+ T Cell Responses and Immunity against Lethal Fungal Pneumonia. *J Immunol* **2018**, *201*, 1717–1726, doi:10.4049/jimmunol.1701241.

110. Tso, G.H.W.; Reales-Calderon, J.A.; Pavelka, N. The Elusive Anti-Candida Vaccine: Lessons From the Past and Opportunities for the Future. *Front Immunol* **2018**, *9*, 897, doi:10.3389/fimmu.2018.00897.
111. Edwards, J.E., Jr; Schwartz, M.M.; Schmidt, C.S.; Sobel, J.D.; Nyirjesy, P.; Schodel, F.; Marchus, E.; Lizakowski, M.; DeMontigny, E.A.; Hoeg, J.; et al. A Fungal Immunotherapeutic Vaccine (NDV-3A) for Treatment of Recurrent Vulvovaginal Candidiasis—A Phase 2 Randomized, Double-Blind, Placebo-Controlled Trial. *Clinical Infectious Diseases* **2018**, *66*, 1928–1936, doi:10.1093/cid/ciy185.
112. Oliveira, L.V.N.; Wang, R.; Specht, C.A.; Levitz, S.M. Vaccines for Human Fungal Diseases: Close but Still a Long Way to Go. *NPJ Vaccines* **2021**, *6*, 33, doi:10.1038/s41541-021-00294-8.
113. Safavi, A.; Kefayat, A.; Abiri, A.; Mahdevar, E.; Behnia, A.H.; Ghahremani, F. In Silico Analysis of Transmembrane Protein 31 (TMEM31) Antigen to Design Novel Multiepitope Peptide and DNA Cancer Vaccines against Melanoma. *Mol Immunol* **2019**, *112*, 93–102, doi:10.1016/j.molimm.2019.04.030.
114. Sluder, A.E.; Raju Paul, S.; Moise, L.; Dold, C.; Richard, G.; Silva-Reyes, L.; Baeten, L.A.; Scholzen, A.; Reeves, P.M.; Pollard, A.J.; et al. Evaluation of a Human T Cell-Targeted Multi-Epitope Vaccine for Q Fever in Animal Models of Coxiella Burnetii Immunity. *Frontiers in Immunology* **2022**, *13*.
115. Akhtar, N.; Kaushik, V.; Grewal, R.K.; Wani, A.K.; Suwattanasophon, C.; Choowongkomon, K.; Oliva, R.; Shaikh, A.R.; Cavallo, L.; Chawla, M. Immunoinformatics-Aided Design of a Peptide Based Multiepitope Vaccine Targeting Glycoproteins and Membrane Proteins against Monkeypox Virus. *Viruses* **2022**, *14*, 2374, doi:10.3390/v14112374.
116. Akhtar, N.; Joshi, A.; Singh, B.; Kaushik, V. Immuno-Informatics Quest against COVID-19/SARS-COV-2: Determining Putative T-Cell Epitopes for Vaccine Prediction. *Infectious Disorders - Drug TargetsDisorders)* **2021**, *21*, 541–552, doi:10.2174/1871526520666200921154149.
117. Oyarzún, P.; Kobe, B. Recombinant and Epitope-Based Vaccines on the Road to the Market and Implications for Vaccine Design and Production. *Hum Vaccin Immunother* **2015**, *12*, 763–767, doi:10.1080/21645515.2015.1094595.
118. Akhtar, N.; Magdaleno, J.S.L.; Ranjan, S.; Wani, A.K.; Grewal, R.K.; Oliva, R.; Shaikh, A.R.; Cavallo, L.; Chawla, M. Secreted Aspartyl Proteinases Targeted Multi-Epitope Vaccine Design for Candida Dubliniensis Using Immunoinformatics. *Vaccines* **2023**, *11*, 364, doi:10.3390/vaccines11020364.
119. Akhtar, N.; Joshi, A.; Kaushik, V.; Kumar, M.; Mannan, M.A. In-Silico Design of a Multivalent Epitope-Based Vaccine against Candida Auris. *Microbial Pathogenesis* **2021**, *155*, 104879, doi:10.1016/j.micpath.2021.104879.
120. Akhtar, N.; Singh, A.; Upadhyay, A.K.; Mannan, M.A.-U. Design of a Multi-Epitope Vaccine against the Pathogenic Fungi Candida Tropicalis Using an in Silico Approach. *J Genet Eng Biotechnol* **2022**, *20*, 140, doi:10.1186/s43141-022-00415-3.
121. Tarang, S.; Kesherwani, V.; LaTendresse, B.; Lindgren, L.; Rocha-Sanchez, S.M.; Weston, M.D. In Silico Design of a Multivalent Vaccine Against Candida Albicans. *Sci Rep* **2020**, *10*, 1066, doi:10.1038/s41598-020-57906-x.
122. Jabin, D.; Kumar, A. T-Cell Epitope-Based Vaccine Prediction against Aspergillus Fumigatus: A Harmful Causative Agent of Aspergillosis. *J Genet Eng Biotechnol* **2022**, *20*, 72, doi:10.1186/s43141-022-00364-x.
123. Araf, Y.; Moin, A.T.; Timofeev, V.I.; Faruqui, N.A.; Saiara, S.A.; Ahmed, N.; Parvez, Md.S.A.; Rahaman, T.I.; Sarkar, B.; Ullah, Md.A.; et al. Immunoinformatic Design of

a Multivalent Peptide Vaccine Against Mucormycosis: Targeting FTR1 Protein of Major Causative Fungi. *Frontiers in Immunology* **2022**, *13*.

124. Pritam, M.; Singh, G.; Kumar, R.; Singh, S.P. Screening of Potential Antigens from Whole Proteome and Development of Multi-Epitope Vaccine against Rhizopus Delemar Using Immunoinformatics Approaches. *J Biomol Struct Dyn* **2022**, 1–28, doi:10.1080/07391102.2022.2028676.
125. Rapin, N.; Lund, O.; Castiglione, F. Immune System Simulation Online. *Bioinformatics* **2011**, *27*, 2013–2014, doi:10.1093/bioinformatics/btr335.
126. Lionakis, M.S.; Drummond, R.A.; Hohl, T.M. Immune Responses to Human Fungal Pathogens and Therapeutic Prospects. *Nat Rev Immunol* **2023**, *23*, 433–452, doi:10.1038/s41577-022-00826-w.
127. Patti, R.K.; Dalsania, N.R.; Somal, N.; Sinha, A.; Mehta, S.; Ghitan, M.; Seneviratne, C.; Kupfer, Y. Subacute Aspergillosis "Fungal Balls" Complicating COVID-19. *Journal of Investigative Medicine High Impact Case Reports* **2020**, *8*, 2324709620966475, doi:10.1177/2324709620966475.
128. Maziarz, E.K.; Perfect, J.R. Cryptococcosis. *Infectious Disease Clinics of North America* **2016**, *30*, 179–206, doi:10.1016/j.idc.2015.10.006.
129. Bertolini, M.; Mutti, M.F.; Barletta, J.A.; Falak, A.; Cuatz, D.; Sisto, A.; Ragusa, M.A.; Fernandez Claros, N.O.; Rolón, M.J. COVID-19 Associated with AIDS-Related Disseminated Histoplasmosis: A Case Report. *Int J STD AIDS* **2020**, *31*, 1222–1224, doi:10.1177/0956462420957518.
130. Huffnagle, G.B.; Noverr, M.C. The Emerging World of the Fungal Microbiome. *Trends Microbiol* **2013**, *21*, 334–341, doi:10.1016/j.tim.2013.04.002.
131. Huseyin, C.E.; O'Toole, P.W.; Cotter, P.D.; Scanlan, P.D. Forgotten Fungi-the Gut Mycobiome in Human Health and Disease. *FEMS Microbiol Rev* **2017**, *41*, 479–511, doi:10.1093/femsre/fuw047.
132. Coker, O.O.; Nakatsu, G.; Dai, R.Z.; Ka, W.; Wu, K.; Wong, S.H.; Ng, S.C.; Ka, F.; Chan, L.; Jao, J.; et al. Enteric Fungal Microbiota Dysbiosis and Ecological Alterations in Colorectal Cancer. **2018**, 1–9, doi:10.1136/gutjnl-2018-317178.
133. Bandara, H.M.H.N.; Panduwawala, C.P.; Samaranayake, L.P. Biodiversity of the Human Oral Mycobiome in Health and Disease. *Oral Diseases* **2019**, *25*, 363–371, doi:10.1111/odi.12899.
134. Skalski, J.H.; Limon, J.J.; Sharma, P.; Gargus, M.D.; Nguyen, C.; Tang, J.; Coelho, A.L.; Hogaboam, C.M.; Crother, T.R.; Underhill, D.M. Expansion of Commensal Fungus Wallemia Mellicola in the Gastrointestinal Mycobiota Enhances the Severity of Allergic Airway Disease in Mice. *PLoS Pathog* **2018**, *14*, e1007260, doi:10.1371/journal.ppat.1007260.
135. Forbes, J.D.; Bernstein, C.N.; Tremlett, H.; Van Domselaar, G.; Knox, N.C. A Fungal World: Could the Gut Mycobiome Be Involved in Neurological Disease? *Front Microbiol* **2019**, *9*, 3249, doi:10.3389/fmicb.2018.03249.
136. Pal, M. Morbidity and Mortality Due to Fungal Infections. *Journal of Applied Microbiology and Biochemistry* **2017**, *1*, doi:10.21767/2576-1412.100002.
137. Fisher, M.C.; Alastruey-Izquierdo, A.; Berman, J.; Bicanic, T.; Bignell, E.M.; Bowyer, P.; Bromley, M.; Brüggemann, R.; Garber, G.; Cornely, O.A.; et al. Tackling the Emerging Threat of Antifungal Resistance to Human Health. *Nat Rev Microbiol* **2022**, *20*, 557–571, doi:10.1038/s41579-022-00720-1.
138. Revie, N.M.; Iyer, K.R.; Robbins, N.; Cowen, L.E. Antifungal Drug Resistance: Evolution, Mechanisms and Impact. *Curr Opin Microbiol* **2018**, *45*, 70–76, doi:10.1016/j.mib.2018.02.005.

139. Cowen, L.E.; Sanglard, D.; Howard, S.J.; Rogers, P.D.; Perlin, D.S. Mechanisms of Antifungal Drug Resistance. *Cold Spring Harbor Perspectives in Medicine* **2015**, *5*, a019752, doi:10.1101/cshperspect.a019752.
140. Arastehfar, A.; Gabaldón, T.; Garcia-Rubio, R.; Jenks, J.D.; Hoenigl, M.; Salzer, H.J.F.; Ilkit, M.; Lass-Flörl, C.; Perlin, D.S. Drug-Resistant Fungi: An Emerging Challenge Threatening Our Limited Antifungal Armamentarium. *Antibiotics* **2020**, *9*, 877, doi:10.3390/antibiotics9120877.
141. CDC Invasive Candidiasis Statistics Available online: https://www.cdc.gov/fungal/diseases/candidiasis/invasive/statistics.html (accessed on 9 March 2023).
142. Pfaller, M.; Neofytos, D.; Diekema, D.; Azie, N.; Meier-Kriesche, H.-U.; Quan, S.-P.; Horn, D. Epidemiology and Outcomes of Candidemia in 3648 Patients: Data from the Prospective Antifungal Therapy (PATH Alliance®) Registry, 2004-2008. *Diagn Microbiol Infect Dis* **2012**, *74*, 323–331, doi:10.1016/j.diagmicrobio.2012.10.003.
143. Horn, D.L.; Neofytos, D.; Anaissie, E.J.; Fishman, J.A.; Steinbach, W.J.; Olyaei, A.J.; Marr, K.A.; Pfaller, M.A.; Chang, C.-H.; Webster, K.M. Epidemiology and Outcomes of Candidemia in 2019 Patients: Data from the Prospective Antifungal Therapy Alliance Registry. *Clinical Infectious Diseases* **2009**, *48*, 1695–1703, doi:10.1086/599039.
144. Berkow, E.L.; Lockhart, S.R. Fluconazole Resistance in Candida Species: A Current Perspective. *Infect Drug Resist* **2017**, *10*, 237–245, doi:10.2147/IDR.S118892.
145. Whaley, S.G.; Berkow, E.L.; Rybak, J.M.; Nishimoto, A.T.; Barker, K.S.; Rogers, P.D. Azole Antifungal Resistance in Candida Albicans and Emerging Non-Albicans Candida Species. *Frontiers in Microbiology* **2017**, *7*.
146. Alexander, B.D.; Johnson, M.D.; Pfeiffer, C.D.; Jiménez-Ortigosa, C.; Catania, J.; Booker, R.; Castanheira, M.; Messer, S.A.; Perlin, D.S.; Pfaller, M.A. Increasing Echinocandin Resistance in Candida Glabrata: Clinical Failure Correlates With Presence of FKS Mutations and Elevated Minimum Inhibitory Concentrations. *Clinical Infectious Diseases: An Official Publication of the Infectious Diseases Society of America* **2013**, *56*, 1724, doi:10.1093/cid/cit136.
147. Perlin, D.S. Echinocandin Resistance in Candida. *Clin Infect Dis* **2015**, *61*, S612–S617, doi:10.1093/cid/civ791.
148. Pham, C.D.; Iqbal, N.; Bolden, C.B.; Kuykendall, R.J.; Harrison, L.H.; Farley, M.M.; Schaffner, W.; Beldavs, Z.G.; Chiller, T.M.; Park, B.J.; et al. Role of FKS Mutations in Candida Glabrata: MIC Values, Echinocandin Resistance, and Multidrug Resistance. *Antimicrob Agents Chemother* **2014**, *58*, 4690–4696, doi:10.1128/AAC.03255-14.
149. Bandres, M.V.; Modi, P.; Sharma, S. Aspergillus Fumigatus. In *StatPearls*; StatPearls Publishing: Treasure Island (FL), 2022.
150. Shishodia, S.K.; Tiwari, S.; Shankar, J. Resistance Mechanism and Proteins in Aspergillus Species against Antifungal Agents. *Mycology 10*, 151–165, doi:10.1080/21501203.2019.1574927.
151. Vahedi Shahandashti, R.; Lass-Flörl, C. Antifungal Resistance in Aspergillus Terreus: A Current Scenario. *Fungal Genet Biol* **2019**, *131*, 103247, doi:10.1016/j.fgb.2019.103247.
152. Satish, S.; Perlin, D.S. Echinocandin Resistance in Aspergillus Fumigatus Has Broad Implications for Membrane Lipid Perturbations That Influence Drug-Target Interactions. *Microbiol Insights* **2019**, *12*, 1178636119897034, doi:10.1177/1178636119897034.

153. Bermas, A.; Geddes-McAlister, J. Combatting the Evolution of Antifungal Resistance in Cryptococcus Neoformans. *Molecular Microbiology* **2020**, *114*, 721–734, doi:10.1111/mmi.14565.
154. Sacheli, R.; Hayette, M.-P. Antifungal Resistance in Dermatophytes: Genetic Considerations, Clinical Presentations and Alternative Therapies. *Journal of Fungi* **2021**, *7*, doi:10.3390/jof7110983.
155. Leidner, F.; Kurt Yilmaz, N.; Schiffer, C.A. Deciphering Antifungal Drug Resistance in Pneumocystis Jirovecii DHFR with Molecular Dynamics and Machine Learning. *J. Chem. Inf. Model.* **2021**, *61*, 2537–2541, doi:10.1021/acs.jcim.1c00403.
156. Wheat, L.J.; Connolly, P.; Smedema, M.; Rogers, P.D. Antifungal Drug Resistance in Histoplasmosis. In *Antimicrobial Drug Resistance: Clinical and Epidemiological Aspects*; Mayers, D.L., Ed.; Infectious Disease; Humana Press: Totowa, NJ, 2009; pp. 987–992 ISBN 978-1-60327-595-8.
157. Ostrosky-Zeichner, L. Combination Antifungal Therapy: A Critical Review of the Evidence. *Clinical Microbiology and Infection* **2008**, *14*, 65–70, doi:10.1111/j.1469-0691.2008.01983.x.
158. Ademe, M. Immunomodulation for the Treatment of Fungal Infections: Opportunities and Challenges. *Front Cell Infect Microbiol* **2020**, *10*, 469, doi:10.3389/fcimb.2020.00469.
159. Marathe, A.; Zhu, Y.; Chaturvedi, V.; Chaturvedi, S. Utility of CHROMagar™ Candida Plus for Presumptive Identification of Candida Auris from Surveillance Samples. *Mycopathologia* **2022**, *187*, 527–534, doi:10.1007/s11046-022-00656-3.
160. Sikora, A.; Hashmi, M.F.; Zahra, F. Candida Auris. In *StatPearls*; StatPearls Publishing: Treasure Island (FL), 2023.
161. Navarro-Arias, M.J.; Hernández-Chávez, M.J.; García-Carnero, L.C.; Amezcua-Hernández, D.G.; Lozoya-Pérez, N.E.; Estrada-Mata, E.; Martínez-Duncker, I.; Franco, B.; Mora-Montes, H.M. Differential Recognition of Candida Tropicalis, Candida Guilliermondii, Candida Krusei, and Candida Auris by Human Innate Immune Cells. *Infection and Drug Resistance* **2019**, *12*, 783, doi:10.2147/IDR.S197531.
162. Garcia-Bustos, V.; Cabañero-Navalon, M.D.; Ruiz-Gaitán, A.; Salavert, M.; Tormo-Mas, M.Á.; Pemán, J. Climate Change, Animals, and Candida Auris: Insights into the Ecological Niche of a New Species from a One Health Approach. *Clin Microbiol Infect* **2023**, *29*, 858–862, doi:10.1016/j.cmi.2023.03.016.
163. Spruijtenburg, B.; Badali, H.; Abastabar, M.; Mirhendi, H.; Khodavaisy, S.; Sharifisooraki, J.; Taghizadeh Armaki, M.; de Groot, T.; Meis, J.F. Confirmation of Fifth Candida Auris Clade by Whole Genome Sequencing. *Emerg Microbes Infect 11*, 2405–2411, doi:10.1080/22221751.2022.2125349.
164. Narayanan, A.; Selvakumar, P.; Siddharthan, R.; Sanyal, K. ClaID: A Rapid Method of Clade-Level Identification of the Multidrug Resistant Human Fungal Pathogen Candida Auris. *Microbiology Spectrum* **2022**, *10*, e00634-22, doi:10.1128/spectrum.00634-22.
165. Szekely, A.; Borman, A.M.; Johnson, E.M. Candida Auris Isolates of the Southern Asian and South African Lineages Exhibit Different Phenotypic and Antifungal Susceptibility Profiles In Vitro. *Journal of Clinical Microbiology* **2019**, *57*, 10.1128/jcm.02055-18, doi:10.1128/jcm.02055-18.
166. Muñoz, J.F.; Welsh, R.M.; Shea, T.; Batra, D.; Gade, L.; Howard, D.; Rowe, L.A.; Meis, J.F.; Litvintseva, A.P.; Cuomo, C.A. Clade-Specific Chromosomal Rearrangements and Loss of Subtelomeric Adhesins in Candida Auris. *Genetics* **2021**, *218*, iyab029, doi:10.1093/genetics/iyab029.

167. Kurakado, S.; Matsumoto, Y.; Sugita, T. Comparing the Virulence of Four Major Clades of Candida Auris Strains Using a Silkworm Infection Model: Clade IV Isolates Had Higher Virulence than the Other Clades. *Med Mycol* **2023**, *61*, myad108, doi:10.1093/mmy/myad108.
168. Ambaraghassi, G.; Dufresne, P.J.; Dufresne, S.F.; Vallières, É.; Muñoz, J.F.; Cuomo, C.A.; Berkow, E.L.; Lockhart, S.R.; Luong, M.-L. Identification of Candida Auris by Use of the Updated Vitek 2 Yeast Identification System, Version 8.01: A Multilaboratory Evaluation Study. *J Clin Microbiol* **2019**, *57*, e00884-19, doi:10.1128/JCM.00884-19.
169. Kathuria, S.; Singh, P.K.; Sharma, C.; Prakash, A.; Masih, A.; Kumar, A.; Meis, J.F.; Chowdhary, A. Multidrug-Resistant Candida Auris Misidentified as Candida Haemulonii: Characterization by Matrix-Assisted Laser Desorption Ionization-Time of Flight Mass Spectrometry and DNA Sequencing and Its Antifungal Susceptibility Profile Variability by Vitek 2, CLSI Broth Microdilution, and Etest Method. *J Clin Microbiol* **2015**, *53*, 1823–1830, doi:10.1128/JCM.00367-15.
170. Mizusawa, M.; Miller, H.; Green, R.; Lee, R.; Durante, M.; Perkins, R.; Hewitt, C.; Simner, P.J.; Carroll, K.C.; Hayden, R.T.; et al. Can Multidrug-Resistant Candida Auris Be Reliably Identified in Clinical Microbiology Laboratories? *J Clin Microbiol* **2017**, *55*, 638–640, doi:10.1128/JCM.02202-16.
171. Sexton, D.J.; Kordalewska, M.; Bentz, M.L.; Welsh, R.M.; Perlin, D.S.; Litvintseva, A.P. Direct Detection of Emergent Fungal Pathogen Candida Auris in Clinical Skin Swabs by SYBR Green-Based Quantitative PCR Assay. *J Clin Microbiol* **2018**, *56*, e01337-18, doi:10.1128/JCM.01337-18.
172. Leach, L.; Zhu, Y.; Chaturvedi, S. Development and Validation of a Real-Time PCR Assay for Rapid Detection of Candida Auris from Surveillance Samples. *Journal of Clinical Microbiology* **2018**, *56*, 10.1128/jcm.01223-17, doi:10.1128/jcm.01223-17.
173. Alvarado, M.; Bartolomé Álvarez, J.; Lockhart, S.R.; Valentín, E.; Ruiz-Gaitán, A.C.; Eraso, E.; de Groot, P.W.J. Identification of Candida Auris and Related Species by Multiplex PCR Based on Unique GPI Protein-Encoding Genes. *Mycoses* **2021**, *64*, 194–202, doi:10.1111/myc.13204.
174. Voelker, R. New Test Identifies Candida Auris. *JAMA* **2018**, *319*, 2164, doi:10.1001/jama.2018.6922.
175. Geremia, N.; Brugnaro, P.; Solinas, M.; Scarparo, C.; Panese, S. Candida Auris as an Emergent Public Health Problem: A Current Update on European Outbreaks and Cases. *Healthcare (Basel)* **2023**, *11*, 425, doi:10.3390/healthcare11030425.
176. Sherry, L.; Ramage, G.; Kean, R.; Borman, A.; Johnson, E.M.; Richardson, M.D.; Rautemaa-Richardson, R. Biofilm-Forming Capability of Highly Virulent, Multidrug-Resistant Candida Auris. *Emerg Infect Dis* **2017**, *23*, 328–331, doi:10.3201/eid2302.161320.
177. Pechacek, J.; Lionakis, M.S. Host Defense Mechanisms against Candida Auris. *Expert Review of Anti-infective Therapy* **2023**, *21*, 1087–1096, doi:10.1080/14787210.2023.2264500.
178. Day, A.M.; McNiff, M.M.; da Silva Dantas, A.; Gow, N.A.R.; Quinn, J. Hog1 Regulates Stress Tolerance and Virulence in the Emerging Fungal Pathogen Candida Auris. *mSphere* **2018**, *3*, e00506-18, doi:10.1128/mSphere.00506-18.
179. Chowdhary, A.; Jain, K.; Chauhan, N. Candida Auris Genetics and Emergence. *Annu Rev Microbiol* **2023**, *77*, 583–602, doi:10.1146/annurev-micro-032521-015858.
180. Jangir, P.; Kalra, S.; Tanwar, S.; Bari, V.K. Azole Resistance in Candida Auris: Mechanisms and Combinatorial Therapy. *APMIS* **2023**, *131*, 442–462, doi:10.1111/apm.13336.

181. Nelson, R. Emergence of Resistant Candida Auris. *Lancet Microbe* **2023**, *4*, e396, doi:10.1016/S2666-5247(23)00143-X.
182. Dominguez, E.G.; Zarnowski, R.; Choy, H.L.; Zhao, M.; Sanchez, H.; Nett, J.E.; Andes, D.R. Conserved Role for Biofilm Matrix Polysaccharides in Candida Auris Drug Resistance. *mSphere* **2019**, *4*, e00680-18, doi:10.1128/mSphereDirect.00680-18.
183. Romera, D.; Aguilera-Correa, J.J.; Gadea, I.; Viñuela-Sandoval, L.; García-Rodríguez, J.; Esteban, J. Candida Auris: A Comparison between Planktonic and Biofilm Susceptibility to Antifungal Drugs. *J Med Microbiol* **2019**, *68*, 1353–1358, doi:10.1099/jmm.0.001036.
184. Chowdhary, A.; Prakash, A.; Sharma, C.; Kordalewska, M.; Kumar, A.; Sarma, S.; Tarai, B.; Singh, A.; Upadhyaya, G.; Upadhyay, S.; et al. A Multicentre Study of Antifungal Susceptibility Patterns among 350 Candida Auris Isolates (2009-17) in India: Role of the ERG11 and FKS1 Genes in Azole and Echinocandin Resistance. *J Antimicrob Chemother* **2018**, *73*, 891–899, doi:10.1093/jac/dkx480.
185. Rybak, J.M.; Cuomo, C.A.; David Rogers, P. The Molecular and Genetic Basis of Antifungal Resistance in the Emerging Fungal Pathogen Candida Auris. *Current Opinion in Microbiology* **2022**, *70*, 102208, doi:10.1016/j.mib.2022.102208.
186. Chow, E.W.L.; Song, Y.; Chen, J.; Xu, X.; Wang, J.; Chen, K.; Gao, J.; Wang, Y. The Transcription Factor Rpn4 Activates Its Own Transcription and Induces Efflux Pump Expression to Confer Fluconazole Resistance in Candida Auris. *mBio* **2023**, e0268823, doi:10.1128/mbio.02688-23.
187. CDC Treatment and Management of C. Auris Infections and Colonization Available online: https://www.cdc.gov/fungal/candida-auris/c-auris-treatment.html (accessed on 29 June 2023).
188. Ishiwata-Kimata, Y.; Kimata, Y. Fundamental and Applicative Aspects of the Unfolded Protein Response in Yeasts. *J Fungi (Basel)* **2023**, *9*, 989, doi:10.3390/jof9100989.
189. Shamu, C.E. Splicing : HACking into the Unfolded-Protein Response. **1998**, 121–123.
190. Hollien, J.; Weissman, J.S. Decay of Endoplasmic Reticulum-Localized mRNAs During the Unfolded Protein Response. *Science* **2006**, *313*, 104–107, doi:10.1126/science.1129631.
191. Tam, A.B.; Koong, A.C.; Niwa, M.; Jolla, L. HHS Public Access. **2015**, *9*, 850–858, doi:10.1016/j.celrep.2014.09.016.Ire1.
192. Guydosh, N.R.; Kimmig, P.; Walter, P.; Green, R. Regulated Ire1-Dependent mRNA Decay Requires No-Go mRNA Degradation to Maintain Endoplasmic Reticulum Homeostasis in S . Pombe. **2017**, *1*.
193. Hernández-Elvira, M.; Torres-Quiroz, F.; Escamilla-Ayala, A.; Domínguez-Martin, E.; Escalante, R.; Kawasaki, L.; Ongay-Larios, L.; Coria, R. The Unfolded Protein Response Pathway in the Yeast Kluyveromyces Lactis. A Comparative View among Yeast Species. *Cells* **2018**, *7*, 106, doi:10.3390/cells7080106.
194. Guerra-Moreno, A.; Ang, J.; Welsch, H.; Jochem, M.; Hanna, J. Regulation of the Unfolded Protein Response in Yeast by Oxidative Stress. *FEBS Letters* **2019**, *593*, 1080–1088, doi:10.1002/1873-3468.13389.
195. Gardner, B.M.; Walter, P. Unfolded Proteins Are Ire1-Activating Ligands That Directly Induce the Unfolded Protein Response. *Science* **2011**, *333*, 1891–1894, doi:10.1126/science.1209126.
196. Ali, M.M.U.; Bagratuni, T.; Davenport, E.L.; Nowak, P.R.; Silva-Santisteban, M.C.; Hardcastle, A.; McAndrews, C.; Rowlands, M.G.; Morgan, G.J.; Aherne, W.; et al. Structure of the Ire1 Autophosphorylation Complex and Implications for the Unfolded Protein Response. *EMBO J* **2011**, *30*, 894–905, doi:10.1038/emboj.2011.18.

197. Kimmig, P.; Diaz, M.; Zheng, J.; Williams, C.C. The Unfolded Protein Response in Fission Yeast Modulates Stability of Select mRNAs to Maintain Protein Homeostasis. **2012**, 1–20, doi:10.7554/eLife.00048.
198. Li, J.; Yu, Q.; Zhang, B.; Xiao, C.; Ma, T.; Yi, X.; Liang, C.; Li, M. International Journal of Medical Microbiology Stress-Associated Endoplasmic Reticulum Protein 1 (SERP1) and Atg8 Synergistically Regulate Unfolded Protein Response (UPR) That Is Independent on Autophagy in Candida Albicans. *International Journal of Medical Microbiology* **2018**, *1*, 0–1, doi:10.1016/j.ijmm.2018.03.004.
199. Saraswat, D.; Kumar, R.; Pande, T.; Edgerton, M.; Paul, J. HHS Public Access. **2016**, *100*, 425–441, doi:10.1111/mmi.13326.Signalling.
200. Hooks, K.B.; Griffiths-Jones, S. Conserved RNA Structures in the Non-Canonical Hac1/Xbp1 Intron. *RNA Biol* **2011**, *8*, 552–556, doi:10.4161/rna.8.4.15396.
201. Sircaik, S.; Román, E.; Bapat, P.; Lee, K.K.; Andes, D.R.; Gow, N.A.R.; Nobile, C.J.; Pla, J.; Panwar, S.L. The Protein Kinase Ire1 Impacts Pathogenicity of Candida Albicans by Regulating Homeostatic Adaptation to Endoplasmic Reticulum Stress. *Cellular Microbiology* **2021**, *23*, doi:10.1111/cmi.13307.
202. Miyazaki, T.; Nakayama, H.; Nagayoshi, Y.; Kakeya, H.; Kohno, S. Dissection of Ire1 Functions Reveals Stress Response Mechanisms Uniquely Evolved in Candida Glabrata. *PLoS Pathogens* **2013**, *9*, e1003160, doi:10.1371/journal.ppat.1003160.
203. Iracane, E.; Donovan, P.D.; Ola, M.; Butler, G.; Holland, L.M. Identification of an Exceptionally Long Intron in the HAC1 Gene of Candida Parapsilosis. *mSphere* **2018**, *3*, e00532-18, doi:10.1128/mSphere.00532-18.
204. Richie, D.L.; Hartl, L.; Aimanianda, V.; Winters, M.S.; Fuller, K.K.; Miley, M.D.; White, S.; McCarthy, J.W.; Latgé, J.-P.; Feldmesser, M.; et al. A Role for the Unfolded Protein Response (UPR) in Virulence and Antifungal Susceptibility in Aspergillus Fumigatus. *PLoS Pathogens* **2009**, *5*, e1000258, doi:10.1371/journal.ppat.1000258.
205. Jung, K.-W.; Lee, K.-T.; Averette, A.F.; Hoy, M.J.; Everitt, J.; Heitman, J.; Bahn, Y.-S. Evolutionarily Conserved and Divergent Roles of Unfolded Protein Response (UPR) in the Pathogenic Cryptococcus Species Complex. *Scientific Reports* **2018**, *8*, 8132, doi:10.1038/s41598-018-26405-5.
206. Cheon, S.A.; Jung, K.-W.; Chen, Y.-L.; Heitman, J.; Bahn, Y.-S.; Kang, H.A. Unique Evolution of the UPR Pathway with a Novel bZIP Transcription Factor, Hxl1, for Controlling Pathogenicity of Cryptococcus Neoformans. *PLoS Pathogens* **2011**, *7*, e1002177, doi:10.1371/journal.ppat.1002177.
207. Cheon, S.A.; Jung, K.-W.; Bahn, Y.-S.; Kang, H.A. The Unfolded Protein Response (UPR) Pathway in Cryptococcus. *Virulence* **2014**, *5*, 341–350, doi:10.4161/viru.26774.
208. Kidd, S.E.; Hagen, F.; Tscharke, R.L.; Huynh, M.; Bartlett, K.H.; Fyfe, M.; MacDougall, L.; Boekhout, T.; Kwon-Chung, K.J.; Meyer, W. A Rare Genotype of <Em>Cryptococcus Gattii</Em> Caused the Cryptococcosis Outbreak on Vancouver Island (British Columbia, Canada). *Proceedings of the National Academy of Sciences of the United States of America* **2004**, *101*, 17258 LP – 17263, doi:10.1073/pnas.0402981101.
209. Kinne, J.; Joseph, M.; Wernery, U.; Nogradi, N.; Hagen, F. Disseminated Cryptococcus Deuterogattii (AFLP6/VGII) Infection in an Arabian Horse from Dubai, United Arab Emirates. *Revista Iberoamericana de Micologia* **2017**, *34*, 229–232, doi:10.1016/j.riam.2017.02.007.
210. Alspaugh, J.A. Virulence Mechanisms and Cryptococcus Neoformans Pathogenesis. *Fungal Genetics and Biology* **2015**, *78*, 55–58, doi:10.1016/j.fgb.2014.09.004.

211. Leopold Wager, C.M.; Hole, C.R.; Wozniak, K.L.; Wormley, F.L. Cryptococcus and Phagocytes: Complex Interactions That Influence Disease Outcome. *Frontiers in Microbiology* **2016**, *7*, 105, doi:10.3389/fmicb.2016.00105.
212. Branco, J.; Miranda, I.M.; Rodrigues, A.G. Candida Parapsilosis Virulence and Antifungal Resistance Mechanisms: A Comprehensive Review of Key Determinants. *J Fungi (Basel)* **2023**, *9*, 80, doi:10.3390/jof9010080.
213. Borgers, M.; Van den Bossche, H.; De Brabander, M. The Mechanism of Action of the New Antimycotic Ketoconazole. *The American Journal of Medicine* **1983**, *74*, 2–8, doi:10.1016/0002-9343(83)90507-7.
214. Blankenship, J.R.; Fanning, S.; Hamaker, J.J.; Mitchell, A.P. An Extensive Circuitry for Cell Wall Regulation in Candida Albicans. *PLoS Pathogens* **2010**, *6*, e1000752, doi:10.1371/journal.ppat.1000752.
215. Thomas, E.; Sircaik, S.; Roman, E.; Brunel, J.-M.; Johri, A.K.; Pla, J.; Panwar, S.L. The Activity of *RTA2*, a Downstream Effector of the Calcineurin Pathway, Is Required during Tunicamycin-Induced ER Stress Response in *Candida Albicans*. *FEMS Yeast Research* **2015**, *15*, fov095, doi:10.1093/femsyr/fov095.
216. Feng, X.; Krishnan, K.; Richie, D.L.; Aimanianda, V.; Hartl, L.; Grahl, N.; Powers-Fletcher, M. V.; Zhang, M.; Fuller, K.K.; Nierman, W.C.; et al. HacA-Independent Functions of the ER Stress Sensor IreA Synergize with the Canonical UPR to Influence Virulence Traits in Aspergillus Fumigatus. *PLoS Pathogens* **2011**, *7*, e1002330, doi:10.1371/journal.ppat.1002330.
217. Rocha, M.C.; Godoy, K.F. de; de Castro, P.A.; Hori, J.I.; Bom, V.L.P.; Brown, N.A.; Cunha, A.F. da; Goldman, G.H.; Malavazi, I. The Aspergillus Fumigatus pkcAG579R Mutant Is Defective in the Activation of the Cell Wall Integrity Pathway but Is Dispensable for Virulence in a Neutropenic Mouse Infection Model. *PLOS ONE* **2015**, *10*, e0135195, doi:10.1371/journal.pone.0135195.
218. Krishnan, K.; Feng, X.; Powers-Fletcher, M. V.; Bick, G.; Richie, D.L.; Woollett, L.A.; Askew, D.S. Effects of a Defective Endoplasmic Reticulum-Associated Degradation Pathway on the Stress Response, Virulence, and Antifungal Drug Susceptibility of the Mold Pathogen Aspergillus Fumigatus. *Eukaryotic Cell* **2013**, *12*, 512–519, doi:10.1128/EC.00319-12.
219. Wiederhold, N. Antifungal Resistance: Current Trends and Future Strategies to Combat. *Infection and Drug Resistance* **2017**, *Volume 10*, 249–259, doi:10.2147/IDR.S124918.
220. Monteiro, C. de A.; Santos, J.R.A. dos Phytochemicals and Their Antifungal Potential against Pathogenic Yeasts. In *Phytochemicals in Human Health*; IntechOpen, 2019 ISBN 978-1-78985-588-3.
221. Thammahong, A.; Puttikamonkul, S.; Perfect, J.R.; Brennan, R.G.; Cramer, R.A. Central Role of the Trehalose Biosynthesis Pathway in the Pathogenesis of Human Fungal Infections: Opportunities and Challenges for Therapeutic Development. *Microbiology and Molecular Biology Reviews* **2017**, *81*, e00053-16, doi:10.1128/MMBR.00053-16.
222. Khan, A.; Moni, S.S.; Ali, M.; Mohan, S.; Jan, H.; Rasool, S.; Kamal, M.A.; Alshahrani, S.; Halawi, M.; Alhazmi, H.A. Antifungal Activity of Plant Secondary Metabolites on Candida Albicans: An Updated Review. *Curr Mol Pharmacol* **2023**, *16*, 15–42, doi:10.2174/1874467215666220304143332.
223. Teodoro, G.R.; Ellepola, K.; Seneviratne, C.J.; Koga-Ito, C.Y. Potential Use of Phenolic Acids as Anti-Candida Agents: A Review. *Front Microbiol* **2015**, *6*, doi:10.3389/fmicb.2015.01420.

224. Vita, D.D.; Simonetti, G.; Pandolfi, F.; Costi, R.; Santo, R.D.; D'Auria, F.D.; Scipione, L. Exploring the Anti-Biofilm Activity of Cinnamic Acid Derivatives in Candida Albicans. *Bioorganic and Medicinal Chemistry Letters* **2016**, *26*, 5931–5935, doi:10.1016/j.bmcl.2016.10.091.
225. Shi, J.; Li, S.; Gao, A.; Zhu, K.; Zhang, H. Tetrandrine Enhances the Antifungal Activity of Fluconazole in a Murine Model of Disseminated Candidiasis. *Phytomedicine* **2018**, *46*, 21–31, doi:10.1016/j.phymed.2018.06.003.
226. Lin, C.-J.; Chang, Y.-L.; Yang, Y.-L.; Chen, Y.-L. Natural Alkaloid Tryptanthrin Exhibits Novel Anticryptococcal Activity. *Medical Mycology* **2021**, *59*, 545–556, doi:10.1093/mmy/myaa074.
227. Nna, P.; Tor-Anyiin, T.; Igoli, J.; Momeni, J. Fagaramide and Pellitorine from the Stem Bark of Zanthoxylum Zanthoxyloides and Their Antimicrobial Activities. *South Asian Research Journal of Natural Products* **2019**, *2*, 1–8.
228. Hamdani, N.; Filali-Ansari, N.; Fdil, R.; Abbouyi, A.E.; Khyari, S. Antifungal Activity of the Alkaloids Extracts from Aerial Parts of Retama Monosperma. *Research Journal of Pharmaceutical, Biological and Chemical Sciences* **2016**, *7*, 965–971.
229. Souza-Moreira, T.M.; Severi, J.A.; Rodrigues, E.R.; Paula, M.I. de; Freitas, J.A.; Vilegas, W.; Pietro, R.C.L.R. Flavonoids from Plinia Cauliflora (Mart.) Kausel (Myrtaceae) with Antifungal Activity. *Natural Product Research* **2019**, *33*, 2579–2582, doi:10.1080/14786419.2018.1460827.
230. Orhan, D.D.; Özçelik, B.; Özgen, S.; Ergun, F. Antibacterial, Antifungal, and Antiviral Activities of Some Flavonoids. *Microbiological Research* **2010**, *165*, 496–504, doi:10.1016/j.micres.2009.09.002.
231. Prasad, S.K.; Bhat, S.S.; Koskowska, O.; Sangta, J.; Ahmad, S.F.; Nadeem, A.; Sommano, S.R. Naringin from Coffee Inhibits Foodborne Aspergillus Fumigatus via the NDK Pathway: Evidence from an In Silico Study. *Molecules* **2023**, *28*, 5189, doi:10.3390/molecules28135189.
232. Chedjou, I.N.; Ngouafong, F.T.; Tchuenguem, R.T.; Dzoyem, J.P.; Ponou, B.K.; Teponno, R.B.; Barboni, L.; Tapondjou, L.A. Siamoside A: A New C-Glycosylated Flavone from Senna Siamea (Lam.) H. S. Irwin & Barneby (Caesalpiniaceae). *Nat Prod Res* **2023**, *37*, 3461–3469, doi:10.1080/14786419.2022.2085699.
233. Wadhwa, K.; Kaur, H.; Kapoor, N.; Brogi, S. Identification of Sesamin from Sesamum Indicum as a Potent Antifungal Agent Using an Integrated in Silico and Biological Screening Platform. *Molecules* **2023**, *28*, 4658, doi:10.3390/molecules28124658.
234. Barros, L.; Dueñas, M.; Alves, C.T.; Silva, S.; Henriques, M.; Santos-Buelga, C.; Ferreira, I.C.F.R. Antifungal Activity and Detailed Chemical Characterization of Cistus Ladanifer Phenolic Extracts. *Industrial Crops and Products* **2013**, *41*, 41–45, doi:10.1016/j.indcrop.2012.03.038.
235. Alves, C.T.; Ferreira, I.C.F.R.; Barros, L.; Silva, S.; Azeredo, J.; Henriques, M. Antifungal Activity of Phenolic Compounds Identified in Flowers from North Eastern Portugal against Candida Species. *Future Microbiol* **2014**, *9*, 139–146, doi:10.2217/fmb.13.147.
236. Elansary, H.O.; Szopa, A.; Klimek-Szczykutowicz, M.; Ekiert, H.; Barakat, A.A.; A. Al-Mana, F. Antiproliferative, Antimicrobial, and Antifungal Activities of Polyphenol Extracts from Ferocactus Species. *Processes* **2020**, *8*, 138, doi:10.3390/pr8020138.
237. Donkia, A.P.T.; Eckhardt, P.; Tsafack, B.T.; Tchuenguem, R.T.; Groß, J.; Ponou, B.K.; Teponno, R.B.; Dzoyem, J.P.; Opatz, T.; Barboni, L.; et al. Constituents of Desmodium Salicifolium (Poir.) DC (Fabaceae) with Antifungal Activity. *Phytochemistry Letters* **2022**, *50*, 100–105, doi:10.1016/j.phytol.2022.05.013.

238. Soberón, J.R.; Sgariglia, M.A.; Pastoriza, A.C.; Soruco, E.M.; Jäger, S.N.; Labadie, G.R.; Sampietro, D.A.; Vattuone, M.A. Antifungal Activity and Cytotoxicity of Extracts and Triterpenoid Saponins Obtained from the Aerial Parts of Anagallis Arvensis L. *J Ethnopharmacol* **2017**, *203*, 233–240, doi:10.1016/j.jep.2017.03.056.
239. Zhang, D.; Fu, Y.; Yang, J.; Li, X.-N.; San, M.M.; Oo, T.N.; Wang, Y.; Yang, X. Triterpenoids and Their Glycosides from Glinus Oppositifolius with Antifungal Activities against Microsporum Gypseum and Trichophyton Rubrum. *Molecules* **2019**, *24*, 2206, doi:10.3390/molecules24122206.
240. Wang, M.-Y.; Peng, Y.; Peng, C.-S.; Qu, J.-Y.; Li, X.-B. The Bioassay-Guided Isolation of Antifungal Saponins from Hosta Plantaginea Leaves. *J Asian Nat Prod Res* **2018**, *20*, 501–509, doi:10.1080/10286020.2017.1329304.
241. Peralta, M.A.; Silva, M.A.D.; Ortega, M.G.; Cabrera, J.L.; Paraje, M.G. Antifungal Activity of a Prenylated Flavonoid from Dalea Elegans against Candida Albicans Biofilms. *Phytomedicine* **2015**, *22*, 975–980, doi:10.1016/j.phymed.2015.07.003.
242. Periferakis, A.; Periferakis, K.; Badarau, I.A.; Petran, E.M.; Popa, D.C.; Caruntu, A.; Costache, R.S.; Scheau, C.; Caruntu, C.; Costache, D.O. Kaempferol: Antimicrobial Properties, Sources, Clinical, and Traditional Applications. *Int J Mol Sci* **2022**, *23*, 15054, doi:10.3390/ijms232315054.
243. Rao, A.; Zhang, Y.; Muend, S.; Rao, R. Mechanism of Antifungal Activity of Terpenoid Phenols Resembles Calcium Stress and Inhibition of the TOR Pathway. *Antimicrob Agents Chemother* **2010**, *54*, 5062–5069, doi:10.1128/AAC.01050-10.
244. Botta, L.; Saladino, R.; Barghini, P.; Fenice, M.; Pasqualetti, M. Production and Identification of Two Antifungal Terpenoids from the Posidonia Oceanica Epiphytic Ascomycota Mariannaea Humicola IG100. *Microbial Cell Factories* **2020**, *19*, 184, doi:10.1186/s12934-020-01445-7.
245. Niu, C.; Wang, C.; Yang, Y.; Chen, R.; Zhang, J.; Chen, H.; Zhuge, Y.; Li, J.; Cheng, J.; Xu, K.; et al. Carvacrol Induces Candida Albicans Apoptosis Associated With Ca2+/Calcineurin Pathway. *Frontiers in Cellular and Infection Microbiology* **2020**, *10*.
246. Nóbrega, R. de O.; Teixeira, A.P. de C.; Oliveira, W.A. de; Lima, E. de O.; Lima, I.O. Investigation of the Antifungal Activity of Carvacrol against Strains of Cryptococcus Neoformans. *Pharmaceutical Biology* **2016**, *54*, 2591–2596, doi:10.3109/13880209.2016.1172319.
247. Tripathi, S.K.; Xu, T.; Feng, Q.; Avula, B.; Shi, X.; Pan, X.; Mask, M.M.; Baerson, S.R.; Jacob, M.R.; Ravu, R.R.; et al. Two Plant-Derived Aporphinoid Alkaloids Exert Their Antifungal Activity by Disrupting Mitochondrial Iron-Sulfur Cluster Biosynthesis. *Journal of Biological Chemistry* **2017**, *292*, 16578–16593, doi:10.1074/jbc.M117.781773.
248. Khan, S.I.; Nimrod, A.C.; Mehrpooya, M.; Nitiss, J.L.; Walker, L.A.; Clark, A.M. Antifungal Activity of Eupolauridine and Its Action on DNA Topoisomerases. *Antimicrobial Agents and Chemotherapy* **2002**, *46*, 1785–1792, doi:10.1128/AAC.46.6.1785-1792.2002.
249. Yang, C.R.; Zhang, Y.; Jacob, M.R.; Khan, S.I.; Zhang, Y.J.; Li, X.C. Antifungal Activity of C-27 Steroidal Saponins. *Antimicrobial Agents and Chemotherapy* **2006**, *50*, 1710–1714, doi:10.1128/AAC.50.5.1710-1714.2006.
250. Trdá, L.; Janda, M.; Macková, D.; Pospíchalová, R.; Dobrev, P.I.; Burketová, L.; Matušinsky, P. Dual Mode of the Saponin Aescin in Plant Protection: Antifungal Agent and Plant Defense Elicitor. *Frontiers in Plant Science* **2019**, *10*, 1448, doi:10.3389/fpls.2019.01448.
251. Zhang, J.-D.; Xu, Z.; Cao, Y.-B.; Chen, H.-S.; Yan, L.; An, M.-M.; Gao, P.-H.; Wang, Y.; Jia, X.-M.; Jiang, Y.-Y. Antifungal Activities and Action Mechanisms of

Compounds from Tribulus Terrestris L. *J Ethnopharmacol* **2006**, *103*, 76–84, doi:10.1016/j.jep.2005.07.006.
252. Jacobs, S.E.; Jacobs, J.L.; Dennis, E.K.; Taimur, S.; Rana, M.; Patel, D.; Gitman, M.; Patel, G.; Schaefer, S.; Iyer, K.; et al. Candida Auris Pan-Drug-Resistant to Four Classes of Antifungal Agents. *Antimicrob Agents Chemother* **2022**, *66*, e0005322, doi:10.1128/aac.00053-22.
253. O'Brien, B.; Liang, J.; Chaturvedi, S.; Jacobs, J.L.; Chaturvedi, V. Pan-Resistant Candida Auris: New York Subcluster Susceptible to Antifungal Combinations. *The Lancet Microbe* **2020**, *1*, e193–e194, doi:10.1016/S2666-5247(20)30090-2.
254. Hashemi, M.M.; Rovig, J.; Holden, B.S.; Taylor, M.F.; Weber, S.; Wilson, J.; Hilton, B.; Zaugg, A.L.; Ellis, S.W.; Yost, C.D.; et al. Ceragenins Are Active against Drug-Resistant Candida Auris Clinical Isolates in Planktonic and Biofilm Forms. *J Antimicrob Chemother* **2018**, *73*, 1537–1545, doi:10.1093/jac/dky085.
255. Iyer, K.R.; Camara, K.; Daniel-Ivad, M.; Trilles, R.; Pimentel-Elardo, S.M.; Fossen, J.L.; Marchillo, K.; Liu, Z.; Singh, S.; Muñoz, J.F.; et al. An Oxindole Efflux Inhibitor Potentiates Azoles and Impairs Virulence in the Fungal Pathogen Candida Auris. *Nat Commun* **2020**, *11*, 6429, doi:10.1038/s41467-020-20183-3.
256. Kubiczek, D.; Raber, H.; Gonzalez-García, M.; Morales-Vicente, F.; Staendker, L.; Otero-Gonzalez, A.J.; Rosenau, F. Derivates of the Antifungal Peptide Cm-P5 Inhibit Development of Candida Auris Biofilms In Vitro. *Antibiotics (Basel)* **2020**, *9*, 363, doi:10.3390/antibiotics9070363.
257. Lara, H.H.; Ixtepan-Turrent, L.; Jose Yacaman, M.; Lopez-Ribot, J. Inhibition of Candida Auris Biofilm Formation on Medical and Environmental Surfaces by Silver Nanoparticles. *ACS Appl. Mater. Interfaces* **2020**, *12*, 21183–21191, doi:10.1021/acsami.9b20708.
258. Liu, J.; Li, Q.; Wang, C.; Shao, J.; Wang, T.; Wu, D.; Ma, K.; Yan, G.; Yin, D. Antifungal Evaluation of Traditional Herbal Monomers and Their Potential for Inducing Cell Wall Remodeling in Candida Albicans and Candida Auris. *Biofouling* **2020**, *36*, 319–331, doi:10.1080/08927014.2020.1759559.
259. Kim, H.-R.; Eom, Y.-B. Antifungal and Anti-Biofilm Effects of 6-Shogaol against Candida Auris. *J Appl Microbiol* **2021**, *130*, 1142–1153, doi:10.1111/jam.14870.
260. Jakab, Á.; Balla, N.; Ragyák, Á.; Nagy, F.; Kovács, F.; Sajtos, Z.; Tóth, Z.; Borman, A.M.; Pócsi, I.; Baranyai, E.; et al. Transcriptional Profiling of the Candida Auris Response to Exogenous Farnesol Exposure. *mSphere 6*, e00710-21, doi:10.1128/mSphere.00710-21.
261. de Alteriis, E.; Maione, A.; Falanga, A.; Bellavita, R.; Galdiero, S.; Albarano, L.; Salvatore, M.M.; Galdiero, E.; Guida, M. Activity of Free and Liposome-Encapsulated Essential Oil from Lavandula Angustifolia against Persister-Derived Biofilm of Candida Auris. *Antibiotics (Basel)* **2021**, *11*, 26, doi:10.3390/antibiotics11010026.
262. Possamai Rossatto, F.C.; Tharmalingam, N.; Escobar, I.E.; d'Azevedo, P.A.; Zimmer, K.R.; Mylonakis, E. Antifungal Activity of the Phenolic Compounds Ellagic Acid (EA) and Caffeic Acid Phenethyl Ester (CAPE) against Drug-Resistant Candida Auris. *J Fungi (Basel)* **2021**, *7*, 763, doi:10.3390/jof7090763.
263. Maione, A.; La Pietra, A.; de Alteriis, E.; Mileo, A.; De Falco, M.; Guida, M.; Galdiero, E. Effect of Myrtenol and Its Synergistic Interactions with Antimicrobial Drugs in the Inhibition of Single and Mixed Biofilms of Candida Auris and Klebsiella Pneumoniae. *Microorganisms* **2022**, *10*, 1773, doi:10.3390/microorganisms10091773.
264. Tran, H.N.H.; Graham, L.; Adukwu, E.C. In Vitro Antifungal Activity of Cinnamomum Zeylanicum Bark and Leaf Essential Oils against Candida Albicans and

Candida Auris. *Appl Microbiol Biotechnol* **2020**, *104*, 8911–8924, doi:10.1007/s00253-020-10829-z.
265. Di Vito, M.; Garzoli, S.; Rosato, R.; Mariotti, M.; Gervasoni, J.; Santucci, L.; Ovidi, E.; Cacaci, M.; Lombarini, G.; Torelli, R.; et al. A New Potential Resource in the Fight against Candida Auris: The Cinnamomum Zeylanicum Essential Oil in Synergy with Antifungal Drug. *Microbiol Spectr* **2023**, *11*, e0438522, doi:10.1128/spectrum.04385-22.
266. Balkrishna, A.; Kharayat, B.; Rastogi, S.; Kabdwal, M.; Haldar, S.; Varshney, A. Withania Somnifera Seed Oil Exhibits Antibiofilm Properties against Drug-Resistant Candida Auris Clinical Isolate through Modulation in Cell Permeability. *J Appl Microbiol* **2023**, *134*, lxad087, doi:10.1093/jambio/lxad087.
267. Kamauchi, H.; Furukawa, M.; Kiba, Y.; Kitamura, M.; Usui, K.; Katakura, M.; Takao, K.; Sugita, Y. Antifungal Activity of Dehydrocurvularin for Candida Spp. through the Inhibition of Adhesion to Human Adenocarcinoma Cells. *J Antibiot (Tokyo)* **2022**, *75*, 530–533, doi:10.1038/s41429-022-00543-5.
268. Marquez, L.; Lee, Y.; Duncan, D.; Whitesell, L.; Cowen, L.E.; Quave, C. Potent Antifungal Activity of Penta-O-Galloyl-β-d-Glucose against Drug-Resistant Candida Albicans, Candida Auris, and Other Non-Albicans Candida Species. *ACS Infect Dis* **2023**, *9*, 1685–1694, doi:10.1021/acsinfecdis.3c00113.
269. Fatima, T.; Fatima, Z.; Hameed, S. Abrogation of Efflux Pump Activity, Biofilm Formation, and Immune Escape by Candidacidal Geraniol in Emerging Superbug, Candida Auris. *Int Microbiol* **2023**, *26*, 881–891, doi:10.1007/s10123-023-00343-3.
270. Arias, L.S.; Butcher, M.C.; Short, B.; McKloud, E.; Delaney, C.; Kean, R.; Monteiro, D.R.; Williams, C.; Ramage, G.; Brown, J.L. Chitosan Ameliorates Candida Auris Virulence in a Galleria Mellonella Infection Model. *Antimicrob Agents Chemother* **2020**, *64*, e00476-20, doi:10.1128/AAC.00476-20.
271. Zeng, H.; Stadler, M.; Abraham, W.-R.; Müsken, M.; Schrey, H. Inhibitory Effects of the Fungal Pigment Rubiginosin C on Hyphal and Biofilm Formation in Candida Albicans and Candida Auris. *J Fungi (Basel)* **2023**, *9*, 726, doi:10.3390/jof9070726.
272. de Groot, T.; Janssen, T.; Faro, D.; Cremers, N.A.J.; Chowdhary, A.; Meis, J.F. Antifungal Activity of a Medical-Grade Honey Formulation against Candida Auris. *J Fungi (Basel)* **2021**, *7*, 50, doi:10.3390/jof7010050.
273. Panda, S.K.; Khan, A.; Swain, S.S.; Aissa, A.; Mukazayire, M.J.; Van Puyvelde, L.; Luyten, W. The Anticandidal Activity of the Diterpenediol 8(14),15-Sandaracopimaradiene-7alpha,18-Diol from Tetradenia Riparia against the Emerging Pathogen Candida Auris. *Phytotherapy Research* **2023**, *37*, 3–6, doi:10.1002/ptr.7638.
274. Watanabe, Y.; Takahashi, S.; Ito, S.; Tokiwa, T.; Noguchi, Y.; Azami, H.; Kojima, H.; Higo, M.; Ban, S.; Nagai, K.; et al. Hakuhybotrol, a Polyketide Produced by Hypomyces Pseudocorticiicola, Characterized with the Assistance of 3D ED/MicroED. *Org Biomol Chem* **2023**, doi:10.1039/d2ob02286a.
275. Bravo-Chaucanés, C.P.; Vargas-Casanova, Y.; Chitiva-Chitiva, L.C.; Ceballos-Garzon, A.; Modesti-Costa, G.; Parra-Giraldo, C.M. Evaluation of Anti-Candida Potential of Piper Nigrum Extract in Inhibiting Growth, Yeast-Hyphal Transition, Virulent Enzymes, and Biofilm Formation. *J Fungi (Basel)* **2022**, *8*, 784, doi:10.3390/jof8080784.
276. Dal Mas, C.; Rossato, L.; Shimizu, T.; Oliveira, E.B.; da Silva Junior, P.I.; Meis, J.F.; Colombo, A.L.; Hayashi, M.A.F. Effects of the Natural Peptide Crotamine from a South American Rattlesnake on Candida Auris, an Emergent Multidrug Antifungal Resistant Human Pathogen. *Biomolecules* **2019**, *9*, 205, doi:10.3390/biom9060205.

277. Parker, R.A.; Gabriel, K.T.; Graham, K.D.; Butts, B.K.; Cornelison, C.T. Antifungal Activity of Select Essential Oils against Candida Auris and Their Interactions with Antifungal Drugs. *Pathogens* **2022**, *11*, 821, doi:10.3390/pathogens11080821.
278. Raber, H.F.; Sejfijaj, J.; Kissmann, A.-K.; Wittgens, A.; Gonzalez-Garcia, M.; Alba, A.; Vázquez, A.A.; Morales Vicente, F.E.; Erviti, J.P.; Kubiczek, D.; et al. Antimicrobial Peptides Pom-1 and Pom-2 from Pomacea Poeyana Are Active against Candidaauris, C. Parapsilosis and C. Albicans Biofilms. *Pathogens* **2021**, *10*, 496, doi:10.3390/pathogens10040496.
279. Raj, S.; Vinod, V.; Jayakumar, J.; Suresh, P.; Kumar, A.; Biswas, R. Antifungal Activity of Syzygium Samarangense Leaf Extracts against Candida. *Lett Appl Microbiol* **2021**, *73*, 31–38, doi:10.1111/lam.13471.
280. Rudramurthy, S.M.; Chakrabarti, A.; Paul, R.A.; Sood, P.; Kaur, H.; Capoor, M.R.; Kindo, A.J.; Marak, R.S.K.; Arora, A.; Sardana, R.; et al. Candida Auris Candidaemia in Indian ICUs: Analysis of Risk Factors. *Journal of Antimicrobial Chemotherapy* **2017**, *72*, 1794–1801, doi:10.1093/jac/dkx034.
281. WHO Best Practices in Phlebotomy. In *WHO Guidelines on Drawing Blood: Best Practices in Phlebotomy*; World Health Organization, 2010.
282. Arendrup, M.C.; Cuenca-Estrella, M.; Lass-Flörl, C.; Hope, W.; EUCAST-AFST EUCAST Technical Note on the EUCAST Definitive Document EDef 7.2: Method for the Determination of Broth Dilution Minimum Inhibitory Concentrations of Antifungal Agents for Yeasts EDef 7.2 (EUCAST-AFST). *Clin Microbiol Infect* **2012**, *18*, E246-247, doi:10.1111/j.1469-0691.2012.03880.x.
283. Madeira, F.; Pearce, M.; Tivey, A.R.N.; Basutkar, P.; Lee, J.; Edbali, O.; Madhusoodanan, N.; Kolesnikov, A.; Lopez, R. Search and Sequence Analysis Tools Services from EMBL-EBI in 2022. *Nucleic Acids Res* **2022**, gkac240, doi:10.1093/nar/gkac240.
284. Kawai, S.; Hashimoto, W.; Murata, K. Transformation of Saccharomyces Cerevisiae and Other Fungi: Methods and Possible Underlying Mechanism. *Bioeng Bugs* **2010**, *1*, 395–403, doi:10.4161/bbug.1.6.13257.
285. Uppala, J.K.; Bhattacharjee, S.; Dey, M. Vps34 and TOR Kinases Coordinate HAC1 mRNA Translation in the Presence or Absence of Ire1-Dependent Splicing. *Mol Cell Biol* **2021**, *41*, e0066220, doi:10.1128/MCB.00662-20.
286. Kim, S.; Chen, J.; Cheng, T.; Gindulyte, A.; He, J.; He, S.; Li, Q.; Shoemaker, B.A.; Thiessen, P.A.; Yu, B.; et al. PubChem 2019 Update: Improved Access to Chemical Data. *Nucleic Acids Research* **2018**, *47*, D1102–D1109, doi:10.1093/nar/gky1033.
287. Molinspiration Molinspiration Cheminformatics Available online: https://www.molinspiration.com/ (accessed on 27 March 2020).
288. Lipinski, C.A.; Lombardo, F.; Dominy, B.W.; Feeney, P.J. Experimental and Computational Approaches to Estimate Solubility and Permeability in Drug Discovery and Development Settings. *Advanced Drug Delivery Reviews* **2001**, *46*, 3–26, doi:10.1016/S0169-409X(00)00129-0.
289. Molsoft Molsoft L.L.C.: Drug-Likeness and Molecular Property Prediction. Available online: http://molsoft.com/mprop/ (accessed on 27 March 2020).
290. Yang, H.; Lou, C.; Sun, L.; Li, J.; Cai, Y.; Wang, Z.; Li, W.; Liu, G.; Tang, Y. admetSAR 2.0: Web-Service for Prediction and Optimization of Chemical ADMET Properties. *Bioinformatics* **2018**, *35*, 1067–1069, doi:10.1093/bioinformatics/bty707.
291. Skrzypek, M.S.; Binkley, J.; Binkley, G.; Miyasato, S.R.; Simison, M.; Sherlock, G. The Candida Genome Database (CGD): Incorporation of Assembly 22, Systematic Identifiers and Visualization of High Throughput Sequencing Data. *Nucleic Acids Research* **2016**, *45*, D592–D596, doi:10.1093/nar/gkw924.

292. Yang, J.; Yan, R.; Roy, A.; Xu, D.; Poisson, J.; Zhang, Y. The I-TASSER Suite: Protein Structure and Function Prediction. *Nature Methods* 2014, *12*, 7–8.
293. Lovell, S.C.; Davis, I.W.; Arendall, W.B.; Bakker, P.I.W.D.; Word, J.M.; Prisant, M.G.; Richardson, J.S.; Richardson, D.C. Structure Validation by Calpha Geometry: Phi,Psi and Cbeta Deviation. *Proteins* **2003**, *50*, 437–450, doi:10.1002/PROT.10286.
294. Schneidman-Duhovny, D.; Inbar, Y.; Nussinov, R.; Wolfson, H.J. PatchDock and SymmDock: Servers for Rigid and Symmetric Docking. *Nucleic Acids Research* **2005**, *33*, W363–W367, doi:10.1093/nar/gki481.
295. Case, D.A.; Cheatham, T.E.; Darden, T.; Gohlke, H.; Luo, R.; Merz, K.M.; Onufriev, A.; Simmerling, C.; Wang, B.; Woods, R.J. The Amber Biomolecular Simulation Programs. *Journal of Computational Chemistry* 2005, *26*, 1668–1688.
296. Wang, J.; Wang, W.; Kollman, P.A.; Case, D.A. Antechamber, An Accessory Software Package For Molecular Mechanical Calculations Correspondence To. *Journal of Chemical Information and Computer Sciences* **2001**, *222*, U403.
297. Toukmaji, A.; Sagui, C.; Board, J.; Darden, T. Efficient Particle-Mesh Ewald Based Approach to Fixed and Induced Dipolar Interactions. *Journal of Chemical Physics* **2000**, *113*, 10913–10927, doi:10.1063/1.1324708.
298. Roe, D.R.; Cheatham, T.E. PTRAJ and CPPTRAJ: Software for Processing and Analysis of Molecular Dynamics Trajectory Data. *Journal of Chemical Theory and Computation* **2013**, *9*, 3084–3095, doi:10.1021/ct400341p.
299. Espinel-Ingroff, A.; Fothergill, A.; Peter, J.; Rinaldi, M.G.; Walsh, T.J. Testing Conditions for Determination of Minimum Fungicidal Concentrations of New and Established Antifungal Agents for Aspergillus Spp.: NCCLS Collaborative Study. *Journal of Clinical Microbiology* **2002**, *40*, 3204–3208, doi:10.1128/JCM.40.9.3204-3208.2002.
300. Prasath, K.G.; Tharani, H.; Kumar, M.S.; Pandian, S.K. Palmitic Acid Inhibits the Virulence Factors of Candida Tropicalis: Biofilms, Cell Surface Hydrophobicity, Ergosterol Biosynthesis, and Enzymatic Activity. *Front Microbiol* **2020**, *11*, 864, doi:10.3389/fmicb.2020.00864.
301. Arthington-Skaggs, B.A.; Jradi, H.; Desai, T.; Morrison, C.J. Quantitation of Ergosterol Content: Novel Method for Determination of Fluconazole Susceptibility of Candida Albicans. *J Clin Microbiol* **1999**, *37*, 3332–3337.
302. Muthamil, S.; Prasath, K.G.; Priya, A.; Precilla, P.; Pandian, S.K. Global Proteomic Analysis Deciphers the Mechanism of Action of Plant Derived Oleic Acid against Candida Albicans Virulence and Biofilm Formation. *Scientific Reports* **2020**, *10*, 5113, doi:10.1038/s41598-020-61918-y.
303. Prasath, K.G.; Sethupathy, S.; Pandian, S.K. Proteomic Analysis Uncovers the Modulation of Ergosterol, Sphingolipid and Oxidative Stress Pathway by Myristic Acid Impeding Biofilm and Virulence in Candida Albicans. *J Proteomics* **2019**, *208*, 103503, doi:10.1016/j.jprot.2019.103503.
304. Semreen, M.H.; Soliman, S.S.M.; Saeed, B.Q.; Alqarihi, A.; Uppuluri, P.; Ibrahim, A.S. Metabolic Profiling of Candida Auris, a Newly-Emerging Multi-Drug Resistant Candida Species, by GC-MS. *Molecules* **2019**, *24*, E399, doi:10.3390/molecules24030399.
305. Sharma, D.; Pramanik, A.; Agrawal, P.K. Evaluation of Bioactive Secondary Metabolites from Endophytic Fungus Pestalotiopsis Neglecta BAB-5510 Isolated from Leaves of Cupressus Torulosa D.Don. *3 Biotech* **2016**, *6*, 210, doi:10.1007/s13205-016-0518-3.

306. Abdullah, R. Insecticidal Activity of Secondary Metabolites of Locally Isolated Fungal Strains against Some Cotton Insect Pests. *Journal of Plant Protection and Pathology* **2019**, *10*, 647–653, doi:10.21608/jppp.2019.79456.
307. Mushtaq, M.Y.; Choi, Y.H.; Verpoorte, R.; Wilson, E.G. Extraction for Metabolomics: Access to The Metabolome. *Phytochemical Analysis* **2014**, *25*, 291–306, doi:10.1002/pca.2505.
308. Leon, C.G.; Lee, J.; Bartlett, K.; Gershkovich, P.; Wasan, E.K.; Zhao, J.; Clement, J.G.; Wasan, K.M. In Vitro Cytotoxicity of Two Novel Oral Formulations of Amphotericin B (iCo-009 and iCo-010) against Candida Albicans, Human Monocytic and Kidney Cell Lines. *Lipids Health Dis* **2011**, *10*, 144, doi:10.1186/1476-511X-10-144.
309. Padmasree, C.; Akhtar, N.; Kumar, N. Vachellia Nilotica, a Potential Plant Source Candidate to Reduce the Oxidative Stress and to Kill the Bacteria. *International Journal of Botany Studies* **2017**, *2*, 25–28.
310. Yang, J.; Yan, R.; Roy, A.; Xu, D.; Poisson, J.; Zhang, Y. The I-TASSER Suite: Protein Structure and Function Prediction. *Nat Methods* **2015**, *12*, 7–8, doi:10.1038/nmeth.3213.
311. Berman, H.M.; Westbrook, J.; Feng, Z.; Gilliland, G.; Bhat, T.N.; Weissig, H.; Shindyalov, I.N.; Bourne, P.E. The Protein Data Bank. *Nucleic Acids Research* **2000**, *28*, 235–242, doi:10.1093/nar/28.1.235.
312. McGinnis, S.; Madden, T.L. BLAST: At the Core of a Powerful and Diverse Set of Sequence Analysis Tools. *Nucleic Acids Res* **2004**, *32*, W20–W25, doi:10.1093/nar/gkh435.
313. Pettersen, E.F.; Goddard, T.D.; Huang, C.C.; Couch, G.S.; Greenblatt, D.M.; Meng, E.C.; Ferrin, T.E. UCSF Chimera--a Visualization System for Exploratory Research and Analysis. *J Comput Chem* **2004**, *25*, 1605–1612, doi:10.1002/jcc.20084.
314. Guex, N.; Peitsch, M.C. SWISS-MODEL and the Swiss-PdbViewer: An Environment for Comparative Protein Modeling. *Electrophoresis* **1997**, *18*, 2714–2723, doi:10.1002/elps.1150181505.
315. Schneidman-Duhovny, D.; Inbar, Y.; Nussinov, R.; Wolfson, H.J. PatchDock and SymmDock: Servers for Rigid and Symmetric Docking. *Nucleic Acids Research* **2005**, *33*, W363–W367, doi:10.1093/nar/gki481.
316. Skrzypek, M.S.; Binkley, J.; Binkley, G.; Miyasato, S.R.; Simison, M.; Sherlock, G. The Candida Genome Database (CGD): Incorporation of Assembly 22, Systematic Identifiers and Visualization of High Throughput Sequencing Data. *Nucleic Acids Research* **2016**, *45*, D592–D596, doi:10.1093/nar/gkw924.
317. Yu, C.S.; Cheng, C.W.; Su, W.C.; Chang, K.C.; Huang, S.W.; Hwang, J.K.; Lu, C.H. CELLO2GO: A Web Server for Protein subCELlular lOcalization Prediction with Functional Gene Ontology Annotation. *PLoS ONE* **2014**, *9*, e99368, doi:10.1371/journal.pone.0099368.
318. Doytchinova, I.A.; Flower, D.R. VaxiJen: A Server for Prediction of Protective Antigens, Tumour Antigens and Subunit Vaccines. *BMC Bioinformatics* **2007**, *8*, 4, doi:10.1186/1471-2105-8-4.
319. Jensen, K.K.; Andreatta, M.; Marcatili, P.; Buus, S.; Greenbaum, J.A.; Yan, Z.; Sette, A.; Peters, B.; Nielsen, M. Improved Methods for Predicting Peptide Binding Affinity to MHC Class II Molecules. *Immunology* **2018**, *154*, 394–406, doi:10.1111/imm.12889.
320. Andreatta, M.; Nielsen, M. Gapped Sequence Alignment Using Artificial Neural Networks: Application to the MHC Class I System. *Bioinformatics* **2015**, *32*, 511–517, doi:10.1093/bioinformatics/btv639.

321. Larsen, J.E.P.; Lund, O.; Nielsen, M. Improved Method for Predicting Linear B-Cell Epitopes. *Immunome Res* **2006**, *2*, 2, doi:10.1186/1745-7580-2-2.
322. María, R.-A.R.; Arturo, C.-V.J.; Alicia, J.-A.; Paulina, M.-L.G.; Gerardo, A.-O. *The Impact of Bioinformatics on Vaccine Design and Development*; IntechOpen, 2017; ISBN 978-953-51-3476-3.
323. Yazdani, Z.; Rafiei, A.; Valadan, R.; Ashrafi, H.; Pasandi, M.S.; Kardan, M. Designing a Potent L1 Protein-Based HPV Peptide Vaccine: A Bioinformatics Approach. *Computational Biology and Chemistry* **2020**, *85*, 107209, doi:10.1016/j.compbiolchem.2020.107209.
324. Gupta, S.; Kapoor, P.; Chaudhary, K.; Gautam, A.; Kumar, R.; Raghava, G.P.S. In Silico Approach for Predicting Toxicity of Peptides and Proteins. *PLoS ONE* **2013**, *8*, e73957, doi:10.1371/journal.pone.0073957.
325. Gozalbo, D.; Maneu, V.; Gil, M.L. Role of IFN-Gamma in Immune Responses to Candida Albicans Infections. *Frontiers in Bioscience - Landmark* **2014**, *19*, 1279–1290, doi:10.2741/4281.
326. Delsing, C.E.; Gresnigt, M.S.; Leentjens, J.; Preijers, F.; Frager, F.A.; Kox, M.; Monneret, G.; Venet, F.; Bleeker-Rovers, C.P.; Veerdonk, F.L. van de; et al. Interferon-Gamma as Adjunctive Immunotherapy for Invasive Fungal Infections: A Case Series. *BMC Infectious Diseases* **2014**, *14*, 166, doi:10.1186/1471-2334-14-166.
327. Dhanda, S.K.; Vir, P.; Raghava, G.P.S. Designing of Interferon-Gamma Inducing MHC Class-II Binders. *Biology Direct* **2013**, *8*, 30, doi:10.1186/1745-6150-8-30.
328. Bui, H.H.; Sidney, J.; Li, W.; Fusseder, N.; Sette, A. Development of an Epitope Conservancy Analysis Tool to Facilitate the Design of Epitope-Based Diagnostics and Vaccines. *BMC Bioinformatics* **2007**, *8*, 361, doi:10.1186/1471-2105-8-361.
329. Altschul, S.; Wootton, J.; Gertz, E.; Agarwala, R.; Morgulis, A.; Schäffer, A.; Yu, Y. Protein Database Searches Using Compositionally Adjusted Substitution Matrices. *The FEBS journal* **2005**, *272*, 5101–5109, doi:10.1111/j.1742-4658.2005.04945.x.
330. Negahdaripour, M.; Eslami, M.; Nezafat, N.; Hajighahramani, N.; Ghoshoon, M.B.; Shoolian, E.; Dehshahri, A.; Erfani, N.; Morowvat, M.H.; Ghasemi, Y. A Novel HPV Prophylactic Peptide Vaccine, Designed by Immunoinformatics and Structural Vaccinology Approaches. *Infection, Genetics and Evolution* **2017**, *54*, 402–416, doi:10.1016/j.meegid.2017.08.002.
331. Hasan, M.; Islam, S.; Chakraborty, S.; Mustafa, A.H.; Azim, K.F.; Joy, Z.F.; Hossain, M.N.; Foysal, S.H.; Hasan, M.N. Contriving a Chimeric Polyvalent Vaccine to Prevent Infections Caused by Herpes Simplex Virus (Type-1 and Type-2): An Exploratory Immunoinformatic Approach. *Journal of Biomolecular Structure and Dynamics* **2019**, *38*, 2898–2915, doi:10.1080/07391102.2019.1647286.
332. Gasteiger, E.; Hoogland, C.; Gattiker, A.; Duvaud, S.; Wilkins, M.R.; Appel, R.D.; Bairoch, A. Protein Identification and Analysis Tools on the ExPASy Server. In *The Proteomics Protocols Handbook*; Walker, J.M., Ed.; Springer Protocols Handbooks; Humana Press: Totowa, NJ, 2005; pp. 571–607 ISBN 978-1-59259-890-8.
333. Magnan, C.N.; Randall, A.; Baldi, P. SOLpro: Accurate Sequence-Based Prediction of Protein Solubility. *Bioinformatics* **2009**, *25*, 2200–2207, doi:10.1093/bioinformatics/btp386.
334. Buchan, D.W.A.; Jones, D.T. The PSIPRED Protein Analysis Workbench: 20 Years On. *Nucleic Acids Research* **2019**, *47*, W402–W407, doi:10.1093/nar/gkz297.
335. Lovell, S.C.; Davis, I.W.; Arendall, W.B.; Bakker, P.I.W.D.; Word, J.M.; Prisant, M.G.; Richardson, J.S.; Richardson, D.C. Structure Validation by Cα Geometry: φ,ψ and Cβ Deviation. *Proteins: Structure, Function and Genetics* **2003**, *50*, 437–450, doi:10.1002/prot.10286.

336. Kozakov, D.; Hall, D.R.; Xia, B.; Porter, K.A.; Padhorny, D.; Yueh, C.; Beglov, D.; Vajda, S. The ClusPro Web Server for Protein-Protein Docking. *Nature Protocols* **2017**, *12*, 255–278, doi:10.1038/nprot.2016.169.
337. Van Der Spoel, D.; Lindahl, E.; Hess, B.; Groenhof, G.; Mark, A.E.; Berendsen, H.J.C. GROMACS: Fast, Flexible, and Free. *J Comput Chem* **2005**, *26*, 1701–1718, doi:10.1002/jcc.20291.
338. Darden, T.; York, D.; Pedersen, L. Particle Mesh Ewald: An N·log(N) Method for Ewald Sums in Large Systems. *The Journal of Chemical Physics* **1993**, *98*, 10089–10092, doi:10.1063/1.464397.
339. Polverini, E.; Coll, E.P.; Tieleman, D.P.; Harauz, G. Conformational Choreography of a Molecular Switch Region in Myelin Basic Protein-Molecular Dynamics Shows Induced Folding and Secondary Structure Type Conversion upon Threonyl Phosphorylation in Both Aqueous and Membrane-Associated Environments. *Biochimica et Biophysica Acta - Biomembranes* **2011**, *1808*, 674–683, doi:10.1016/j.bbamem.2010.11.030.
340. van Oss, C.J. The Extended DLVO Theory. In *Interface Science and Technology*; van Oss, C.J., Ed.; The Properties of Water and their Role in Colloidal and Biological Systems; Elsevier, 2008; Vol. 16, pp. 31–48.
341. Grote, A.; Hiller, K.; Scheer, M.; Münch, R.; Nörtemann, B.; Hempel, D.C.; Jahn, D. JCat: A Novel Tool to Adapt Codon Usage of a Target Gene to Its Potential Expression Host. *Nucleic Acids Research* **2005**, *33*, W526–W531, doi:10.1093/nar/gki376.
342. Pote, S.T.; Sonawane, M.S.; Rahi, P.; Shah, S.R.; Shouche, Y.S.; Patole, M.S.; Thakar, M.R.; Sharma, R. Distribution of Pathogenic Yeasts in Different Clinical Samples: Their Identification, Antifungal Susceptibility Pattern, and Cell Invasion Assays. *Infect Drug Resist* **2020**, *13*, 1133–1145, doi:10.2147/IDR.S238002.
343. Pincus, D.H.; Orenga, S.; Chatellier, S. Yeast Identification — Past, Present, and Future Methods. *Medical Mycology* **2007**, *45*, 97–121, doi:10.1080/13693780601059936.
344. Ozcan, K.; Ilkit, M.; Ates, A.; Turac-Bicer, A.; Demirhindi, H. Performance of Chromogenic Candida Agar and CHROMagar Candida in Recovery and Presumptive Identification of Monofungal and Polyfungal Vaginal Isolates. *Medical Mycology* **2010**, *48*, 29–34, doi:10.3109/13693780802713224.
345. Ghelardi, E.; Pichierri, G.; Castagna, B.; Barnini, S.; Tavanti, A.; Campa, M. Efficacy of Chromogenic Candida Agar for Isolation and Presumptive Identification of Pathogenic Yeast Species. *Clinical Microbiology and Infection* **2008**, *14*, 141–147, doi:10.1111/j.1469-0691.2007.01872.x.
346. Badiee, P.; Alborzi, A. Susceptibility of Clinical Candida Species Isolates to Antifungal Agents by E-Test, Southern Iran: A Five Year Study. *Iran J Microbiol* **2011**, *3*, 183–188.
347. Alastruey-Izquierdo, A.; Melhem, M.S.C.; Bonfieti, L.X.; Rodriguez-Tudela, J.L. Susceptibility Test for Fungi: Clinical and Laboratorial Correlations in Medical Mycology. *Rev Inst Med Trop Sao Paulo* **2015**, *57*, 57–64, doi:10.1590/S0036-46652015000700011.
348. Sanguinetti, M.; Posteraro, B. Susceptibility Testing of Fungi to Antifungal Drugs. *J Fungi (Basel)* **2018**, *4*, 110, doi:10.3390/jof4030110.
349. CDC Antifungal Susceptibility Testing and Interpretation Available online: https://www.cdc.gov/fungal/candida-auris/c-auris-antifungal.html (accessed on 3 July 2023).

350. CDC Antimicrobial Resistance in Candida Available online: https://www.cdc.gov/fungal/diseases/candidiasis/antifungal-resistant.html (accessed on 3 July 2023).
351. Hooks, K.B.; Griffiths-Jones, S. Conserved RNA Structures in the Non-Canonical Hac1/Xbp1 Intron. *RNA Biol* **2011**, *8*, 552–556, doi:10.4161/rna.8.4.15396.
352. Guo, F.; Li, S.C.; Wang, L.; Zhu, D. Protein-Protein Binding Site Identification by Enumerating the Configurations. *BMC Bioinformatics* **2012**, *13*, 158, doi:10.1186/1471-2105-13-158.
353. Laskowski, R.A.; Swindells, M.B. LigPlot+: Multiple Ligand-Protein Interaction Diagrams for Drug Discovery. *Journal of Chemical Information and Modeling* **2011**, *51*, 2778–2786, doi:10.1021/ci200227u.
354. Jha, A.; Kumar, A. Multiple Drug Targeting Potential of Novel Ligands Against Virulent Proteins of Candida Albicans. *International Journal of Peptide Research and Therapeutics* **2020**, *26*, 921–942, doi:10.1007/s10989-019-09897-1.
355. Jha, A.; Vimal, A.; Bakht, A.; Kumar, A. Inhibitors of CPH1-MAP Kinase Pathway: Ascertaining Potential Ligands as Multi-Target Drug Candidate in Candida Albicans. *International Journal of Peptide Research and Therapeutics* **2019**, *25*, 997–1010, doi:10.1007/s10989-018-9747-0.
356. Singulani, J. de L.; Galeane, M.C.; Ramos, M.D.; Gomes, P.C.; dos Santos, C.T.; de Souza, B.M.; Palma, M.S.; Fusco Almeida, A.M.; Mendes Giannini, M.J.S. Antifungal Activity, Toxicity, and Membranolytic Action of a Mastoparan Analog Peptide. *Frontiers in Cellular and Infection Microbiology* **2019**, *9*.
357. Treshchalin, I.D.; Sletta, H.; Borgos, S.E.; Pereverzeva, E.P.; Voeĭkova, T.A.; Ellingsen, T.E.; Zotchev, S.B. Comparative analysis of in vitro antifungal activity and in vivo acute toxicity of the nystatin analogue S44HP produced via genetic engineering. *Antibiot Khimioter* **2005**, *50*, 18–22.
358. Chandler, C.E.; Hernandez, F.G.; Totten, M.; Robinett, N.G.; Schatzman, S.S.; Zhang, S.X.; Culotta, V.C. Biochemical Analysis of CaurSOD4, a Potential Therapeutic Target for the Emerging Fungal Pathogen Candida Auris. *ACS Infect Dis* **2022**, *8*, 584–595, doi:10.1021/acsinfecdis.1c00590.
359. Hu, Z.; He, B.; Ma, L.; Sun, Y.; Niu, Y.; Zeng, B. Recent Advances in Ergosterol Biosynthesis and Regulation Mechanisms in Saccharomyces Cerevisiae. *Indian Journal of Microbiology* **2017**, *57*, 270, doi:10.1007/s12088-017-0657-1.
360. Rodrigues, M.L. The Multifunctional Fungal Ergosterol. *mBio* **2018**, *9*, e01755-18, doi:10.1128/mBio.01755-18.
361. Dabur, R.; Gupta, A.; Mandal, T.K.; Singh, D.D.; Bajpai, V.; Gurav, A.M.; Lavekar, G.S. Antimicrobial Activity of Some Indian Medicinal Plants. *Afr J Tradit Complement Altern Med* **2007**, *4*, 313–318.
362. Khameneh, B.; Iranshahy, M.; Soheili, V.; Fazly Bazzaz, B.S. Review on Plant Antimicrobials: A Mechanistic Viewpoint. *Antimicrobial Resistance & Infection Control* **2019**, *8*, 118, doi:10.1186/s13756-019-0559-6.
363. Elleuche, S.; Pöggeler, S. Carbonic Anhydrases in Fungi. *Microbiology (Reading)* **2010**, *156*, 23–29, doi:10.1099/mic.0.032581-0.
364. Hall, R.A.; De Sordi, L.; MacCallum, D.M.; Topal, H.; Eaton, R.; Bloor, J.W.; Robinson, G.K.; Levin, L.R.; Buck, J.; Wang, Y.; et al. CO2 Acts as a Signalling Molecule in Populations of the Fungal Pathogen Candida Albicans. *PLoS Pathog* **2010**, *6*, e1001193, doi:10.1371/journal.ppat.1001193.
365. Schlicker, C.; Hall, R.A.; Vullo, D.; Middelhaufe, S.; Gertz, M.; Supuran, C.T.; Mühlschlegel, F.A.; Steegborn, C. Structure and Inhibition of the CO2-Sensing

Carbonic Anhydrase Can2 from the Pathogenic Fungus Cryptococcus Neoformans. *J Mol Biol* **2009**, *385*, 1207–1220, doi:10.1016/j.jmb.2008.11.037.
366. Jungbluth, M.; Mösch, H.-U.; Taxis, C. Acetate Regulation of Spore Formation Is under the Control of the Ras/Cyclic AMP/Protein Kinase A Pathway and Carbon Dioxide in Saccharomyces Cerevisiae. *Eukaryot Cell* **2012**, *11*, 1021–1032, doi:10.1128/EC.05240-11.
367. Cummins, E.P.; Selfridge, A.C.; Sporn, P.H.; Sznajder, J.I.; Taylor, C.T. Carbon Dioxide-Sensing in Organisms and Its Implications for Human Disease. *Cell Mol Life Sci* **2014**, *71*, 831–845, doi:10.1007/s00018-013-1470-6.
368. Supuran, C.T.; Capasso, C. A Highlight on the Inhibition of Fungal Carbonic Anhydrases as Drug Targets for the Antifungal Armamentarium. *Int J Mol Sci* **2021**, *22*, 4324, doi:10.3390/ijms22094324.
369. Dostál, J.; Brynda, J.; Blaha, J.; Macháček, S.; Heidingsfeld, O.; Pichová, I. Crystal Structure of Carbonic Anhydrase CaNce103p from the Pathogenic Yeast Candida Albicans. *BMC Structural Biology* **2018**, *18*, 14, doi:10.1186/s12900-018-0093-4.
370. Spivak, A.Y.; Khalitova, R.R.; Nedopekina, D.A.; Gubaidullin, R.R. Antimicrobial Properties of Amine- and Guanidine-Functionalized Derivatives of Betulinic, Ursolic and Oleanolic Acids: Synthesis and Structure/Activity Evaluation. *Steroids* **2020**, *154*, 108530, doi:10.1016/j.steroids.2019.108530.
371. Siddiqui, S.A.; Rahman, A.; Rahman, M.O.; Akbar, M.A.; Ali, M.A.; Al-Hemaid, F.M.A.; Elshikh, M.S.; Farah, M.A. A Novel Triterpenoid 16-Hydroxy Betulinic Acid Isolated from Mikania Cordata Attributes Multi-Faced Pharmacological Activities. *Saudi Journal of Biological Sciences* **2019**, *26*, 554–562, doi:10.1016/j.sjbs.2018.03.002.
372. Innocente, A.; Casanova, B.B.; Klein, F.; Lana, A.D.; Pereira, D.; Muniz, M.N.; Sonnet, P.; Gosmann, G.; Fuentefria, A.M.; Gnoatto, S.C.B. Synthesis of Isosteric Triterpenoid Derivatives and Antifungal Activity. *Chemical Biology & Drug Design* **2014**, *83*, 344–349, doi:10.1111/cbdd.12251.
373. Mazumder, A.H.; Das, J.; Kumar Gogoi, H.; Chattopadhyay, P.; Singh, L.; Paul, S.B. In Vitro Activity of Some Medicinal Plants from Cachar District, Assam (India) against Candida Albicans. *Pharmacognosy Journal* **2012**, *4*, 35–39, doi:10.5530/pj.2012.33.6.
374. Paul, S.B.; Mazumder, A.H.; Gogoi, H.K.; Gogoi, B.J.; Chaurasia, A.; Singh, L.; Srivastava, R.B. Evaluation of In Vitro Antioxidant Activity of Some Plants of Cachar District, Assam. *Pharmacognosy Journal* **2010**, *2*, 289–292, doi:10.1016/S0975-3575(10)80118-X.
375. Karamać, M.; Kosińska, A.; Pegg, R.B. Content of Gallic Acid in Selected Plant Extracts. *Pol. J. Food Nutr. Sci.* **2006**, *56*, 55–58.
376. Genwali, G.R.; Acharya, P.P.; Rajbhandari, M. Isolation of Gallic Acid and Estimation of Total Phenolic Content in Some Medicinal Plants and Their Antioxidant Activity. *Nepal Journal of Science and Technology* **2013**, *14*, 95–102, doi:10.3126/njst.v14i1.8928.
377. Giftson, J.S.; Jayanthi, S.; Nalini, N. Chemopreventive Efficacy of Gallic Acid, an Antioxidant and Anticarcinogenic Polyphenol, against 1,2-Dimethyl Hydrazine Induced Rat Colon Carcinogenesis. *Investigational New Drugs* **2010**, *28*, 251–259, doi:10.1007/s10637-009-9241-9.
378. Kahkeshani, N.; Farzaei, F.; Fotouhi, M.; Alavi, S.S.; Bahramsoltani, R.; Naseri, R.; Momtaz, S.; Abbasabadi, Z.; Rahimi, R.; Farzaei, M.H.; et al. Pharmacological Effects of Gallic Acid in Health and Diseases: A Mechanistic Review. *Iranian Journal of Basic Medical Sciences* **2019**, *22*, 225–237, doi:10.22038/ijbms.2019.32806.7897.

379. Yang, K.; Zhang, L.; Liao, P.; Xiao, Z.; Zhang, F.; Sindaye, D.; Xin, Z.; Tan, C.; Deng, J.; Yin, Y.; et al. Impact of Gallic Acid on Gut Health: Focus on the Gut Microbiome, Immune Response, and Mechanisms of Action. *Front Immunol* **2020**, *11*, 580208, doi:10.3389/fimmu.2020.580208.
380. Kroes, B.H.; van den Berg, A.J.; Quarles van Ufford, H.C.; van Dijk, H.; Labadie, R.P. Anti-Inflammatory Activity of Gallic Acid. *Planta Medica* **1992**, *58*, 499–504, doi:10.1055/s-2006-961535.
381. Patel, S.S.; Goyal, R.K. Cardioprotective Effects of Gallic Acid in Diabetes-Induced Myocardial Dysfunction in Rats. *Pharmacognosy Research* **2011**, *3*, 239–245, doi:10.4103/0974-8490.89743.
382. Huang, P.-J.; Hseu, Y.-C.; Lee, M.-S.; Senthil Kumar, K.J.; Wu, C.-R.; Hsu, L.-S.; Liao, J.-W.; Cheng, I.-S.; Kuo, Y.-T.; Huang, S.-Y.; et al. In Vitro and in Vivo Activity of Gallic Acid and Toona Sinensis Leaf Extracts against HL-60 Human Premyelocytic Leukemia. *Food and Chemical Toxicology* **2012**, *50*, 3489–3497, doi:10.1016/j.fct.2012.06.046.
383. Nabavi, S.F.; Habtemariam, S.; Jafari, M.; Sureda, A.; Nabavi, S.M. Protective Role of Gallic Acid on Sodium Fluoride Induced Oxidative Stress in Rat Brain. *Bulletin of Environmental Contamination and Toxicology* **2012**, *89*, 73–77, doi:10.1007/s00128-012-0645-4.
384. Gandhi, G.R.; Jothi, G.; Antony, P.J.; Balakrishna, K.; Paulraj, M.G.; Ignacimuthu, S.; Stalin, A.; Al-Dhabi, N.A. Gallic Acid Attenuates High-Fat Diet Fed-Streptozotocin-Induced Insulin Resistance via Partial Agonism of PPARγ in Experimental Type 2 Diabetic Rats and Enhances Glucose Uptake through Translocation and Activation of GLUT4 in PI3K/p-Akt Signaling Pathway. *European Journal of Pharmacology* **2014**, *745*, 201–216, doi:10.1016/j.ejphar.2014.10.044.
385. Bayramoglu, G.; Kurt, H.; Bayramoglu, A.; Gunes, H.V.; Degirmenci, İ.; Colak, S. Preventive Role of Gallic Acid on Hepatic Ischemia and Reperfusion Injury in Rats. *Cytotechnology* **2015**, *67*, 845–849, doi:10.1007/s10616-014-9724-1.
386. Wen, L.; Qu, T.-B.; Zhai, K.; Ding, J.; Hai, Y.; Zhou, J.-L. Gallic Acid Can Play a Chondroprotective Role against AGE-Induced Osteoarthritis Progression. *Journal of Orthopaedic Science: Official Journal of the Japanese Orthopaedic Association* **2015**, *20*, 734–741, doi:10.1007/s00776-015-0718-4.
387. DailyMed GALLIC ACID- Gallicum Acidum Liquid.
388. Li, Z.J.; Liu, M.; Dawuti, G.; Dou, Q.; Ma, Y.; Liu, H.G.; Aibai, S. Antifungal Activity of Gallic Acid In Vitro and In Vivo. *Phytotherapy Research* **2017**, *31*, 1039–1045, doi:10.1002/ptr.5823.
389. Carvalho, R.S.; Carollo, C.A.; Magalhães, de J.C.; Palumbo, J.M.C.; Boaretto, A.G.; Sá, e I.C.N.; Ferraz, A.C.; Lima, W.G.; Siqueira, de J.M.; Ferreira, J.M.S. Antibacterial and Antifungal Activities of Phenolic Compound-Enriched Ethyl Acetate Fraction from Cochlospermum Regium (Mart. Et. Schr.) Pilger Roots: Mechanisms of Action and Synergism with Tannin and Gallic Acid. *South African Journal of Botany* **2018**, *114*, 181–187, doi:10.1016/j.sajb.2017.11.010.
390. Marra, A. Can Virulence Factors Be Viable Antibacterial Targets? *Expert Review of Anti-infective Therapy* **2004**, *2*, 61–72, doi:10.1586/14787210.2.1.61.
391. Heras, B.; Scanlon, M.J.; Martin, J.L. Targeting Virulence Not Viability in the Search for Future Antibacterials. *British Journal of Clinical Pharmacology* **2015**, *79*, 208–215, doi:10.1111/bcp.12356.
392. Kaur, J.; Cao, X.; Abutaleb, N.S.; Elkashif, A.; Graboski, A.L.; Krabill, A.D.; AbdelKhalek, A.H.; An, W.; Bhardwaj, A.; Seleem, M.N.; et al. Optimization of Acetazolamide-Based Scaffold as Potent Inhibitors of Vancomycin-Resistant

Enterococcus. *Journal of Medicinal Chemistry* **2020**, *63*, 9540–9562, doi:10.1021/acs.jmedchem.0c00734.
393. Adhikari, U.K.; Tayebi, M.; Rahman, M.M. Immunoinformatics Approach for Epitope-Based Peptide Vaccine Design and Active Site Prediction against Polyprotein of Emerging Oropouche Virus. *Journal of Immunology Research* **2018**, *2018*, 6718083, doi:10.1155/2018/6718083.
394. Liu, W.; Xie, Y.; Ma, J.; Luo, X.; Nie, P.; Zuo, Z.; Lahrmann, U.; Zhao, Q.; Zheng, Y.; Zhao, Y.; et al. IBS: An Illustrator for the Presentation and Visualization of Biological Sequences. *Bioinformatics* **2015**, *31*, 3359–3361, doi:10.1093/bioinformatics/btv362.
395. Tarang, S.; Kesherwani, V.; LaTendresse, B.; Lindgren, L.; Rocha-Sanchez, S.M.; Weston, M.D. In Silico Design of a Multivalent Vaccine Against Candida Albicans. *Scientific Reports* **2020**, *10*, 1–7, doi:10.1038/s41598-020-57906-x.
396. Ben-Yedidia, T.; Arnon, R. Epitope-Based Vaccine against Influenza. *Expert Review of Vaccines* 2007, *6*, 939–948.
397. Tahir Ul Qamar, M.; Saleem, S.; Ashfaq, U.A.; Bari, A.; Anwar, F.; Alqahtani, S. Epitope-Based Peptide Vaccine Design and Target Site Depiction against Middle East Respiratory Syndrome Coronavirus: An Immune-Informatics Study. *Journal of Translational Medicine* **2019**, *17*, 362, doi:10.1186/s12967-019-2116-8.
398. Oyarzún, P.; Kobe, B. Recombinant and Epitope-Based Vaccines on the Road to the Market and Implications for Vaccine Design and Production. *Human Vaccines and Immunotherapeutics* **2016**, *12*, 763–767, doi:10.1080/21645515.2015.1094595.
399. Singh, S.; Uppuluri, P.; Mamouei, Z.; Alqarihi, A.; Elhassan, H.; French, S.; Lockhart, S.R.; Chiller, T.; Edwards, J.E.; Ibrahim, A.S. The NDV-3A Vaccine Protects Mice from Multidrug Resistant Candida Auris Infection. *PLoS Pathogens* **2019**, *15*, e1007460, doi:10.1371/journal.ppat.1007460.
400. María, R.R.; Arturo, C.J.; Alicia, J.A.; Paulina, M.G.; Gerardo, A.O. The Impact of Bioinformatics on Vaccine Design and Development. In *Vaccines*; InTech, 2017.
401. Adhikari, U.K.; Tayebi, M.; Rahman, M.M. Immunoinformatics Approach for Epitope-Based Peptide Vaccine Design and Active Site Prediction against Polyprotein of Emerging Oropouche Virus. *Journal of Immunology Research* **2018**, *2018*, 6718083, doi:10.1155/2018/6718083.
402. Gozalbo, D.; Maneu, V.; Gil, M.L. Role of IFN-Gamma in Immune Responses to Candida Albicans Infections. *Frontiers in Bioscience - Landmark* **2014**, *19*, 1279–1290, doi:10.2741/4281.
403. Delsing, C.E.; Gresnigt, M.S.; Leentjens, J.; Preijers, F.; Frager, F.A.; Kox, M.; Monneret, G.; Venet, F.; Bleeker-Rovers, C.P.; van de Veerdonk, F.L.; et al. Interferon-Gamma as Adjunctive Immunotherapy for Invasive Fungal Infections: A Case Series. *BMC Infectious Diseases* **2014**, *14*, 166, doi:10.1186/1471-2334-14-166.
404. Forstnerič, V.; Ivičak-Kocjan, K.; Plaper, T.; Jerala, R.; Benčina, M. The Role of the C-Terminal D0 Domain of Flagellin in Activation of Toll like Receptor 5. *PLOS Pathogens* **2017**, *13*, e1006574, doi:10.1371/journal.ppat.1006574.
405. Gupta, S.K.; Bajwa, P.; Deb, R.; Chellappa, M.M.; Dey, S. Flagellin a Toll-like Receptor 5 Agonist as an Adjuvant in Chicken Vaccines. *Clinical and Vaccine Immunology* 2014, *21*, 261–270.
406. Shanmugam, A.; Rajoria, S.; George, A.L.; Mittelman, A.; Suriano, R.; Tiwari, R.K. Synthetic Toll Like Receptor-4 (TLR-4) Agonist Peptides as a Novel Class of Adjuvants. *PLoS ONE* **2012**, *7*, e30839, doi:10.1371/journal.pone.0030839.
407. Akhtar, N.; Kaushik, V.; Grewal, R.K.; Wani, A.K.; Suwattanasophon, C.; Choowongkomon, K.; Oliva, R.; Shaikh, A.R.; Cavallo, L.; Chawla, M. Immunoinformatics-Aided Design of a Peptide Based Multiepitope Vaccine Targeting

Glycoproteins and Membrane Proteins against Monkeypox Virus. *Viruses* **2022**, *14*, 2374, doi:10.3390/v14112374.
408. Akhtar, N.; Singh, A.; Upadhyay, A.K.; Mannan, M.A. Design of a Multi-Epitope Vaccine against the Pathogenic Fungi Candida Tropicalis Using an in Silico Approach. *J Genet Eng Biotechnol* **2022**, *20*, 140, doi:10.1186/s43141-022-00415-3.
409. Akhtar, N.; Joshi, A.; Singh, J.; Kaushik, V. Design of a Novel and Potent Multivalent Epitope Based Human Cytomegalovirus Peptide Vaccine: An Immunoinformatics Approach. *Journal of Molecular Liquids* **2021**, *335*, 116586, doi:10.1016/j.molliq.2021.116586.
410. Hasan, M.; Islam, S.; Chakraborty, S.; Mustafa, A.H.; Azim, K.F.; Joy, Z.F.; Hossain, M.N.; Foysal, S.H.; Hasan, M.N. Contriving a Chimeric Polyvalent Vaccine to Prevent Infections Caused by Herpes Simplex Virus (Type-1 and Type-2): An Exploratory Immunoinformatic Approach. *Journal of Biomolecular Structure and Dynamics* **2019**, doi:10.1080/07391102.2019.1647286.
411. Kaushik, V.; G, S.K.; Gupta, L.R.; Kalra, U.; Shaikh, A.R.; Cavallo, L.; Chawla, M. Immunoinformatics Aided Design and In-Vivo Validation of a Cross-Reactive Peptide Based Multi-Epitope Vaccine Targeting Multiple Serotypes of Dengue Virus. *Frontiers in Immunology* **2022**, *13*.
412. Shukla, M.; Chandley, P.; Rohatgi, S. P120 Vaccine Induced Protection by Secreted Aspartyl Proteinase 2 from Candida Parapsilosis in Candida Tropicalis Mediated Murine Systemic Candidiasis: A Role of B-Cells and Antibodies. *Medical Mycology* **2022**, *60*, myac072P120, doi:10.1093/mmy/myac072.P120.